

**A Comparative Study on Surface and Foam Properties  
of Natural and Synthetic Surfactants and  
Characterization of Natural Surfactants**

A Thesis Submitted

To

**Sikkim University**



In Partial Fulfilment of the Requirement for the  
**Degree of Doctor of Philosophy**

By

**Ambika Pradhan**

Department of Physics  
School of Physical Sciences  
July 2018

# Dedication

To my parents

*Mr. Dhruba Kumar Pradhan*

and

*Mrs. Geeta Pradhan*

for their constant encouragement,  
support and inspiration.

To my beloved husband

*Dr. Ashish Pradhan*

and son

*Master Avanish Pradhan*

for their love, support,  
encouragement and trust.

# Acknowledgements

First of all, I would like to express my gratitude to my supervisor, Dr. Amitabha Bhattacharyya for his invaluable guidance, inspirational encouragement, for his patience and constant support throughout my Ph.D course.

I would like to sincerely and wholeheartedly thank Dr. Archana Tiwari for her valuable discussions and suggestions for spectroscopic analysis. The faculty members, Professor A. K. Pathak, Dr. Subir Mukhopadhyaya, Dr. Ajay Tripathi, Dr. Hemam Dinesh Singh and Dr. Dhurba Rai for their valuable discussion, encouragement and insightful comments during this work, so my heartfelt gratitude to all of them.

I am deeply obliged to Dr. Biswajit Gopal Roy for his courteous assistance, valuable discussion and insightful comments for chromatography and spectroscopy experiments. I thankfully acknowledge the Head of the Department of Chemistry, Dr. Somendra Nath Chakraborty, for his insightful discussions and granting permission to perform the chromatography and spectroscopy experiments in his Department.

I would like to acknowledge Dr. Rakesh Kumar Ranjan for granting permission to use the density attachment balance for surface tension experiments. I thankfully acknowledge the Head of the Department of Horticulture, Dr. Laxuman Sharma, for granting permission to perform UV-Vis experiments in his Department. I wish to acknowledge the Head of the Department of Microbiology, Dr. Hare Krishna Tiwari for granting permission to use the pH meter.

I am deeply obliged to Dr. T. K. Mandal, Research Officer In-charge,

Ayurveda Regional Research Institute, Sikkim and Mr. Manoj Chettri, the Range Officer, Lloyd Botanic Garden, Darjeeling, for identifying and authenticating the plant parts.

I would like to thank Mr. Yogesh Chettri for building the jack for surface tension measurement. I thankfully acknowledge Dr. Kabindra Tamang and late Mrs. Kamali Mothey, for providing information on some natural surfactants.

I am indebted to Mr. Sayak Das for his constant support, encouragement, helpful discussions and comments for this work. I am deeply obliged to Mr. Samuzal Bhuyan, Mr. Karan Chhetri, Mr. Susant Mondal, Mr. Ankit Malla Thakuri for their invaluable assistance with chromatography experiments and hospitality.

I would like to thank the laboratory assistants of the Department of Physics, Mr. Bikram Thapa and Mr. Nar Bahadur Subba, Department of Chemistry, Mr. Binod Chettri, Department of Geology, Mr. Bhanu Manger and Department of Microbiology, Mrs. Radha Basnett for their help.

I am thankful to Mr Rajesh Rawat for his assistance in handling of softwares. I wish to acknowledge Mr. Prajwal Chettri and Ms. Laden Sherpa for their assistance in FTIR measurements. I would like to express my thanks to Ms. Trisha Mondal for her encouragement, support and for being such a wonderful person. I am thankful to Mr. Yam Prasad Rai, Mr. Umesh Dhakal, Mr. Ronal Rai, Ms. Asha Tongbram, Ms. Smita Rai, Mr. Indra Hang Subba, Mr. Bheem Singh Jatav, Ms. Chandrima Paul and Mr. Nishal Rai for their help, support and encouragement. I am also thankful to all my friends for their support all along the work.



Last but not the least, I pay my special gratitude to my parents, husband, son, sister and in-laws for their unconditional love, constant support and encouragement.

I would like to acknowledge UGC Non-Net Fellowship for financial support. I thank Sikkim University for providing me the opportunity to do my Ph.D.

Many remain unthanked by name, a heartfelt gratitude to all those who have helped me during this years.

***Ambika Pradhan***

*July 2018*

# Abstract

Surfactants or surface active agents are molecules exhibiting various interfacial activities. Amphiphilicity of surfactants is responsible for surface tension reduction, exhibiting a wide range of pharmaceutical and industrial applications.

Foaming is an important property of surfactants. Foam is a system of gas phase distributed in a liquid phase. They have varied applications in the everyday world. Synthetic surfactants are used extensively today. After use, they enter the aquatic environment and cause damage. Keeping in view the environmental burden, it is desirable to substitute synthetic surfactants with naturally obtained molecules as renewable and bio-compatible alternatives. In search of such alternatives, I have investigated a few plant based natural surfactants.

This thesis presents detailed investigations of surface and foam properties of natural surfactants extracted from *Sapindus mukorossi*, *Albizia procera*, *Zephyranthes carinata*, *Acacia concinna* and *Juglans regia*. Some synthetic surfactants have been studied as a reference. In addition, I have also performed preliminary characterization of the natural surfactants using Thin Layer Chromatography (TLC), Column Chromatography (CC), High Performance Liquid Chromatography (HPLC), UV-Visible Spectroscopy (UV-Vis), Fourier Transform Infrared Spectroscopy (FTIR) and Gas Chromatography Mass Spectrometry (GC-MS). Also, the thesis discusses one shot two dimensional drainage in foams using natural surfactant systems. While *Sapindus mukorossi* and *Acacia concinna* have been studied earlier, this

thesis gives the first ever reports on surfactant activities of *Albizia procera*, *Zephyranthes carinata* and *Juglans regia*.

The surface tension studies reveal that good surface tension reduction was observed for all the natural surfactants with a low critical micelle concentration (CMC). The natural surfactants are acid balanced and exhibited good wetting ability. *Juglans regia* is an exception. On addition of salt, the foaming increases and then decreases when surfactant concentration is below the CMC. Above CMC, foaming decreases with increase in salt. The natural surfactants show good cleaning and emulsification at higher concentrations. Emulsion stability decreases in the region of micelle formation. Thus natural surfactants exhibit remarkable surface active characteristics.

An important parameter for studying the efficacy of a surfactant is Dirt Dispersion (DD) or the amount of dirt present in the foam. It is difficult to rinse this dirt and it may redeposit. DD is quantified for the first time. I also studied its variation with concentration. Quantification of DD reveals interesting results. The amount of dirt present in foam increases, reaches a maximum and then decreases with increase in concentration. The concentration at which maximum amount of dirt attaches to the foam corresponds to the CMC, as revealed by surface tension measurements. Thus this approach gives a rapid, easy, low cost effective tool to measure CMC.

Preliminary characterization of the natural surfactants was performed to understand the chemical profile of the natural surfactants. TLC studies revealed the presence of saponin possessing a large number of polar and non-polar compounds. The presence of saponin was supported by UV-Vis results. FTIR spectra showed characteristic triterpenoid saponin absorptions

of OH, C=O, C-H, and C=C. Glycoside linkages to the saponinins was shown by absorptions of C-O-C. A large number of compounds were observed by HPLC and good separation was achieved using water-methanol solvent system. GC-MS showed the presence of diverse classes of compounds belonging to alcohols, esters, aldehydes and fatty acids.

To quantitatively understand the mechanism of foam stability, I performed forced drainage experiments on *Sapindus mukorossi* and *Acacia concinna* systems. Drainage is the flow of intervening liquid due to gravity, surface tension and viscosity. It plays an important role in determining foam stability. This is the first study of drainage in plant based surfactants. Similar drainage profile was observed by both the systems. The vertical drainage profile reveals a power law behaviour for front position and a Poiseuille type flow, similar to synthetic surfactants. The drainage wave initially produced a conic shape downstream and later became an expanding ellipsoid. Liquid fraction studies showed that drainage wave moves with Gaussian distributions both vertically and horizontally. Along the vertical, the normal Gaussian distribution distorts after 20 seconds indicating two types of flow occurring simultaneously.

Our results suggest that the plant derived natural surfactants possess an enormous potential to be used as surface active agents which could provide useful input to various industries.

# List of Publications

- A. Pradhan and A. Bhattacharyya. Shampoos then and now: Synthetic versus natural. *Journal of Surface Science and Technology*, 30, 59-76, 2014.
- A. Pradhan and A. Bhattacharyya. *Modern aspects in Materials Physics and Chemistry, Chapter 3: Investigating natural surfactants as a green alternative: A review*, Lap Lambert Academic Publishing, Deutschland, Germany, 2015.
- A. Pradhan and A. Bhattacharyya. Quest for an eco-friendly alternative surfactant: Surface and foam characteristics of natural surfactants. *Journal of Cleaner Production*, 150, 127-134, 2017.
- A. Pradhan and A. Bhattacharyya. Dispersion of ink in foam quantified: An alternative approach to critical micelle concentration. Accepted for publication by *Journal of Surfactants and Detergents*.

# Contents

<b>I</b>	<b>INTRODUCTION</b>	<b>1</b>
<b>1</b>	<b>Introduction</b>	<b>2</b>
1.1	Introduction . . . . .	2
1.2	Outline . . . . .	11
<b>2</b>	<b>Literature Review</b>	<b>14</b>
2.1	Surfactants . . . . .	14
2.1.1	Application of Surfactants . . . . .	17
2.1.2	Classification of surfactants . . . . .	18
2.1.3	Surface Tension . . . . .	21
2.1.4	Surface Tension Measurement . . . . .	22
2.1.5	Micelles and Critical Micelle Concentration . . . . .	25
2.1.6	Methods of Estimating CMC . . . . .	28
2.2	Foams . . . . .	30
2.2.1	Structure of Foam . . . . .	32
2.2.2	Young-Laplace Equation . . . . .	33
2.2.3	Foaming Ability and Stability . . . . .	35
2.2.4	Test for Foamability and Stability . . . . .	37

CONTENTS x

2.2.5	Drainage in Foams . . . . .	38
2.2.6	Foam Drainage Equation . . . . .	41
2.2.7	Applications of Foam . . . . .	43
2.3	Emulsions . . . . .	44
2.3.1	Surfactants as Emulsifying Agent . . . . .	47
2.4	Surface Wetting . . . . .	48
2.5	Dirt Dispersion . . . . .	49
2.6	Environmental Effects . . . . .	50
2.7	Natural Surfactants . . . . .	51
2.7.1	Saponins as Surfactants and Emulsifiers . . . . .	54
2.7.2	Applications of Saponin . . . . .	55
2.8	Plants Used in this Study . . . . .	56
2.8.1	<i>Sapindus mukorossi</i> (Ritha) . . . . .	57
2.8.2	<i>Albizia procera</i> (Seto Siris) . . . . .	57
2.8.3	<i>Zephyranthes carinata</i> (Pyagi Phool) . . . . .	58
2.8.4	<i>Acacia concinna</i> (Shikakai) . . . . .	59
2.8.5	<i>Juglans regia</i> (Okhar) . . . . .	59

**II EXPERIMENTAL TECHNIQUES 61**

**3 Material and Methods 62**

3.1	Materials . . . . .	62
3.1.1	Natural Surfactants . . . . .	62
3.1.2	Synthetic Surfactants . . . . .	64
3.1.3	Other Materials . . . . .	65

<i>CONTENTS</i>	xi
-----------------	----

3.2	Experimental Techniques . . . . .	66
3.2.1	Extraction of Natural Surfactants . . . . .	66
3.2.2	Preparation of Synthetic Surfactants . . . . .	69
3.2.3	Surface Activity Measurements . . . . .	69
3.2.4	Characterization Techniques . . . . .	80
3.2.5	Forced Drainage Experiment . . . . .	96
3.3	Conclusion . . . . .	99

<b>III</b>	<b>RESULTS AND DISCUSSION</b>	<b>100</b>
------------	-------------------------------	------------

<b>4</b>	<b>Surface and Foam Properties</b>	<b>101</b>
----------	------------------------------------	------------

4.1	Introduction . . . . .	101
4.2	Surface Tension Measurements . . . . .	102
4.3	Surface Wetting Measurements . . . . .	106
4.4	Foaming . . . . .	107
4.4.1	Foaming Ability . . . . .	107
4.4.2	Foam Stability . . . . .	108
4.4.3	Effect of Salt on Foaming . . . . .	110
4.4.4	Effect of Salt on Foam Stability . . . . .	113
4.5	Emulsification . . . . .	115
4.6	pH Measurements . . . . .	116
4.7	Conductivity Measurements . . . . .	117
4.8	Viscosity Measurements . . . . .	119
4.8.1	Effect of Salt on Viscosity . . . . .	120
4.9	Cleaning . . . . .	121



4.10 Conclusion . . . . .	122
<b>5 Dirt in Foam: New Approach to Measure CMC</b>	<b>124</b>
5.1 Introduction . . . . .	125
5.2 Dirt Dispersion Measurements . . . . .	126
5.3 Surface Tension Measurements . . . . .	128
5.4 Comparison of the two methods . . . . .	129
5.5 Conclusions . . . . .	131
<b>6 Preliminary Characterization of Natural Surfactants</b>	<b>132</b>
6.1 Introduction . . . . .	132
6.2 <i>Albizia procera</i> . . . . .	134
6.2.1 Thin Layer Chromatography Analysis . . . . .	134
6.2.2 Column Chromatography . . . . .	136
6.2.3 UV-Visible Spectroscopy . . . . .	136
6.2.4 HPLC Analysis . . . . .	138
6.2.5 FTIR Analysis . . . . .	141
6.2.6 GC-MS Analysis . . . . .	143
6.3 <i>Juglans regia</i> . . . . .	146
6.3.1 Thin Layer Chromatography Analysis . . . . .	146
6.3.2 Column Chromatography . . . . .	147
6.3.3 UV-Visible Spectroscopy . . . . .	148
6.3.4 HPLC Analysis . . . . .	149
6.3.5 FTIR Analysis . . . . .	152
6.3.6 GC-MS Analysis . . . . .	153
6.4 <i>Zephyranthes carinata</i> . . . . .	156

6.4.1	Thin Layer Chromatography Analysis . . . . .	156
6.4.2	Column Chromatography . . . . .	158
6.4.3	UV-Visible Spectroscopy . . . . .	158
6.4.4	HPLC Analysis . . . . .	160
6.4.5	FTIR Analysis . . . . .	162
6.4.6	GC-MS Analysis . . . . .	164
6.5	<i>Sapindus mukorossi</i> . . . . .	167
6.5.1	Thin Layer Chromatography Analysis . . . . .	167
6.5.2	UV-Visible Spectroscopy . . . . .	168
6.5.3	HPLC Analysis . . . . .	170
6.5.4	FTIR Analysis . . . . .	170
6.5.5	GC-MS Analysis . . . . .	172
6.6	<i>Acacia concinna</i> . . . . .	175
6.6.1	Thin Layer Chromatography Analysis . . . . .	175
6.6.2	Column Chromatography . . . . .	176
6.6.3	UV-Vis Spectroscopy . . . . .	177
6.6.4	HPLC Analysis . . . . .	178
6.6.5	FTIR Analysis . . . . .	180
6.6.6	GC-MS Analysis . . . . .	183
6.7	Conclusion . . . . .	184
<b>7</b>	<b>Two-Dimensional One-Shot Forced Drainage</b>	<b>186</b>
7.1	Introduction . . . . .	186
7.2	<i>Sapindus mukorossi</i> . . . . .	189
7.2.1	Drainage Profile . . . . .	189

*CONTENTS* xiv

7.2.2 Drainage Profile Shape . . . . . 191

7.2.3 Liquid Fraction along Vertical and Horizontal Positions 192

7.2.4 Effect of added dye on Surface Tension . . . . . 193

7.3 *Acacia concinna* . . . . . 195

7.3.1 Drainage Profile . . . . . 195

7.3.2 Drainage Profile Shape . . . . . 196

7.3.3 Liquid Fraction along Vertical and Horizontal Position 197

7.4 Conclusion . . . . . 199

**IV CONCLUSIONS 201**

**8 Concluding Remarks and Future Prospects 202**

8.1 Conclusion . . . . . 202

8.2 Future Prospects . . . . . 206

**V APPENDIX 207**

# List of Figures

1.1	Schematic diagram of a surfactant molecule. . . . .	3
1.2	Orientation of hydrophilic heads and hydrophobic tails at air-water interface forming a monolayer. Some surfactant molecules are seen to form a micelle. . . . .	4
1.3	Structure of typical saponin molecule. . . . .	7
2.1	Mechanism of stain removal from fabric by surfactant. . . . .	17
2.2	Classification of surfactants. . . . .	19
2.3	The molecular structure of (a) sodium dodecyl sulphate (b) n-dodecyl-hexaethylene oxide (c) cetyl trimethylammonium bromide (d)N,N-dimethyl-N-dodecylglycine dodecylbetaine. . .	20
2.4	Schematic representation of surface tension with concentration. . . . .	26
2.5	Variation of physical properties with surfactant concentration. . . . .	27
2.6	The structure of dry and wet foam. . . . .	33
2.7	The structure and geometry of dry foam. . . . .	34
2.8	Mechanism involved in destability of emulsion. . . . .	45
2.9	Schematic representation of complete and partial wetting. . . . .	49
2.10	Structures of (a) triterpenoid (b) steroid sapogenins. . . . .	53

3.1	(a) <i>Sapindus mukorossi</i> fruit pulp (b) <i>Albizia procera</i> leaves (c) <i>Zephyranthes carinata</i> bulbs (d) <i>Acacia concinna</i> pods (e) <i>Juglans regia</i> bark. . . . .	64
3.2	(a) <i>Sapindus mukorossi</i> (b) <i>Albizia procera</i> (c) <i>Zephyranthes</i> <i>carinata</i> (d) <i>Acacia concinna</i> (e) <i>Juglans regia</i> . . . . .	69
3.3	Experimental set-up for surface tension measurements (a)Wilhelmy plate arrangement (b) Schematic representation of the medium.	70
3.4	Experimental set-up for foam formation (a)Photograph show- ing Bikerman's method (b) Schematic representation of the system showing the foam height as 'h'. . . . .	73
3.5	Photograph showing emulsion formed with <i>Sapindus mukorossi</i> extract. The emulsion formed did not separate for 2 hours. . .	75
3.6	Photograph of conductivity measurement. . . . .	76
3.7	Photograph taken while performing viscosity measurements. .	78
3.8	Dirt dispersion of <i>Sapindus mukorossi</i> extract at various con- centrations. (a) $5.47 \times 10^{-4}$ g/cc (b) $1.09 \times 10^{-3}$ g/cc (c) $2.19 \times 10^{-3}$ g/cc (d) $4.38 \times 10^{-3}$ g/cc (e) $8.75 \times 10^{-3}$ g/cc (f) $1.75 \times 10^{-2}$ g/cc (g) $3.50 \times 10^{-2}$ g/cc. . . . .	79
3.9	Photograph taken while performing Thin Layer Chromato- graphy on <i>Sapindus mukorossi</i> extract. . . . .	82
3.10	Photograph taken while performing Column Chromatography.	85
3.11	Schematic representation of High Performance Liquid Chro- matography. . . . .	86
3.12	High Performance Liquid Chromatography setup. . . . .	87
3.13	Transition between electronic states in a molecule. . . . .	89

3.14	Block diagram of UV-Vis Spectrophotometer. . . . .	90
3.15	Schematic diagram of FTIR Spectrometer. . . . .	94
3.16	Schematic diagram of Gas Chromatography Mass Spectrometry. . . . .	95
3.17	(a) Photograph of one-shot two-dimensional forced drainage experiment with <i>Sapindus mukorossi</i> solution when 0.5 ml solution was added from top (b) One-shot two-dimensional forced drainage setup. . . . .	98
4.1	Variation of surface tension with surfactant concentration at $20 \pm 2$ °C. . . . .	103
4.2	Wetting time of surfactant solutions at $20 \pm 2$ °C. . . . .	106
4.3	Foaming behaviour of surfactant solutions (a),(b) Bikerman's method (c),(d) Bartsch test at $20 \pm 2$ °C. . . . .	108
4.4	Variation of <i>R5</i> value with surfactant concentration (a),(b) Bikerman's method (c),(d)Barstch test at $20 \pm 2$ °C. . . . .	109
4.5	The effect of salt on foam height below CMC at $20 \pm 2$ °C. . . . .	110
4.6	The effect of salt on foam height at CMC at $20 \pm 2$ °C. . . . .	111
4.7	The effect of salt on foam height above CMC at $20 \pm 2$ °C. . . . .	112
4.8	<i>R5</i> as a function of added salt concentration below CMC at $20 \pm 2$ °C. . . . .	113
4.9	<i>R5</i> as a function of added salt concentration at CMC at $20 \pm 2$ °C. . . . .	114
4.10	<i>R5</i> as a function of added salt concentration above CMC at $20 \pm 2$ °C. . . . .	114
4.11	Emulsion stability of surfactant solutions at $20 \pm 2$ °C. . . . .	116

4.12	Variation of pH with surfactant concentration at $20 \pm 2$ °C. . .	117
4.13	Conductivity as a function of surfactant solutions at $20 \pm 2$ °C.	118
4.14	Variation of viscosity of surfactant solutions at $20 \pm 2$ °C. . .	119
4.15	Effect of salt on viscosity of surfactant solutions at $20 \pm 2$ °C.	120
4.16	Cleaning ability of surfactant solutions at $20 \pm 2$ °C. . . . .	122
5.1	Variation of dirt dispersion with surfactant concentration at $20 \pm 2$ °C. . . . .	127
5.2	Surface tension of <i>Sapindus mukorossi</i> with and without ink as a function of surfactant concentration at $20 \pm 2$ °C. . . . .	128
6.1	TLC plates for methanol extract of <i>Albizia procera</i> derivatized with PMA using (a) (Chloroform: Glacial acetic acid: Meth- anol: Water [8:4:1.5:1]) (b) (Petroleum ether: Ethyl acetate [80:20]). . . . .	134
6.2	Column purified fractions of methanol extract of <i>Albizia pro- cera</i> . . . . .	136
6.3	UV-Vis absorption spectra for extracts of <i>Albizia procera</i> . . .	137
6.4	HPLC chromatogram for methanol extract of <i>Albizia procera</i> . .	138
6.5	HPLC chromatogram of column purified fraction B8 for meth- anol extract of <i>Albizia procera</i> . . . . .	140
6.6	FTIR spectra for extracts of <i>Albizia procera</i> . . . . .	141
6.7	GC-MS chromatogram of methanol extract of <i>Albizia procera</i> .	144

6.8	TLC plates for methanol extract of <i>Juglans regia</i> : (a) short wavelength (254 nm) (b) derivatized with PMA using (Chloroform: Glacial acetic acid: Methanol: Water [8:4:1.5:1]); using (Petroleum ether: Ethyl acetate [90:10]) (c) short wavelength (d) long wavelength (366 nm) (e) derivatized with PMA. . . .	146
6.9	Column purified fractions for methanol extract of <i>Juglans regia</i> .	148
6.10	UV-Visible spectra for extracts of <i>Juglans regia</i> . . . . .	148
6.11	HPLC chromatogram for methanol extract of <i>Juglans regia</i> . .	150
6.12	HPLC chromatogram of column purified fraction Y1 for methanol extract of <i>Juglans regia</i> . . . . .	150
6.13	FTIR spectra for extracts of <i>Juglans regia</i> . . . . .	152
6.14	GC-MS chromatogram for methanol extract of <i>Juglans regia</i> .	155
6.15	TLC plates for methanol extract of <i>Zephyranthes carinata</i> : using (Chloroform: Glacial acetic acid: Methanol: Water [8:4:1.5:1]) (a) short wavelength (254 nm) (b) long wavelength (366 nm) (c) derivatized with PMA; using (Petroleum ether: Ethyl acetate [90:10]) (d) short wavelength (e) derivatized with PMA. . . . .	156
6.16	Column purified fractions for methanol extract of <i>Zephyranthes carinata</i> . . . . .	158
6.17	UV-Visible absorption spectra for extracts of <i>Zephyranthes carinata</i> . . . . .	159
6.18	HPLC chromatogram for methanol extract of <i>Zephyranthes carinata</i> . . . . .	160



6.19	HPLC chromatogram of column purified fraction U5 for methanol extract of <i>Zephyranthes carinata</i> . . . . .	161
6.20	FTIR spectra for extracts of <i>Zephyranthes carinata</i> . . . . .	162
6.21	GC-MS chromatogram for methanol extract of <i>Zephyranthes carinata</i> . . . . .	166
6.22	TLC plates for methanol extract of <i>Sapindus mukorossi</i> : using (Chloroform: Glacial acetic acid: Methanol: Water [8:4:1.5:1]) (a) short wavelength (254nm) (b) derivatized with PMA; using (Petroleum ether: Ethyl acetate [50:50]) (c) short wavelength (d) derivatized with PMA. . . . .	167
6.23	UV-Visible absorption spectra for extracts of <i>Sapindus mukorossi</i> .	169
6.24	HPLC chromatogram for the methanol extract of <i>Sapindus mukorossi</i> . . . . .	170
6.25	FTIR spectra for extracts of <i>Sapindus mukorossi</i> . . . . .	171
6.26	GC-MS chromatogram for the methanol extract of <i>Sapindus mukorossi</i> . . . . .	173
6.27	TLC plates for methanol extract of <i>Acacia concinna</i> derivatized with anisaldehyde-sulphuric acid reagent using (a) (Chloroform: Glacial acetic acid: Methanol: Water [8:4:1.5:1]) (b) (Petroleum ether: Ethyl acetate [80:20]). . . . .	175
6.28	Column purified fractions for methanol extract of <i>Acacia concinna</i> . . . . .	177
6.29	UV-Vis absorption spectra for extracts of <i>Acacia concinna</i> . . . . .	177
6.30	HPLC chromatogram for methanol extract of <i>Acacia concinna</i> .	179

6.31	HPLC chromatogram of column purified fraction I6 for methanol extract of <i>Acacia concinna</i> . . . . .	180
6.32	FTIR spectra for extracts of <i>Acacia concinna</i> . . . . .	181
6.33	GC-MS chromatogram for methanol extract of <i>Acacia concinna</i> . . . . .	183
7.1	Snapshot of 2 D drainage for <i>Sapindus mukorossi</i> , 0.5 ml liquid added. Photograph shows precursor movement after 10 seconds.	189
7.2	(a) Position of wave front along vertical and horizontal directions as a function of time (b) Variation of vertical and horizontal velocity with time. . . . .	190
7.3	Shape of the drainage pattern. The vertical axis is shown upwards, hence the shape should be visualised in reverse. . . .	191
7.4	(a) Profiles of liquid fraction along the vertical and horizontal (b) Position of the wetting front moving through the foam. . . .	193
7.5	Surface tension as a function of amount of dye added. . . . .	194
7.6	Snapshot of 2 D drainage for <i>Acacia concinna</i> , 0.5 ml liquid added. Photograph shows precursor movement after 10 seconds.	195
7.7	(a) Position of wave front along vertical and horizontal directions (b) Variation of vertical and horizontal velocity with time. . . . .	196
7.8	Shape of the drainage pattern. . . . .	197
7.9	(a) Profiles of liquid fraction along the vertical and horizontal (b) Position of the wetting front moving through the foam. . . .	198

# List of Tables

3.1	Natural surfactants used for the present study. . . . .	63
3.2	Synthetic surfactants used for the present study. . . . .	65
4.1	Surface properties of surfactants at $20 \pm 2$ °C. . . . .	104
5.1	CMC obtained by dirt dispersion and surface tension method.	130
6.1	<i>R<sub>f</sub></i> value on TLC plate for methanol extract of <i>Albizia procera</i> .	135
6.2	UV-Vis absorption peaks for extracts of <i>Albizia procera</i> . . . .	138
6.3	HPLC for methanol extract of <i>Albizia procera</i> . . . . .	139
6.4	Functional groups present in extracts of <i>Albizia procera</i> . . . .	142
6.5	Chemical constituents for methanol extract of <i>Albizia procera</i> by GC-MS . . . . .	145
6.6	<i>R<sub>f</sub></i> value on TLC plate for methanol extract of <i>Juglans regia</i> . . . .	147
6.7	UV-Vis absorption for extracts of <i>Juglans regia</i> . . . . .	149
6.8	HPLC for methanol extracts of <i>Juglans regia</i> . . . . .	151
6.9	Functional groups present in extracts of <i>Juglans regia</i> . . . . .	153
6.10	Chemical constituents for methanol extract of <i>Juglans regia</i> by GC-MS. . . . .	154

6.11 <i>R<sub>f</sub></i> value on TLC plate for methanol extract of <i>Zephyranthes carinata</i> . . . . .	157
6.12 UV-Vis absorption for extracts of <i>Zephyranthes carinata</i> . . .	159
6.13 HPLC for methanol extracts of <i>Zephyranthes carinata</i> . . . . .	161
6.14 Functional groups present in the extracts of <i>Zephyranthes carinata</i> . 163	
6.15 Chemical constituents for methanol extract of <i>Zephyranthes carinata</i> by GC-MS. . . . .	165
6.16 <i>R<sub>f</sub></i> value on TLC plate for methanol extract of <i>Sapindus mukorossi</i> . 168	
6.17 UV-Vis absorption for extracts of <i>Sapindus mukorossi</i> . . . . .	169
6.18 HPLC chromatogram for the methanol extract of <i>Sapindus mukorossi</i> . . . . .	171
6.19 Functional groups present in extracts of <i>Sapindus mukorossi</i> . 172	
6.20 Chemical constituents for methanol extract of <i>Sapindus mukorossi</i> by GC-MS. . . . .	174
6.21 <i>R<sub>f</sub></i> value on TLC plate for methanol extract of <i>Acacia concinna</i> . 176	
6.22 UV-Vis absorption for extracts of <i>Acacia concinna</i> . . . . .	178
6.23 HPLC for methanol extracts of <i>Acacia concinna</i> . . . . .	179
6.24 Functional groups present in extracts of <i>Acacia concinna</i> . . . . .	181
6.25 Chemical constituents for methanol extract of <i>Acacia concinna</i> by GC-MS. . . . .	184

# Abbreviations

- CMC: Critical Micelle Concentration
- CAC: Critical Aggregation Concentration
- DD : Dirt Dispersion
- TLC: Thin Layer Chromatography
- CC : Column Chromatography
- HPLC: High Performance Liquid Chromatography
- UV-Vis: UV-Visible Spectroscopy
- FTIR: Fourier Transform Infrared Spectroscopy
- GC-MS: Gas Chromatography-Mass Spectrometry
- PMA: Phosphomolybdic Acid
- TFA: Trifluoroacetic acid
- NIST: National Institute of Standard and Technology
- O/W: Oil-in-water
- W/O: Water-in-oil
- *R<sub>f</sub>*: Retention Factor

# Part I

## INTRODUCTION

# Chapter 1

## Introduction

### 1.1 Introduction

Surfactants or surface active agents are amphiphilic substances exhibiting a dual affinity also known as polar-apolar duality. The polar (hydrophilic) or water loving portion comprises of hetero atoms such as oxygen, sulphur, phosphorus or nitrogen included in the functional groups such as alcohols, ether, ester, acid sulfate, phosphate, amide etc. The non-polar (hydrophobic) or water hating portion consists of one or more hydrocarbon chains of alkyl or alkylbenzene type [1] (Figure 1.1). The hydrophilic part undergoes electrostatic interactions like hydrogen bonding, dipolar interactions, ionic bonding with the surrounding molecules whereas the hydrophobic part interacts with its neighbouring non-polar structures through Van der Waals interactions. This results in the adsorption and aggregation of the molecules. Due to its double affinity, surfactants migrate to the surface or interfaces and orient with the polar part in water and non-polar part in air thus altering the surface

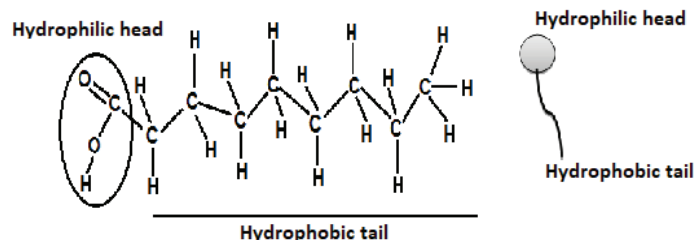


Figure 1.1: Schematic diagram of a surfactant molecule.

free energy. Depending on the nature of the hydrophilic group surfactants are classified as anionic, cationic, zwitterionic and non-ionic surfactants [2].

When surfactants are added to water, they adsorb at the air-water interface forming a monolayer. This reduces the surface or interfacial tension. With increase in concentration, a stage is reached when no further molecules can be accommodated at the surface. The molecules then assemble in the bulk to form aggregates called micelles. Here the hydrophobic part associates in the interior while the hydrophilic part faces the aqueous medium, as shown in Figure 1.2. Surfactants thus either interact with the surfaces or self aggregate to form micelles in solution. Various techniques such as surface tension, osmotic pressure [3], viscosity [4], conductivity [5], light scattering [6], dye solubilization, fluorimetry [7] etc. are used to demonstrate micellar aggregation. All these properties abruptly change over a narrow concentration range. The threshold concentration at which the properties of the surfactant solution change due to micelle formation is termed as the Critical Micelle Concentration (CMC).

One important property of a surfactant is surface wetting. Surfactants are also known as wetting agents as they lower the surface tension of the



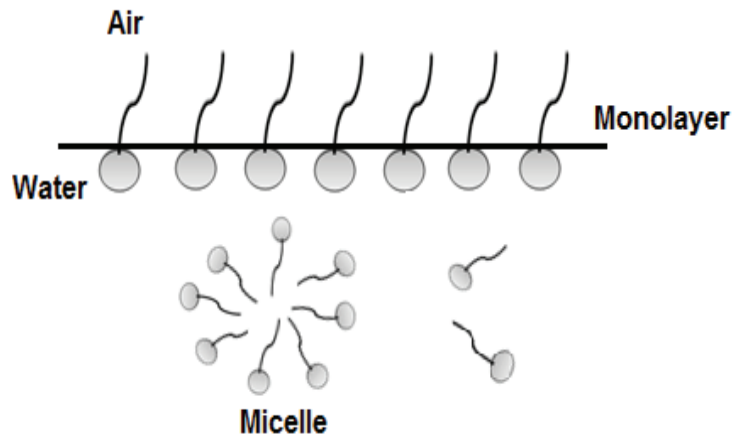


Figure 1.2: Orientation of hydrophilic heads and hydrophobic tails at air-water interface forming a monolayer. Some surfactant molecules are seen to form a micelle.

liquid which enhances easier spreading over surfaces. The dual nature of the surfactant molecule is responsible for enhanced wetting of water. This in turn allows water to penetrate a surface and enter into the dirt. The hydrophobic or the oleophilic part of the surfactant attracts and emulsifies the grease or dirt whereas the hydrophilic part dissolves in water. This simultaneous action causes the dirt or grease to disperse in water [8].

Foaming is a characteristic of a surface active substance. When a surfactant is added to water and agitated, foam is formed. Foam is a collection of gas bubbles uniformly distributed throughout a continuous liquid phase [9]. It is produced when surface tension of water is reduced and air is forced in to form bubbles. Foam plays an important role in foods and personal care products like espresso coffee, creams, lotions and shampoo [10]. It is also important in many industries like petroleum, metallurgy, brewing, fire fight-

ing and separating, isolating or spreading of chemicals [11]. Thus the study of foam is useful in engineering, chemistry, physics and food science with its wide range of applications [12]. Our present work is on aqueous foam.

The flow of liquid through a foam caused by gravity and capillarity is known as drainage [13]. It is one of the important factors which destabilizes foam. Thus this process is of great importance in the study of foams. Gravitational forces drain the liquid out of the foam. The liquid films between the bubbles become thinner, fragile and finally break as the foam dries up. Thus stability of foam depends on drainage [14]. The present work studies one shot two dimensional drainage in natural surfactant systems using a rectangular Hele-Shaw cell.

An important parameter for studying cleaning ability of surfactants or surfactant efficacy is Dirt Dispersion (DD), the quantity of dirt remaining in the foam [15]. It is difficult to rinse this dirt and it may redeposit at the surface. To the best of our knowledge, DD has so far been studied qualitatively by eye estimation only [16]. This work is the first to report quantification of DD. I have measured DD as a function of concentration and used it to determine CMC of surfactants. This is a new low cost method of determining CMC.

Another important characteristic of surfactants is their ability to form stable oil-water emulsions. Surfactants act as emulsifiers by adsorbing at the oil-water interface and reducing interfacial tension. Emulsion is important in food, personal care products, paints, polishes and pesticides [17].

Thus surfactants play an important role in a wide array of industries including detergents, paints, flotation, surface wetting preparation of nano-

particles, emulsions, pharmaceuticals, cosmetics, food products, remediation processes and paper products [1].

Due to its wide applications, large number of synthetic surfactants are in industrial and domestic usage. They get dispersed in different environment sections such as water, soil and sediments etc [18]. In 2006, 12.5 million tonnes of surfactants were produced world wide [19] while 3 million tonnes of surfactants were produced in Western Europe in 2007 [20]. The consumption of one non-ionic surfactant (polyethoxylated nonylphenol) in United States was approximately 172 thousand tonnes in 2010 [21]. Ultimately, all these surfactants would go into the environment. Most surfactants are manufactured using synthetic chemical processes and are not biodegradable leading to serious environmental problems [22, 23]. These surfactants cause health hazards such as irritation of eyes, respiratory diseases and dermatitis [24, 25]. Synthetic surfactants enter the aquatic system and hampers the environment. Studies have shown that synthetic surfactants inhibit the filtering activity of mussels and oysters [26]. Toxicity test of seven surfactants on six fresh water microbes show that all surfactants are toxic. However, non-ionic surfactants are less toxic, followed by anionic and cationic surfactants [27].

The environment concerned world of today requires not only surface active properties of a surfactant but also biodegradability and low toxicity [28]. In comparison to synthetic surfactants, natural surfactants are renewable as they are obtained from continuous ecological cycles, easy to obtain in large quantities, biodegradable, and have less toxic breakdown products [29]. There is thus an increasing trend to move towards a more sustainable production of surfactants by using natural products. Thus researches on envir-

environment friendly surfactants are being initiated of which, one study could be on natural surfactants. The sources of natural surfactants include plants, bacteria or fungi, humic acid, fatty acid esters of sugars or amides of amino acids. They can be obtained using different techniques like extraction, filtration, precipitation and distillation [30].

The best known plant based surfactant is called saponin. Saponins are naturally occurring glycosides mostly produced by plants but also produced by some lower marine animals and bacteria. Saponins constitute a fat soluble nucleus known as the aglycone which can either be triterpenoid or alkaloid steroids. The aglycone nucleus is attached to one or more sugar chains called glycones through ether or ester bonds, [31, 32] as shown in Figure 1.3 [33].

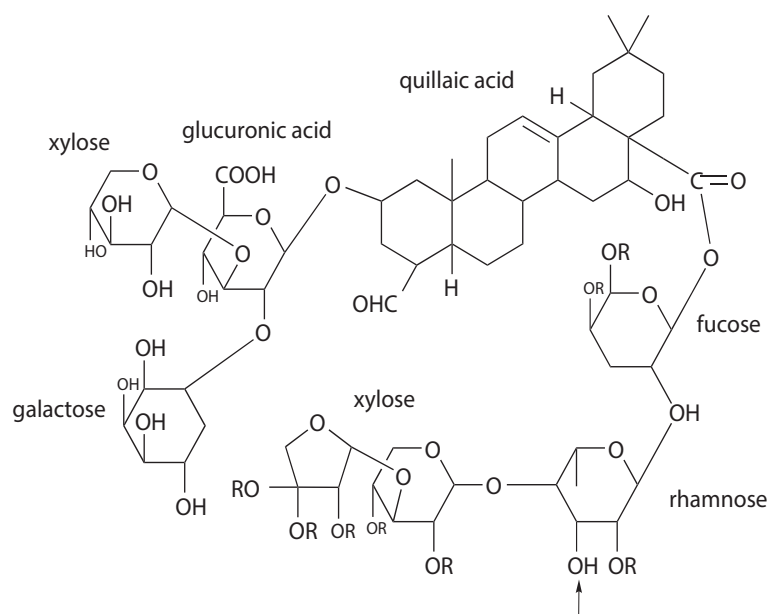


Figure 1.3: Structure of typical saponin molecule.

Due to the simultaneous presence of sugar chains and aglycone, saponins possess surface active properties. They have the ability to form stable

foams in aqueous solutions. Studies have shown that Endod (*Phytolacca dodocandra* L'Herit) saponin could be completely biodegraded in 10 days [34]. Saponins are used to treat many diseases and they are used in environmental control activities such as control of oil spills, bioremediation of contaminated soils and detoxification of industrial effluents [35].

Recent trends in industries is to search for natural alternatives and avoid synthetic products. Keeping this in mind, I have studied extracts obtained from five plant sources namely *Sapindus mukorossi*, *Acacia concinna*, *Albizia procera*, *Zephyranthes carinata* and *Juglans regia* as natural surfactants. This is the first report of surface active properties of *Albizia procera*, *Zephyranthes carinata* and *Juglans regia*. These plants have been chosen as traditional cleansing agents in the regions of West Bengal and Sikkim around Gangtok. These natural surfactants have been studied with an objective to evaluate their surface, foam and drainage characteristics. The natural surfactants have been characterized using various techniques. Some synthetic surfactants have also been studied as a reference.

In order to search for potential natural plant based surfactants having various surface, foam and drainage characteristics the following parameters were determined:

- **Determination of surface tension:** Limited experiments were performed on surface tension as a function of concentration and temperature during my M. Phil. However, the CMC could not be investigated. In the present study, surface tension of the solutions was again measured by Wilhelmy Plate technique. This technique uses a filter paper/platinum plate kept fixed with respect to the liquid surface. Sur-

face tension is obtained by measuring the downward force experienced on the plate due to the liquid meniscus using a microbalance. Variation of surface tension with concentration was studied. Initially, the surface tension reduces with increase in surfactant concentration after which it remains constant. This concentration at which surface tension remained constant is the CMC. Our studies aimed at estimating the CMC of the different solutions which is an important parameter of a surfactant.

- **Foaming Ability and Stability:** Our previous study in M.Phil. investigated the foaming ability and stability of various natural surfactants with respect to concentration using Bikerman's Method and Barstch Test. Foam generation is an important criteria in evaluation of a surfactant. In the present study, the foaming ability and stability were investigated as a function of addition of salt by Bikermam's Method.
- **pH and Conductivity:** The conductivity of natural and synthetic surfactants was studied as a function of concentration. The abrupt increase in conductivity of a surfactant solution gives an idea about the region of micelle formation. Study of the pH of the surfactant solution is important as a solution of pH close to the skin causes less damage to the hair and skin. The solution pH was measured as a function of concentration.
- **Viscosity:** Viscosity of natural and synthetic surfactants was studied as a function of concentration. Viscosity affects foam stability as high

viscosity tends to stabilize foam. The study of viscosity also gives an idea of formation of micelles.

- **Surface Wetting:** Wetting ability was determined to compare detergent efficacies by Canvas Disc Wetting test with a slight modification. A cotton cloth was used instead of a canvas disc. The cloth was floated on the surface of the solution. Wetting time was measured as the time taken for the cloth to begin to sink [36].
- **Emulsifying power:** The stability and type of oil-water emulsion depends on the nature of surfactant used. Emulsifying power of surfactants were studied using the Barstch test. Equal volumes of surfactant solutions and oil were shaken in a measuring cylinder. The separation of aqueous phases were monitored with time for the emulsions formed.
- **Dirt Dispersion:** Dispersion of dirt in foam is a test of the surfactant's efficacy. In previous studies it was studied only by eye estimation. In this study two bottles of surfactant solution were taken and India ink was added to one bottle. The bottles were simultaneously shaken, photographed and the gray scale of the foams analyzed. Dirt dispersion was measured by taking the ratio of the gray scale at the same height for the foams. This study is the first attempt to quantify the amount of dirt present in the foam.
- **Cleaning ability of Surfactants:** In order to evaluate the amount of dirt removed by surfactants, cleaning action was measured as a percentage of dirt removed.

- **Characterization of Natural Surfactants:** The natural surfactant (saponin) present in the various plant samples was analyzed and characterized using Thin Layer Chromatography (TLC), Column Chromatography (CC), High Performance Liquid Chromatography (HPLC), UV-Visible spectroscopy (UV-Vis), Fourier Transform Infrared Spectroscopy (FTIR) and Gas Chromatography-Mass Spectrometry (GC-MS).
- **Observation of Drainage in Foams:** The stability of foam depends on three processes, drainage, Ostwald ripening and coalescence. The process of drainage in natural surfactant system was investigated. This study focussed on one shot forced drainage with fresh liquid along with a dye added to foam of different bubble sizes. Drainage velocity was studied as a function of surfactant concentration. This work is an extension of the previous work done on one surfactant with 2 ml of liquid added from the top. As a precaution the effect of the added dye on surface tension is also investigated.

The research work presented in this thesis has endeavoured to investigate the potential of five plant based natural surfactants with the goal of finding an alternative to synthetic ones.

## 1.2 Outline

The work presented in this thesis provides a pathway for the use of natural surfactants as an alternative to synthetic surfactants. Several aspects of sur-



face as well as foam properties of the natural and synthetic surfactants have been examined. The drainage characteristics of natural surfactant have also been investigated. The natural surfactants extracted have been characterized using different techniques. The thesis is organized as follows:

Chapter 2 provides the technical background for the thesis. It summarizes different research works related to the field. The background on surfactants and their applications, classifications, surface tension and its measurement, micelles, critical micelle concentration and its measurement are discussed. In addition, foam structure and applications, foaming ability, stability and drainage are also presented. Emulsions with applications, surfactant as emulsifiers, surface wetting, environmental effects of surfactants, natural surfactants and its applications are discussed. Finally, plants used to obtain natural surfactant are described.

Chapter 3 gives the details of experimental techniques and procedures such as Wilhelmy Plate method for surface tension, pH, conductivity and viscosity measurements. The experimental procedures for emulsification, wetting, cleaning, dirt dispersion, two dimensional drainage in Hele's Shaw cell are also described. The experimental procedures and techniques for characterization of the natural surfactants used in the work are also discussed. The details of the materials (natural and synthetic surfactants) and extraction of the natural surfactant used in this work are also reported.

Chapter 4 describes the measurements of surface and foam characteristics of the surfactants such as surface tension, surface wetting, emulsification, pH and conductivity, viscosity and cleaning.

Chapter 5 describes quantification of the dirt present in the foam and

provides a new approach to measure the CMC of the surfactants. This is the first report on quantification of dirt in foam. The results obtained from dirt dispersion measurements are compared with surface tension measurements.

Chapter 6 describes the preliminary characterization of the plant based natural surfactants using different techniques. The results are discussed.

Chapter 7 presents the results of two-dimensional one shot drainage in natural surfactant systems *Sapindus mukorossi* and *Acacia concinna*. The analysis and explanations regarding the type of flow of the liquid in vertical and horizontal directions are given. This chapter also attempts to provide explanations for the results obtained, in the light of other works and theories. The results are compared with the results for synthetic systems.

Chapter 8 provides the overall summary of the thesis and the potential avenues for further work.

The letters of identification and authentication of parts of the plant are provided in the Appendix. The publications related to the thesis are placed at the end. Copies of the certificates of conference presentations made during the Ph.D. programme are also provided.

# Chapter 2

## Literature Review

The main motivation of the present study is to search for potential natural plant based surfactants having good surface and foam properties. This chapter describes the fundamental theory and a literature review describing surfactants, it's applications and types. Then I describe surface tension measurement, critical micelle concentrations, foams, emulsions, surface wetting, natural surfactants (saponins). The chapter ends with a description of the plants used in this study to obtain natural surfactants. Reviews on environmental effects of surfactants have also been reported.

### 2.1 Surfactants

Surfactants are a class of amphiphilic molecules consisting of two distinctly different parts; an ionic or dipolar hydrophilic head and a polar hydrophobic tail covalently bounded with one another. The head is soluble in water. The polar tail is insoluble in water but soluble in oil and other non-polar solvents.

The presence of these two parts gives these molecules their unique properties [37]. The hydrophobic part consists of hydrocarbon/fluorocarbon/siloxane chains and can be branched or linear consisting of 8-18 carbon atoms. The hydrophilic head may be ionic or non-ionic.

At a low concentration, surfactants adsorb on the surfaces or interface of the system and alter the surface or interfacial free energy. The minimum amount of work required to create an interface is the interfacial free energy. When the surfactant is added to water, the hydrogen bonds are disrupted by the hydrophobic group in the interior of water increasing the free energy of the system. This leads to concentration of the surfactant molecules on the surface as less work is required to bring a surfactant molecule than a water molecule to the surface. Thus the surface tension gets reduced.

The presence of hydrophilic group prevents the surfactant from being expelled completely from water. The surfactant molecules pack together and orient at the interface with the hydrophilic group in water and hydrophobic group away from water. They form a single molecule layer called a monolayer [38].

Minimization of free energy is also achieved in the bulk by another mechanism that comes into play above a particular concentration. The surfactant molecules organize themselves in structures wherein the hydrophobic groups face one another and the hydrophilic groups face the water forming clusters called micelles. The concentration at which micelles appear in the solution is termed critical micelle concentration (CMC) [39]. After the CMC is achieved, the increase in concentration only adds to the formation of more and bigger micelles.

The adsorption of surfactant molecules at an interface provides an expanding force against the interfacial tension. This lowers the interfacial tension. The lowering of interfacial tension is illustrated by the Gibbs adsorption equation for a binary isothermal system

$$\Gamma_s = -(1/RT)(d\gamma/\ln C_s) \quad (2.1)$$

where  $\Gamma_s$  is the surface excess of surfactant solution,  $C_s$  is the surfactant solution concentration and  $\gamma$  is the surface or interfacial tension,  $R$  is the universal gas constant and  $T$  is the absolute temperature. The above equation can be applied to dilute surfactant solutions forming a monolayer. The area per adsorbed molecule  $a_s$  is given by

$$a_s = 1/(N_A\Gamma_s) \quad (2.2)$$

where  $N_A$  is Avogadro's number [2].

The mechanism of action of a surfactant includes roll-up mechanism, emulsification and solubilization as shown in Figure 2.1. In roll-up mechanism, the surfactant lowers the oil/solution and fabric/solution interfacial tensions and removes the stain out of the fabric. During emulsification the surfactant molecules decrease the oil/solution interfacial tensions and emulsifies the oil droplets. The solubilization mechanism involves the interaction of the micelles of a surfactant in water with the dirt, which spontaneously dissolves to form a stable and clear solution. Thus the surfactants, by lowering the interfacial tension between two interfaces such as air-water, water/stain,

stain/fabric etc. play a vital role in entrapping the oil phase. Due to the lower surface tension of the surfactant solution, the oil/dirt/grease gets removed or lifted up in water forming emulsions. The hydrophilic head remains in water and pulls the oil towards water. The oil thus gets removed when rinsed with water [40].

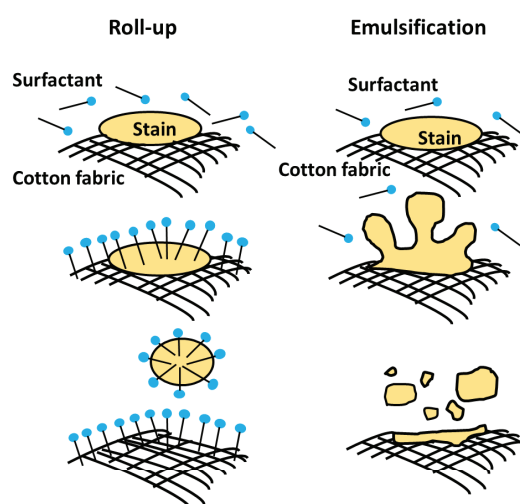


Figure 2.1: Mechanism of stain removal from fabric by surfactant.

### 2.1.1 Application of Surfactants

Surfactants have a large range of applications related to chemical, biochemical, pharmaceutical and other industries. This includes detergents, paints, paper coatings, dyestuff, personal care products, fibres, softeners, inks, flotation, enhanced oil recovery and separation processes [1]. Surfactants are used as lubricating agents. In pharmaceutical industry surfactants are used as enhancers for precutaneous absorption by disordering the lipid layer and denaturing keratin [41]. Surfactants are also used as flocculating agents

[42], in respiratory distress therapy [43], in hard gelatine capsules [44], as lubricating agents for the removal of ear wax [45].

Every sector of industry uses surfactants as an important class of industrial chemicals. The worldwide production of surfactants is around 12.5 million tonnes per year, growing at a rate of about 0.5 million tonnes per year. The consumption of surfactant as household detergents is about 60%, 30% in industrial and technical applications, 7% in industrial and institutional cleaning and 3% in personal care products. Asia accounts for the largest global detergent consumption of 33% [19].

### 2.1.2 Classification of surfactants

Surfactants can be classified into four main divisions according to the composition of the head group as given in Figure 2.2 [46].

#### Anionic Surfactants

The most commonly used surfactants are anionic surfactants which accounts for approximately 50% of worldwide production. They dissociate into an amphiphilic anion and a cation when dissolved in water. The head group is negatively charged whereas the counter ion is positively charged. The cation generally consist of an alkali metal like  $\text{Na}^+$  and  $\text{K}^+$  or a quaternary ammonium [46]. The commonly used surfactants include alkyl benzenesulphonates, alkyl sulphates, sodium dodecyl sulphate, ether sulphates, lignin sulphonates etc. [47]. The molecular structure of sodium dodecyl sulphate is shown in Figure 2.3(a). They are usually used in cleaning formulations.

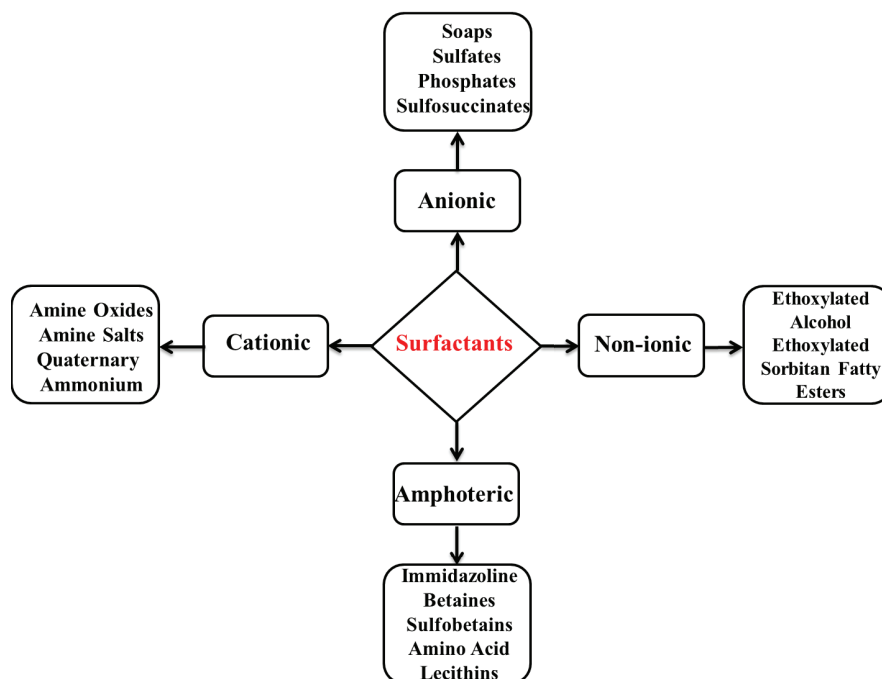


Figure 2.2: Classification of surfactants.

### Non-ionic Surfactants

The second most commonly used surfactants are the non-ionic surfactants which account for 43% of the world's production [47]. These surfactants do not ionize when dissolved in water. The head group does not have a charge. The hydrophilic moieties comprise of alcohol, phenol, ether, ester or amide coming from naturally-occurring fatty acids. The hydrophobic moieties are alkyl or alkylbenzene type [46]. Non-ionic surfactants include ethoxylated alcohols, ethoxylated amines, ethoxylated acids, ethoxylated esters, polysorbates, alkyl polyglycosides etc [48]. The molecular structure of surfactant n-dodecyl-hexaethylene oxide is illustrated in Figure 2.3(b). These surfactants are used in low temperature detergency as wetting agents and emulsifiers. The present work deals with plant based non-ionic natural surfactants.



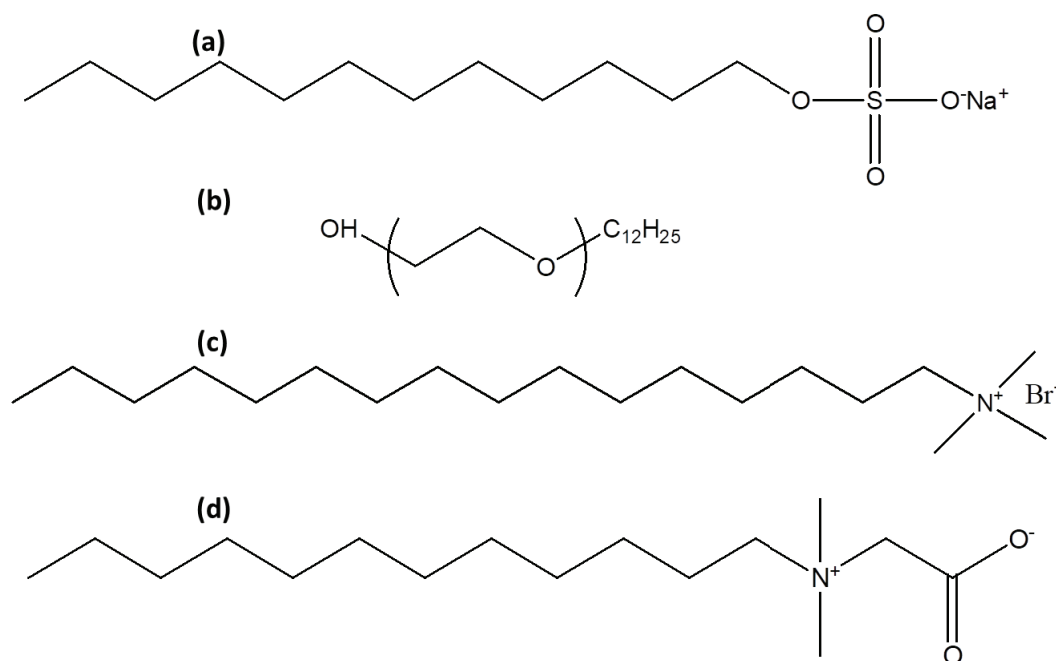


Figure 2.3: The molecular structure of (a) sodium dodecyl sulphate (b) n-dodecyl-hexaethylene oxide (c) cetyl trimethylammonium bromide (d) N,N-dimethyl-N-dodecylglycine dodecylbetaine.

### Cationic Surfactants

Cationic surfactants dissociate into an amphiphilic cation and an anion when dissolved in water. The head group is positively charged whereas the counter ion is negatively charged. These surfactants include cetyl trimethyl ammonium bromide, alkyl quaternary ammonium salts, benzylalkyldimethyl ammonium salts, amidoamine quaternaries etc [48]. The molecular structure of cetyl trimethylammonium bromide is shown in Figure 2.3(c). These surfactants have commercial importance in corrosion inhibition, flotation collectors for mineral ores, fabric softeners, hair conditioners etc [38, 46].

### **Amphoteric or Zwitterionic Surfactants**

These surfactants exhibit both anionic and cationic dissociation properties as the head group comprises of both positive and negative charges. The pH determines which group dominates. They are anionic at alkaline pH and cationic at acidic pH. They are used in pharmaceuticals, cosmetics, baby shampoos where biological compatibility and low toxicity is of utmost importance [48]. These surfactants have good dermatological properties and cause less irritation to the skin. These include N,N-dimethyl-N-dodecylglycine dodecylbetaine, alkylamino acids, alkylbetaines, alkylaminobetaines, imidazoline-derived amphoterics and sulfobetaines etc [46]. Figure 2.3(d) shows the molecular structure of N,N-dimethyl-N-dodecylglycine dodecylbetaine.

### **2.1.3 Surface Tension**

Surface tension/ surface free energy is the work required to increase the surface area isothermally and reversibly per unit area. The forces responsible for attraction of molecules in a liquid are dispersion, hydrogen bonding, dipole-dipole and dipole-induced-dipole forces. In the bulk liquid, a molecule experiences the same attractive and repulsive forces in all directions whereas these forces are lacking in one direction for the molecule at the surface. This asymmetry results in surface energy or surface tension [29]. The surface has a tendency to contract spontaneously minimizing the surface area. Gas bubbles and rain drops tend to adopt a spherical shape reducing the total surface free energy. The surface tension can also be defined as the contracting force per unit length around a surface. It is the work required to expand

a surface against the contracting forces which increases the surface energy accompanying this expansion. Work done ( $W$ ) to increase the surface area by  $\Delta A$  is given as

$$W = \gamma \times \Delta A \quad (2.3)$$

Surface tension can also be expressed as surface energy per unit area [2]. The surface tension between water and air is 72 mN/m or dynes/cm. The more polar the compound, higher is the surface tension due to strong intermolecular interactions. Surface tension is the measure of the difference in nature of the two phases (namely gas and air) meeting at that surface [1]. Surfactant concentration is responsible for decrease in surface tension and influences properties like foaming, spreading, emulsification etc.

#### 2.1.4 Surface Tension Measurement

Surface tension is measured using various techniques like Wilhelmy Plate, du Nouy Ring, Pendant drop, Maximum bubble pressure etc. Different measurement techniques are employed depending on the purpose and the type of experiments performed. Some commonly used techniques are described below.

##### **Wilhelmy Plate Method**

Wilhelmy plate uses a microbalance for direct measurement of surface tension. A vertical thin plate made of platinum, glass, mica or filter paper serves as a Wilhelmy plate. The plate is held in a fixed position dipping into the horizontal surface of the liquid. The vertical force  $F$  required to lift the plate

from the air-water interface is measured using the microbalance. The surface tension  $\gamma$  can be calculated by the equation

$$\gamma = F/(L \cos \theta) \quad (2.4)$$

where  $F$  is the force on the plate,  $L$  the plate perimeter and  $\theta$  the contact angle. Assuming  $\theta$  to be zero, equation (1.4) becomes

$$\gamma = F/L \quad (2.5)$$

For static measurements, the plate is kept in contact with liquid during the complete cycle of measurement. In the detachment mode, the force required to separate the plate from the interface is measured [49]. The present work uses this technique to measure surface tension.

### **Pendant Drop Method**

The technique uses the shape of the drop to determine the parameters necessary for surface tension measurement. The stability of the hanging drop depends on its shape. The surface tension can be determined by

$$\gamma = \Delta G \rho r_0^2 / f(V/r_0^3) \quad (2.6)$$

where  $V$  is the volume of the pendant drop,  $G$  the gravitational constant,  $\Delta\rho$  the density difference between liquid and gaseous medium, and  $r_0$  the radius of the capillary tip.  $f(V/r_0^3)$  is a functional relationship dependent on  $V/r_0^3$  [50].

**du Nouy Ring Method**

In this technique, a platinum ring is submerged under the surface of the liquid. The ring is then lifted up along with the meniscus of the liquid. The maximum force required to raise the ring until the meniscus breaks is measured by a balance [51]. The force required to lift a platinum du Nouy ring of wire radius  $R_W$  and ring radius  $R_R$  from the solution surface is given by [50]

$$\gamma = PF/(4\pi R_R) \quad (2.7)$$

where  $\gamma$  is the surface tension,  $P$  the force necessary to detach the ring from the solution surface, and  $V$  the volume of solution displaced by the pull of the ring.  $F$  is the Harkins-Jordan correction factor given by

$$F = f(R_R/R_W, R_R/V) \quad (2.8)$$

**Maximum Bubble Pressure Method**

In this technique air is blown through a thin capillary into the solution for which the surface tension is to be measured. Due to the blowing of air, bubbles are formed at the opening of the capillary. Maximum value of the pressure is obtained when the bubble radius equals the capillary radius. Using the Young-Laplace equation the surface tension can then be determined.

$$\gamma = \Delta P \times R/2 \quad (2.9)$$

where  $\Delta P$  is the pressure difference between the gas bubble and the liquid

and  $R$  is the radius of the bubble [52].

### 2.1.5 Micelles and Critical Micelle Concentration

Surfactants distort the structure of water by breaking the hydrogen bond and increasing the free energy. This distortion leads to more adsorption of surfactant molecules at air-water interface resulting in decrease of surface tension. As the concentration of the surfactant is increased, the surfactant molecules form micelles with hydrophilic head towards water and hydrophobic tails inside. The word micelle was coined by J. W. McBain in 1920 to describe colloidal sized particles of soaps and detergents [53].

Thus micelle formation is a spontaneous process which results from attainment of a minimum free energy state. Increase of entropy is central driving force for micelle formation. This occurs when the hydrophobic part of the surfactants get removed from water and the ordered structure of water molecules around this region of the molecule is lost [54]. The diameter of micelle is about 2 to 3 nm due to which it is not visible under light microscope. In a micelle there are approximately 60 to 100 surfactant molecules [55]. It can be seen from nuclear magnetic resonance [56] and ultrasonic measurements that the rate constant for the disassociation of a micelle to a monomer is  $10^{-2}$  to  $10^{-9}$  seconds<sup>-1</sup>. The length of hydrocarbon chain, dissociation degree, aggregation numbers and additives are responsible for the life time of a micelle. Micelles are complex dynamic structures which are continuously being formed as well as broken down in solution.

Micelle formation is an important property of the surfactant as phenom-

ena like detergency and solubilization depend on its existence [1, 39]. After CMC is attained any added surfactant contributes to the formation of more or bigger micelles. The schematic diagram of the behaviour of surface tension with concentration is illustrated in Figure 2.4.

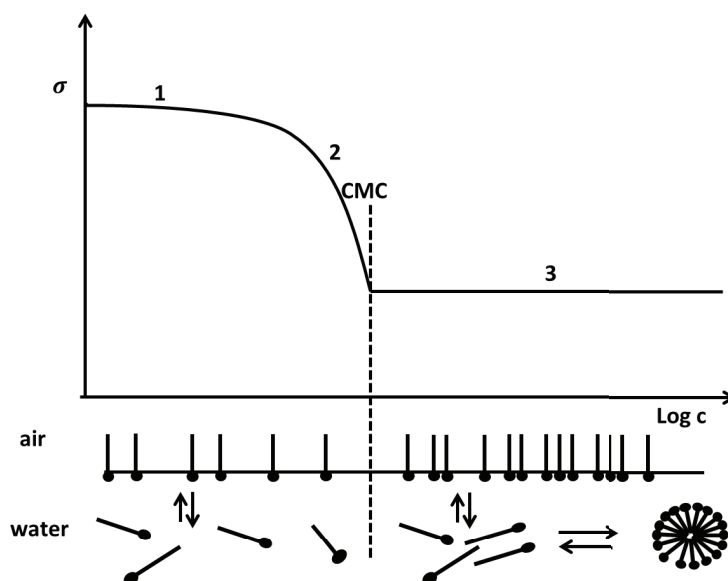


Figure 2.4: Schematic representation of surface tension with concentration.

The efficiency of a surfactant is monitored by measuring the CMC. A lower CMC suggests that the surfactant is more efficient. CMC is considered to be a fingerprint evidence of micellization [57]. The chemical properties of surfactant vary above and below the CMC. CMC is important in different industries. Surfactant must be present at higher concentration than CMC as surface tension reduction, foaming or emulsification can be achieved only when a significant number of micelles are present. CMC is also important as above this value maximum surfactant absorption takes place. Below CMC, the physico-chemical properties like conductivity, electromotive force of ionic surfactants exhibit the properties of strong electrolyte. Above CMC, these

properties change drastically. Various techniques like surface tension, optical turbidity, electric conductivity, osmotic coefficient, density, sound velocity, diffusion, viscosity, refractive index, solubilization and ultra centrifugal sedimentation are employed to measure CMC. CMC of a surfactant can be determined from the inflection point of any physico-chemical property of the solution against concentration [2]. At CMC the physico-chemical properties change over a narrow concentration range [1] as illustrated in Figure 2.5.

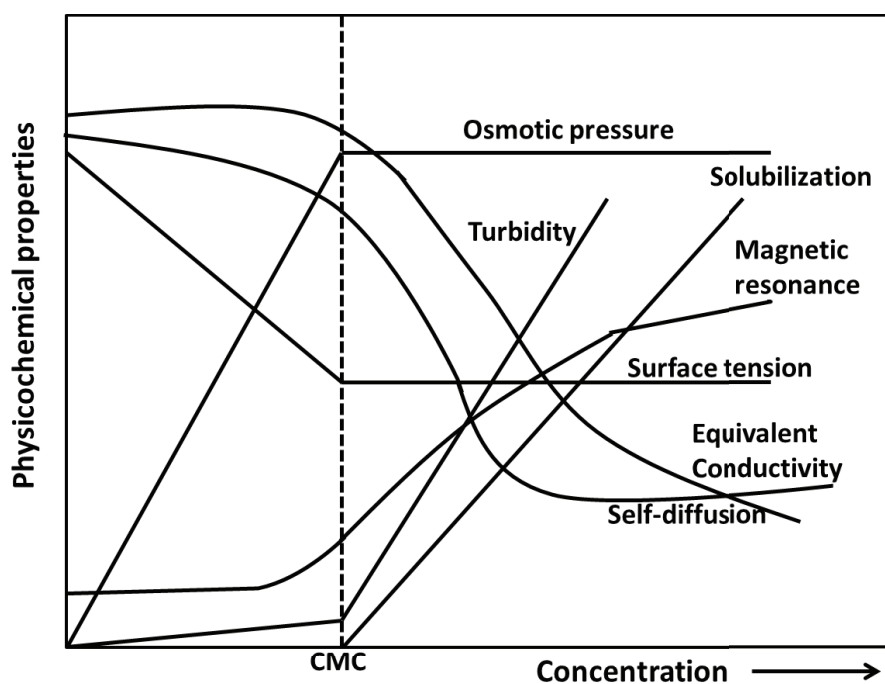


Figure 2.5: Variation of physical properties with surfactant concentration.

The various factors on which CMC of a surfactant depends are length of hydrocarbon chain, number of double bonds, charge of the polar head group, presence of additives in the solution like salt or alcohols, temperature, pH and pressure [58]. As the hydrophobic character (the number of carbon atoms) of the amphiphile increases, the CMC decreases. An increase in



number of double bonds increases the CMC. Non-ionic surfactants have a much lower CMC. The CMC decreases with increase in temperature to a minimum and then it increases. In a surfactant based formulation, salts are added to control viscosity, stability, appearance and consistency. The CMC of ionic surfactants are significantly lowered by the addition of salt. For non-ionic surfactants, the effect of salt is small. Addition of alcohols also lowers the CMC in a significant way [59].

### 2.1.6 Methods of Estimating CMC

The different methods of estimating the CMC of a surfactant solution are described below.

#### Surface Tension

CMC is best estimated from the surface tension isotherm. Initial increase in surfactant concentration leads to more adsorption to the surface resulting in surface tension reduction. Beyond CMC, the surface gets saturated with adsorbed surfactants and additional surfactants contribute to micelle formation. Hence surface tension becomes constant. This break in the surface tension isotherm is the point of micellisation or CMC [38].

#### Conductivity

This method of CMC estimation is suitable for ionic surfactants. The equivalent conductivity of surfactant solution as a function of the square root of concentration decreases slightly in the pre-micellar region like any conven-

tional electrolyte. Beyond CMC, a large decrease is seen due to incomplete dissociation of the surfactants present in micellar form. This discontinuity can be used to determine the CMC [38].

### **Colorimetric Technique**

This technique is based on solubilization of oil-soluble dye. The solubility of a normal solvent-insoluble compound is studied against the surfactant concentration. The solubility is low and constant at low concentrations but after a certain concentration it increases abruptly. The point at which the solubility increases abruptly corresponds to CMC [60].

### **Dye Micellization Method**

This method studies the variation of absorbance of dye-surfactant solution with concentration. At low concentrations, the absorption is small. The absorbance increases suddenly at a higher concentration. After this the absorbance curve flattens as most of the dye shifts to the micelle, depleting the dye phase. The portion near the inflection point is extrapolated to the point where absorbance matches that of the dye in absence of surfactant. This value is the CMC [61].

### **Fluorescence Probe Technique**

This technique uses a hydrophobic fluorescent dye such as pyrene and pyrene-3-carboxaldehyde which exhibits different fluorescence characteristics depending upon the properties of the solubilizing medium. These probes show different behaviour in micellar and non-micellar solutions. The change of be-

haviour with surfactant concentration is used to determine the CMC. Initially fluorescence is a constant with concentration and then decreases sharply. The concentration at which the break occurs is the CMC [62].

## 2.2 Foams

Foam is the result of non-equilibrium dispersion of gas in a liquid containing surface active substances. Random packing of bubbles in a relatively small amount of liquid results in the formation of foam. Production of foam is the result of introduction of air or other gases beneath the surface of a liquid that expands and encloses the gas within a liquid film. Pure liquids do not foam as gas bubbles introduced rupture immediately on contact with each other or escape very fast from the liquid.

Formation of foam requires solutes that absorb at the liquid gas interface. A surfactant added to the liquid prevents foam rupture by absorbing at the air water interface, or by reducing drainage of the liquid from the foam lamellae. Thus for the formation and stability of foam, surfactants play a vital role [38]. Foam has important applications in personal and house-hold products, enhanced oil recovery, food industry, washing, fire fighting, separating, isolating and other applications. It is common in soaps, detergents, food products like espresso coffee, chocolate mousse, meringues, beer etc. It is therefore essential to understand how foam is formed and how it changes with time.

Low density, high viscosity and large interfacial area are important characteristics of foam. Foam consists of honeycomb structure of gas cells sep-

arated by thin liquid films [1]. It behaves like a gas (volume is proportional to temperature and pressure), liquid (it can flow and fill a vessel) and solid (it can support small shears and bubble distortion takes place without rearrangement). Foams are thermodynamically unstable systems. It is a non-Newtonian fluid with a well-defined structure and can be opaque or transparent, soft or rigid and conducting or insulating. This complex nature of foam is due to the fact that it organizes at different length scales from the surfactants being absorbed at the gas-fluid interface to the interconnected fluid channels, bubbles and the sample. Properties of foam also depend on bubble diameter, liquid fraction, dimension and shape as well as chemical composition of the sample.

Formation of foam requires bubble production in a solution. The bubbles are produced by various processes, namely:

a) Nucleation: This can be achieved by foaming gas in liquid by rapid pressure drop; e.g. shaving foam flowing out of a pressurized can.

b) Gas entrainment: This includes massaging shampoo into hair, agitating laundry solution with hands, pouring solution from a height.

c) Direct introduction of gas into a liquid: This method is used for drinks, which release a burst of gas when the can is opened [11].

d) Direct bubbling of a gas into the surfactant solution (Bikerman's method): This is a reproducible and quantifiable process widely used to produce foam for studies and research [63].

Most foam that we are acquainted with is water based or aqueous foam (detergent foam, cosmetic foam, beer foam, fire retardant). There also exist non-aqueous foams like geological foam, metal foam, solid foam (foam rub-

ber, bath sponge), synthetic foam (flexible foam core, expandable foam fill), integral skin foam (arm rests, baby seats, shoe soles and mattresses) etc. Liquid foam is one of the examples of soft matter with a well-defined structure. Aqueous or liquid foam comprises of various sizes of gas bubbles separated by layers of liquid lamella of various thickness formed on a continuous liquid network [64]. In this work we have concentrated on aqueous foam.

### 2.2.1 Structure of Foam

A foam is a gas-liquid mixture which strongly depends on the liquid fraction ' $\phi$ ' defined as the volume ratio of liquid and foam given as

$$\phi = V_{liquid}/V_{foam} \quad (2.10)$$

Foams are classified as *wet* or *dry*, depending on the liquid fraction. Wet or *Kugelschaum* foam corresponds to a liquid fraction higher than 0.15 e.g. freshly poured beer. The bubbles appear like a packing of spheres as shown in Figure 2.6. Wet foams are stabilized by high viscosity and surface elasticity. Due to the presence of enough liquid the cell edges become rounded and there is no coalescence.

Due to gravity the liquid between the bubbles gradually flows down. Dry or *Polyederschaum* foam correspond to foam with liquid fraction less than 0.05 e.g. detergent foams. In dry foam gas bubbles are separated by thin liquid films. This results in polyhedral bubbles. The structure of foam was first described by Joseph Plateau. The polyhedral bubbles get arranged in such a way that three films meet symmetrically along a line at an angle of

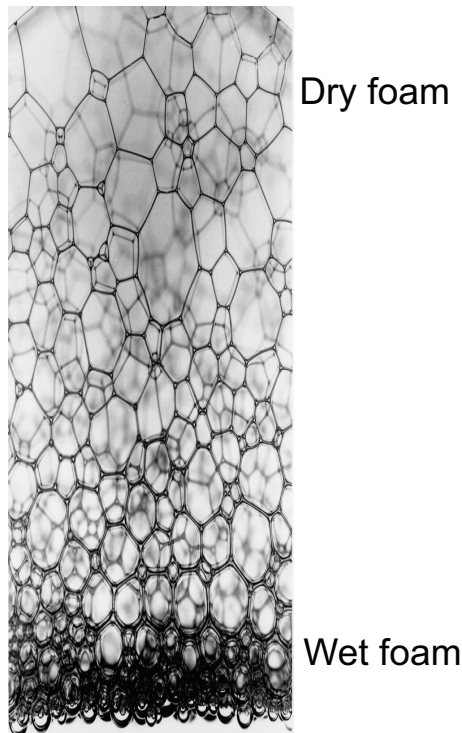


Figure 2.6: The structure of dry and wet foam.

$120^\circ$ . Four such lines meet at a vertex at the tetrahedral angle of  $104.97^\circ$  as shown in Figure 2.7. The thin films forming the faces of polyhedral bubbles are known as lamella. The lines of intersection of three films are called Plateau borders. The vertices where four Plateau borders meet are called nodes. The factors related to the components of foam include the density  $\rho$ , bulk viscosity of the liquid  $\eta$ , surface tension  $\gamma$ , surface viscosity  $\eta_s$  and the diffusivity of the gas [13].

### 2.2.2 Young-Laplace Equation

Young-Laplace equation governs the local equilibrium of a gas/liquid interface. It relates the pressure difference across the interface to the surface

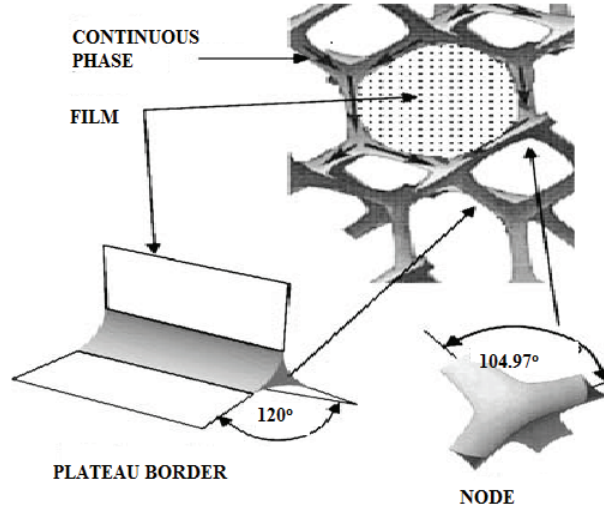


Figure 2.7: The structure and geometry of dry foam.

tension. Surfactants decrease the surface tension of water, which creates pressure difference across the curved surface of the bubble. The pressure outside the bubble is less than the pressure inside. The pressure difference for a spherical bubble of radius  $R$  is given by the Young-Laplace equation

$$\Delta P = P_G - P_L = 2\gamma/R \quad (2.11)$$

Here  $P_G$  and  $P_L$  are the pressures of the gas and liquid respectively. In case of bubbles having complex geometry, the two principal radii of curvature  $R_1$  and  $R_2$  have to be used in the equation.

$$\Delta P = \gamma(1/R_1 + 1/R_2) \quad (2.12)$$

Surface tension measurement techniques like pendant drop, spinning drop and maximum bubble-pressure use the Young-Laplace equation [65]. This

equation can also explain liquid drainage from lamellae into Plateau borders under the influence of gravity. The internal (Laplace) pressure of small bubbles provides the driving force for diffusion of gas through the lamellae into larger bubbles leading to phenomena like Ostwald ripening [66].

### 2.2.3 Foaming Ability and Stability

Foam producing power of surfactant solution is the ability of the surfactant solution to attain lower surface tension in a short time when new interface is being created [67]. It is the gas/air entrapment capacity of the surfactant solution. When the foam is being generated, surfactant monomers adsorb on the freshly created interface from the bulk solution. In case of low CMC the monomer gets depleted which results in breakdown of the micelles to provide additional monomers. Stable micelles in the solution cannot provide monomers quickly which results in higher dynamic surface tension and less foam. Disintegration of unstable micelles resupplies the depleted monomer and thus foaming is enhanced [68].

The foaming ability and stability of surfactant solution is dependent on the chemical composition and properties of the adsorbed surfactant molecules. It depends on rate of adsorption from solution to liquid/gas interface, rheology of the adsorbed surfactant layer, gaseous diffusion out of and into the bubble, bubble size, surface tension, bulk viscosity, presence of electrolyte, temperature and pressure [1].

The ability of the foam to sustain the gas for a long time to maintain bubble size, liquid content and foam volume is referred to as stability of foam.



The decay of foam is a measure of foam stability. As the bulk viscosity of the foaming solution and surface viscosity of the adsorbed surfactant layer at air-water interface increases, the foaming stability also increases. Stability of foam decreases in the presence of an electrolyte as the electrical repulsion between the ionic surfactant molecules at the interface decreases [69].

Surface elasticity and viscosity are responsible for foam stability. Drainage of the liquid from the foam lamella to Plateau border results in lower surfactant adsorption due to thinning of the film. This increases the surface tension and leads to surface contraction. The resulting surface tension gradient forces the liquid from a low tension region to a high tension region. The expansion arising due to gravity or capillarity is opposed by higher surface tension. Thus the loss of liquid between the interfaces is balanced by a counter flow of liquid. This surface tension driven liquid transport provides a resistive force to the thinning film and further thinning is prevented. This mechanism of foam stabilization is called Gibbs-Marangoni effect [65].

Foam undergoes self-destruction as its stability is affected by various processes. Three natural processes are responsible for stability of foam, namely:

a) Drainage: Liquid drainage is a natural phenomenon caused by gravity as well as surface pressure imbalance in foam lamellae and Plateau borders. Due to the draining liquid the foam bubbles approach each other. The spherical bubbles become polyhedral corresponding to a transition from wet to dry foam. The bubbles may collapse due to collision leading to film thinning and increased surface tension [67].

b) Ostwald Ripening: It is a process where larger droplets grow due to the diffusion of smaller droplets. Disproportion in bubble size causes gas mo-

lecules to diffuse from small bubbles to large ones. This causes growth of the bubble size with time at the expense of number of bubbles [70]. The pressure gradient may also arise due to lamella permeability which is dependent on the type of the surfactant, liquid and gas phases.

c) **Coalescence:** Due to the thinning of the foam film (dry foam), the film between two adjacent bubbles ruptures to form a single large bubble and this process is called coalescence. It is an extremely rapid process which is difficult to observe [71].

Thus foam can be stabilized by taking into account all these processes and controlling the thinning of the foam lamella. Stability of the foam also depends on particle size, shape, concentration and the type of surfactant [72]. The stability of foam increases by the presence of hydrophilic particles as they collect at the Plateau border and slow down drainage. These particles may also shield the foam bubbles and decrease the diffusion of gas, resulting in stable foam [67].

#### 2.2.4 Test for Foamability and Stability

The foaming ability and stability can be monitored by different techniques:

a) **Bartsch Test/Shaking Tube Method:** A known volume of liquid is taken in a tube of standard size and shaken in a standard way. The height of the resulting form is measured [73].

b) **Ross-Miles Method:** A fixed volume of surfactant solution is poured onto the bed of the same solution from a constant height. Foam volume is measured after the last drop has fallen [38].

c) **Bikerman's Method:** The Bikerman's technique quantifies the foaming ability and stability of a surfactant using a simple method. A known volume of the solution is taken in a cylindrical column and a gas is bubbled into it at a constant rate resulting in the production of foam. The foam produced accumulates into the column, with the fresh foam pushing up the older foams. As the foam column rises, the liquid in between the bubbles drains to the bottom until the foam breaks. When the rate of foam formation matches the rate of breakage of foam, a steady state is achieved. After reaching the steady state the gas flow is turned off. The maximum height attained by the foam is the foaming ability [63].

The stability of foam is determined by measuring the foam volume as a function of time. Foam stability is expressed as  $R5$  parameter, the ratio of foam height after 5 minutes to maximum foam height.

### 2.2.5 Drainage in Foams

Generation of foam results in an increase of Gibbs free energy of the system thus making it thermodynamically unstable. Foams are unstable dispersions by their nature and collapse given sufficient time. The rupture of the film is generally caused by thermal perturbations. When the liquid drains from lamella to the Plateau borders there is reduction in the thickness of the lamella. The liquid flows through the interconnected Plateau border network resulting in reduction of total liquid fraction with time. Drainage from the lamella to Plateau border can be understood by considering the Young-Laplace equation discussed earlier. Laplace's law states that reduc-

tion of radius of curvature increases the pressure. The radius of curvature of the Plateau border is much larger than that of the lamella which results in higher pressure in the lamella. This pressure difference creates a driving force. The liquid drains into the Plateau borders, this phenomenon is called Plateau border suction [74]. The rate of drainage depends not only on the size of the Plateau borders, gas/liquid interface properties which can be changed by the adsorbed surfactant molecules but also on the rate of internal foam destruction by bubble coalescence.

During drainage, the foam at the top is dry with polyhedral bubbles with thin edges while at the bottom is wet having spherical bubbles. Depending on the surface mobility parameters e.g. bubble size, interfacial properties etc., two drainage regimes have been observed, namely Poiseuille flow (channel dominated) or plug flow (node dominated), depending on the viscosity of the surfactant solution. Poiseuille flow is the flow of liquid in the channels with zero velocity at the boundaries. Plug flow is liquid flow with a uniform velocity throughout the cross section. This allows more liquid to flow through the Plateau borders [75].

The stability and other rheological properties of foam system are associated with drainage. This process has been extensively studied both experimentally and theoretically for various surfactants and for different gravitational and geometrical conditions [76]. The studies on foam drainage have industrial importance. Many technological properties of foam depend on the liquid fraction and rate of drainage [77].

Drainage can be studied under different conditions, namely free drainage, forced drainage and pulsed drainage. Free drainage is a naturally occurring

physical process in aqueous foams. The liquid present in freshly prepared foam drains immediately and the foam eventually attains an equilibrium state under gravity, viscosity and capillary pressure between adjacent bubbles. Many experiments were performed on free drainage in the middle of the 20th century.

Forced drainage can be achieved by continuously adding liquid at the top of a foam column. It is a steady flow of liquid through static foam. Forced drainage experiments were first performed by Leonard and Lemlich in 1965 [78]. Forced drainage has been extensively studied to compute dynamic and geometric parameters of foams [9].

Pulsed drainage is the flow of the liquid in foam column when the liquid is introduced at the top periodically [13]. It is the evolution of a small volume of liquid introduced into a foam with a very low liquid content. The injected liquid is pulled downwards by gravity and spread in all directions by capillarity [75].

Forced drainage experiments showed that the velocity  $v$  of injected liquid (drainage velocity) varied with  $Q$ , the rate of solution addition as a power law

$$v \sim Q^\beta \tag{2.13}$$

where  $\beta$  is an exponent ( $\sim 0.5$ ) [79]. Comparing forced drainage experiments in two dimensions with numerical simulations of drainage equation showed that the vertical movement of drainage wave was due to gravity and horizontal movement due to capillarity [13]. Foam drainage in two dimension with two inputs showed that along the vertical direction at the centre of the

two nozzles, the spreading speed is nearly constant for a fixed separation [77]. Simulations of two dimensional Poiseuille flow foam drainage with a narrow input in a rectangular Hele-Shaw cell under 8 different gravities (from 9.8 to 0  $m s^{-2}$ ) showed that the motion of drainage wave fronts in both horizontal and vertical directions were well described by the power law [80].

### 2.2.6 Foam Drainage Equation

Drainage in foam takes place through Plateau borders, the curved triangular channels of liquid separating the bubbles. Considering the continuity and the balance in pressure, the drainage equation can be written as

$$\frac{\partial \alpha}{\partial \tau} + \frac{\partial}{\partial \xi} \left( \alpha^2 - \frac{\sqrt{\alpha}}{2} \frac{\partial \alpha}{\partial \xi} \right) = 0 \quad (2.14)$$

This equation represents a continuity equation for a flow rate provided in brackets. The above equation is achieved by taking dimensionless coordinates corresponding to vertical position  $x$  (measured downwards) and time  $t$  by defining  $x = \xi x_0$  and  $t = \tau t_0$ . The units are defined by  $x_0 = \sqrt{\frac{C\gamma}{\rho g}}$  and  $t_0 = \frac{\eta^*}{\sqrt{C\gamma\rho g}}$ . Here the physical parameters are surface tension  $\gamma$ , liquid density  $\rho$ , acceleration due to gravity  $g$  and effective viscosity  $\eta^*$ . The constant  $C$  is given by  $C = \sqrt{\sqrt{3} - \frac{\pi}{2}}$  which is related to the triangular cross section of the Plateau borders. The area of cross section  $A$  of the Plateau border is reduced to dimensionless variable  $\alpha$  by scaling it as  $A = \alpha x_0^2$ . The liquid fraction is obtained by  $\phi_l = \frac{NA}{S}$  where  $N$  is the number of Plateau borders,  $S$  is the cross section of the tube and  $x_0^2$  is the capillary constant [81].

### Drainage Equation in Two Dimensions

Assuming that the liquid flows through the Plateau borders only, the Poiseuille flow drainage equation for two-dimension is given by

$$150\mu \frac{\partial A}{\partial t} + \rho g \frac{\partial A^2}{\partial z} - \frac{1}{3} C\gamma \nabla^2 A^{\frac{3}{2}} = 0 \quad (2.15)$$

where  $z$  and  $x$  are the vertical and horizontal coordinates. The differential operator is  $\nabla = (\frac{\partial}{\partial x}, \frac{\partial}{\partial z})$ .

The equation 2.15 can be written in terms of dimensionless quantities by introducing length scale as  $x_0 = 2^{7/12} 12^{-1/2} V_b^{1/3} = 0.433 V_b^{1/3}$ . Here the bubble volume,  $V_b = \frac{4\pi}{3} (\frac{d}{2})^3$  [82]. A dimensionless Plateau border area  $\alpha = A/x_0^2$  is chosen, so that the liquid fraction  $\phi_1$  becomes numerically equal to  $\alpha$ . The time scale is take as  $t_0 = 150\mu x_0 / (C\gamma)$ . The Bond number  $B_0 = \rho g x_0^2 / (C\gamma)$  is introduced to measure the importance of gravitational flow over surface tension [83]. Taking the vertical coordinates as  $\xi = z/x_0$  and horizontal as  $\eta = x/x_0$  respectively, we get

$$\frac{\partial \alpha}{\partial t} + \frac{\partial}{\partial \xi} (B_0 \alpha^2 - \frac{\sqrt{\alpha}}{2} \frac{\partial \alpha}{\partial \xi}) - \frac{\partial}{\partial \eta} (\frac{\sqrt{\alpha}}{2} \frac{\partial \alpha}{\partial \eta}) = 0 \quad (2.16)$$

Equation 2.16 represents the two dimensional drainage equation where the terms in parentheses are the flow rates along the vertical and horizontal directions [13].

### 2.2.7 Applications of Foam

- **Home, personal care products, food and beverages:** Foam is used by each and every individual at home in the form of toothpaste, shower gel, shampoo, shaving foam, whipped cream, hair mousse, cleaning products, detergents, coffee, beer, champagne, dessert mousse, bread, cake, ice cream, whipped cream etc. Foam makes the food soft and creates a sensation of lightness and creaminess. The high backscattering of light is associated with brightness of foam and thus cleanliness [1, 84].
- **Industries:** Foams used in various industries are outlined below:
  - a) **Fire fighting:** Fire caused by burning liquid cannot be extinguished by water due to fact that the burning liquid is generally lighter than water. Thus fire-fighting foam comes into application where it spreads on the surface of the burning liquid and spontaneously extinguishes the on-going fire as well as suppresses re-ignition. Fire fighting foam is generated by mechanical agitation of a dilute surfactant solution, water and air [85].
  - b) **Agriculture:** Surfactants are used for removing contamination from soil by solubilising the contamination in foam and helping microorganisms to degrade it [86].
  - c) **Petroleum extraction, removal of oil spills:** Recovery of petroleum is enhanced by using foam [87]. The oil spilled on sea water causes economic and environmental damage. Foams of polyurethanes are applied on oil spill to provide a neat method for clean-up [88].



d) Ore purification: Separation of metals is done using the process of flotation. Pulverized ore is mixed with a surfactant solution and is agitated to form foam. Bubbles along with the hydrophobic particles rises up to form foam while the hydrophilic part settles at the bottom. This process is carried out in various steps for enhanced recovery [89].

## 2.3 Emulsions

Emulsions are colloidal suspension of two or more immiscible liquids where one is dispersed as minute globules into the other, stabilized by emulsifiers. Emulsions have variety of applications including food emulsions like mayonnaise, butter salad creams, desserts and beverages; personal care and cosmetics, hand creams, lotions, hair sprays; pharmaceuticals like anaesthetics of O/W emulsions, lipid emulsions and latex emulsions. Emulsions are also used in polishes, pesticides and metal cutting oils. The process of mixing two liquids in order to prepare emulsion is known as emulsification [90]. Oil droplets dispersed in a continuous aqueous phase vary in shape and size depending on the composition and process conditions. Emulsions can be classified as either oil-in-water (O/W) where the dispersing medium is water and water-in-oil (W/O) type where the dispersing medium is oil. The type of emulsion formed depends on many factors like oil-water ratio, molecular structure and concentration of the surfactant, presence or absence of electrolytes, temperature and pressure [91].

The O/W emulsions are generally produced with hydrophilic surfactants while W/O are stabilized by surfactants that are more soluble in oil than in

water [92]. The ability of an emulsion to keep its properties unchanged over a period of time is referred to as emulsion stability. The stability of emulsion is dependent on a large number of factors including the nature of interfacial film, the viscosity of the continuous medium, oil-water ratio, droplet size distribution, temperature and presence of electrostatic or steric barriers on the droplet [1]. Emulsion properties as well as stability depend on many phenomena like creaming, coalescence, flocculation, Ostwald ripening etc. They are illustrated in Figure 2.8.

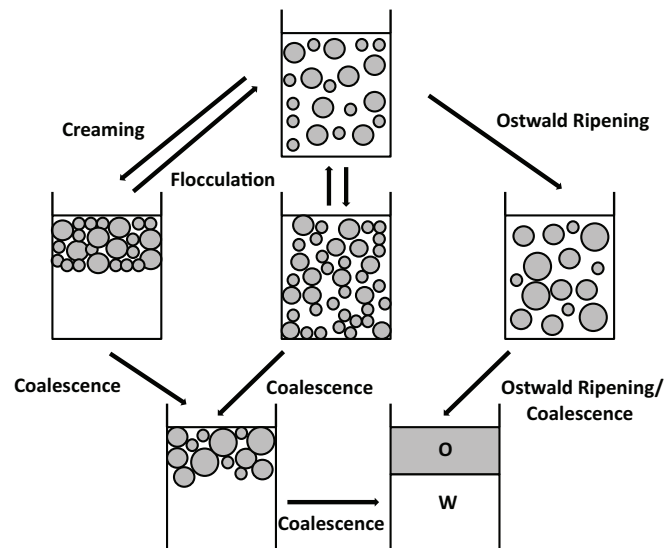


Figure 2.8: Mechanism involved in destability of emulsion.

*Creaming:* Droplets of emulsion differ in density from the continuous medium and move up or down through the continuous phase due to gravity. Droplets of lower densities move up to form a layer of emulsion droplets at the top known as creaming. Since the density of oil is lower than water, the droplets of O/W emulsions undergo creaming. Creaming can be reduced by reducing droplet size, minimizing density difference between the two phases

and increasing droplet concentration [93].

*Coalescence:* Emulsion droplets frequently collide with each other due to Brownian motion, gravity or mechanical agitation leading to aggregation. Coalescence is the merging of two or more droplets to form a single large droplet by rupture of the film separating them. This results in the formation of a layer of oil at the top of O/W emulsion [94]. It is an irreversible process. The driving force for coalescence is surface or film fluctuation which leads to closer approach of the droplets where the Van der Waals forces are strong to prevent separation. The rupture of film depends on the properties of the emulsifier absorbed at the droplets and also on the continuous phase properties. Prevention of droplet coalescence is an important factor in emulsion stabilization which can be achieved by reducing droplet contact and film rupture [17].

*Flocculation:* Aggregation of droplets as a result of Van der Waals attraction, without any change in primary droplet size is flocculation. It occurs when repulsive forces are insufficient to keep the droplets beyond the influence of Van der Waals attraction [95]. Flocculation is considered as an instability process which can be reversible (weak flocculation) or irreversible (strong flocculation) [96]. The creaming rate of the emulsion depends on flocculation. The presence of flocs increases the emulsion viscosity which may not be favourable for some food products [97]. Creating a network of flocs in emulsion is advantageous in modifying or controlling the texture of some products. For this an understanding of flocculation is important. The effective way to control the rate and extent of flocculation is to regulate the colloidal interactions like steric, electrostatic, hydrophobic, etc. between the

droplets.

*Ostwald Ripening:* The process of gradual growth of smaller to larger droplets due to mass transport of soluble dispersed phase through the continuous phase [98] is Ostwald ripening. Instability in food emulsion may be caused due to Ostwald ripening. It can be reduced by using emulsifiers that do not increase the oil solubility so that the bubble size remains small.

### 2.3.1 Surfactants as Emulsifying Agent

The ability to form emulsion is one of the important characteristics of a surfactant. Surfactants help to stabilize the emulsion by reducing the interfacial tension at oil-water interface. Due to their amphiphilic character, the surfactants have their hydrophilic moiety in water and hydrophobic moiety in oil. They replace the water and oil molecules at the original interface. This leads to reduction of interfacial energy as the direct contact between oil and water has been reduced [93].

When large amount of surfactant adsorbs at the interface, the interfacial tension is reduced and a barrier is formed by the surfactant molecules delaying the coalescence of droplets by electrostatic and/or steric repulsion. The formation of an emulsion requires input energy to disperse one liquid as droplets into the other liquid increasing interfacial area [91]. The time required by the surfactant to adsorb at the interface is important. The surfactant must quickly adsorb at the interface for the interfacial tension to be modified to facilitate droplet disruption and prevent coalescence. Low concentration of surfactant fails to provide a protective layer around the droplets

due to which the droplets tend to coalesce as they collide [93].

## 2.4 Surface Wetting

The phenomenon of spreading of a liquid droplet on a surface is known as wetting [99]. It involves one interface being replaced by another and also the interaction of a liquid with a solid. It helps to determine solid/liquid interactions and to characterize a surface. There are three types of wetting related to interface replacement namely spreading, immersional and adhesional [100]. Wetting is important for the removal of oil and dirt. It is controlled by surface tension, diffusion, concentration and composition of the surfactant solution and the nature of the surface to be wet [101]. It plays a vital role in industries such as froth flotation, oil recovery, surface cleaning, cosmetics and detergency [102]. Wetting of a surface depends on its contact angle, the angle between the solid-liquid and liquid-air interface. Complete wetting occurs when the contact angle is  $0^{\circ}$  and non-wetting occurs when the contact angle is  $180^{\circ}$ . Both are ideal cases, in actual situation the values lie between  $0^{\circ}$  and  $180^{\circ}$  [8]. Figure 2.9 illustrates a schematic representation of complete and partial wetting.

Wetting is directly associated with contact angle measurement as well as surface tension of the liquid. It can be enhanced using aqueous solutions of various surfactants. Surfactant molecules increase the rate of interfacial replacement by reducing the surface tension of water. The solution can easily penetrate and wet the surface. In addition, the wettability of surface increases due to adsorption of surfactant at the solid liquid interface which

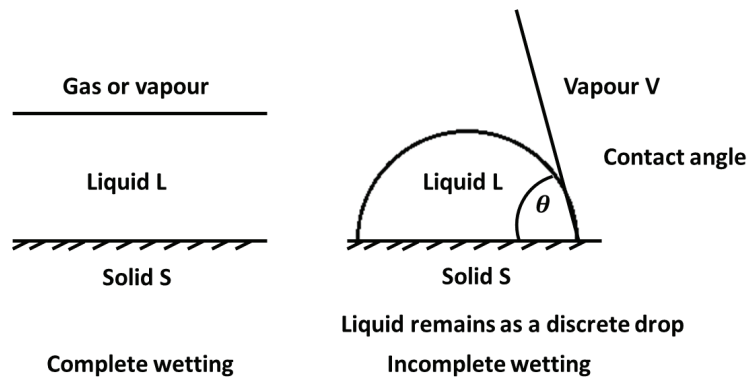


Figure 2.9: Schematic representation of complete and partial wetting.

reduces contact angle. Increase in wetting ability is important where complete contact of a solid surface with the liquid is required such as in textile industries where wetting of fibres is necessary for effective dyeing and cleaning [8].

## 2.5 Dirt Dispersion

The cleaning ability of a surfactant can also be studied by Dirt Dispersion (DD). It is the quantity of dirt that gets attracted to foam. The dirt that is present in the foam is difficult to rinse while cleaning and it may redeposit at the surface. The efficacy of a surfactant is defined in terms of DD. DD has been investigated by many workers only qualitatively by eye estimation [16].

## 2.6 Environmental Effects

The surfactants after use are disposed and dispersed to different sections of the environment. Surfactants enter the aquatic environment through wastewater discharges [103]. Thus either directly (wastewater discharges) or indirectly (contaminated rivers) the marine system receives almost continuous input of surfactants [104]. Poor degradation of surfactants based on alkylbenzenesulphonates cause the rivers and lakes receiving city waste waters to be covered with thick foams. This curtails photosynthesis and oxygen dissolution and cause ecological damage. Around 1965, environmental laws were passed in developed countries to restrict the use of alkylbenzene sulphonates, leading to the development of linear alkylbenzene sulphonates [19]. Phosphate content of surfactants cause eutrophication, a slow ageing process during which a lake, river, bay etc. deteriorates into a marsh and gets extinct. The important factor in eutrophication is the large growth of algae which consumes the dissolved oxygen from water and causes suffocation to fishes, other aquatic plants and animal life [105].

Studies on effects of surfactants on various aquatic organism, showed acute and chronic toxicities caused by synthetic surfactants [27, 106]. Linear alkylbenzene sulphonate, an anionic surfactant has toxic effect on aquatic faunas, floras in soil [107], growth and development of plankton [108] and aquatic life [109]. The filtering activity of oysters and mussels are inhibited by synthetic surfactants [26]. Toxicity of surfactants passes in animals through animal feeding and skin penetration. Higher concentration of surfactants in water lead to their penetration into the gills, blood, kidney, pan-

creas, gallbladder, liver and causes aquatic toxicity effect [110]. The toxic effects of seven surfactants on six fresh water microbes showed that cationic surfactants are more toxic than anionic and non-ionic surfactants [27]. The toxic effects of surfactants on humans, aquatic plants, microorganisms, invertebrates and crustaceans also follow a similar trend [111]. Problems arise in the reproductive systems of fish grown in surfactant contaminated waters [112].

High surfactant content in water affects the growth of algae and other microorganisms which results in decreased productivity of water bodies thereby affecting the food chain. Toxic metabolites of surfactants in waste-water and digested sludge cause many problems. Surfactants cause health hazards like dermatitis, respiratory irritation, eye irritation etc. [113]. Sodium dodecyl benzene sulfonate when absorbed through the skin results in damage of liver and it is carcinogenic [114].

In spite of these problems, environmental hazard causing surfactants are excessively used and get deposited on land and water systems [115]. With regard to the effects of surfactants on the environment, it becomes necessary to search for a suitable alternative to overcome these problems. One of the alternatives could be natural surfactants.

## 2.7 Natural Surfactants

Naturally available substances present in plants and animals, and fatty acid esters of sugars and amides which help to reduce surface tension are called natural surfactants [30, 116]. Potential advantages of these surfactants are



biodegradability, lower toxicity, biocompatibility and low cost. The natural surfactants are effective at extreme conditions like temperature, pH and salinity [117]. The major class of surfactants obtained from nature includes oleochemical surfactants, microbial surfactants and plant based surfactants. The oleochemical surfactants are obtained from plant oils (like palm oil, coconut oil) and animal fats like fish oil, tallow etc by suitable chemical reaction. Microbial surfactants commonly known as biosurfactants are produced by yeast, bacteria and fungi. Biosurfactants are ionic as well as non-ionic having antibacterial and antiviral properties. Plant based surfactants are called saponins which comes from the latin word *sapo* which means soap. Saponins are non-ionic in nature. Its name comes from its ability to form stable foams in aqueous solutions [118]. This work is based on studies on saponins.

Saponins are non-volatile naturally occurring surface active glycosides with high molecular weight consisting of one or more sugar chains connected to a triterpene (C30) or a steroid (C27) aglycone backbone. The non-sugar part (aglycone) of the saponin is known as the sapogenin. The combination of hydrophobic (fat soluble) sapogenin with a hydrophilic (water-soluble) sugar part makes a saponin a surfactant. Foaming is an important property used in identification and quantification of saponin containing plant species. Saponins reduce the surface tension of water and give stable foams. According to the structure of sapogenin, the saponins are divided into two major classes namely (1) triterpenoid and (2) steroid as shown in Figure 2.10.

Depending on the number of sugar chains, saponins are classified as monodesmosidic or bidesmosidic. Monodesmosidic saponins consist of a

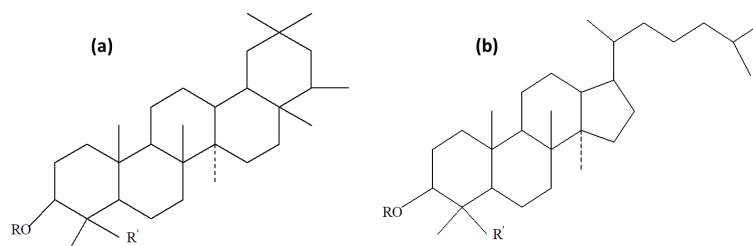


Figure 2.10: Structures of (a) triterpenoid (b) steroid sapogenins.

single sugar chain generally attached at C-3. Bidesmosidic saponins comprises of two sugar chains one attached through an ether linkage at C-3 and the other attached through an ester linkage at C-28 (triterpene saponin) or an ether linkage at C-26 (furanol saponins) [119]. The sugar chains are generally galactose, glucose, glucuronic acid, methylpentose, xylose and rhamnose [120]. Large number of functional groups like (-OH, -COOH, -CH<sub>3</sub>) are present in both steroidal and triterpene sapogenins.

Saponin is present in large number of plants. Some lower marine organisms like sea cucumbers use it as a defence. The commonly eaten plants containing saponin are soyabeans, chickpea, peanuts and spinach [121]. Triterpenoid saponins are found in beans, soyabeans, peas, sugar beet, spinach, quinoa, tea whereas steroidal saponins are found in oats, capsicum, aubergine, tomato, potato, onion, garlic and asparagus [122]. Saponin concentrations in these products range from 0.1 to 2% in dry matter [123]. They are bitter in taste and cause throat irritation. Many plant drugs and folk medicines contain saponin [124] which are weakly acidic due to the hydrolysis of glycosides [125]. Water and alcohols like methanol and ethanol are the most common extraction solvents for saponins.

### 2.7.1 Saponins as Surfactants and Emulsifiers

Saponins are surface active compounds having detergent, wetting, foaming and emulsifying properties, due to their amphiphilic nature [126]. The foaming property of saponin is due to the combination of the non-polar sapogenin and water soluble side chain, a structure similar to most synthetic surfactants having hydrophilic and lipophilic parts. The lipophilic part may consist of steroidal or triterpene structure while the hydrophile consist of sugar chain differing in length, branching, substitution and composition (glucose, galactose, rhamnose, arabinose, xylose, apiose and uronic acid) making it a non-ionic surfactant. The best foaming characteristics are exhibited by one sugar chain saponins. As the number of sugar chains (two or three) increases the foaming decreases.

The emulsifying properties of saponin are not affected by alkaline or acidic conditions due to their non-ionic nature. Saponins form micelle-like aggregates when mixed with water [127]. An abrupt change in many physical properties is observed when the concentration reaches the CMC, micelles are formed. The micelle forming property as well as the number of monomers in a micelle is affected by temperature, pH and salt concentration. CMC increases with temperature and pH while it decreases with salt concentration. Surface activity and emulsion stability is strongly influenced by the presence and location of carboxylic acid in the saponin molecule [128].

### 2.7.2 Applications of Saponin

Saponins exhibit a variety of useful biological properties such as antioxidant, antimicrobial, anticarcinogenic, antidiarrheal, anticoagulant, antiinflammatory, antiulcerogenic, antioxytoxic, immunostimulant. They exhibit other properties like hypocholesterolemic, neuroprotective anticoagulant, hepatoprotective, hypoglycemic, antiallergic, antihepatotoxic, antifungal, antiviral, cytotoxic, inhibition of dental caries and platelet aggregation [122, 129]. Saponins are also useful in diabetic retinopathy and reproduction. The antimicrobial property of saponins provides a defense system to inhibit mould and to protect plants from insects [130]. Physicochemical and biological properties of saponins have led to large number of applications in food, cosmetics, agriculture products and pharmaceuticals. The market demand for saponins has increased in recent years due to its natural sources as well as biological activities. Being natural non-ionic surfactants they have widespread use as detergent, foaming and emulsifying agents [131]. Saponins are being used as natural surfactants in personal care products like shower gels, liquid soaps, hair conditioner, mouth washes and toothpastes [132]. Saponins have also been marketed as bioactive ingredients in cosmetic formulations [133] and prevention of acne [134].

In addition to surface activity, they are used as feed additives [135], vegetable and bacterial growth regulators [136] and also for soil remediation [137]. The commercial sources of saponins include soap bark tree (*Quillaja saponaria*), horse chestnut (*Aesculus hippocastanum*) soapwort (*Saponaria officinalis*) and Mohave yucca (*Yucca schidigera*) extracts [131] while tea

seeds have also been investigated [135]. The concentration of saponin in *Quillaja saponaria* and *Yucca schidigera* are very high reaching 10% of dry matter. The extracts of Quillaja are used for food, beverages as well as an emulsifier due to its foaming properties. They are also used in ore separation, photographic emulsions, cosmetics and shampoos [127].

Saponins are also used as health beneficial food components due to their anticancer and cholesterol lowering properties, e.g. onion, garlic, soyabean etc [127]. Pharmaceutical application of saponin include immunological adjuvants [138], active ingredients in natural health products [131] and as a raw material for hormone production [129]. The triterpene type saponin is patented as an effective component for fire-fighting foams in United States [139]. Thus saponin, a natural surfactant, causes lesser environmental burden in addition to its varied applications in food, agriculture, cosmetics and pharmaceutical industries leading to extraction and identification of saponin in different plant species.

## 2.8 Plants Used in this Study

Natural surfactants have thus gained importance due to economical, health and environmental aspects. Due to the enormous application of saponin in various fields, a study was conducted to evaluate saponin as natural surfactants for its surface active properties from the regions of Sikkim and West Bengal. Saponin extracted from five different plants were studied and are described in detail below.

### 2.8.1 *Sapindus mukorossi* (Ritha)

*Sapindus mukorossi* (Ritha or soapnut) is a deciduous tree growing in tropical and sub-tropical Asia [140]. It belongs to *Sapindaceae* family. The fruit is traditionally used as a shampoo, to clean woollen fabrics and to restore the brightness of precious ornaments. It is known for antimicrobial property and is used for treatment of common cold, pimples, constipation, nausea, migraine, epilepsy, chlorosis, eczema, psoriasis and gonorrhoea [140]. It has been used for the development of spermicides [141] as well as for the formulation of contraceptive cream [142]. It can be used in oil recovery, in contaminated soil washing [143, 144], solubilization of foreign materials present in muga silk [145], for biodiesel production etc [146]. Antibacterial and antifungal properties of the extract make it a potential candidate to cure dental caries [147]. The saponin has been classified as non-toxic and non-dermal irritation by the toxicological test on rats and rabbits [148]. It has also been reported that external use of saponin in washing has no toxic effects on human eyes and skin [137]. Large number of studies on *Sapindus mukorossi* have dealt with extraction, isolation and identification of saponin [149, 150, 151, 152] but very few investigations have focussed on the surfactant activity of this plant [24, 36, 117, 153].

### 2.8.2 *Albizia procera* (Seto Siris)

*Albizia procera* (Seto Siris or White Siris) is a medium sized deciduous tree which grows in moist deciduous and semi evergreen hill and swamp forest of sub-Himalayan tracts, Gujarat, South India and Andamans. It belongs to

the family *Fabaceae*. It has been used for hedges, street trees and also as animal feed. This plant is traditionally used as anticancer agent [154] and in the treatment of pain, convulsions, delirium and septicemia [155]. The bark is used for the treatment of rheumatism, diarrhea, haemorrhage, for stomach-ache, pregnancy related problems, as an astringent, while the leaves are used on ulcers, wounds and have insecticidal properties [156]. It is also used for urinary tract infections, haemorrhoids, fistula and worm infections. Aerial parts demonstrate promising hepatoprotective effect suggesting that it could be used as a therapeutic agent for protection from overdose of paracetamol [157]. The gum obtained from this plant can be used as a drug release retardant in controlled release matrix systems [158]. Studies show that the bark can be used as anti-HIV-1 IN agent for treating HIV infections [159]. To our knowledge this is the first report of surface active properties of the leaves and stem of *Albizia procera* [25].

### 2.8.3 *Zephyranthes carinata* (Pyagi Phool)

*Zephyranthes carinata* (Pyagi Phool or Pink Rain Lily) is a perennial flowering plant growing in the moist areas of the Himalayas. It belongs to *Amaryllidaceae* family. It has bright pink flowers with globular 2-3 cm bulbs. It is used in Chinese medicine to treat fever and also as a poultice for abscesses. It is widely used as an ornamental plant [160, 161]. Isolation of phenolic base named carinatine and pretazettine from the bulbs of has been reported [162]. The lectins were studied for antiviral activity against a strain of vaccinia virus in vitro [163]. The isolation, structural elucidation and cytotoxic

activities of alkaloid have been reported [164, 165]. It was also seen that alkaloid fraction exhibited significant acetylcholinesterase inhibitory activity [166]. According to our literature survey and our knowledge this is the first report of surface active properties of the bulbs.

#### 2.8.4 *Acacia concinna* (Shikakai)

*Acacia concinna* (Shikakai) is a bush found in tropical rainforests of southern Asia belonging to the family *Fabaceae*. It is also called *fruit for hair*. The pods contain saponins of acaciatic acid with acidic pH, beneficial for the scalp. The pods are traditionally used for washing hair, promoting hair growth and also as foaming agent [25]. The plant is used as a purgative, emetic and an expectorant [167]. The seeds have been used as a folk medicine. It has been investigated as an eco-friendly acidic surfactant type catalyst for different chemical synthesis [168]. Immunological adjuvant activity of the saponins has also been reported [169]. Large number of studies on isolation and characterization of the seeds [170] and pods have been carried out [171, 172, 173, 174, 175]. Surfactant activity studies of the pods are relatively very few [25, 176].

#### 2.8.5 *Juglans regia* (Okhar)

*Juglans regia* (Okhar or walnut) of family *Juglandaceae*, is a woody, deciduous and frost tender tree around 20 m high. It is found in China, Iraq, Mexico, Spain, Turkey, Nepal, India (forest in Himalayas). It is traditionally used in Indian (Ayurvedic) and Greco-Arab (Unani-tibb) medicine for the



treatment of different ailments like sinusitis, cold stomach ache and cancer. The bark is dull blackish brown and is used as a toothcleaner and as a dye for colouring lips [177], in arthritis, skin diseases, toothache, hair growth [178]. It is also used for anti-inflammatory, blood purifier, anticancer and laxative activities [179]. The leaves are used as an astringent, antimicrobial, antifungal, antihelminthic, diuretic and detoxifier [180] and also for treatment of fever, rheumatic pain [181], diabetes, asthma [182], prostate and vascular disturbance [183], scalp itching, dandruff, sunburn and superficial burns [184]. The bark of this plant is used as a protective agent against toxicity of anticancer drugs and cyclophosphamide [185]. Bark extracts have also been reported to exhibit antibacterial, anticandidal, antioxidant [186], antifungal [187, 188] and antimicrobial activities [189]. In folk medicine the shell is used to heal malaria [190]. This is the first report of surface active properties of the bark of *Juglans regia*.

## Part II

# EXPERIMENTAL TECHNIQUES

# Chapter 3

## Material and Methods

This chapter describes the materials used in the thesis and the experimental techniques used to study them. I begin with a description of the plant based and synthetic surfactants studied. This is followed by the details of the experimental techniques used in this work.

This chapter discusses the techniques used to characterize natural surfactants such as Thin Layer Chromatography, Column Chromatography, UV-Vis Spectroscopy, Fourier Transform Infrared Spectroscopy and Gas Column Mass Spectrometry. Also, one shot forced drainage experiment in natural surfactant system is described.

### 3.1 Materials

#### 3.1.1 Natural Surfactants

Natural plant based surfactants used for this study are outlined in Table 3.1.

Table 3.1: Natural surfactants used for the present study.

Scientific Name	Common Name	Family	Part Used	Habitat
<i>Sapindus mukorossi</i> Gaertn.	Ritha	<i>Sapindaceae</i>	Fruit pulp	India Nepal
<i>Albizia procera</i> (Roxb.) Benth.	Seto Siris	<i>Fabaceae</i>	Leaves	Himalayas, Gujarat, South India
<i>Zephyranthes carinata</i> Herbert	Pyagi Phool	<i>Amyrilladaceae</i>	Bulb	Himalayas
<i>Acacia concinna</i> DC.	Shikakai	<i>Fabaceae</i>	Fruit(Pods)	Asia, Central and South India
<i>Juglans regia</i> Linn.	Okhar	<i>Juglanduceae</i>	Bark	China, Iraq, Nepal, Himalayas

### Sample Collection

The plants were bought/collected from various areas of Darjeeling, Siliguri and Sikkim as given below.

- *Sapindus mukorossi* pulps and *Acacia concinna* pods were bought from local market, Mahavirsthan in Siliguri.
- *Albizia procera* leaves were collected from Neeha Busty in South Sikkim.
- *Zephyranthes carinata* bulbs were collected from Mirik in Darjeeling.
- *Juglans regia* barks were collected from Bhutia Busty in Darjeeling.

### Identification of the Plants

The plants have been identified, referred and authenticated by Dr T. K. Mandal, Research Officer (S-2), Central Council for Research in Ayurvedic

Sciences, Department Of AYUSH (Ayurveda, Yoga and Naturopathy, Unani, Siddha and Homoeopathy), Ministry of Health and Family Welfare, Government of India, Ayurveda Regional Research Institute, Tadong, Gangtok, Sikkim, India. Some plant parts have also been identified by Mr. Manoj Chettri, Range Officer, Directorate of Forests, Lloyd Botanic Garden, Darjeeling, Government of West Bengal. The letters of identification of the plant parts are provided in Appendix. Figure 3.1 below shows the parts of the plants used to extract surfactants.

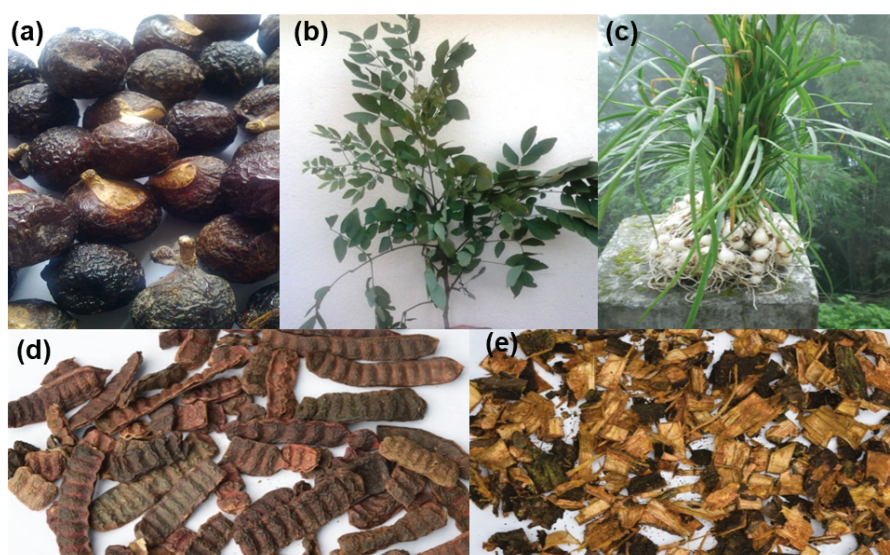


Figure 3.1: (a) *Sapindus mukorossi* fruit pulp (b) *Albizia procera* leaves (c) *Zephyranthes carinata* bulbs (d) *Acacia concinna* pods (e) *Juglans regia* bark.

### 3.1.2 Synthetic Surfactants

Synthetic surfactants, available in the local market used in this study are mentioned in Table 3.2. They were bought from the local market. Samples were weighed using a digital balance.

Table 3.2: Synthetic surfactants used for the present study.

Powdered Surfactant	Liquid Surfactant	Shampoo
Henko (Batch No. C/HSCP15/0313)	Ezee (Lot No. 130114B )	Johnson's Baby Shampoo (Lot No. BB9087)

### 3.1.3 Other Materials

The materials and chemicals used to carry out this study are listed as follows:

- Millipore Milli-Q water of resistivity 18.2 M $\Omega$ cm, surface tension 71.5 mN/m and pH 6.5-7 was used to prepare surfactant solutions.
- Whatman Filter paper No. 1 was used to filter surfactant solutions and as Wilhelmy Plate for surface tension measurements.
- Salt (Tata, Batch number-AF115A2) was used to study effect of additives.
- Refined soyabean oil (Fortune, Batch number-(AH) SB06C05) was used for studying emulsifying properties.
- Coconut oil (Parachute oil, Lot number- KA003), paraffin wax (from candles available in the market) and hexane (high purity grade from Merck) were used for studying cleaning.
- India ink (Camel, Batch number A1205) was used for dirt dispersion measurements.
- Cotton bleached Poplin cloth Sort No. 22125003 from Manoj Fabrics, Ahmedabad, India was used for studying wetting and cleaning properties.

- Colouring dye (blue) and nitrogen gas (99% pure)- for drainage experiments.
- Pre-coated TLC plates (Silica gel 60 F254 (Merck)) were used in Thin Layer Chromatography.
- Silica gel (Merck 60-120 mesh, 15×100 cm) was used for Column Chromatography.
- Ethanol, chloroform, acetone, methanol, petroleum ether, n-butanol, ethyl acetate, glacial acetic acid, sulphuric acid, phosphomolybdic acid were used for extraction and characterization of the natural surfactants. All the chemicals were of high purity grade and obtained from Merck.

## 3.2 Experimental Techniques

### 3.2.1 Extraction of Natural Surfactants

Natural surfactants were extracted using water and methanol. Water extracts were used to study surface, foam and drainage characteristics while methanol extract were used for characterization.

Before extraction of natural surfactant, the required parts were segregated. The outer pericarp of *Sapindus mukorossi* and the pods of *Acacia concinna* were separated from the seeds. *Albizia procera* leaves were separated from the stem while *Zephyranthes carinata* bulbs were segregated from the leaves. The bark of *Juglans regia* were chopped into small pieces. The segregated parts of the plants were thoroughly washed with water and shade

dried at room temperature ( $20 \pm 2$ )<sup>0</sup>C. The dried sample were crushed using a mortar and pestle and weighed with a digital balance.

### Water Extraction

The plant samples were extracted with water. *Sapindus mukorossi* (30 gm), *Albizia procera* (30 gm), *Zephyranthes carinata* (30 gm), *Acacia concinna* (30 gm), *Juglans regia* (30 gm) were soaked in 100 ml Milli-Q water and macerated for 24 hours at room temperature. The solutions obtained were filtered in Whatman filter paper no. 1 using a Buchner funnel.

### Calculation of Concentration

Initially the concentration of the natural surfactant was calculated with the help of a specific gravity bottle. The concentration  $C$  was taken as

$$C = \rho_{water} \times (m_3 - m_2)/(m_2 - m_1) \quad (3.1)$$

where  $\rho_{water}$  is density of water,  $m_1$  is mass of empty bottle,  $m_2$  is mass of bottle filled with water,  $m_3$  is mass of bottle filled with solution.

Later, the concentration was calculated following the method developed by Kommalapati et al. and Roy et al. with slight modifications [137, 191]. The filtrate obtained was evaporated with a rotary evaporator (Buchi, Switzerland/R-3) at 40-50 <sup>0</sup>C on a water bath. *Sapindus mukorossi* gave a brownish paste (10.5 gm), *Albizia procera* gave a yellowish green paste (1.4 gm), *Zephyranthes carinata* gave a whitish paste ( 2.7 gm), *Acacia concinna* gave a reddish brown paste (11.5 gm) while *Juglans regia* gave a dark brown



paste (1.3 gm). The extracts were weighed and dissolved in Milli-Q water and diluted as required. All the experiments were performed at least thrice and an average of the results were taken.

### **Methanol Extraction**

Powdered plant samples *Sapindus mukorossi* (90 gm), *Zephyranthes carinata* (90 gm) and *Juglans regia* (90 gm) were extracted with 450 ml 70 % methanol by maceration for 72 hours at room temperature. The other two plant samples *Albizia procera* (40 gm) and *Acacia concinna* (40 gm) were extracted with 200 ml 70 % methanol by maceration for 72 hours at room temperature. The extracts were filtered through Whatman filter paper no. 1 in a Buchner funnel. The filtrate was evaporated and concentrated to about 50 ml with a rotary evaporator (Buchi, Switzerland/R-3) at 40-50 °C on a water bath. 100 ml of Milli-Q water and 250 ml of water-saturated n-butanol were added to the concentrated extract and shaken several times in a separating funnel. The process was repeated several times. The upper n-butanol layer was separated and the solvent was evaporated and concentrated to about 10 ml to get the saponin extract [192, 193]. *Sapindus mukorossi* gave a brownish paste (20 gm), *Albizia procera* gave a yellowish green paste (3 gm), *Zephyranthes carinata* gave a whitish paste (3 gm), *Acacia concinna* gave a reddish brown paste (6 gm) while *Juglans regia* gave a dark brown paste (10 gm). The extracts were diluted with methanol for further investigations. Figure 3.2 illustrates saponin obtained from different plant extracts.

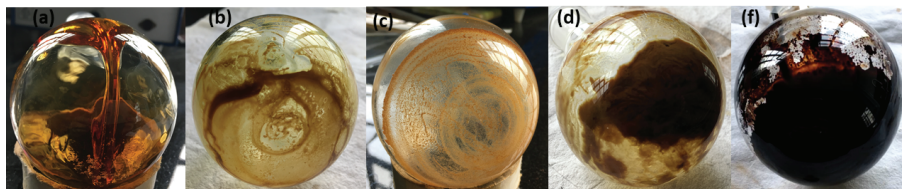


Figure 3.2: (a) *Sapindus mukorossi* (b) *Albizia procera* (c) *Zephyranthes carinata* (d) *Acacia concinna* (e) *Juglans regia*.

### 3.2.2 Preparation of Synthetic Surfactants

The weighed samples were dissolved in 100 ml Milli-Q water and the concentrations were calculated. It was further diluted as required.

### 3.2.3 Surface Activity Measurements

Properties like surface tension, foaming, wetting, emulsification, viscosity, conductivity, dirt dispersion and cleaning are essential criteria to characterize surface active materials. The various surface activity measurements are underlined below.

#### Surface Tension Measurements

The most common method of determination of CMC is by surface tension. Surface tension decreases with increase in concentration and then remains constant after reaching CMC. The CMC values were obtained from the break in the surface tension vs concentration plots. This method is fast, convenient as well as non- destructive to the surfactant.

Surface tension was measured by Wilhelmy plate method [49, 194] using a Sartorius CPA-225 D Semi-Micro Balance with Density Measurement Attachment at room temperature as shown in Figure 3.3. Whatman filter

paper no. 1 was used as the plate. The filter paper was hung to the density attachment of the balance with an S hook. A 100 ml glass beaker containing 80 ml of surfactant solution was placed on a jack, which was placed right below the filter paper. The beaker was raised so that the filter paper went partially into the solution and was held for about 30 minutes. The beaker was lowered so that the lower end of the filter paper just touched the liquid surface. The balance reading was made zero.

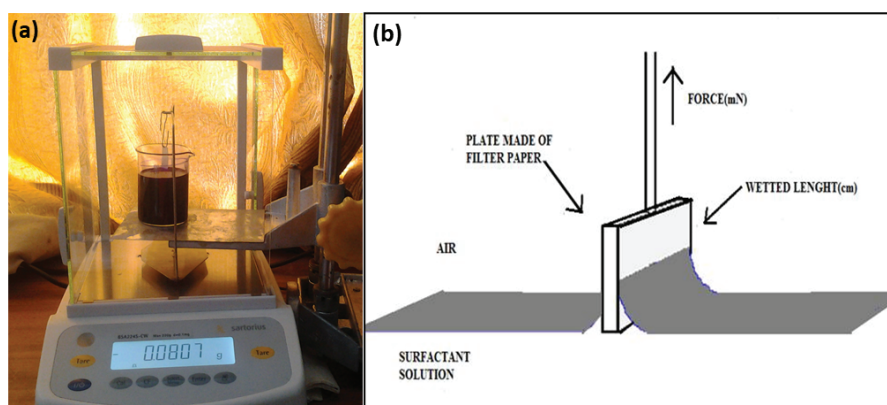


Figure 3.3: Experimental set-up for surface tension measurements (a) Wilhelmy plate arrangement (b) Schematic representation of the medium.

The force  $F$  acting vertically on the filter paper by the liquid meniscus was measured using the balance. Thus this force applied to the filter paper is equal to the weight of the liquid meniscus lifted over the horizontal surface of the surfactant solution. The beaker was lowered so that the filter paper came out of the liquid surface. This measured the surface tension of the surfactant solution. The surface tension is related to the force measured and plate dimensions as described in Chapter 2, equations 2.4 and 2.5.

The beaker was cleaned with a detergent and washed thoroughly with Milli-Q water, ethanol and finally rinsed with acetone before the experiment.

It was then dried with a drier. The Wilhelmy Plate was made of 2.5 cm by 1 cm filter paper. The paper was first dipped in chloroform and left to dry for some time. It was then dipped in Milli-Q water before the experiments were performed. The paper was made completely wet before the experiment so that the contact angle between the paper and the solution is zero. Freshly prepared stock solutions were diluted to different concentrations and were thoroughly mixed using a magnetic stirrer. The samples were stabilized for 10-15 minutes before the measurements.

### **Foam Formation**

Formation of foam and its stability are one of the important parameter to characterize a surfactant. The foaming ability and stability of the surfactant solution depends on the chemical properties and composition of adsorbed surfactant molecules. The foaming ability and stability of the surfactants were investigated by Bikerman's method and Bartsch test previously in my M. Phil. work. In the present work the effect of salt on foaming capacity and stability were studied using Bikerman's method. The Bikerman's method of foam production is the most productive way to produce foam as mechanical work is not required for air entrapment in the formation of bubbles [195].

**Bikerman's Method:** Foam was generated by bubbling nitrogen gas at a constant pressure through 40 ml surfactant solution placed in a cylindrical column of length 100 cm and diameter 4.43 cm with a fritted glass filter G-2 at the bottom for gas dispersion. A solution was poured into the column in a manner that no foam was produced. A gas flow rate of 2 litre/min was maintained with a flow meter. The bubbling of gas was continued until

the foam reached a constant height, a state of dynamic equilibrium. This condition of equilibrium is attained when the rate of foam formation at the bottom is equal to the rate of collapse of bubbles at the top. The equilibrium height or foam volume attained by the foam showed the foaming ability.

After equilibrium condition is reached, the foam column height became stable and the gas flow was terminated. The foam thus formed was allowed to collapse without any disturbances. The decline of foam height against time was monitored using a stop watch [196, 197, 198]. The duration of the experiment depended on the nature as well as stability of foam from minutes to hours to even days. The stability of foam was measured by finding the  $R5$  value defined as the ratio of the foam height at 5 minutes to initial height [199]. The effect of salt on foam height and stability with concentration was measured for different surfactants. This experiment was carried out at a room temperature of  $(20 \pm 2)^{\circ}\text{C}$ . Every measurement was repeated at least thrice and an average was taken. The experimental set-up is shown in Figure 3.4.

**Barstch Test:** Barstch test is also known as shaking tube method. A 100 ml measuring cylinder was taken in which 40 ml surfactant solution was added and vigorously shaken by hand. The shaking had an amplitude of 5 cm and a frequency of 3 Hz. The measuring cylinder was left to stand and the maximum height obtained was taken as the foaming ability. The decay of foam (foam stability) was monitored using a stop watch [199].

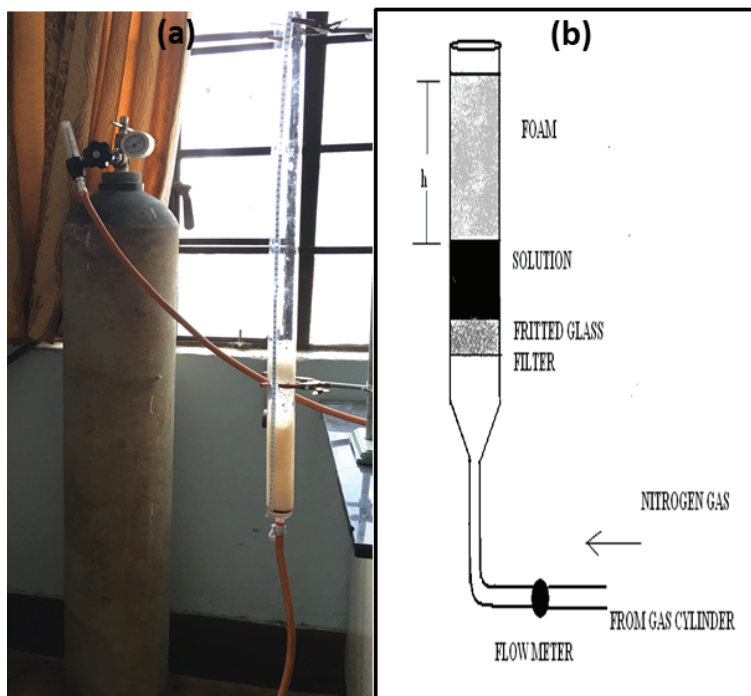


Figure 3.4: Experimental set-up for foam formation (a) Photograph showing Birkman's method (b) Schematic representation of the system showing the foam height as 'h'.

### Surface Wetting Measurements

Surface wetting is an important parameter in characterizing the properties of surface active substances. It is the capacity of the liquid to maintain a contact with a solid surface, due to the intermolecular interactions when two surfaces are brought together. The wetting test evaluates the ease with which a surfactant solution can wet a given surface. The shorter it takes for a solution of surface active substance to wet the surface, better is the wetting agent.

Wetting was conducted on  $(5 \times 5)$  cm cotton Poplin cloth using Canvas disc wetting test with slight modification at  $(20 \pm 2)^{\circ}$  C. 400 ml of surfactant

solution was taken in a 500 ml beaker. The cloth was floated on the surface of the solution. As the cloth touched the solution, a stop watch was started and was stopped at the time the cloth began to sink in the solution. The time required for the cloth to begin to sink was measured as wetting or sinking time. The test was repeated several times using the same surfactant solutions but with a fresh cloth each time for the test and an average of the wetting time were taken [200, 201].

The yarn count of the cloth was  $(6593 \pm 26.7)$  cm/g, surface mass  $(8.929 \pm 0.013) \times 10^3$  g/cm<sup>2</sup>, single thread linear mass  $(1.52 \pm 0.04) \times 10^4$  g/cm and thread count  $(130.8 \pm 2.2)$ /cm<sup>2</sup>. The cloth had a water absorption capacity of  $(95.25 \pm 1.33)$  %.

### **Emulsification**

Formation of stable emulsion is an essential characteristic of surfactants. The nature of surfactant is responsible for formation of W/O emulsion or O/W emulsion. In this work, I have investigated the efficacy of surfactant to stabilize O/W emulsion at a room temperature of  $(20 \pm 2)^0$  C.

Emulsification properties were investigated by taking 20 ml of surfactant solution and 20 ml of refined oil in a 100 ml measuring cylinder. The measuring cylinder was sealed from the top and vigorously shaken by hand until a homogenous mixture was obtained. The frequency of shaking was around 3 Hz with an amplitude of 5 cm. The cylinder was left to stand. The separation of the surfactant solution from the emulsion was monitored with of a stop watch. The time required for the separation of 10 ml of surfactant solution from the emulsion was taken as a measure of emulsion stability [202].

The emulsion formed is shown in Figure 3.5.



Figure 3.5: Photograph showing emulsion formed with *Sapindus mukorossi* extract. The emulsion formed did not separate for 2 hours.

### pH Measurements

pH of the surfactant solutions were measured at room temperature using Thermo Scientific Orion 2 star pH Bench top. The pH meter was routinely calibrated by the standards and buffers. Fresh surfactant solutions in Milli-Q water were prepared. After proper mixing with the help of a magnetic stirrer, the beakers were properly sealed with parafilm and the measurements taken [24, 203].

### Conductivity Measurements

Electrical conductivities of aqueous surfactant solutions are low at low concentrations and a sharp increase in conductance is seen owing to micelle



formation. The study of conductivity is important above CMC to estimate the region of micelle formation.



Figure 3.6: Photograph of conductivity measurement.

The conductivity measurements were performed with La Motte Conductivity/Temperature/pH pocket TRACER at room temperature as shown in Figure 3.6. The cells were calibrated with standard solutions before measurements. Fresh surfactant solutions were prepared in Milli-Q water. The solutions were mixed with a magnetic stirrer. The change in the nature of plots were considered as the CMC [203].

### Viscosity Measurements

Fluids are generally considered to be consisting of molecular layers arranged one on top of the other. Application of a shearing force on the liquid helps it to flow. However, frictional forces between the layers offer obstruction to this flow. The measure of frictional resistance is termed as viscosity of a liquid. Numerous methods exist for measuring viscosity  $\eta$ . The most commonly

method used to measure viscosity is based on Poiseuille's law given by,

$$\eta = \frac{\pi r^4 t P}{8 v l} \quad (3.2)$$

where  $v$  is the volume in  $\text{cm}^3$  of the liquid flowing at time  $t$  seconds through a tube of radius  $r$  cm, length  $l$  under hydrostatic pressure  $P$ . The viscosity of a liquid with respect to water is called the relative viscosity  $\eta_r$ . If  $t_s$  and  $t_w$  are the times of flow of surfactant solution and water respectively, then

$$\eta_r = \frac{\eta_s}{\eta_w} = \frac{t_s P_s}{t_w P_w} \quad (3.3)$$

As pressure ( $P$ ) is proportional to the density ( $\rho$ ), we get

$$\eta_s = \frac{\eta_w t_s \rho_s}{t_w \rho_w} \quad (3.4)$$

where subscripts  $s$  and  $w$  indicate the surfactant solution and water respectively. Viscosity measurement is essential for surfactants as it gives information about the region of micelle formation and also the types of micelles formed. Aqueous surfactant solutions containing spherical micelles have low viscosity [204]. Also, high viscosity stabilizes the foam.

The viscosities of the surfactant solutions were obtained using an Ubbelohde Cannon Fenske Direct flow capillary viscometer (size 50, constant 0.00437) suspended vertically in a stand as shown in Figure 3.7. The viscometer was cleaned and dried before every measurement. Fresh surfactant solutions were prepared in Milli-Q water in a beaker. The solutions were mixed with a magnetic stirrer. A constant volume of surfactant solution was



Figure 3.7: Photograph taken while performing viscosity measurements.

poured into the viscometer. The time of flow of the solution through the capillary was measured with a stop watch. The measurement was done thrice and an average of the measurement was taken. Viscosities were calculated using the equation 3.4 [204, 205].

### **Dirt Dispersion**

The quantity of dirt remaining in the foam, that is Dirt Dispersion (DD), is an important parameter to study the cleaning ability of a surfactant. Dirt that remains in the foam is difficult to rinse while cleaning and may redeposit at the surface. Thus, efficacy of a surfactant is expressed in terms of DD [201].

Dirt dispersion in foam was studied by preparing fresh surfactant solutions in Milli-Q water in a beaker at room temperature. The surfactant solutions were mixed properly with a magnetic stirrer. Two 30 ml bottles

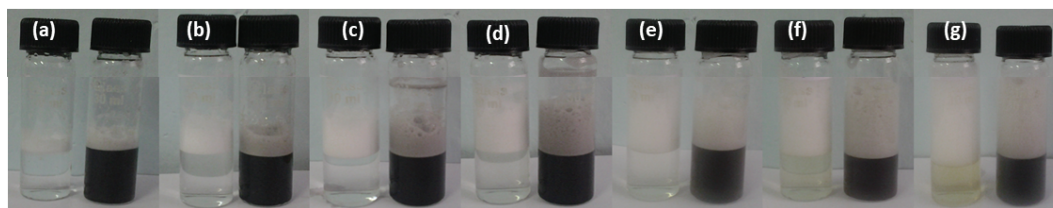


Figure 3.8: Dirt dispersion of *Sapindus mukorossi* extract at various concentrations. (a)  $5.47 \times 10^{-4}$  g/cc (b)  $1.09 \times 10^{-3}$  g/cc (c)  $2.19 \times 10^{-3}$  g/cc (d)  $4.38 \times 10^{-3}$  g/cc (e)  $8.75 \times 10^{-3}$  g/cc (f)  $1.75 \times 10^{-2}$  g/cc (g)  $3.50 \times 10^{-2}$  g/cc.

were taken and 10 ml of surfactant solution were added to these bottles. One drop ( $\sim 0.03$  ml) of India ink was added to one bottle and mixed with the solution. India ink was used as a model of dirt even though the behaviour of ink and dirt may not be the same. The two bottles were simultaneously shaken by hand until a foam was formed. The bottles were left to stand and photographed against a white background. Adobe<sup>®</sup> Photoshop<sup>®</sup> 7.0 was used to analyze the gray scale of the foams in the photographs. DD was measured as the ratio of gray scale at the same height for the two foams. Figure 3.8 shows dirt dispersion at various concentrations. This is the first approach for quantification of dirt as previously it has been studied only qualitatively by eye estimation as heavy, moderate and light [15, 16, 206].

### Cleaning

The most important aspect of a surfactant is removal of dirt, oil and grease. The ability to remove dirt is a characteristic property of a surface active substance. Cleaning action was tested on a  $(5 \times 5)$  cm piece of cotton Poplin cloth at room temperature. The cloth was soaked in water for 24 hours, dried and weighed ( $W_1$ ). Simulated dirt was prepared by taking 1

gm of coconut oil, 1 gm of paraffin wax in 100 ml of hexane. The cloth was dipped in simulated dirt. The cloth was then dried and weighed ( $W_2$ ). 400 ml of surfactant solution was taken in a 500 ml beaker. This cloth was placed in the surfactant solution for half an hour and shaken. The cloth was taken out, washed with water, dried and weighed ( $W_3$ ) [36]. The percentage of cleaning was expressed using equation,

$$C = \frac{(W_2 - W_3)}{(W_2 - W_1)} \times 100 \quad (3.5)$$

### 3.2.4 Characterization Techniques

A large number of techniques can be used to determine and estimate the presence of active components in the plant extracts. The most useful and popular tools used for this purpose include chromatographic and spectroscopic techniques. The information generated from these techniques could provide a complete understanding of the system. The presence of active constituents and chemical composition of the natural surfactants present in the plant extracts were characterized using the following techniques.

#### Thin Layer Chromatography

Thin layer chromatography (TLC) is a common and efficient technique used to separate a wide variety of compounds of chemical and biochemical interest. It is also known as planar chromatography. Chromatography was first introduced by Mikhail Tswett in 1906. In 1938, Nikolai Arkadevich Izmailov and Maria Semenovna Schreiber designed TLC with slight modification [207].

It is a simple, quick and inexpensive method to know different components and identify compounds present in a mixture. TLC uses a stationary and a mobile phase under the principle of solubility *Like Dissolves Like*. The stationary phase consists of a solid sheet like glass, plastic or aluminium coated with absorbent materials like silica powder, aluminium oxide or cellulose. The mobile phase comprises of a single or a mixture of solvents. The mobile phase is made to rise in the stationary phase by capillary action. The sample is introduced into the mobile phase through a capillary tube. The compounds get separated due to their solubility and retardation in mobile and stationary phases. Compounds which dissolve in the mobile phase move up the plate and others remain or travel to a smaller extent on the stationary phase [208].

The movement of the compounds are expressed by its retention factor or retardation factor ( $R_f$ ) given by:

$$R_f = \frac{\text{Distance travelled by the compound}}{\text{Distance travelled by the solvent front}} \quad (3.6)$$

After the experiment is over, the TLC spots are studied. The  $R_f$  value can be calculated by the TLC spots obtained when observed under UV light or when heated after being sprayed with spraying agent. The distance travelled by the compound and the solute front is noted and  $R_f$  calculated using equation 3.6.

TLC studies for this work were carried out following the methods provided by Wagner et al [192]. Various solvent systems were used for eluting the TLC plates. Better separation was observed in the solvent system Chloroform:

Glacial acetic acid: Methanol: Water in the ratio 8:4:1.5:1. The solvents were poured into a chromatographic glass chamber to a height of 0.5 cm. The solvents were kept inside the chamber for 30 minutes to ensure proper saturation. The prepared saponin extracts 20  $\mu\text{l}$  were dissolved in methanol and applied on pre-coated TLC plates (Silica gel 60 F254 (Merck)) using capillary tubes at a distance of 1 cm from the edge of the plate. The applied spots on the plate were dried at room temperature and the plates were placed inside the glass chamber at an angle of  $15^\circ$  approximately as shown in Figure 3.9.

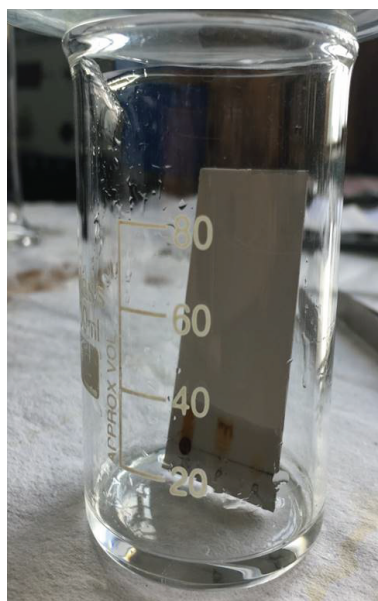


Figure 3.9: Photograph taken while performing Thin Layer Chromatography on *Sapindus mukorossi* extract.

The chamber was left undisturbed until the solvent front reached 1 cm from the top of the coated portion of the plate. The plates were taken out gently and the solvent front was marked with pencil. The spots on the plates were detected using UV light obtained from the UV chamber (Zenith

Glasswares and Instrument Corporation) at short wavelength (254 nm), long wavelength (366 nm) and derivatized using spraying reagents like anisaldehyde-sulphuric acid reagent and Phosphomolybdic Acid (PMA) to identify the compounds. TLC plates were dipped in anisaldehyde-sulphuric acid reagent or Phosphomolybdic Acid (PMA) and the plates were heated for 5-10 minutes at 100 °C for the development of color in separated bands. The colour of the spots were observed and the  $R_f$  values calculated [209].

### Staining Agents

- **Phosphomolybdic Acid (PMA):** 1.2 grams of Phosphomolybdic Acid was mixed in 25 ml ethanol.
- **Anisaldehyde-sulphuric acid reagent:** 0.5 ml anisaldehyde was mixed with 10 ml glacial acetic acid. 85 ml of methanol and 5 ml of sulphuric acid was added [210].

### Column Chromatography

Column Chromatography (CC) is useful for separation and purification of compounds. It is a form of adsorption chromatography in which the stationary phase is a solid and the mobile phase is a liquid. A solid adsorbent is placed in a vertical glass column (stationary phase) and the solvent (mobile phase) is added from the top of the column and allowed to flow down either by gravity or by application of external pressure. The solvent flows through the stationary phase dissolving the compounds being studied. Various components in the mixture have different interactions with mobile and stationary



phases. As a result these components are carried over different distances by the mobile phase. The different compounds get separated as individual components or elutants which are collected at different time scales as solvent drips from the bottom of the column [211].

Adsorbents used for CC include silica, alumina, calcium carbonate, calcium phosphate etc. Solvent selection depends on the nature of the solvent and the adsorbent. Separation of the components of the mixture depends on the polarity of the solvent and adsorbent activity. Good but slower separation is achieved if adsorbent activity is high and solvent polarity is low and vice versa. Thus proper selection of the eluting solvent is essential for CC.

Preliminary purification of the saponins of the different extracts were performed using CC on silica gel (Merck 60-120 mesh, 15×100 cm) [212]. A column 100 cm long and 2 cm in diameter was thoroughly washed with detergent, rinsed with Milli-Q water and allowed to dry. A small piece of cotton was inserted into the lower part of the column when the column was fully dry. The column was held vertically by a clamp to a stand and a funnel was attached to the open end. Silica gel was poured into the column, after which the solvent (petroleum ether) was poured down the column. Homogenous packing of the column was obtained by the flow of the solvent as shown in Figure 3.10.

The saponin extracts were dissolved in methanol and were thoroughly mixed with silica gel until the solvent evaporated. The extracts mixed with silica gel were applied to the top of column as evenly as possible as distortion of the column packing would lead to distorted bands. Initially 100 % petroleum ether was used to run the column. Later, gradual increase of 2-5



Figure 3.10: Photograph taken while performing Column Chromatography.

% ethyl acetate in petroleum ether was used to run the column. Finally, the column was run with methanol. This was carried out in order to increase the adsorption of different components. Various fractions of the extract were eluted using varying proportion of petroleum ether, ethyl acetate and later with methanol and were monitored by TLC [209]. Fractions having same number of spots with same  $R_f$  values were combined and evaporated to give major fractions.

### **High Performance Liquid Chromatography**

High Performance Liquid Chromatography (HPLC) also known as High Pressure Liquid Chromatography is an analytical technique used for separation, identification and quantification of constituents of mixture of compounds.

Here a high pressure upto 400 atm is applied with a pump to force the solvent containing the sample to enter a column containing solid adsorbent material. The adsorbent is a granular material made of silica or polymers of size  $2\ \mu\text{m}$  to  $50\ \mu\text{m}$ . The adsorbent acts as stationary phase. The pressurized fluid consisting of solvents namely water, acetonitrile and methanol acts as a mobile phase. The interaction of each sample component varies leading to a difference of flow rates for each component. This in turn leads to separation of components. The time at which a particular analyte rises and comes out of the column is taken as the retention time [213, 214].

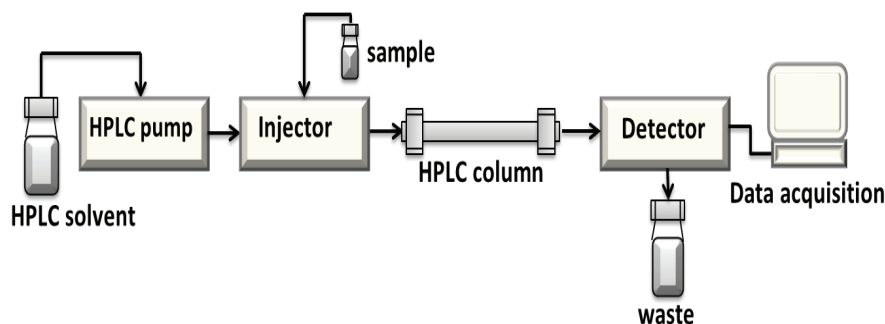


Figure 3.11: Schematic representation of High Performance Liquid Chromatography.

The basic components of HPLC system are shown in Figure 3.11 and discussed below [215]:

- **Solvent Reservoir:** The different solvents (polar as well as non-polar) which constitute the mobile phase are kept in glass containers. The relative quantities of polar and non-polar solvents can be varied depending on the composition of the sample.
- **Pump:** The mobile phase is pumped from the solvent reservoir into

the column and then to the detector. The pressure applied depends on the dimensions of the column, particle size, composition of the mobile phase and the flow rate.

- **Sample Injector:** The sample is injected through computerized infusion framework.
- **Columns:** The columns consist of cleaned stainless steel around 50 mm to 300 mm in length with inward distance across around 2 to 5 mm. The columns are loaded with solid adsorbent (stationary phase).
- **Detector:** The detectors help to distinguish the analytes as they come out from the chromatographic column. Generally used are ultra violet detectors, refractive index detectors etc.
- **Data Collection Devices or Integrators:** The signals generated by the detectors are collected by the computer as a chromatograph.



Figure 3.12: High Performance Liquid Chromatography setup.

HPLC analysis were performed using an Agilent technologies 1200 infinity series along with a Diode Array Detector (DAD) attached to it as shown in Figure 3.12. The sample was dissolved in 2 ml methanol and passed through 0.22  $\mu\text{m}$  syringe filter. The mobile phase consisted of two solutions (A and B). Solution A corresponds to 0.1 % Trifluoroacetic Acid (TFA) (v/v) in water and B 0.1 % Trifluoroacetic acid (TFA) in methanol (v/v). However, the gradient profile was water and methanol in varying proportions. The flow rate was set at 1 mL/min. The injection volume of the sample was 5  $\mu\text{L}$ . Total running time of the sample was around 50 minutes. The experiment was conducted at room temperature.

### Ultra-Violet Visible Spectroscopy

The Ultra-violet Visible Spectroscopy (UV-Vis) uses electromagnetic radiations between 190 nm to 800 nm. The sample molecules when exposed to light have energy

$$E = h\nu \quad (3.7)$$

where  $E$  is the energy in Joule,  $h$  is Planck's constant and  $\nu$  is the frequency in Hertz. When this energy matches the electronic transition within the molecule, the electrons are transferred from the ground state to an excited state. This results in the absorbance of light. The frequency of the light absorbed is related to the energy difference between the ground and excited states [216].

Absorption wavelength is larger when the difference between ground and excited state is small and vice versa. The absorption intensity depends on

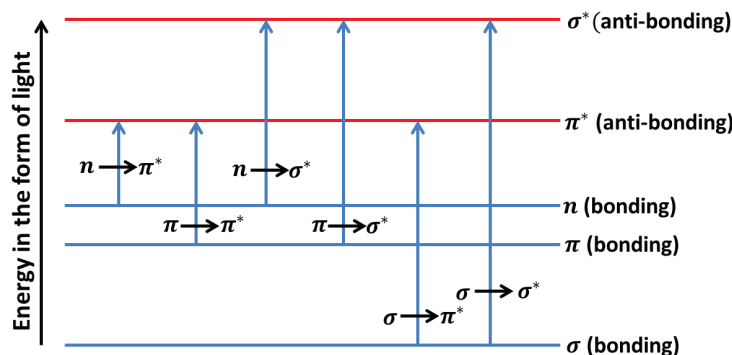


Figure 3.13: Transition between electronic states in a molecule.

the interaction probability between energy radiated and electronic system. The wavelength at which absorption takes place is recorded by the spectrophotometer. The maximum absorbance wavelength is represented as  $\lambda_{max}$ .

Total energy of a molecule consists of sum of electronic, vibrational and rotational energy. Absorption of energy in the UV region causes changes in the molecules electronic energy. The  $\pi$ -electrons or the non-bonding electrons ( $n$ -electrons) of the molecules, absorb UV or visible light to excite to higher anti-bonding molecular orbitals. The transition between the bonding and anti-bonding electronic states is illustrated in Figure 3.13. The basic principle behind absorbance of light by the molecules in the solution is given by Beer-Lambert's law.

$$A = \log \frac{I_0}{I} = \epsilon \times b \times c \quad (3.8)$$

where  $A$  is measured absorbance (arb. units),  $I_0$  and  $I$  are intensities of the reference and sample beam respectively,  $\epsilon$  is molar absorptivity ( $M^{-1} \text{ cm}^{-1}$ ),  $b$  is sample path length (cm) and  $c$  is solution concentration (M).

The schematic representation of the UV-Vis spectrophotometer is illus-

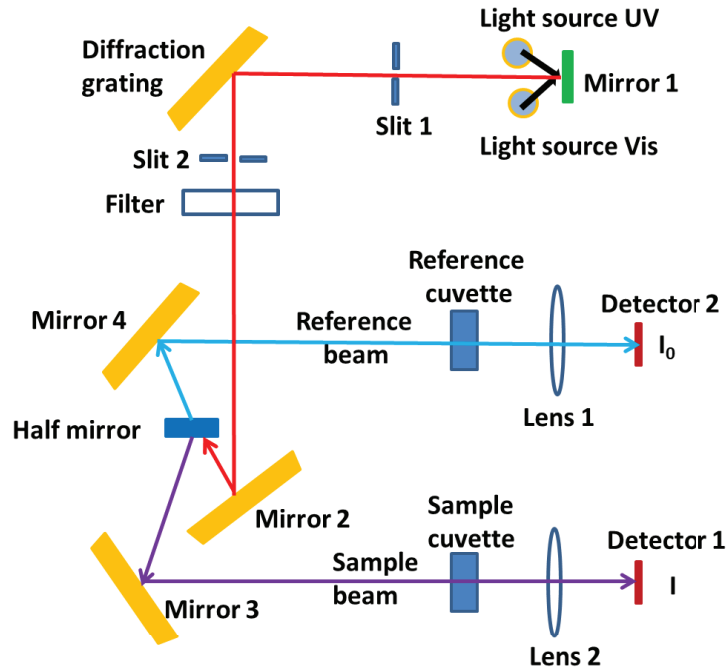


Figure 3.14: Block diagram of UV-Vis Spectrophotometer.

trated in Figure 3.14. UV-Vis spectrophotometer comprises of five components.

- **Source:** The deuterium discharge lamp acts as a light source for UV measurements while tungsten- halogen lamp is used for visible and Near Infra Red (NIR) measurements. The lamp swaps automatically when the scanning takes place between UV and visible regions.
- **Monochromator:** The light enters through the entrance slits into the monochromator. The collimated beam is split into its component wavelength by a grating or a prism. Radiation of one particular wavelength leaves the exit slit. This beam splits into two halves as it passes a set of mirrors.

- **Sample:** One half of the beam passes through the sample solution contained in a transparent quartz cuvette and the other half passes through the reference, an identical cuvette containing only the solvent. The scattering and reflection losses are minimized by using highly polished faces of the cuvette.
- **Detector:** The two beams are fed into detectors. The commonly used detectors are photomultiplier tubes which amplify the resulting spectrum.
- **Computer:** The detectors are connected to the computer to get the desired output [217, 218].

A Perkin Elmer Lambda 35 UV-Vis spectrophotometer was used for the measurement. The peak positions were evaluated using Gaussian peak fitting. The samples were prepared both in water and methanol.

### Fourier Transform Infrared Spectroscopy

Fourier Transform Infrared Spectroscopy (FTIR) is a valuable tool for identification and characterization of compounds or functional groups present. The FTIR spectra of pure compounds are considered to be molecular fingerprint. Unknown compounds can be identified by comparing their spectra with those to a library of known compounds.

Infrared spectroscopy (IR) is based on the principle that chemical bonds in a molecule vibrate at specific frequencies. The infrared region of the electromagnetic spectrum have frequencies in the range  $\sim 4000 \text{ cm}^{-1}$  to  $\sim 600$



$\text{cm}^{-1}$ . When a molecule is exposed to infra-red rays, it absorbs at characteristic frequencies but transmits all other frequencies. The difference of charge in the electric fields of atoms in a molecule produces a net dipole moment. Due to this net dipole moment the molecules interact with the infrared photons causing excitation to higher vibrational states. Each interatomic bond vibrates with different vibrations (stretching or bending) yielding different infrared spectrum [219]. Functional groups are thus detected by identifying the characteristic frequencies as an absorption band in the infrared spectrum. The vibrational frequency is given by:

$$\nu = \frac{1}{2\pi} \sqrt{\frac{k}{\mu}} \quad (3.9)$$

where  $k$  is the force constant and  $\mu$  is the reduced mass.

The infrared spectrum of a molecule is divided into functional group region ( $4000 \text{ cm}^{-1}$  to  $1500 \text{ cm}^{-1}$ ) and fingerprint region ( $1500 \text{ cm}^{-1}$  to  $400 \text{ cm}^{-1}$ ). The bending vibrations are associated with the finger print region whereas the functional group region include stretching vibrations [220]. Strong peaks are generally produced by stretching vibrations than bending. Conversely, weaker bending mode of vibration can be helpful in discriminating similar types of bonds like aromatic substitution. The different components of an FTIR spectrometer are shown in Figure 3.15.

- **Source:** The radiation source consists of an inert solid electrically heated to  $1000 \text{ }^{\circ}\text{C}$  to  $1800 \text{ }^{\circ}\text{C}$ . The different types of sources used are Globar (constructed of silicon carbide), Nernst glower (constructed of rare-earth oxides) and Nichrome coil. These sources produce continu-

ous radiation with varying radiation energy profiles.

- **Interferometer:** The radiation produced passes through the interferometer. The radiant beams are divided due to changes in the relative position of the moving mirror to the fixed mirror generating an optical path difference between the beams producing repetitive interference signals. The resulting beam thus passes through the sample.
- **Sample:** The beam from the interferometer enters the sample where specific frequencies of energy characteristic of the sample get absorbed.
- **Detector:** The beam from the sample passes to the detector. The frequently used detectors consist of mercury cadmium telluride and triglycine sulphate. The detector detects time domain signal which gets converted into frequency domain spectrum with the help of Fourier transform.
- **Computer:** The measured digitized signal from the detector is sent to the computer for Fourier transformation and is presented as an infrared spectrum.

FTIR is a time domain (i.e. radiant power data is recorded as a function of time) spectroscopy where all the frequencies are examined simultaneously. The measurement performed with FTIR gives high resolution better accuracy and high signal to noise ratio. IR spectroscopy can study any sample in any state (liquid, powders, films etc.).

The presence of different functional groups in the plant extracts were analyzed using Bruker, Germany/ Alpha FTIR spectrometer. Before measure-

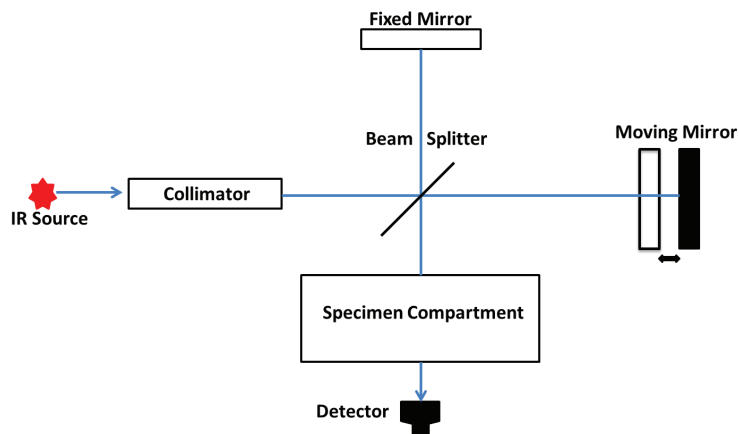


Figure 3.15: Schematic diagram of FTIR Spectrometer.

ments the instrument was calibrated against air. The spectra were obtained between  $4000\text{-}400\text{ cm}^{-1}$  with a resolution of  $4\text{ cm}^{-1}$ .

### Gas Chromatography-Mass Spectrometry

Gas Chromatography-Mass Spectrometry (GC-MS) is an analytical technique to detect and identify various substances within the sample that combines the separation properties of gas-liquid chromatography with the detection features of mass spectrometry [221].

GC-MS consists of two main components. GC is a type of chromatography which uses carrier gas such as helium or nitrogen as the mobile phase. The capillary column consists of a fine solid support coated with a nonvolatile liquid as a stationary phase. The stream of helium gas helps the sample to pass through the column. Different components present in the sample take different times to pass through the column resulting in the separation of the components. The MS acts as a detector for GC. The sample exiting the GC column gets fragmented by ionization. It generally uses electron impact and

chemical ionization techniques. The fragments thus obtained are sorted by mass to obtain a fragmentation pattern also referred as a molecular fingerprint. The fragmentation pattern of given sample is unique thus identifying the characteristic property of that component.

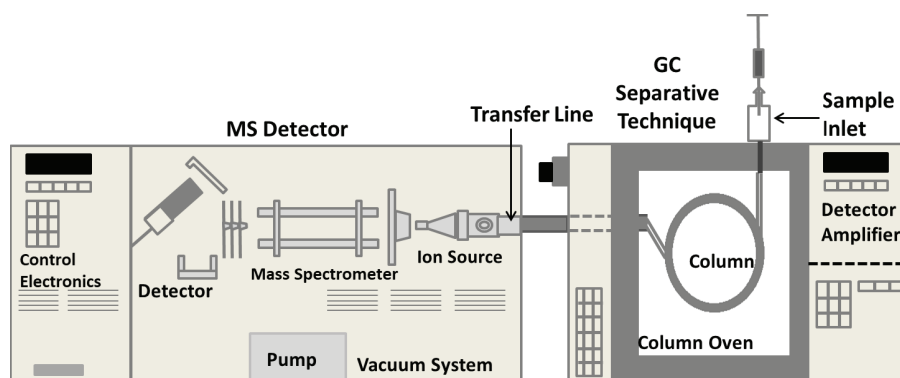


Figure 3.16: Schematic diagram of Gas Chromatography Mass Spectrometry.

Thus GC-MS fragments and identifies the analyte on the basis of its mass to charge ratio ( $m/z$ ). A specific spectral peak is obtained by each component present in the sample. Retention time is taken as the time elapsed between injection and elution of sample which helps to distinguish various components in the sample. The quantity of sample present depends on the size of the peaks measured from the baseline to the tip of the peak. The spectra thus obtained is stored in the computer and then analyzed. GC-MS system is shown in Figure 3.16.

GC-MS was carried out on a 7890 Agilent Gas Chromatograph coupled to a mass spectrometer 240-MS/4000 MS. Agilent CP8994 column composed of 5% phenyl methyl with a capillary J and W VF-5ms, measuring  $30 \text{ m} \times 0.25 \text{ mm} \times 0.25 \mu\text{m}$  was used at  $325^\circ\text{C}$ . Helium gas at a flow rate of  $1 \text{ ml/min}$  was used as a carrier gas. The injection volume of the sample was  $1 \mu\text{l}$  with

a split ratio 20:1. Inlet temperature was maintained at 250 °C. The temperature of the oven was programmed initially at 50°C for 2 minutes, with an increase of 10°C/minutes to 250°C for 5 minutes. The mass range was from 30 to 650 m/z. The total running time for a sample was about 32 minutes. GC-MS was analyzed using electron ionization system with ionization energy 70 eV. The data was evaluated using total ion count for compound identification and quantification. Spectra of the components were compared with the database of spectrum of known components stored in the GC-MS library. Identification of the components and interpretation of GC-MS data was conducted using data base obtained from National Institute of Standard and Technology (NIST). The retention time, molecular formula, molecular weight of the plant samples were obtained. This work was performed at Metagenepro Tech, Hyderabad.

### 3.2.5 Forced Drainage Experiment

Aqueous foam consists of a dense packing of gas bubbles in a small amount of surfactant solution. The liquid fraction is an important structure parameter for studying the properties of foam [80]. Dry foam has a low liquid fraction while wet foam has a high liquid fraction. In aqueous foam there exists a small amount of surfactant solution in interstitial channels between the bubbles. Large density difference in the gas causes the liquid to drain out of the foam due to gravity. This phenomena of flow of the liquid due to gravity and capillarity is called drainage. Drainage thus influences the liquid fraction of a foam which is important for its stability. It is thus a complex physico-

chemical hydrodynamic process [222]. Studies on foam drainage contributes to improve industrial processes like recovery of oil, metallic foam productions, refining of ores, brewing and separation technology [77]. Forced foam drainage consists of constantly pouring a surfactant solution into a foam at a constant flow-rate. The liquid flows through network of channels between bubbles as a result of gravity and capillarity [80].

Preliminary one-shot forced drainage in one and two-dimensions have been performed in my M.Phil. work. This work is an extension of the previous work. Here drainage wave is investigated with smaller bubble size, higher concentration of the surfactant solution as well as high resolution camera using two natural surfactant systems *Sapindus mukorossi* and *Acacia concinna*. Using the gray scale as the indication of liquid fraction, we have studied the drainage profile as well as the shape of the drainage pattern.

### One-Shot Two-Dimensional Forced Drainage

One-shot two-dimensional forced drainage was studied as described by Hutzler et al. [13] with a slight modification at room temperature. The experiment was performed using a Hele-Shaw cell. The cuboidal glass cell was made by fixing four rectangular glass plates, as shown in Figure 3.17. The cell is 26.7 cm high, 15.0 cm wide and 10.8 cm thick.

The surfactant solutions were prepared by extracting 300 gm of *Sapindus mukorossi* or 320 gm of *Acacia concinna* in 2500 ml of Milli-Q water. The concentration of *Sapindus mukorossi* and *Acacia concinna* solution were  $4.69 \times 10^{-2}$  g/cc and  $5.25 \times 10^{-2}$  g/cc respectively.

The surfactant solution was poured into the Hele-Shaw cell. Nitrogen

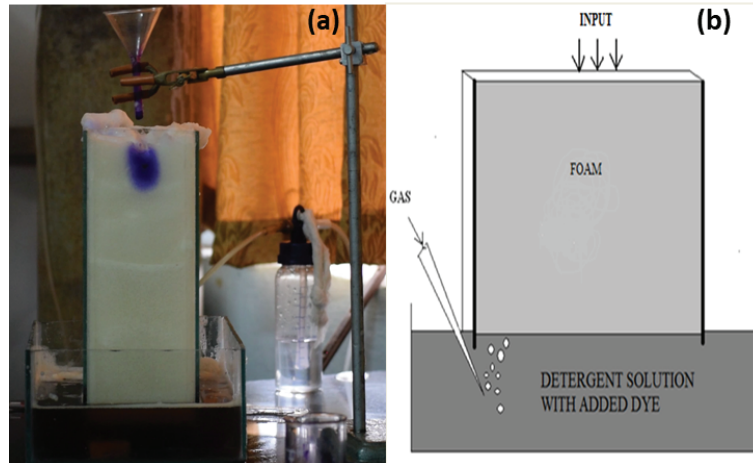


Figure 3.17: (a) Photograph of one-shot two-dimensional forced drainage experiment with *Sapindus mukorossi* solution when 0.5 ml solution was added from top (b) One-shot two-dimensional forced drainage setup.

gas at a flow rate of 2 litre/min was bubbled through a porous glass frit of diameter 30 mm G-1 inside the surfactant solution filling the Hele-Shaw cell with monodisperse foam of small bubbles of diameter approximately 1 mm. The flow of gas was continued until a uniform steady foam was produced.

40 ml of the surfactant solution was taken separately and 1 gm of dye added to it. The solution was thoroughly mixed using a magnetic stirrer. 0.5 ml of this solution was added from the top of the Hele-Shaw cell with the help of a funnel within one second near the center of the cell. The sharp contrast between the blue colour of input solution and white background of dry foam made the drainage wave easily visible [83]. The variation of foam colour was monitored with the help of a digital camera (Nikon D3000, with 24.2 MP) mounted on a stand in front of the cell to provide high quality pictures. The movement of the drainage wave along the vertical and horizontal direction was monitored visually which gave an idea of flow of liquid due

to gravity (vertically) and capillarity (horizontally). The wave velocity both horizontally and vertically along with other parameters were determined.

Analysis of the drainage wave pattern was done using Adobe® Photoshop® 7, by analysing the gray scale value or the intensity represented by K (in CMYK Colour model).

### **3.3 Conclusion**

The experimental details and characterization techniques employed to study the various properties of the natural surfactants extracts have been discussed. Each of the techniques described and the instruments used provides information of the extracts of plant samples which could be correlated to determine the properties of these natural surfactants. Schematic representation of the experimental setup have also been provided and discussed.



## Part III

# RESULTS AND DISCUSSION

# Chapter 4

## Surface and Foam Properties

Keeping in view the environment related problems of synthetic surfactants discussed in Chapter 2, it is desirable to find an alternative. For this search on environmental-friendly alternatives, it is important to investigate the surface activity and foam properties of natural surfactants. This chapter deals with the results obtained from surface tension, foaming, wetting, emulsification, viscosity, pH, conductivity and cleaning experiments of natural surfactants and attempts to provide explanations for the results obtained. Surface activity of synthetic surfactants have also been studied as a reference. In addition, the effect of salt as an additive has been investigated.

### 4.1 Introduction

The wide use of surfactants in various fields lead to the basis of surfactant science being recognised as a separate field [117]. Advancement in surfactant technology lead to the synthesis of huge quantity and variety of surfactants.

Domestic as well as industrial usage disperses these surfactants in diverse sections of the environment imposing serious environmental concerns [23] as discussed in Chapter 2. There is thus an increasing interest in searching safe and green less toxic surfactants [28]. One such alternative could be natural surfactants obtained directly from plants, bacteria, fungi, amides of amino acids or fatty acid esters of sugars [30, 116].

In this work, saponin, a plant-based natural surfactant has been extracted from five plants namely *Sapindus mukorossi*, *Albizia procera*, *Juglans regia*, *Zephyranthes carinata* and *Acacia concinna*. These plants have been traditionally used as cleansing agents in the nearby regions of West Bengal and Sikkim. This is the first ever report on the surfactant activity of *Albizia procera*, *Juglans regia* and *Zephyranthes carinata*. Three commonly used synthetic surfactants Henko, Ezee and Johnson's Baby Shampoo have also been investigated as reference.

## 4.2 Surface Tension Measurements

Surface tension studies is an essential technique to study the surface activity of a surfactant. It is a parameter to study the interactions between surface active and non-surface active components at a surface. Surfactants adsorb at the air-water interface resulting in reduction of surface tension [202, 223].

The details of the surface tension measurements using Wilhelmy plate technique is discussed in Chapter 3. Surface tension decreases with increase in concentration and then remains constant after CMC as shown in Figure

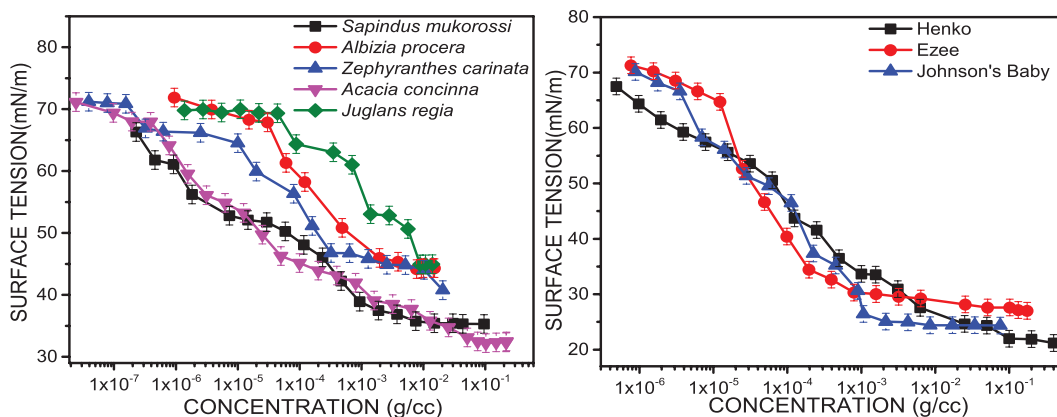


Figure 4.1: Variation of surface tension with surfactant concentration at  $20 \pm 2$  °C.

4.1. The rapid decrease in surface tension is due to the breakage of hydrogen bonds when adsorption takes place at air-water interface resulting in decrease of energy for increasing of interfacial area [90]. Surface tension reduction by the natural surfactants is slightly higher compared to the synthetic ones, as illustrated in Table 4.1. This could be due to slow micellization in water [202].

Reduction of surface tension from 72 mN/m to 32-37 mN/m indicates good surface activity and detergency [224]. This implies *Sapindus mukorossi* and *Acacia concinna* possess good detergency like the synthetic surfactants while *Albizia procera*, *Juglans regia* and *Zephyranthes carinata* show moderate detergency. Lower surface tension helps the washing liquid to penetrate into the fibre and completely wet it [90].

On further increasing the concentration beyond CMC, surfactants form micelles [2]. Addition of more surfactants contributes only to micelle formation, the surface tension remains constant. Many properties change on crossing the CMC, thus making it an important parameter [225]. Table 4.1

Table 4.1: Surface properties of surfactants at  $20 \pm 2$  °C.

Surfactants	CMC (Surface Tension) (g/cc)	Reduced Surface Tension (mN/m)	Corresponding Concentration (g/cc)	Effectiveness (mN/m)	CMC (Conduc- (-tivity) (g/cc)
<i>Sapindus mukorossi</i> Gaertn.	$7.50 \times 10^{-3}$	$35.30 \pm 0.2$	$9.50 \times 10^{-2}$	$36.70 \pm 0.2$	$2.00 \times 10^{-2}$
<i>Albizia procera</i> (Roxb.) Benth.	$7.00 \times 10^{-3}$	$44.33 \pm 0.2$	$1.51 \times 10^{-2}$	$26.67 \pm 0.2$	$2.00 \times 10^{-3}$
<i>Zephyranthes carinata</i> Herbert	$6.40 \times 10^{-4}$	$40.76 \pm 0.2$	$2.05 \times 10^{-2}$	$31.24 \pm 0.2$	$6.00 \times 10^{-3}$
<i>Acacia concinna</i> DC.	$7.00 \times 10^{-2}$	$32.35 \pm 0.2$	$2.20 \times 10^{-1}$	$39.65 \pm 0.2$	$7.00 \times 10^{-3}$
<i>Juglans regia</i> Linn.	$8.80 \times 10^{-3}$	$44.95 \pm 0.2$	$1.40 \times 10^{-2}$	$27.05 \pm 0.2$	$1.00 \times 10^{-3}$
Johnson's Baby Shampoo	$2.00 \times 10^{-3}$	$24.35 \pm 0.2$	$7.56 \times 10^{-2}$	$47.65 \pm 0.2$	$7.00 \times 10^{-3}$
Ezee	$7.97 \times 10^{-4}$	$21.01 \pm 0.2$	$1.75 \times 10^{-1}$	$50.99 \pm 0.2$	$3.00 \times 10^{-3}$
Henko	$1.00 \times 10^{-1}$	$21.20 \pm 0.2$	$4.00 \times 10^{-1}$	$58.80 \pm 0.2$	$1.00 \times 10^{-3}$

shows the CMC of surfactants. The values are comparable to CMCs of other natural surfactants [226]. Slow micellization in water of *Acacia concinna* and *Sapindus mukorossi* is responsible for efficient surface tension reduction. Greater surface tension reduction of *Acacia concinna* and *Sapindus mukorossi* indicate that surfactants pack closely at the air-water interface, similar to the synthetic surfactants [227]. All the surfactants exhibited low CMC except *Acacia concinna* and Henko. This indicates that micellar solubilization begins at a higher concentration for these surfactants. Natural surfactants consist of a large number of surfactant molecules having varying molecular structures. This changes the hydrophobicity of the molecules and in turn the CMC. Ionic surfactants exhibit a higher CMC attributed to ion-ion repulsion of the head groups [226].

Surface pressure or effectiveness  $\pi_{CMC}$  is defined as

$$\pi_{CMC} = \gamma_0 - \gamma \quad (4.1)$$

where surface tension of pure water is taken as  $\gamma_0$  and of surfactant solution as  $\gamma$ . The efficiency of surfactant adsorption at the air-water interface can be estimated by  $\pi_{CMC}$  [228]. Thus *Acacia concinna* and *Sapindus mukorossi* show greater effectiveness similar to the synthetic surfactants. Moderate effectiveness is shown by *Albizia procera*, *Juglans regia*, and *Zephyranthes carinata* (Table 4.1).

### 4.3 Surface Wetting Measurements

Surface wetting is a vital parameter depending on surface tension, concentration, nature of the surface to be wet and diffusion. It is a complex phenomena playing an important role in the removal of oils, dirt and grease. Reduced surface tension of the surfactant solutions enhances the penetration of liquid through the surface and wet it completely [36]. Wetting behaviour is important in cleaning.

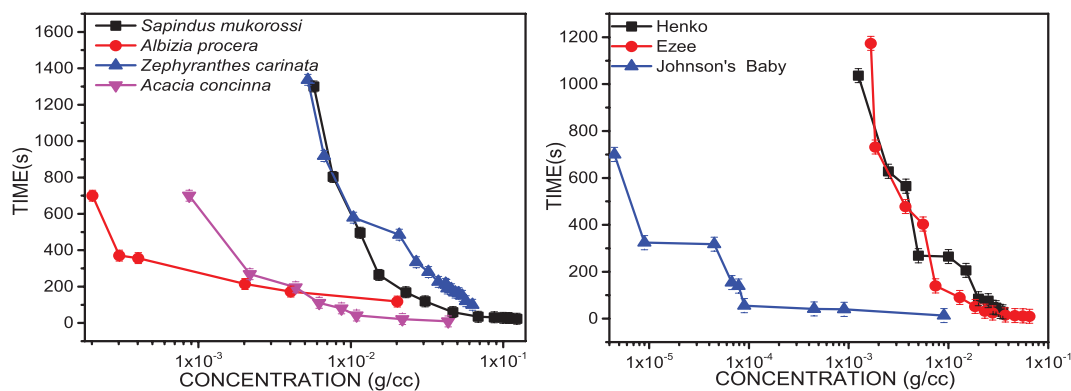


Figure 4.2: Wetting time of surfactant solutions at  $20 \pm 2$  °C.

Figure 4.2 illustrates the wetting time of surfactant solutions. Good wetting was shown by *Albizia procera* and *Acacia concinna* similar to synthetic surfactants. Moderate wetting was shown by *Sapindus mukorossi* and *Zephyranthes carinata*. Qualitatively, the wetting behaviour of natural surfactants was similar to synthetic surfactants.

Good wetting indicates sufficient reduction of surface tension and enhanced penetration into the surface. The results are in good agreement with surface tension measurements for most surfactants. Interestingly, *Juglans regia* did not exhibit any change in wetting ability from pure water even

though the surface tension reduced significantly. The wetting results for *Albizia procera* and *Sapindus mukorossi* were not in good agreement with the surface tension results. This signifies that wetting is a complex phenomena governed by other factors and not only by surface tension.

## 4.4 Foaming

Foaming ability and stability is an essential property in detergent evaluation of surface active substances. Formation of foam requires creation of new interfaces. High surface elasticity and viscosity leads to rapid absorption at the interfaces and hence high foaming power [229].

### 4.4.1 Foaming Ability

This study was conducted in my previous work in M.Phil. For the sake of completeness the results have also been incorporated. Foaming was studied using Bikerman's methods and Bartsch test as described in Chapter 3. The foaming behaviours of the surfactants are illustrated in Figure 4.3.

Good quality thick foam was produced by *Sapindus mukorossi* and *Acacia concinna*, similar to synthetic surfactants. This may be due to large amount of saponin present helping the reduction of surface tension and creation of large surface area required for foaming [90].

It is observed that foaming power increases with increase of surfactant concentration. This is due to the presence of more surfactant in the films to stabilize the foam [25]. Similar foaming trend was seen by both tests (Figure 4.3). Bikerman's method produced large amount of foam compared



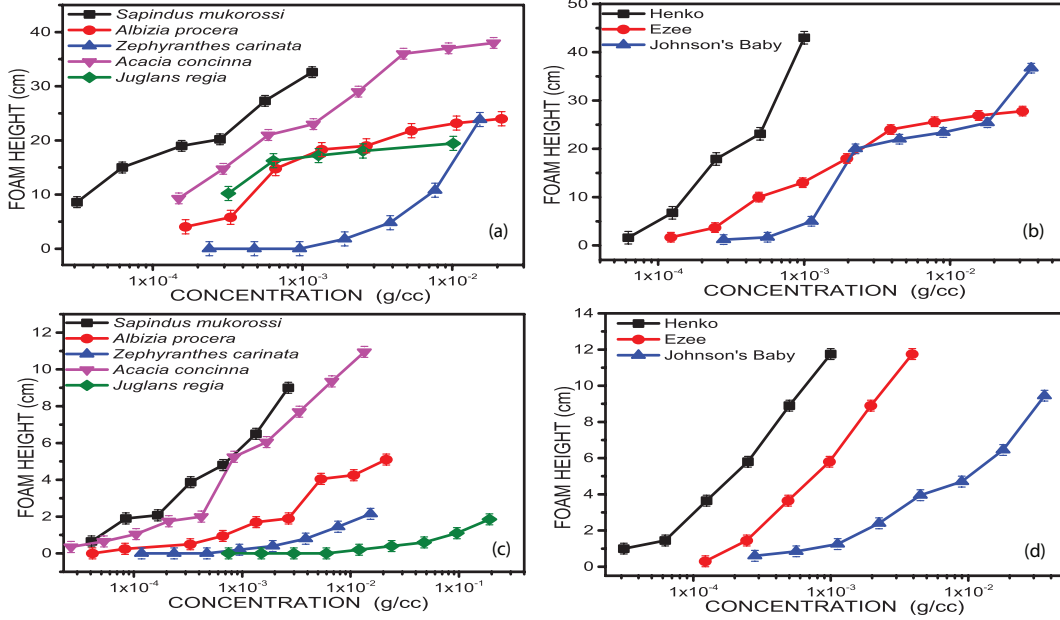


Figure 4.3: Foaming behaviour of surfactant solutions (a),(b) Bikerman's method (c),(d) Bartsch test at  $20 \pm 2$  °C.

to Bartsch test as it involved more gas.

#### 4.4.2 Foam Stability

Foam is an unstable system and is prone to rupture and decay. The stability of foam is defined by the  $R5$  parameter given by

$$R5 = \frac{h_5}{h_0} \times 100 \quad (4.2)$$

where maximum foam height is  $h_0$  and foam height at 5 minutes is  $h_5$ . An  $R5$  value of 50 % gives the cut-off between low stability foam and metastable foam. Figure 4.4 shows the variation of  $R5$  parameter with concentration. *Acacia concinna* and *Sapindus mukorossi* showed a sharp transition from

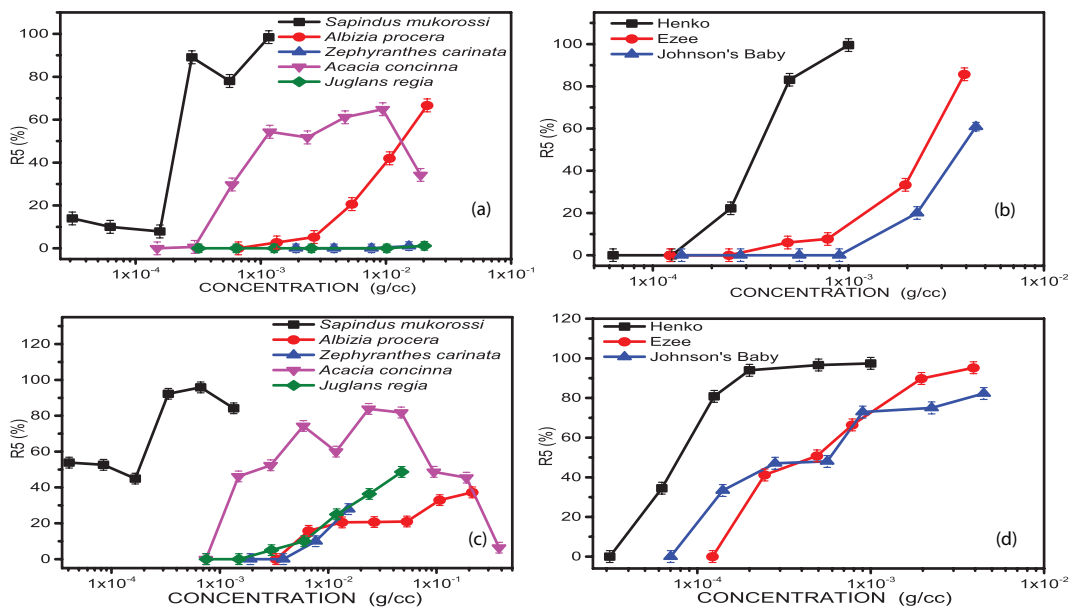


Figure 4.4: Variation of  $R_5$  value with surfactant concentration (a),(b) Bikerman's method (c),(d)Barstch test at  $20 \pm 2$  °C.

low stability to metastable foam, similar to synthetic surfactants. This is not observed in *Albizia procera*, *Zephyranthes carinata* and *Juglans regia*. This implies *Acacia concinna* and *Sapindus mukorossi* produce more stable foam than other natural surfactants.

The cut off concentration for Bikerman's method is higher than for Barstch test, which may be due to variations in the mechanisms of foam formation (Figure 4.4). In the Bikerman's method, a large amount of air is abruptly introduced into the liquid resulting in a lot of foam. The foam is unstable because enough surfactant is not able to adsorb at the interfaces. Introduction of a small amount of air in the Barstch test results in less foam. Here the vigorous shaking moves a large amount of surfactant molecules to the interfaces, making the foam stable.

### 4.4.3 Effect of Salt on Foaming

The effect of salt on foaming was studied for my Ph.D. In many commercial products, salts are added to surfactant solution to increase viscosity. As high viscosity stabilizes the foam and these two parameters are interrelated, the effect of salt on foaming ability and stability was investigated below CMC, at CMC and above CMC.

#### Below and at CMC

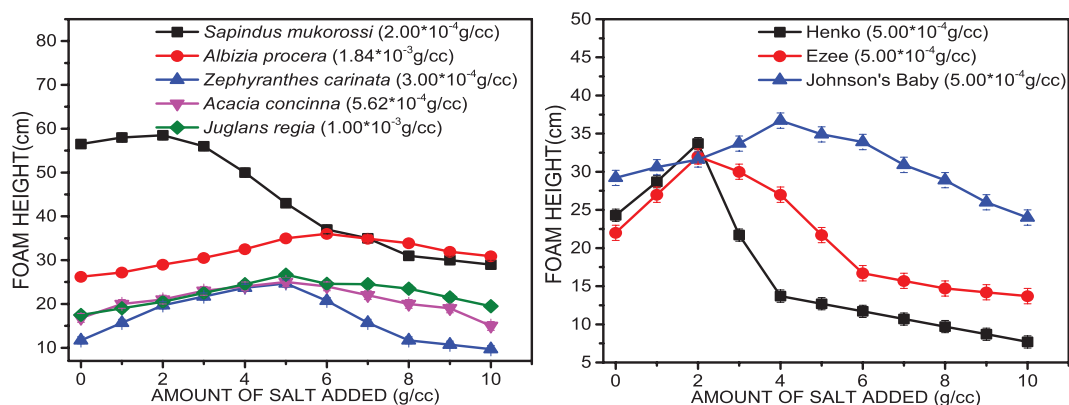


Figure 4.5: The effect of salt on foam height below CMC at  $20 \pm 2$  °C.

Figures 4.5 and 4.6 illustrate the profile of foaming ability of surfactant solutions at different salt concentrations. The foaming ability increases with salt concentration up to a concentration after which it decreases, both below and at CMC. Increase in foaming ability indicates improvement in surfactant adsorption in the presence of salt.

When salt is added to a surfactant solution below CMC, it tends to come to the interface with the surfactant molecules. This reduces the repulsion between the surfactant molecules. More surfactant molecules can be accom-

modated at the surface, thereby reducing the surface tension. Increase in salt concentration results in a more efficiently packed surfactants. This decreases the repulsion between two monolayers which are on two sides of a film. This leads to more structured liquid in the lamella, having higher viscosity and lower film drainage rate [230].

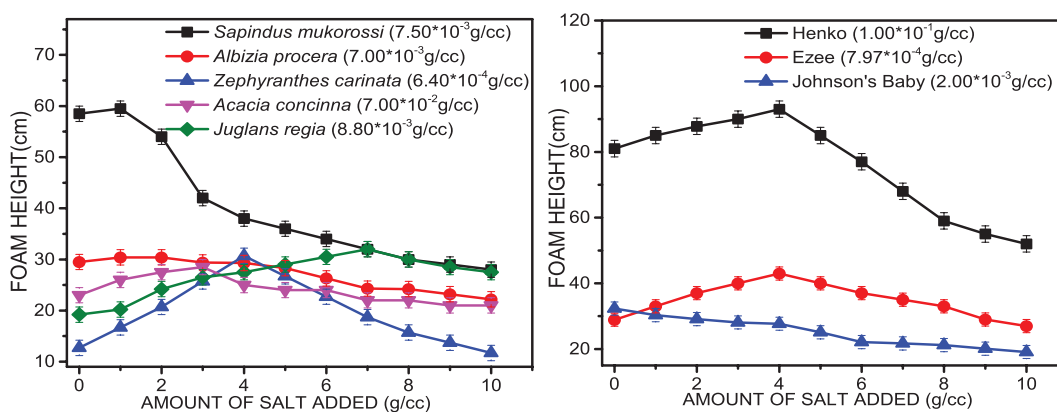


Figure 4.6: The effect of salt on foam height at CMC at  $20 \pm 2$  °C.

The increase in foaming with the addition of salt is concentration dependent. Henko, Ezee and *Zephyranthes carinata* showed similar behaviour. The maximum amount of salt concentration after which foaming decreases was 4 g/cc for these surfactants. At higher salt concentration, foaming decreases. This decrease may be due to high ionic strength which reduces the Coulombic forces in the molecules [231]. At higher salt concentration, the double layer repulsion of the film gets reduced due to which the surfactants move closer to each other. They may either be attracted by Van der Waal's forces or be repelled due to electrostatic repulsion. During the formation of film, large amount of charge leads to charge repulsion and reduced surfactant molecules at the air-water interface which leads to decrease in surface viscosity and

foam stability [232].

As seen from Figures 4.5 and 4.6, salt concentration decreased the foaming ability of the surfactants. *Sapindus mukorossi* and Henko showed a more distinct decrease in foaming ability compared to other surfactants both below and at CMC. The behaviour shown by ionic and non-ionic surfactants are similar to those observed by other workers [233].

### Above CMC

The addition of salt depresses foaming for both natural and synthetic surfactants beyond CMC as shown in Figure 4.7. This decrease may be due to the formation of micelles which enhances the electrostatic repulsion between the adsorbed and non-adsorbed molecules. This results in reduced adsorption at the air-water interface and decreases foaming. Decrease in foam height was more prominent in *Sapindus mukorossi* and *Acacia concinna*, similar to synthetic surfactants.

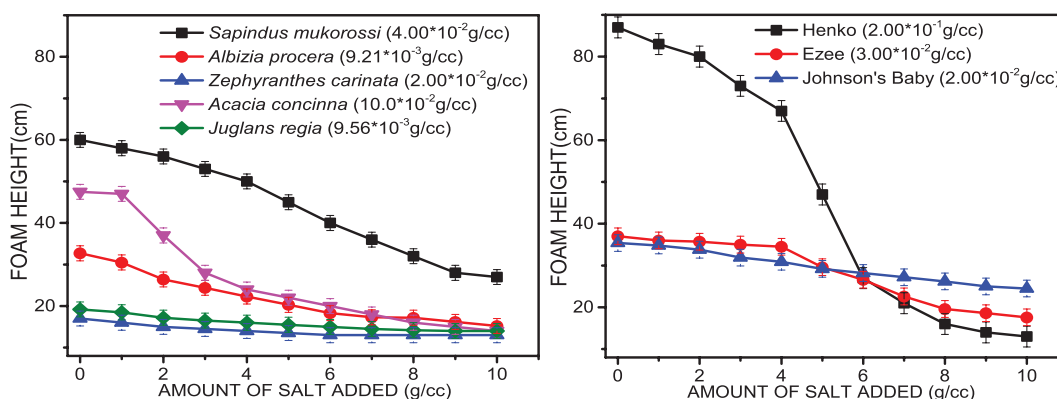


Figure 4.7: The effect of salt on foam height above CMC at  $20 \pm 2$  °C.

#### 4.4.4 Effect of Salt on Foam Stability

The effect of salt on stability of foam was evaluated by calculating the  $R5$  value.

##### Below and at CMC

Figures 4.8 and 4.9 illustrate the behaviour of foam when salt was added below and at CMC. It was observed that the  $R5$  value decreases with increasing concentration of salt. The foam disappeared at a faster rate than pure surfactants solutions.

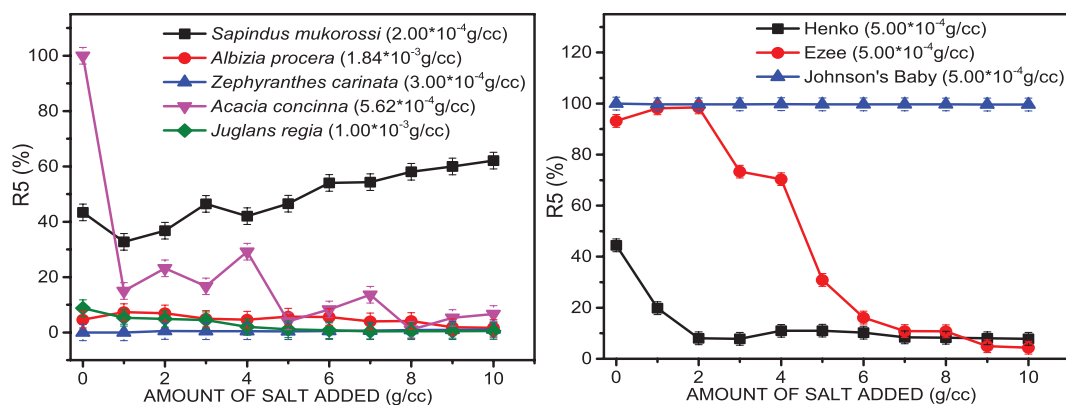


Figure 4.8:  $R5$  as a function of added salt concentration below CMC at  $20 \pm 2$  °C.

Salt had a negative effect on stability of foam of *Acacia concinna*, *Juglans regia*, *Albizia procera* and *Zephyranthes carinata* similar to two synthetic surfactants. However, the stability of Johnson's baby Shampoo was not affected by salt. *Sapindus mukorossi* exhibited a different behaviour, the stability decreased and then increased with the addition of salt. Decrease in stability may be attributed to a decrease in hydrophobic forces between air bubbles.

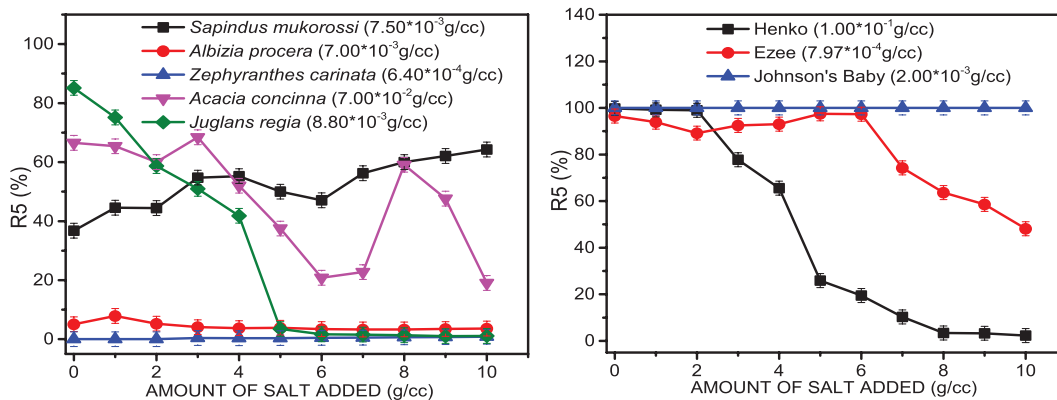


Figure 4.9:  $R_5$  as a function of added salt concentration at CMC at  $20 \pm 2$  °C.

Above CMC

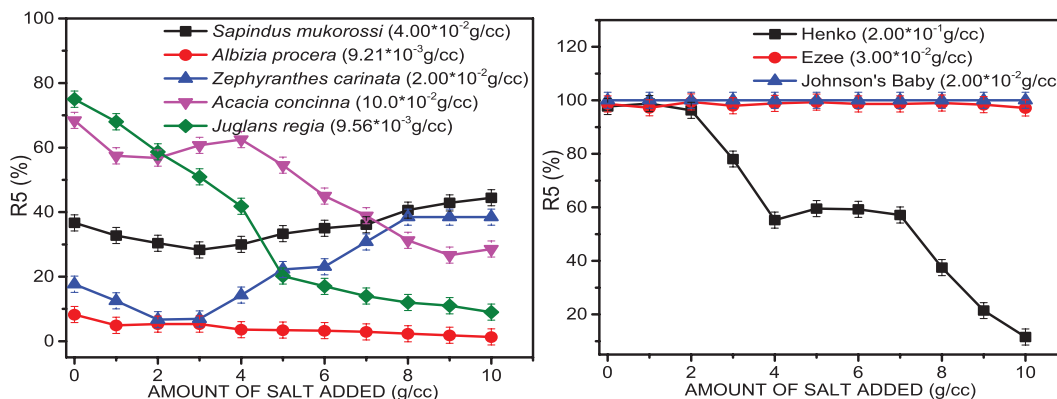


Figure 4.10:  $R_5$  as a function of added salt concentration above CMC at  $20 \pm 2$  °C.

The effect of salt on the stability above CMC was very different as shown in Figure 4.10. Ezee and Johnson’s Baby Shampoo’s were not affected by the addition of salt. This may be due to positive surface elasticity or Gibbs-Marangoni effect.

The foam stability of *Sapindus mukorossi* and *Zephyranthes carinata* decreased and then increased. These results can be attributed to a rapid de-

crease in hydrophobic forces between air bubbles. The foam stability of Henko, *Acacia concinna*, *Juglans regia* and *Albizia procera* decreased with the addition of salt, which may be attributed to a decrease in the electrostatic repulsion in foam films at high electrolyte concentrations. Decreased stability may also be due to increased drainage rate due to disproportionation and bubble coalescence immediately after foam formation [234].

## 4.5 Emulsification

Surfactants diffuse in oil-water interface and reduce the interfacial tension. Thus less energy is required at oil-water interface to form an emulsion. Surfactants are thus widely used as emulsifiers to stabilize emulsion droplets [235]. The emulsifying power of surfactants was evaluated using the procedure described in Chapter 3.

Figure 4.11 shows emulsifying behaviour of surfactants. Higher concentrations of *Sapindus mukorossi* produced very stable emulsions. This emulsion did not separate for almost 2 hours. Emulsion stability increases with increase in concentration, decreases and then increases again. The region at which the stability decreases is the region where micelles begin to form, as confirmed by surface tension measurements.

The low emulsion stability at low concentrations is probably due to less adsorption of surfactants at the oil water interface [236]. At very high surfactant concentrations, emulsion stability decreases as a result of rapid droplet coalescence [237]. *Sapindus mukorossi* exhibited higher stability of emulsions, followed by *Zephyranthes carinata* and *Acacia concinna*. Some of these nat-



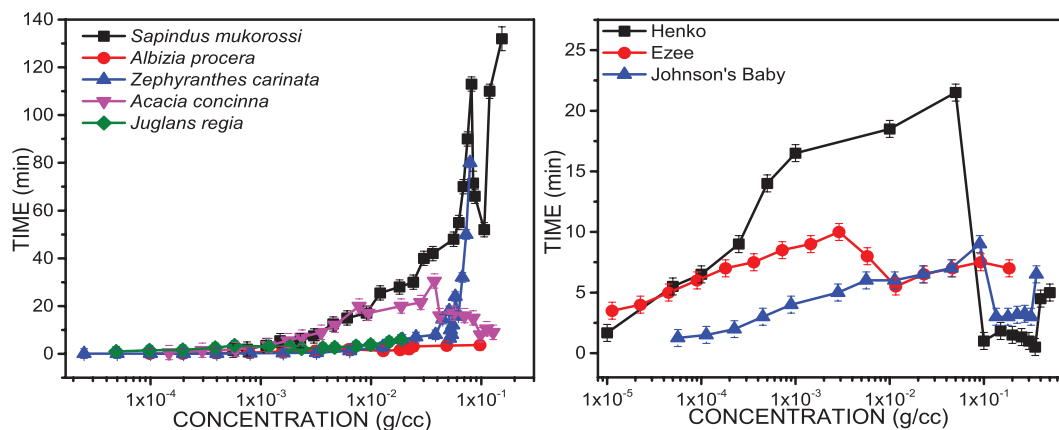


Figure 4.11: Emulsion stability of surfactant solutions at  $20 \pm 2$  °C.

ural surfactants showed better emulsifying properties compared to synthetic surfactants. Stable emulsions are produced when surfactant adsorption produces repulsive interactions between the droplets thereby providing an energy barrier against rupture [202].

## 4.6 pH Measurements

The pH of surfactant solutions were examined as described in Chapter 3. pH of a solution similar to human skin ( $\sim 5.5$ ) causes lesser damage to the skin and hair. Study of the pH of surfactant solutions is important as the net charge on the molecule and the repulsive force between them changes with pH [24].

It is observed from Figure 4.12 that *Acacia concinna*, *Sapindus mukorossi*, *Zephyranthes carinata* are acidic. This acidic nature accounts for hydrolysis of non-ionic glucuronic groups [137]. *Albizia procera* and *Juglans regia* showed less acidic characteristics similar to Ezee and Johnson's Baby Sham-

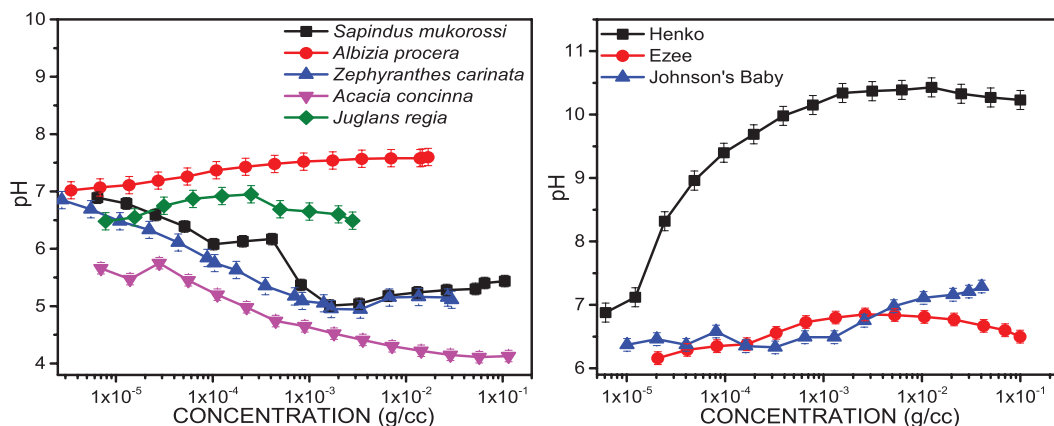


Figure 4.12: Variation of pH with surfactant concentration at  $20 \pm 2$  °C.

poo. Henko showed basic characteristics. The pH of solutions of *Acacia concinna*, *Sapindus mukorossi*, *Zephyranthes carinata* and *Juglans regia* decreased with concentration. An increase was shown by *Albizia procera* similar to synthetic surfactants.

## 4.7 Conductivity Measurements

Conductivity measurements were performed to examine the micellar aggregation behaviour of the surfactants. Figure 4.13 presents the conductivity of surfactant solutions as a function of concentration.

At lower concentrations, the conductivity is low and almost constant. This is attributed to the hydrophilic part of the molecule being enclosed by water molecules resulting in low conductivity. At higher concentrations, conductivity begins to increase rapidly. The increase is generally observed near the regions where micelles start to form. This increase is attributed to more or bigger micelles and intermicellar interaction [117].

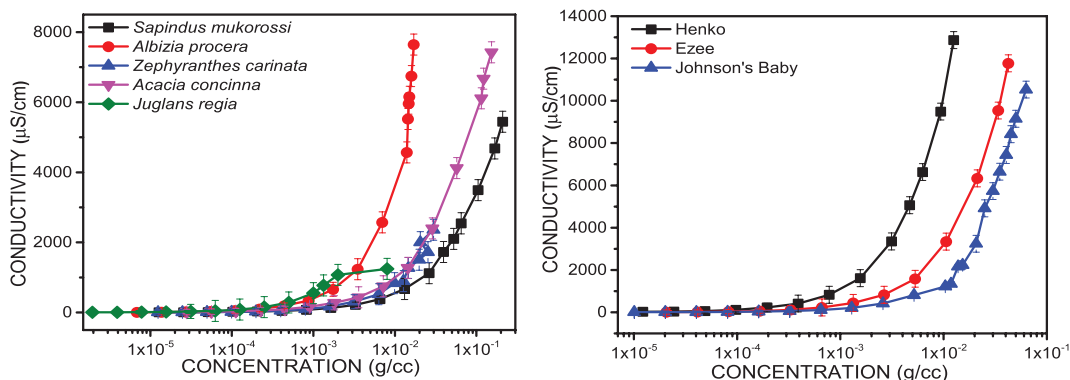


Figure 4.13: Conductivity as a function of surfactant solutions at  $20 \pm 2$  °C.

Conductivity of natural surfactants can also increase due to hydrolysis of glucuronic groups. The conductivities of *Sapindus mukorossi*, *Albizia procera*, *Juglans regia*, *Acacia concinna*, *Zephyranthes carinata* and Johnson's Baby Shampoo increase at a higher concentration than Henko and Ezee. The CMC obtained for *Sapindus mukorossi*, *Zephyranthes carinata*, Johnson's Baby Shampoo and Ezee by conductivity measurements is higher than those with surface tension measurements as illustrated in Table 4.1. This difference is attributed to the presence of surface active impurities that saturates the interface at concentrations below CMC generating a prominent minimum in the surface tension isotherm [238]. Alternatively surface tension gives the concentration at which surfactants stop coming to the surface while conductivity changes occur only when a certain number of micelles have been formed. Thus surface tension gives a lower value of CMC. Surface tension measures surfactant behaviour at the air-water interface. Conductivity measurements are important for evaluating the bulk properties of the solution.

This discrepancy in CMC obtained by different techniques has also been

observed by other workers [226, 239]. However smaller CMC is obtained for *Albizia procera*, *Juglans regia*, *Acacia concinna* and Henko by conductivity method (Table 4.1). Also, the samples studied are extracted from plants having several surfactants. This makes the changes difficult to detect by the surface tension measurements [240].

## 4.8 Viscosity Measurements

Micelle formation affects many physical properties, one of which is viscosity. This parameter depends on the number and size of particles in solutions. Viscosity was measured using the procedure discussed in Chapter 3.

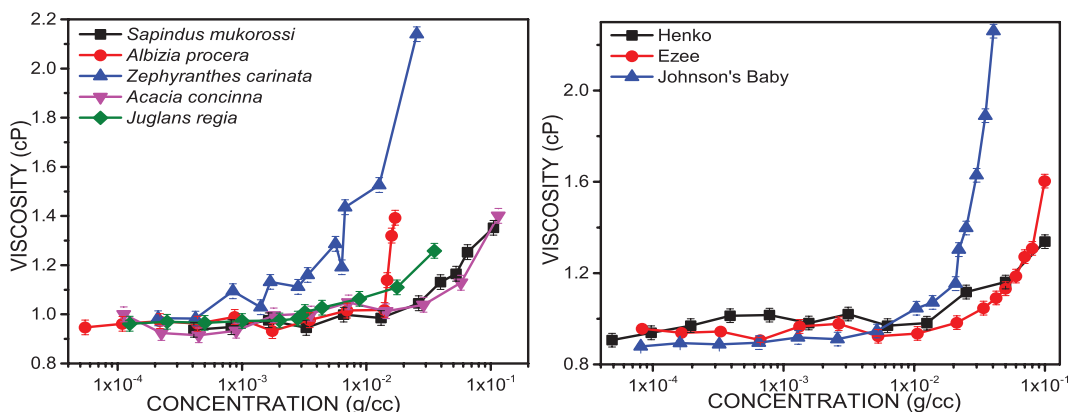


Figure 4.14: Variation of viscosity of surfactant solutions at  $20 \pm 2$  °C.

Figure 4.14 shows the change of viscosities with concentration. All the surfactants showed a similar increase in viscosity with concentration. At higher concentrations, the viscosities rapidly increased.

At low concentrations, molecules are present in the form of monomers. The hydrophilic moieties are enclosed by water molecules. This results in

an increase in viscosity. All the surfactants exhibit a gradual increase in viscosity at lower concentrations.

With increase in surfactant concentration viscosities increase rapidly after a certain point for all surfactants. This rapid increase is probably due to the formation of micelles. The increase in viscosities far beyond CMC, is attributed to more micelle formation and also the interaction between micelles coming close to each other [137, 225].

The maximum viscosity was shown by *Zephyranthes carinata*, which was similar to Johnson's Baby Shampoo. Moderate viscosity was seen for *Albizia procera*, *Juglans regia*, *Acacia concinna*, *Sapindus mukorossi* similar to Henko and Ezee. At lower concentrations, the viscosity of *Zephyranthes carinata* increased rapidly. The concentration at which rapid increase was observed is the region at which micelles begin to form as confirmed by surface tension studies.

#### 4.8.1 Effect of Salt on Viscosity

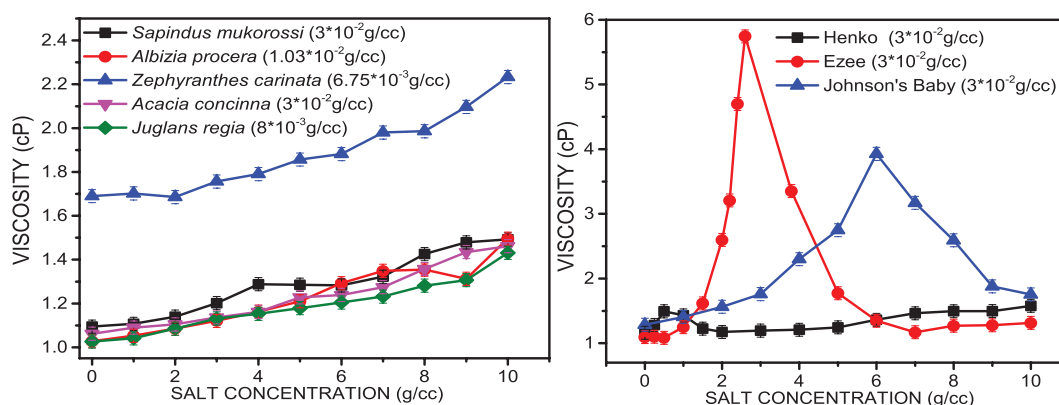


Figure 4.15: Effect of salt on viscosity of surfactant solutions at 20 ± 2 °C.

Presence of electrolytes like salt endorses surfactant adsorption and thus enhances surface viscosity [241]. Additives like salt are important for increasing viscosity in surfactant solutions for ionic surfactants. The effect of salt on the viscosities of surfactant solutions is shown in Figure 4.15. For synthetic surfactants, viscosity increases with increase in salt concentration up to a concentration and then decreases.

Ionic surfactants have a specific charge density. Addition of salt (sodium ions) lowers the charge density of the micelle surface. This reduces the electrostatic repulsion between micelles and they are able to pack closely. This creates a thicker solution, with a higher viscosity. When more salt is added, too much ion causes a higher charge density and the micelles begin to repel each other. This repulsion results in a decrease in viscosity [242].

Addition of salt to the natural surfactants causes a small increase in viscosity. This confirms that natural surfactants are in general non-ionic in nature.

## 4.9 Cleaning

The primary and essential characteristic of a surfactant is the removal of grease, dirt, dust and soil. Cleaning action was studied using the method described in Chapter 3. Figure 4.16 shows the cleaning properties of surfactant solutions. As seen, the trend in cleaning action is similar for all the surfactants, though there is substantial difference in the amount of dirt removed. *Acacia concinna* exhibited a greater cleaning ability similar to Johnson's Baby Shampoo which may be due to sufficient surface tension reduction and

higher wetting ability. Moderate cleaning was seen for *Zephyranthes carinata*, similar to Ezee and Henko.

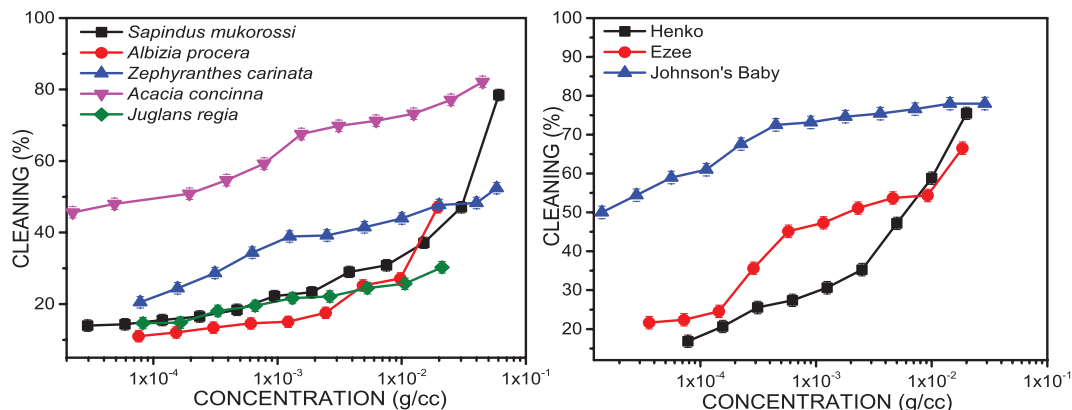


Figure 4.16: Cleaning ability of surfactant solutions at  $20 \pm 2$  °C.

The cleaning ability of *Sapindus mukorossi* shoots up at CMC. This high cleaning ability at higher concentration is due to adequate surface tension reduction. Higher cleaning action was shown by *Zephyranthes carinata* at lower concentrations as compared to *Sapindus mukorossi*. This may be due to early micelle formation. Even though the surface tension of *Sapindus mukorossi* was sufficiently reduced, cleaning ability was moderate due to lower wetting ability. Thus cleaning action is dependent on wetting ability and surface tension. The lower cleaning ability shown by *Albizia procera* and *Juglans regia* is perhaps due to high surface tension and lower wetting ability.

## 4.10 Conclusion

The surface and foam measurements show that natural surfactants are at par with the synthetic ones. Out of these, *Albizia procera*, *Zephyranthes carinata* and *Juglans regia* have been studied for the first time for their surface activity.

The results obtained showed greater surface tension reduction of *Sapindus mukorossi* and *Acacia concinna* indicating good detergency. Moderate detergency was shown by *Albizia procera*, *Juglans regia*, *Zephyranthes carinata*. The pH measurements reveal that *Sapindus mukorossi*, *Acacia concinna*, *Zephyranthes carinata* are acid balanced while *Albizia procera* and *Juglans regia* are less acidic. Foam produced by Bikerman's method is in large amount with lower stability while Bartsch test produces less, but stable foam. This is probably due to different mechanism involved.

Addition of salt on foaming revealed that there exists an optimum limit for maximum foaming below and at CMC. Above CMC, foaming appears to decrease, which is attributed to enhanced electrostatic repulsion between absorbed and non-absorbed particles and also due to reduced adsorption at the air-water interface. Addition of salt showed a negative effect on foam stability below and at CMC except Johnson's Baby Shampoo and *Sapindus mukorossi*. Beyond CMC, different surfactants showed different behaviour.

*Sapindus mukorossi* and *Zephyranthes carinata* showed good emulsifying characteristics and may find industrial applications. All the surfactants showed decrease in emulsion stability in the region of micelle formation. The effect of salt on viscosity is more pronounced for synthetic surfactants. The natural surfactants exhibited a relatively small effect on viscosity on addition of salt. This also showed that the natural surfactants are non-ionic in nature.

The natural surfactants are at par with synthetic surfactants in terms of foaming, cleaning, wetting and show better stability of emulsion and viscosity. Thus these natural surfactants are potential candidates for good surface activity useful for many food and cosmetic industries.



## Chapter 5

# Dirt in Foam: New Approach to Measure CMC

As we saw in Chapter 4, surfactants when added to water form closed structures called micelles at the Critical Micelle Concentration (CMC). The CMC and the formation of micelles are characteristics of surfactants. It is an important parameter for solubilization. This chapter describes the measurement of CMC of surfacants using a Dirt Dispersion (DD) approach. DD or the amount of dirt present in the foam was previously studied only through eye estimation. India ink has been used as a model for dirt. We have quantified the measurement of DD. This leads to a new approach to estimate the CMC of non-ionic surfactants. The CMC obtained from DD is compared to that measured using surface tension. This chapter also attempts to provide explanations of the results obtained.

## 5.1 Introduction

The amphiphilic nature of the surfactants with simultaneous presence of hydrophilic and hydrophobic moieties demonstrate interesting concentration dependent solubilization behaviour in aqueous solutions. The details of surfactants and the formation of micelles has already been described in detail in Chapter 2. Formation of micelles or self-aggregation in solution is responsible for various applications of surfactants like emulsion stabilization, detergency, drug delivery etc [3].

Determination of CMC of surfactant is essential for various applications. Micelles help the surfactant solution to solubilize or mobilize hydrophobic materials. Micelles start to form generally at a lower concentration than CMC. After CMC more and bigger micelles are formed. Studies have shown characteristic changes in many properties of solutions at CMC [243]. Various techniques have been employed to study different physical properties which can differentiate between monomers and micelles [244]. CMCs have been studied using surface tension, density, osmotic pressure [3], light scattering [6], UV-Visible spectrophotometry [245], conductivity [5], viscosity, refractive index [4, 246], fluorimetric method [7], chromatography [247] and nuclear magnetic resonance [248]. The CMC values obtained are found to be slightly different as they detect different aspects of micelle formation [240, 249, 250]. All these methods mentioned above are very sensitive and require sophisticated instrumental techniques and are expensive to perform.

In case of mixed solutions, aggregation is seen between surfactants and non surface active materials. The concentration at which significant aggreg-

ation occurs between a surfactant and a non surface active solute due to electrostatic attraction in the solution is known as Critical Aggregation Concentration (CAC) [251].

Dirt Dispersion, the amount of dirt remaining in the foam is a vital parameter while studying cleansing ability of surfactants. Dirt remaining in the foam is difficult to rinse as it may redeposit at the surface to be cleaned [201]. The efficacy of a surfactant can thus be expressed by the amount of dirt remaining in the foam. It has been observed that inspite of many workers studying DD, it has been conducted at a single concentration and only by eye estimation [15, 16, 206, 252]. The present study quantifies DD as a function of surfactant concentration and uses it to determine the CMC of natural surfactants.

In order to verify the occurrence of aggregation between the surfactants and India ink, the surface tension of *Sapindus mukorossi* solution with and without the same ink concentration was measured.

## 5.2 Dirt Dispersion Measurements

The experimental details of DD measurements is discussed in Chapter 3. This work quantifies DD by investigating it at different concentrations using photography and appropriate image processing software as illustrated in Figure 5.1. By comparing the gray scale of foams I have quantified the DD measurements. This provides an easy approach to study the variation of DD with concentration.

It is observed from Figure 5.1 that all surfactants (natural and synthetic)

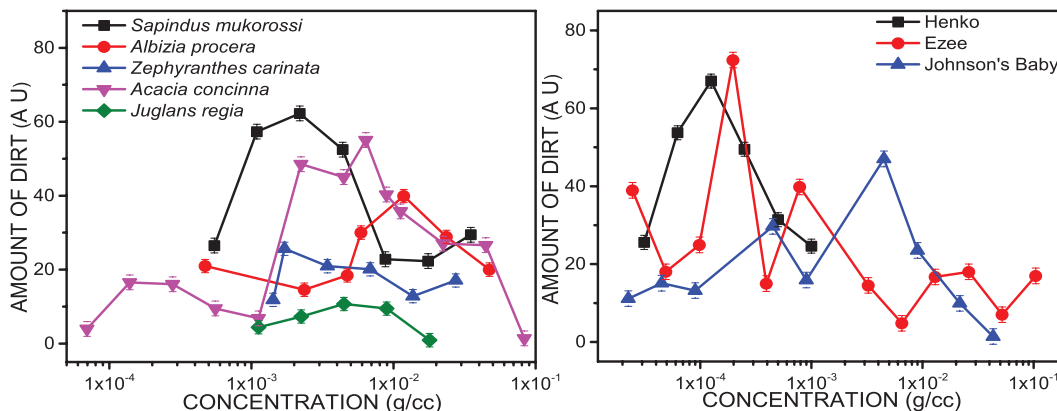


Figure 5.1: Variation of dirt dispersion with surfactant concentration at  $20 \pm 2$  °C.

exhibit a similar trend. The amount of dirt present in the foam is low at very low concentrations. DD increases with increase in concentration, reaches a maximum and then decreases as the concentration increases. The concentration at which DD reaches the maximum is observed to be in the region of micelle formation or CMC.

*Acacia concinna* and Ezee show a pattern where DD increases and decreases twice as concentration is increased. In these cases, the maximum value of DD in foam is taken as the CMC. This increase and decrease pattern may be due to the presence of different types of surfactants. Table 5.1 illustrates the CMC values obtained by the DD approach.

The variation of DD with concentration can be explained as follows. At low concentrations, the foam obtained contains very little surfactant. Thus the foam attracts little dirt. Increase in concentration results in more surfactant in the foam than in solution. Thus the foam attracts more dirt as compared to the solution. This process continues till the formation of micelles or CMC.

Beyond CMC, where the micelles have been formed, the dirt gets suspended in the solution as well as in the foam. This results in a competition between the foam and the solution, as observed by the decrease in dirt attracted towards the foam. Thus DD becomes maximum at the region where the micelles start to form.

Alternately, the ink may probable form complexes with the surfactants above CAC. Thus in the region between CAC and CMC, the absorption in the foam appears high. After this concentrations the ink may probably get solubilized into the micelles and thus do not go into the foam.

### 5.3 Surface Tension Measurements

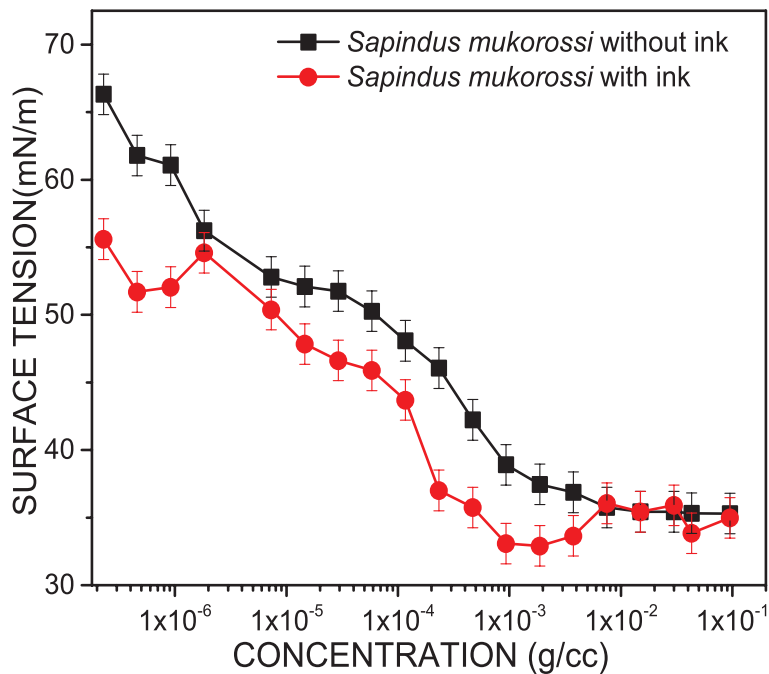


Figure 5.2: Surface tension of *Sapindus mukorossi* with and without ink as a function of surfactant concentration at  $20 \pm 2$  °C.

The surface tension curves illustrated in Figure 4.1 show a break in the region of formation of micelles. As seen, after CMC there is no significant change in surface tension. The CMC values obtained from surface tension measurements are illustrated in Table 5.1.

The effect of India ink on surface tension of a surfactant was studied for *Sapindus mukorossi*. This is illustrated in Figure 5.2. It was observed that the surface tension reduced by around 5 mN/m in the region below the CMC on addition of ink. The reduction is around 10 mN/m, below a concentration of  $2 \times 10^{-6}$  g/cc. Above CMC, there was no significant difference seen. However, the presence of a CAC could not be deduced as no clear pattern was visible.

## 5.4 Comparison of the two methods

The data obtained by the DD method are compared to those obtained by surface tension measurements (Table 5.1). It is observed that the CMC values obtained are close by with some exceptions. *Acacia concinna* and Henko show the maximum deviation in the values, while *Albizia procera* shows the minimum deviation. Nevertheless the values obtained by these two methods are within an order of magnitude with each other except Henko. This may be as the surfactants taken were non-ionic with the exception of Henko. Variation in CMC measured by different techniques have also been observed by other researchers [61, 253].

It is observed that the CMC obtained by surface tension are smaller than those by DD method. This may be due to fact that surface tension gives the

Table 5.1: CMC obtained by dirt dispersion and surface tension method.

S.No	Surfactants	Dirt Dispersion CMC(g/cc)	Surface Tension CMC(g/cc)	Deviation ( $\delta$ )
1	<i>Sapindus mukorossi</i> Gaertn.	$2.20 \times 10^{-3}$	$7.50 \times 10^{-3}$	0.707
2	<i>Albizia procera</i> (Roxb.) Benth.	$1.10 \times 10^{-2}$	$7.00 \times 10^{-3}$	0.364
4	<i>Zephyranthes carinata</i> Herbert	$1.70 \times 10^{-3}$	$6.40 \times 10^{-4}$	0.624
5	<i>Acacia concinna</i> DC.	$6.00 \times 10^{-3}$	$7.00 \times 10^{-2}$	0.914
3	<i>Juglans regia</i> Linn.	$4.50 \times 10^{-3}$	$8.80 \times 10^{-3}$	0.489
6	Johnson's Baby Shampoo	$4.50 \times 10^{-3}$	$2.00 \times 10^{-3}$	0.556
7	Ezee	$1.97 \times 10^{-4}$	$7.97 \times 10^{-4}$	0.753
8	Henko	$1.25 \times 10^{-4}$	$1.00 \times 10^{-1}$	0.999

concentration at which surfactant stops moving up to the surface. However, DD measures the concentration at which dirt starts moving towards the bulk, a point when sufficient micelles have already been formed, giving a higher value of CMC.

Some surfactants such as *Acacia concinna*, Johnson's Baby Shampoo and Henko exhibit a higher CMC by surface tension method. This could be explained as the appearance of smaller macro-structures like dimers, that attract small amounts of dirt. This process is not detected by surface tension measurements [253]. Thus in these cases CMC values are higher for surface tension measurements. It is also to be mentioned that the samples studied are obtained from plants having several surfactants instead of a single surfactant,

thus making the change in surface tension difficult to detect [240]. On the other hand, the maximum obtained in DD is clear, making determination of CMC easier.

Thus DD approach could provide an alternative to other experimental techniques to measure CMC of non-ionic surfactants due to its simplicity and requirement of less amount of sample.

## 5.5 Conclusions

The present study quantifies Dirt Dispersion in foams and studies its variation with concentration for the first time. Our quantification studies show that DD increases, reaches a maximum and then decreases with increase in concentration. The maximum dirt in the foam corresponds to CMC or the region of micelle formation. This new approach of CMC determination is rapid, easy, inexpensive and requires very little sample. The CMC for complex mixtures can also be easily determined, where the surface tension curves are not smooth. It requires only a digital camera and a computer with appropriate software. The information thus obtained is easy to interpret. The CMC values obtained from DD approach are in agreement with those obtained from surface tension measurements. Thus this approach could be an easy low cost method for CMC determination for non-ionic surfactants.



## Chapter 6

# Preliminary Characterization of Natural Surfactants

After investigating the surface and foam properties of natural surfactants in Chapter 4, it is essential to examine their chemical profiles and characterize them. The solvent based extracts were separated using chromatographic techniques and the separated compounds were studied by spectral analysis.

### 6.1 Introduction

In order to introduce natural surfactants as an alternative to synthetic surfactants, a knowledge of the components of natural surfactants (saponin) is necessary. Saponins are a major group of secondary metabolites present in plants as discussed in detail in Chapter 2. They are self-decomposable [34] in addition to having surface activity comparable to synthetic surfactants. Due to their structural complexity saponins exhibit interesting chemical, biolo-

gical and physical properties. Saponins have applications in food processes as a natural surfactant, as a preservative in controlling food spoilage by micro-organisms, as an emulsifying agent. They also have pharmaceutical applications [254, 255].

Various techniques can be employed to isolate and study the saponins present in plant extracts. The most popular and useful tools for this purpose are a combination of chromatography and spectroscopy. In the present study, chromatography methods like Thin Layer Chromatography (TLC), Column Chromatography (CC) and High Performance Liquid Chromatography (HPLC) were used to examine, identify and separate the components present in the methanol extracts. TLC is a simple, quick and inexpensive method that provides an idea of the number of compounds present [208]. By comparing the  $R_f$  value of the unknown compounds with that of known compounds, one can quantify the kind of compounds involved. CC is a purification technique to isolate desired compounds from a mixture [211]. HPLC is one of the most powerful technique to identify the number of components and it relates to the closest match with the reference compounds available as per the database. It is a powerful technique for saponin determination as it can be effectively used for highly polar compounds [214].

Spectral characteristics help to identify compounds by comparing with known data from the literature and various database. Ultra Violet-Visible Spectroscopy (UV-Vis), Fourier Transform Infrared Spectroscopy (FTIR) and Gas Chromatography-Mass Spectrometry (GC-MS) measurements were carried out for this purpose. Preliminary information about the composition of the extracts can be obtained from the UV-Vis spectra. Pharmacologically

active compounds are aromatic in nature and hence show absorption in the UV range. UV-Vis spectroscopy can identify unsaturated bonds [256]. FTIR is a widely used technique for identification of functional groups present [219]. GC-MS is a sophisticated technique for analysis of phyto constituents and structure elucidation of compounds. It has a very high sensitivity of detecting compounds [257].

## 6.2 *Albizia procera*

### 6.2.1 Thin Layer Chromatography Analysis

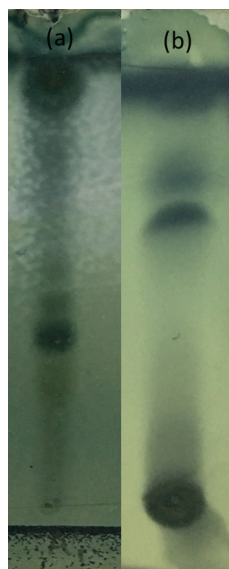


Figure 6.1: TLC plates for methanol extract of *Albizia procera* derivatized with PMA using (a) (Chloroform: Glacial acetic acid: Methanol: Water [8:4:1.5:1]) (b) (Petroleum ether: Ethyl acetate [80:20]).

TLC was performed in methanol extract of *Albizia procera*. Various solvent systems were used for eluting the TLC plates. Good separation was

observed in the solvent system (Chloroform: Glacial acetic acid: Methanol: Water [8:4:1.5:1]) as shown in Figure 6.1(a).

Table 6.1:  $R_f$  value on TLC plate for methanol extract of *Albizia procera* .

Solvent System	No. of spots	( $R_f$ ) Derivatised with PMA
Chloroform: Glacial acetic acid: Methanol:Water (8:4:1.5:1)	4	0.79
		0.53
		0.48
		0.35
PET. Ether:Ethyl acetate (80:20)	2	0.75 0.64

The number of compounds present in the extract was monitored by the number of spots with different  $R_f$  values [192]. TLC did not show any spot when visualised under short wavelength (254 nm) and long wavelength (366 nm). TLC analysis showed four bands when derivatised with PMA. The corresponding  $R_f$  values are shown in Table 6.1. The band with  $R_f$  values 0.79 (bluish green) was due to non-polar compounds while the bands with  $R_f$  value 0.53 (light green), 0.48 (light green) and 0.35 (dark green) were due to polar compounds. The  $R_f$  value of 0.48 indicated the presence of saponin [258, 259, 260, 261]. The long tail like structure above the spot with  $R_f$  value 0.53 indicated the presence of inseparable non-polar compounds.

In order to see the compounds of the uppermost part, a non-polar solvent system (Petroleum ether: Ethyl acetate:[80:20]) was used. Two spots having  $R_f$  value 0.64 and 0.75 were obtained as shown in Figure 6.1 (b).

### 6.2.2 Column Chromatography

The eluted fractions of the methanol extract of *Albizia procera* were separated by CC. 105 fractions were obtained. Five fractions (Figure 6.2) which showed the distinct spots, as monitored by TLC, were analysed with UV-Vis and FTIR. The fraction that showed the best separation was monitored by HPLC. CC was unsuccessful in separating pure components from the extract.

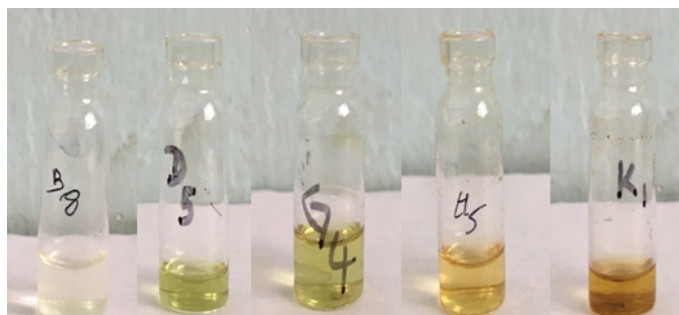


Figure 6.2: Column purified fractions of methanol extract of *Albizia procera*.

### 6.2.3 UV-Visible Spectroscopy

The spectra obtained from UV-Vis provides preliminary information about the nature of compounds present. Figure 6.3 shows the absorbance peaks for the water and methanol extracts and column purified fractions. The UV-Vis analysis is summarized in Table 6.2.

Absorbance peaks shown in the first and second row are in the range of 213 to 247 nm. This absorbance is attributed to  $\pi$ - $\pi^*$  electronic transitions due to presence of C=C multi double bonds in benzene rings. Absorption between 200-400 nm indicates the presence of unsaturated groups [256]. Absorption at 243 nm indicates the presence of carbonyl group/conjugation in

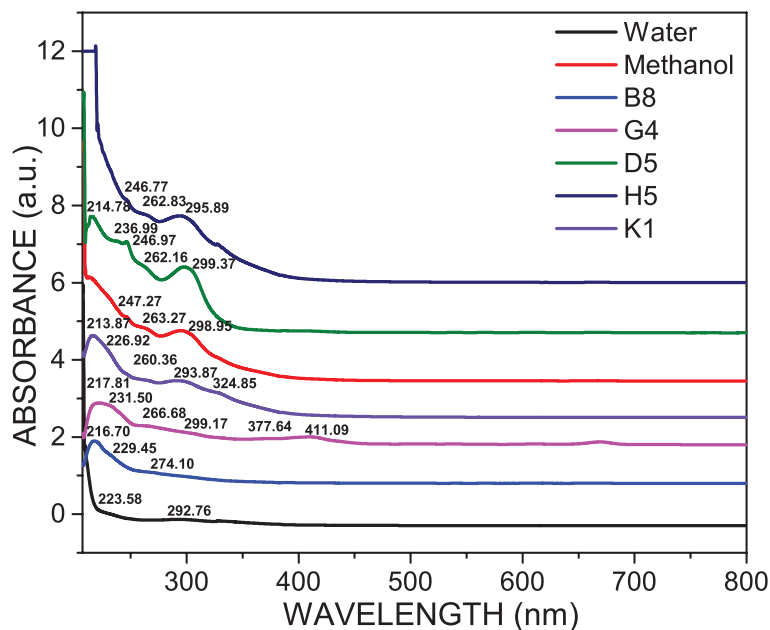


Figure 6.3: UV-Vis absorption spectra for extracts of *Albizia procera*.

the molecules. Saponin shows absorption at 200-250 nm [170, 172, 262]. Some saponins also exhibit absorption in the range of 250-350 nm [263, 264]. Thus absorption around 213 nm to 247 nm are attributed to the presence of saponin (Figure 6.3).

Absorption peaks at longer wavelengths are due to  $n-\pi^*$  electronic transitions due to presence of C=O bonds. The absorption peak in the above range suggests that the compounds in methanol and water extract have chromophores and hence absorption can take place.

Methanol extract and Fraction H5 of *Albizia procera* showed large absorbance which indicated a bigger molecule. Column purified fractions exhibited prominent peaks which were not observed for water and methanol extracts. This may be attributed to efficient removal of impurities during CC. Absorption at 280 nm is considered to be due to the presence of phenolic compounds.

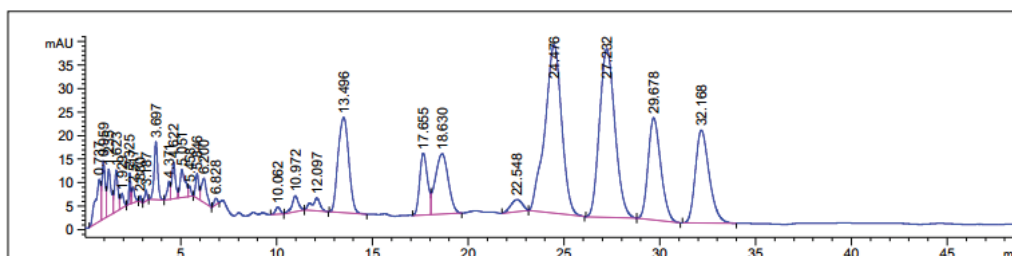
Table 6.2: UV-Vis absorption peaks for extracts of *Albizia procera* .

Water Extract nm	Methanol Extract nm	Fract. B8 nm	Fract. D5 nm	Fract. G4 nm	Fract. H5 nm	Fract. K1 nm
-	-	216.70	217.81	214.78	-	213.87
223.58	247.47	229.45	231.50	236.99	246.77	226.92
-	263.27	274.10	266.68	262.16	262.83	260.36
292.76	298.95	-	377.64	299.37	295.89	299.17
-	-	-	411.09	-	-	324.85

The results also indicated the presence of various aromatic compounds. Absorption in the range of 240-285 nm and 300-500 nm indicates the presence of flavonoids [265].

### 6.2.4 HPLC Analysis

HPLC analysis was carried out for methanol extract of *Albizia procera* and column purified fraction B8. The UV-Vis spectra were employed for choosing appropriate wavelengths for HPLC monitoring. HPLC profile was detected at a wavelength of 200-400 nm using a Diode Array Detector (DAD). The chromatograms obtained at a wavelength of 260 nm are shown in Figures 6.4 and 6.5.

Figure 6.4: HPLC chromatogram for methanol extract of *Albizia procera*.

The elution on HPLC system were performed using methanol-water and acetonitrile-water eluents of various compositions. Acetonitrile-water [50:50, 80:20, 70:30] mobile phase could not adequately resolve the peaks in the sample. Hence a system of methanol and water [50:50] with 0.1 % trifluoroacetic acid (TFA) was chosen as mobile phase at a flow rate 1 mL/min. This solvent system gave better peak separation. Saponins generally contain glucuronic acid moiety that ionizes in aqueous solution causing peak broadening. In order to improve the shape of the peak of glucuronic acid containing saponins, TFA, an ion-suppression reagent was added to the mobile phase. TFA was chosen due to its low UV absorbance making sample detection possible without the drift of baseline [266].

Table 6.3: HPLC for methanol extract of *Albizia procera* .

Methanol Extract		Column Purified Fraction B8	
Retention Time (minutes)	Area (%)	Retention Time (minutes)	Area (%)
10.062	0.2693	1.965	35.6653
12.097	0.8512	2.809	4.0438
13.496	8.2193	17.555	4.0438
17.655	3.9371	21.085	31.0716
18.630	6.2929	-	-
22.548	1.0877	-	-
24.476	22.7861	-	-
27.233	21.0237	-	-
29.678	10.4510	-	-
32.168	10.4128	-	-

Based on the retention time and the availability of peaks the number of compounds could be identified. The retention time and the area of the peak(%) are illustrated in Table 6.3. The methanol extract showed eleven



distinct peaks (Figure 6.4) for retention time 0 to 45 minutes. The peaks before the retention time of 5 minutes could not be separated. There were only eight prominent peaks with significant height and area ( $> 1\%$ ).

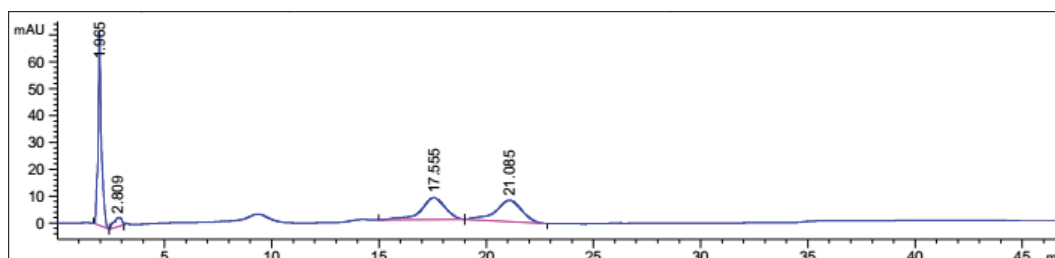


Figure 6.5: HPLC chromatogram of column purified fraction B8 for methanol extract of *Albizia procera*.

As seen from Figure 6.5, in the chromatogram, the column purified fraction contained four peaks indicating that four classes of compounds still exist after purification. This showed that CC could not isolate a particular compound.

A prominent peak (Figure 6.4) for the methanol extract with 22.79 % area was observed at retention time 24.48 minutes, similar to that observed for the isolated fraction (Figure 6.5) at 21.09 minutes. The peaks showing lower retention time upto 14 minutes represent O-H group connected to benzene ring, making it acidic and polar. Peaks showing retention time beyond 25 minutes signify least number of O-H groups attached and hence are non-polar. The compounds that absorb in the UV range may possess chromatophoric groups like phenol, benzene etc.

The peaks in the chromatogram showed the presence of compounds that are thought to represent derivatives of saponin compounds [267]. Peaks with retention time 10-20 minutes signify the presence of saponin [266, 268]. Slight

differences may be due to difference in the HPLC methods. Apart from the prominent peaks, some peaks having area  $< 1\%$  were detected. They could be due to the presence of compounds in small quantities.

### 6.2.5 FTIR Analysis

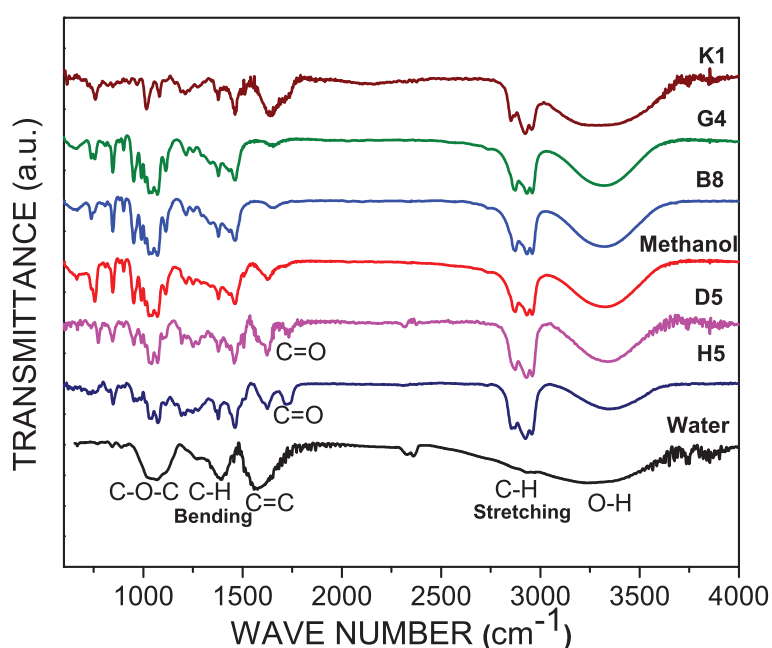


Figure 6.6: FTIR spectra for extracts of *Albizia procera*.

The water, methanol and column purified fractions were analysed with FTIR between 4000 and 500  $\text{cm}^{-1}$ . The results are shown in Figure 6.6. The spectra represent the functional groups of the compounds. The functional groups are allocated based on identification of the spectral peaks and matching the frequency with the corresponding chemical group that absorbs in the mid-infrared region. The various functional groups detected are given in Table 6.4.

Table 6.4: Functional groups present in extracts of *Albizia procera*.

Functional Groups	Water Extract cm <sup>-1</sup>	Methanol Extract cm <sup>-1</sup>	Fract. B8 cm <sup>-1</sup>	Fract. D5 cm <sup>-1</sup>	Fract. G4 cm <sup>-1</sup>	Fract. H5 cm <sup>-1</sup>	Fract. K1 cm <sup>-1</sup>
O-H	3227	3321	3322	3326	3320	3334	3258
C-H Stretching	2931	2959	2957	2962	2960	2955	2954
		2931	2931	2928	2929	2926	2921
		2871	2875	2872	2874	2855	2848
C=O	-	-	-	1731	-	1718	-
C=C	1567	1626	1653	1621	1647	1620	1628
C-H Bending	1385	1462	1462	1455	1463	1465	1463
		1378	1381	1378	1376	1374	1378
C-O-C	1064	1112	1214	1247	1216	1185	1204
		1071	1113	1194	1111	1072	1083
		1032	1071	1071	1075	1031	1017

The FTIR spectrum exhibited the presence of hydroxyl, alkyl, ether and ester groups. Presence of broad hydroxyl (OH), carbonyl(C=O), C-H (stretching and bending), and C=C (skeletal vibration from sp<sup>2</sup> carbon rings) demonstrated characteristic oleanane triterpenoid saponin absorptions. The infrared absorbance of oleanane-type triterpenoid saponins are characterized by the C=O group due to the presence of oleanolic acid/ester. Column purified fractions D5 and H5 showed prominent peaks indicating the presence of C=O. This peak characterizes oleanane-type triterpenoid saponins. It is evident that after purification C=O functional group became distinct in the two fractions. The water, methanol and other column purified fractions did not show the presence of C=O functional group. This functional group was not dominant in these samples. The absorptions of C-O-C indicated glycoside linkages to the sapogenins, the non-sugar part (aglycone) of the saponin [269].

In methanol extracts, Fractions B8 and G4 sharp peak of C-O-C is observed compared to Fractions D5, K1 and H5. The observed changes in FTIR are attributed to the efficient removal of compounds with the functional group during purification. The absorption due to the C-H bending for water, methanol and column purified fractions indicates a saturation in the compound. The functional group C=C indicates the presence of conjugated unsaturation in the compound. This is supported by the absorption in UV-Vis at 247.47 nm for methanol and 246.77 nm for Fraction H5 [270].

Similar functional groups were present in water, methanol and column purified fractions. This indicates that saponins are easily detectable in water and methanol extracts [271]. Large absorbance of OH is seen for water as compared to methanol and column purified fractions. Prominent C-H stretching is observed for methanol and column purified fractions as compared to water. Water extracts exhibit prominent and broader peak absorptions of C-O-C indicating the presence of bigger molecules.

### 6.2.6 GC-MS Analysis

GC-MS is a combined technique used to identify various compounds present in a sample. The GC-MS graphical representation of the methanol extract of *Albizia procera* is shown in Figure 6.7.

The analysis lead to identification of various compounds constituting of the plant extract. The data was interpreted using National Institute of Standard and Technology (NIST) database. The name of the compound, its molecular weight and structure were ascertained. The methanol extract

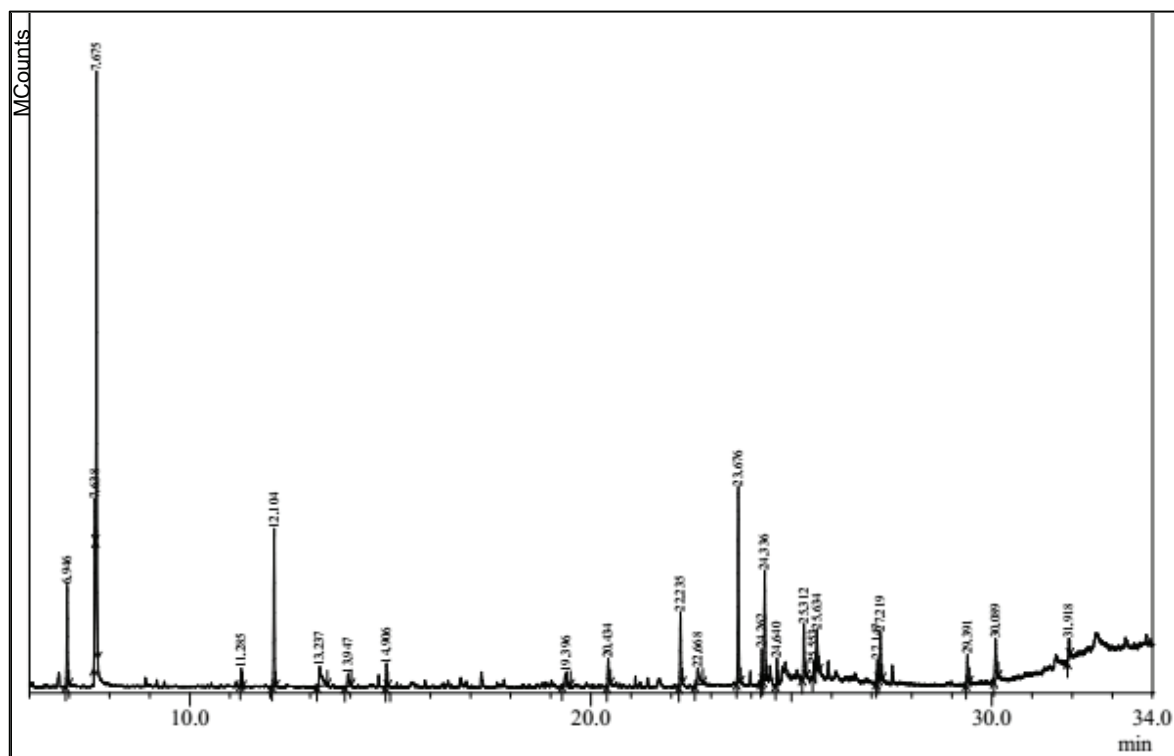


Figure 6.7: GC-MS chromatogram of methanol extract of *Albizia procera*.

showed 23 bioactive phytochemical compounds such as alcohol, esters, aromatic substances and fatty acids. Table 6.5 illustrates the prominent compounds present along with their retention time, peak area in percentage, molecular formula and molecular weight. The GC-MS spectrum contained five major peaks and many small peaks. The relative concentrations of the various compounds were indicated by the peak area. The peaks having lower retention times are due to the less polar compounds [256].

Table 6.5: Chemical constituents for methanol extract of *Albizia procera* by GC-MS .

Peak No.	Retention Time (minutes)	Peak Area (%)	Molecular Formula	Molecular Mass (g/mol)	IUPAC Name of Compound
1	6.946	5.80	C <sub>8</sub> H <sub>16</sub> O <sub>2</sub>	144.21	Butanoic acid, butyl ester
2	7.675	25.15	C <sub>8</sub> H <sub>18</sub> O	130.23	2-Ethyl- 1-hexanol
3	12.104	8.31	C <sub>12</sub> H <sub>26</sub> O <sub>2</sub>	202.34	1-Butoxyl-1-isobutoxy butane
4	23.676	11.61	C <sub>19</sub> H <sub>40</sub> O <sub>2</sub> Si	328.61	Palmitic Acid, TMS derivative
5	24.336	7.33	C <sub>22</sub> H <sub>38</sub> O <sub>2</sub>	334.54	Cyclopropanoic acid, 2-[[2-[2-ethylcyclopropyl]methylcyclopropyl], methyl]- methyl ester

One of the compound present in the extract is hexadecanoic acid, methyl ester. It is a palmitic acid compound which may have biological properties such as anti-oxidant, pesticide, lubricant activities and hemolytic 5-alpha is a reductase inhibitors [272]. Palmitic acid is a good source of toiletry and

laundry soap [273]. The presence of fatty acids and aromatic components in the extract highlights the pharmacological properties of the plant [274].

## 6.3 *Juglans regia*

### 6.3.1 Thin Layer Chromatography Analysis

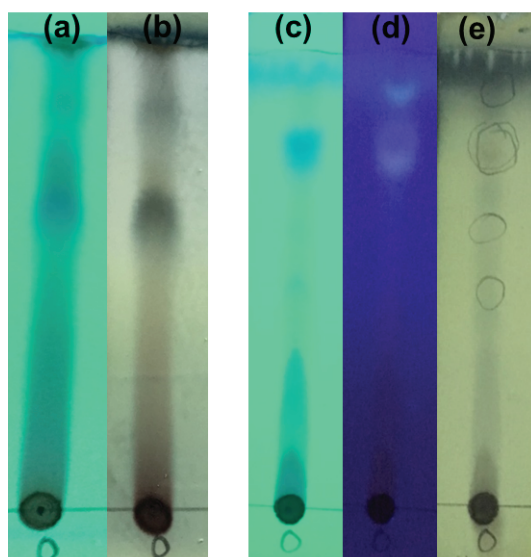


Figure 6.8: TLC plates for methanol extract of *Juglans regia*: (a) short wavelength (254 nm) (b) derivatized with PMA using (Chloroform: Glacial acetic acid: Methanol: Water [8:4:1.5:1]); using (Petroleum ether: Ethyl acetate [90:10]) (c) short wavelength (d) long wavelength (366 nm) (e) derivatized with PMA.

Different solvent systems were tried out for eluting the TLC plates to get a good results. The solvent system, (Chloroform: Glacial acetic acid: Methanol: Water [8:4:1.5:1]) gave a good separation, shown in Figure 6.8(a)(b).

The resulting TLC patterns were observed at short wavelength (254 nm) and derivatised with PMA. TLC analysis showed two spots in short wavelength

and when derivatised with PMA. The corresponding  $R_f$  values were calculated (Table 6.6). The band with  $R_f$  value 0.83 (light grey) was due to non-polar compounds while that with  $R_f$  0.62 (dark grey) was due to polar compounds. The tail like structure above  $R_f$  0.62 was due to inseparable non-polar compounds. The  $R_f$  value obtained was similar to the value for saponin as present in the literature [259, 260, 261].

Table 6.6:  $R_f$  value on TLC plate for methanol extract of *Juglans regia*.

Solvent System	No. of Spots	( $R_f$ ) Short wavelength 254 nm	( $R_f$ ) Long wavelength 366 nm	( $R_f$ ) Derivatised with PMA
Chloroform: Glacial acetic acid: Methanol:Water (8:4:1.5:1)	2	0.83 0.62	- -	0.83 0.62
PET.ether:Ethyl acetate (90:10)	5	- 0.78 0.60 0.46 0.24	0.90 0.78 - - -	0.90 0.78 0.60 0.46 0.24

A non-polar solvent system (Petroleum ether: Ethyl acetate [90:10]) was used to study the non polar compounds. This is illustrated in Table 6.6. When the TLC was viewed under short wavelength, four spots were obtained. Two spots were obtained when viewed under long wavelength and five spots were obtained when derivatised with PMA (Figure 6.8 (c),(d),(e)).

### 6.3.2 Column Chromatography

CC for methanol extract of *Juglans regia* eluted 90 fractions. Four fractions (Figure 6.9) which showed distinct spots monitored by TLC were analyzed



with UV-Vis. One fraction was further monitored by FTIR and HPLC.



Figure 6.9: Column purified fractions for methanol extract of *Juglans regia*.

### 6.3.3 UV-Visible Spectroscopy

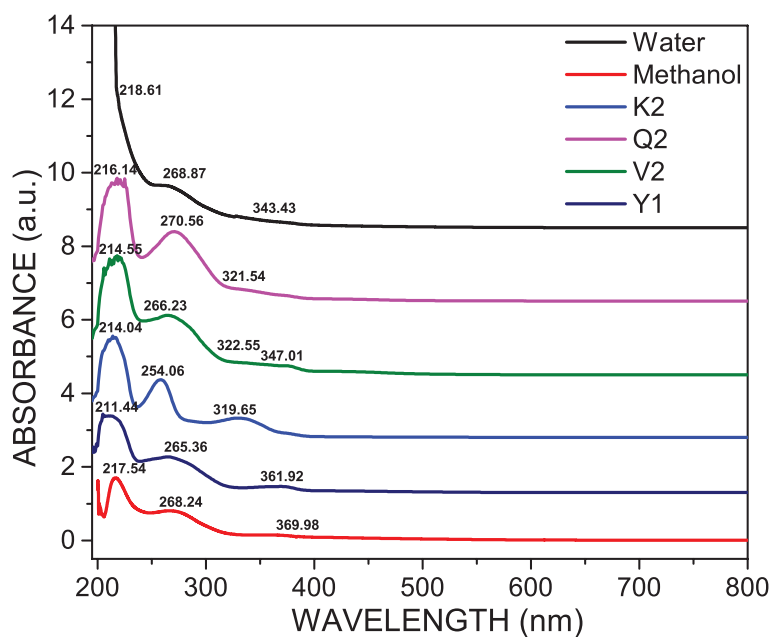


Figure 6.10: UV-Visible spectra for extracts of *Juglans regia*.

The absorbance peaks for the water, methanol and column purified fractions are shown in Figure 6.10. Table 6.7 illustrates the absorbance of *Juglans*

*regia*. The peaks in the first row are around 215 nm and are attributed to  $\pi$ - $\pi^*$  electronic transitions due to presence of (C=C) multi double bonds in the benzene rings. Presence of unsaturated groups is shown by absorption between 200-400 nm [256].

Table 6.7: UV-Vis absorption for extracts of *Juglans regia*.

<b>Water Extract nm</b>	<b>Methanol Extract nm</b>	<b>Fract. K2 nm</b>	<b>Fract. Q2 nm</b>	<b>Fract. V2 nm</b>	<b>Fract. Y1 nm</b>
218.61	217.54	214.04	216.14	214.55	211.44
268.87	268.24	254.06	270.56	266.23	265.36
-	-	319.65	321.54	322.55	-
343.43	369.98	-	-	347.01	361.92

The peaks at longer wavelength around 254 nm to 370 nm account for  $n$ - $\pi^*$  electronic transitions attributed to presence C=O group. Prominent peaks were obtained for methanol and column purified fractions as compared to water extract. Prominent absorption around 211 nm to 219 nm show the presence of saponin in *Juglans regia* (Figure 6.10) [170, 172, 262].

### 6.3.4 HPLC Analysis

The methanol extract of *Juglans regia* and one column purified fraction Y1 were subjected to HPLC for further analysis at a wavelength of 200-400 nm. Figures 6.11 and 6.12 show the chromatograms at a wavelength of 260 nm.

Different solvent systems were tried on HPLC. Acetonitrile-water could not adequately resolve the peaks. Good peak separations were obtained using methanol and water [50:50] for methanol extract and [30:70] for column purified fraction Y1 with 0.1 % TFA. The flow rate was maintained at 1

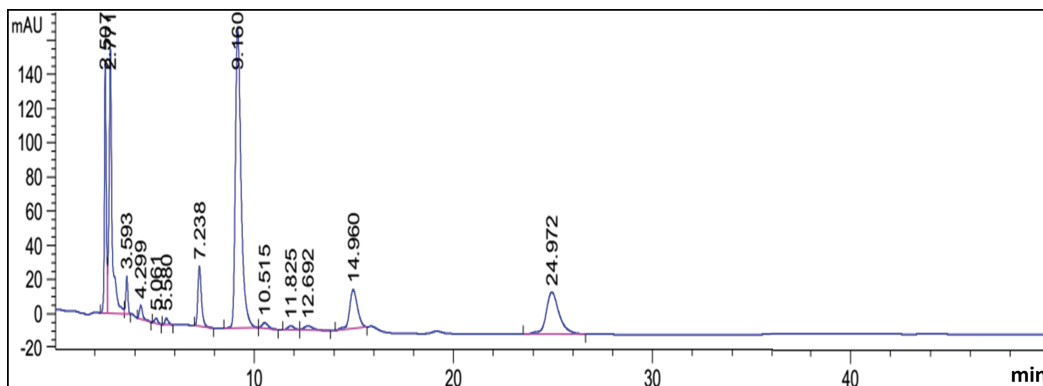


Figure 6.11: HPLC chromatogram for methanol extract of *Juglans regia* .

mL/min.

The retention time and peak area are illustrated in Table 6.8. The methanol extract showed 13 distinct peaks (Figure 6.11) for retention times 0 to 45 minutes. The peaks before 2.5 minutes could not be separated. Only six peaks had significant height and area. Apart from them some peaks with area  $< 1\%$  were detected. These could be due to the presence of small quantity of compounds.

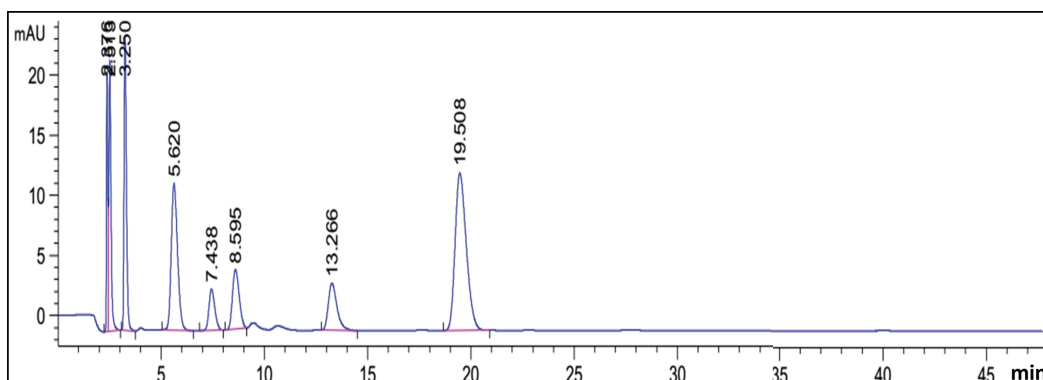


Figure 6.12: HPLC chromatogram of column purified fraction Y1 for methanol extract of *Juglans regia* .

The chromatogram for column purified fraction Y1 (Figure 6.12) con-

Table 6.8: HPLC for methanol extracts of *Juglans regia*.

Methanol Extract		Column Purified Fraction Y1	
Retention Time (minutes)	Area (%)	Retention Time (minutes)	Area (%)
2.507	10.4232	2.376	6.3263
2.771	18.9667	2.513	10.7293
3.593	1.8300	3.250	13.0901
4.299	1.0303	5.620	17.1720
5.061	0.3771	7.438	4.5816
5.580	0.5069	8.595	7.5423
7.238	4.9967	13.266	7.6154
9.160	39.9100	19.508	32.9430
10.515	0.7472	-	-
11.825	0.5528	-	-
12.692	0.7553	-	-
14.960	7.1752	-	-
24.972	12.7285	-	-

tained eight peaks indicating that eight classes of compounds still exist. The peaks obtained were sharp, distinct and prominent with significant height and area ( $> 4\%$ ). This could be due to the removal of some less abundant compounds during CC.

The elution with lower retention time indicates the presence of polar compounds and higher retention time non-polar compounds. The peaks in the chromatogram are similar to those obtained for saponins using the same solvent system [267].

### 6.3.5 FTIR Analysis

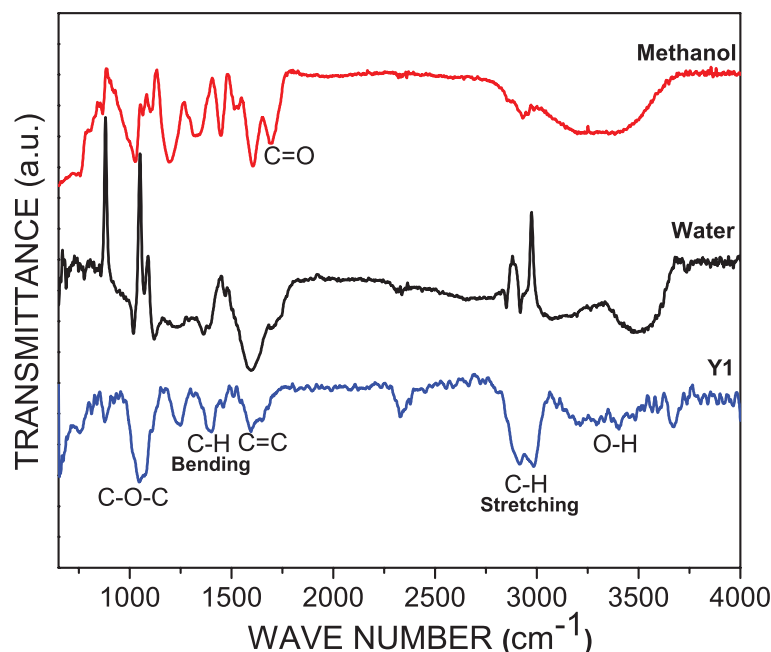


Figure 6.13: FTIR spectra for extracts of *Juglans regia*.

Figure 6.13 illustrates the FTIR spectra. The different functional groups present are outlined in Table 6.9. Characteristic oleanane triterpenoid saponin absorptions were seen showing the presence of OH, C=O, C-H and C=C. Oleanane-type triterpenoid saponins are characterized by C=O bond due to the presence of oleanolic acid/ester. Water and methanol extracts showed the presence of C=O indicating oleanane-type triterpenoid saponins. Column purified fraction Y1 did not exhibit peak corresponding to C=O group. The observed changes in the FTIR spectrum is attributed to efficient removal of the carbonyl group during purification. The absorption peaks due to C-O-C indicated glycoside linkages to the sapogenins [269].

The functional groups present in water, methanol and column purified

Table 6.9: Functional groups present in extracts of *Juglans regia*.

Functional Groups	Water Extract $\text{cm}^{-1}$	Methanol Extract $\text{cm}^{-1}$	Fraction Y1 $\text{cm}^{-1}$
O-H	3490	3305	3300
C-H	2918	2930	2983
Stretching	-	2848	2913
C=O	1697	1691	-
C=C	1595	1604	1658
	-	1533	1595
C-H	1362	1446	1390
Bending	-	1313	-
C-O-C	1117	1189	1235
	1069	1027	1045
	1017	-	-

fraction were similar indicating that saponins are easily detectable in the extracts [271]. The C-H stretching peak is sharper for the column purified fraction Y1. Prominent glycoside linkages to the sapogenins, C-O-C is seen for methanol and column purified fractions compared to water. Water extracts exhibit prominent and broader peak for absorptions of C=C indicating bigger molecules.

### 6.3.6 GC-MS Analysis

The GC-MS chromatogram of methanol extract is presented in Figure 6.14. The extract showed the presence of 10 bioactive phytochemical compounds belonging to alcohol, esters, polyphenol, aldehyde and fatty acids groups. Among the different bioactive compounds, five compounds were present in high quantity illustrated in Table 6.10. The GC-MS spectrum exhibited five major peaks and many small peaks attributed to presence of compounds in

smaller quantities [256].

Table 6.10: Chemical constituents for methanol extract of *Juglans regia* by GC-MS.

Peak No.	Retention Time (minutes)	Peak Area (%)	Molecular Formula	Molecular Mass (g/mol)	IUPAC Name of Compound
1	8.871	25.929	C <sub>8</sub> H <sub>18</sub> O	130.23	(S)-(+)-5-Methyl-1-heptanol
2	15.18	28.238	C <sub>6</sub> H <sub>6</sub> O <sub>3</sub>	126.11	1,2,3-Benzenetriol
3	19.856	14.350	C <sub>11</sub> H <sub>14</sub> O <sub>2</sub>	178.23	Benzaldehyde, 4-butoxy
4	25.141	9.667	C <sub>21</sub> H <sub>38</sub> O <sub>2</sub>	322.52	n-Propyl 9,12-octadecadienoate
5	25.213	7.194	C <sub>18</sub> H <sub>30</sub> O <sub>2</sub>	182.30	Methyl 8,11,14-heptadecatrienoate

The compound 1,2,3-Benzenetriol (Pyrogallol) was a major constituent in *Juglans regia* extract. It is a cofactor to xanthine oxidase inhibitory activity [275] and inhibits the growth of lung cancer cells [276]. It is used as a photographic developer, in the manufacture of some dyes [277]. Methyl 8,11,14-heptadecatrienoate is used as an antibiotic [278]. It also has antibac-

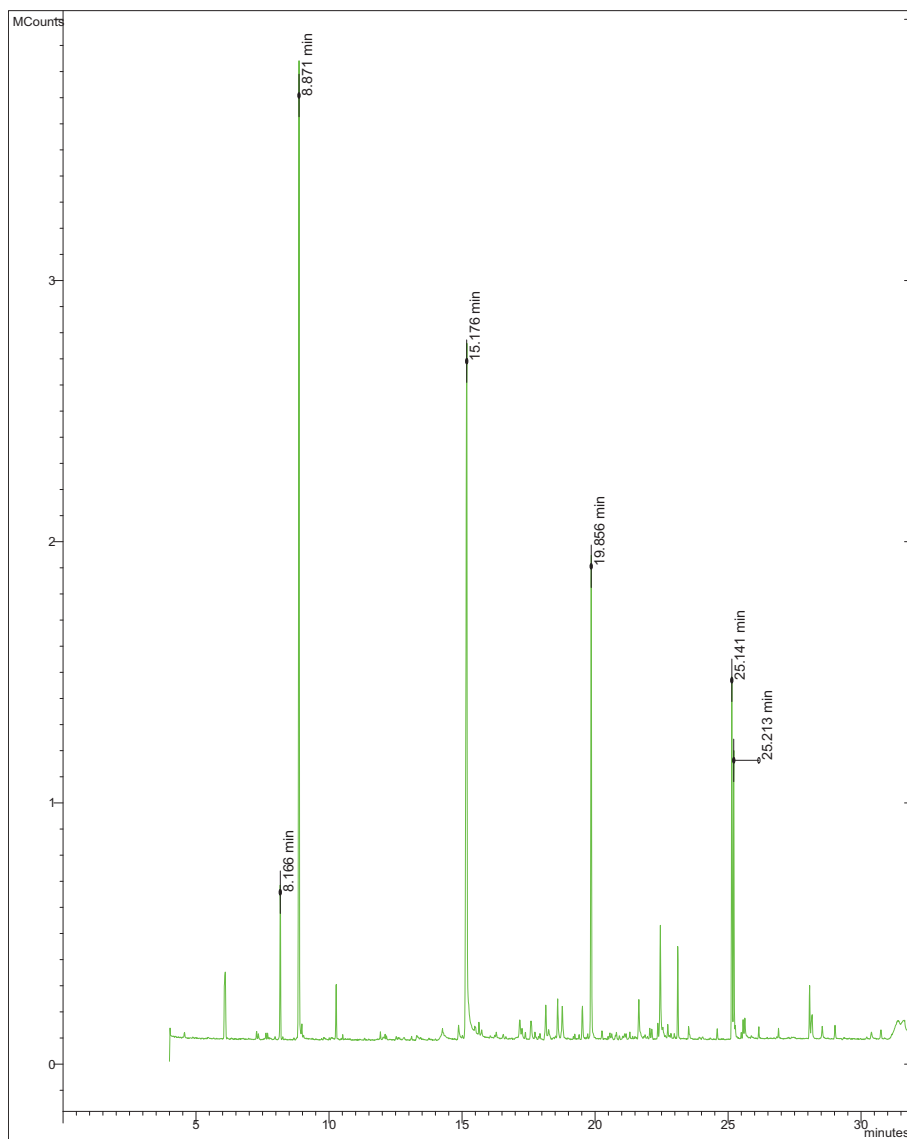


Figure 6.14: GC-MS chromatogram for methanol extract of *Juglans regia*.



terial and pharmaceutical properties [279]. The GC-MS analysis showed the presence of fatty acids, highlighting the pharmacological properties of the plant [274].

## 6.4 *Zephyranthes carinata*

### 6.4.1 Thin Layer Chromatography Analysis

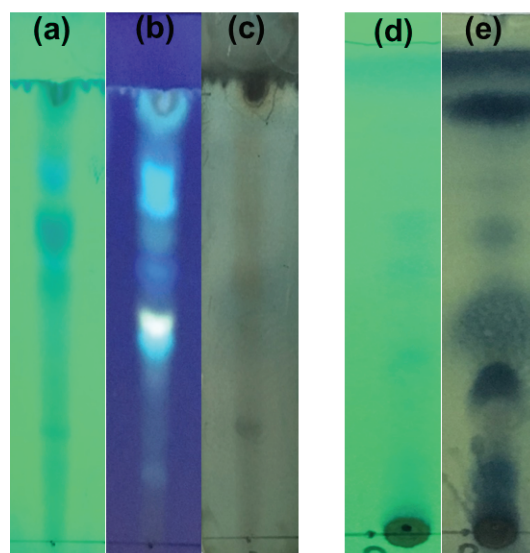


Figure 6.15: TLC plates for methanol extract of *Zephyranthes carinata*: using (Chloroform: Glacial acetic acid: Methanol: Water [8:4:1.5:1]) (a) short wavelength (254 nm) (b) long wavelength (366 nm) (c) derivatized with PMA; using (Petroleum ether: Ethyl acetate [90:10]) (d) short wavelength (e) derivatized with PMA.

Compounds present in methanol extract of *Zephyranthes carinata* were first analysed by TLC. The solvent system (Chloroform: Glacial acetic acid: Methanol: Water [8:4:1.5:1]) gave best separation as shown in Figure 6.15. The TLC patterns were observed at short wavelength, long wavelength and

were derivatised with PMA. The spots seen and the corresponding  $R_f$  values are illustrated in Table 6.11. The spots with  $R_f$  values 0.910, 0.757 and 0.658 are attributed to the presence of non-polar compounds, spots having  $R_f$  values 0.216, 0.450, 0.486, 0.541, 0.586 to polar compounds. The broader spot above  $R_f$  value 0.757 indicated the presence of inseparable non-polar compounds. Spots at  $R_f$  values of 0.450 and 0.486 indicate the presence of saponin [258, 259, 260, 261].

Table 6.11:  $R_f$  value on TLC plate for methanol extract of *Zephyranthes carinata*.

Solvent System	No. of Spots	( $R_f$ ) Short wavelength 254 nm	( $R_f$ ) Long wavelength 366 nm	( $R_f$ ) Derivatised with PMA
Chloroform: Glacial acetic acid: Methanol:Water (8:4:1.5:1)	6	0.910	0.910	-
		0.757	0.757	-
		0.658	0.658	-
		0.586	0.568	-
		-	-	0.541
		-	0.486	-
PET.ether:Ethyl acetate (90:10)	5	-	0.450	-
		0.216	-	0.216
		0.817	-	0.817
		0.720	-	0.720
		0.596	-	0.596
0.480	-	0.480		
-	-	0.202		

The non-polar compounds were analysed using the solvent system (Petroleum ether: Ethyl acetate:[90:10]). The spots obtained are shown in Figure 6.15,  $R_f$  values are shown in Table 6.11.

### 6.4.2 Column Chromatography

The methanol extract of *Zephyranthes carinata* eluted 70 fractions under CC. Four fractions (Figure 6.16) showing distinct spots in TLC were further analysed with UV-Vis. One fraction was monitored with HPLC.

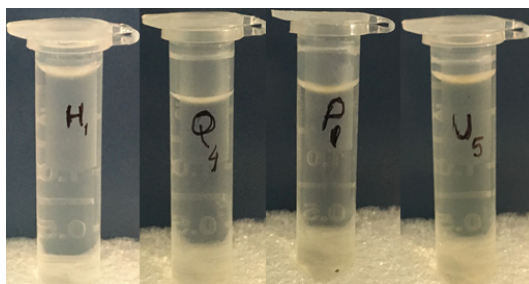


Figure 6.16: Column purified fractions for methanol extract of *Zephyranthes carinata*.

### 6.4.3 UV-Visible Spectroscopy

Figure 6.17 shows the absorbance peaks for the extracts of *Zephyranthes carinata*. Absorption peaks shown in the first two rows of Table 6.12 are around 223 nm to 244 nm. The  $\pi$ - $\pi^*$  electronic transitions due to presence of C=C multi double bonds in the rings are responsible for such absorption. Presence of unsaturated groups are exhibited by absorption in the range of 200-400 nm [256]. The absorption peaks in the first two rows, in the range 223 to 243 nm are attributed to the presence of saponin [170, 262, 263, 264].

Absorption at longer wavelengths are attributed to  $n$ - $\pi^*$  electronic transitions due to presence of C=O group. Absorption peaks suggest that compounds in water, methanol and column purified fractions have chromophores.

Absorption shown by methanol extract is slightly different from water

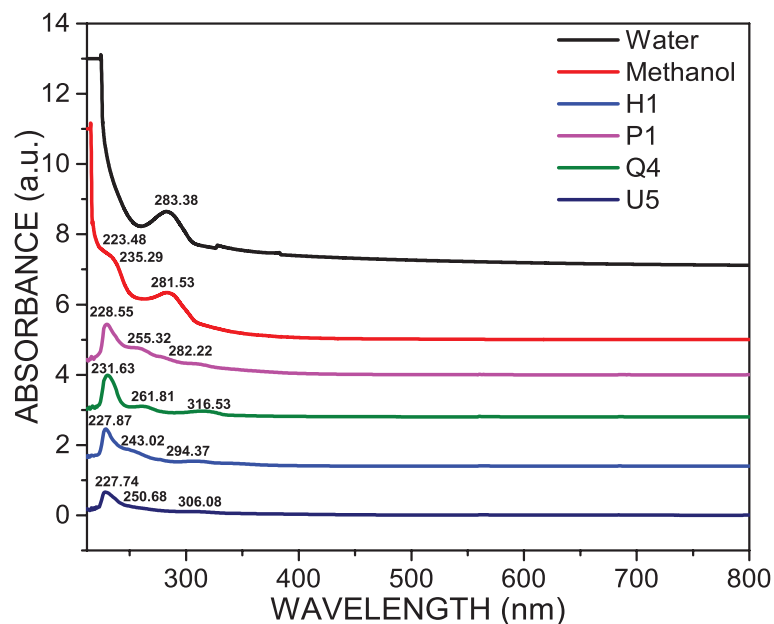


Figure 6.17: UV-Visible absorption spectra for extracts of *Zephyranthes carinata*.

Table 6.12: UV-Vis absorption for extracts of *Zephyranthes carinata*.

Water Extract nm	Methanol Extract nm	Fract. H1 nm	Fract. Q4 nm	Fract. P1 nm	Fract. U5 nm
-	223.48	227.87	231.63	228.55	227.74
-	235.29	243.02	-	-	-
-	-	-	261.81	255.32	250.00
283.38	281.53	294.37	316.53	282.22	306.08

extract. This may be accounted to the differences in the types of surfactants extracted by the solvents. Column purified fractions exhibited prominent peaks which are not observed for water and methanol extracts which may be attributed to removal of impurities during CC. Absorption at 280 nm is considered due to the presence of phenolic compounds. Absorption in the range of 240-285 nm and 300-500 nm indicates the presence of flavonoids [265].

#### 6.4.4 HPLC Analysis

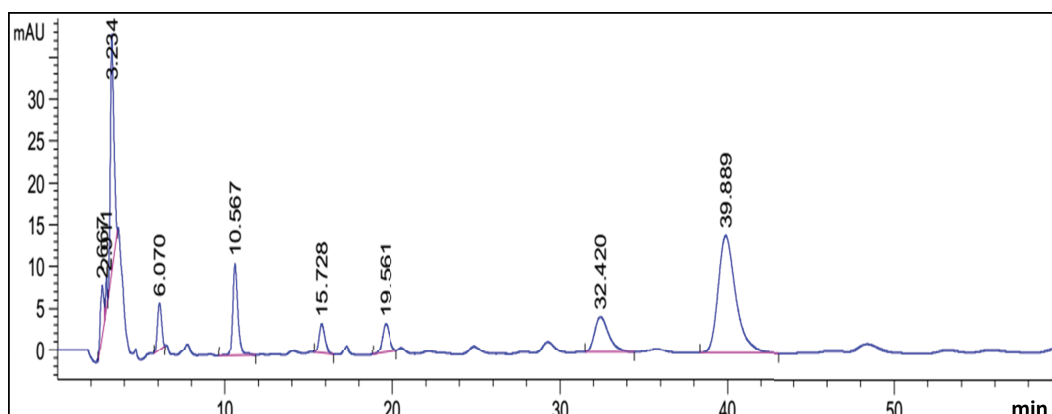


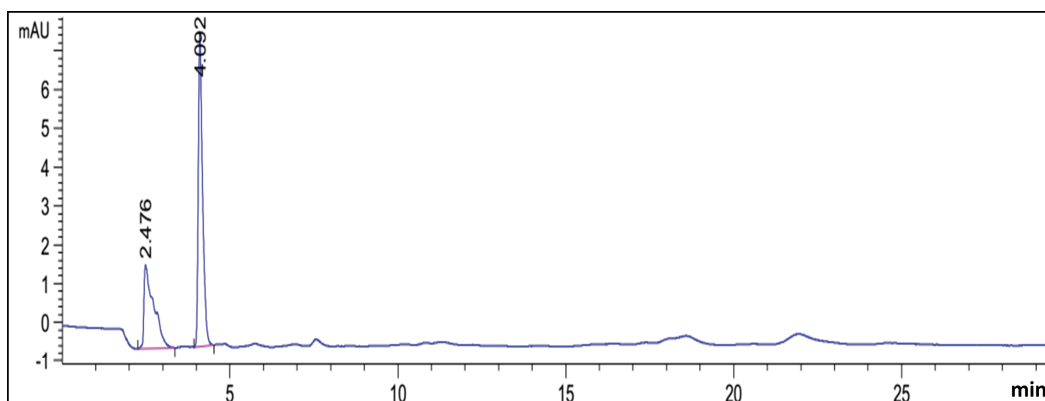
Figure 6.18: HPLC chromatogram for methanol extract of *Zephyranthes carinata*.

Figures 6.18 and 6.19 show the HPLC chromatograms of methanol extract and column purified fraction U5 at 260 nm. Solvent systems methanol-water and acetonitrile-water of various compositions were used. The acetonitrile-water [50:50, 80:20, 70:30] mobile phase could not adequately resolve the peaks. Hence methanol and water [15:85] with 0.1 % TFA was chosen at a flow rate 1 mL/min.

Table 6.13: HPLC for methanol extracts of *Zephyranthes carinata*.

Methanol Extract		Column Purified Fraction U5	
Retention Time (minutes)	Area (%)	Retention Time (minutes)	Area (%)
2.667	3.6299	2.476	37.5923
2.911	1.0025	4.092	62.4077
3.234	17.1768	-	-
6.070	4.1099	-	-
10.567	10.0928	-	-
15.728	3.7666	-	-
19.561	4.4601	-	-
32.420	10.9669	-	-
39.889	44.7945	-	-

The peaks and their retention times are illustrated in Table 6.13. The methanol extract showed nine peaks (Figure 6.18) for retention times 0 to 55 minutes. Peaks before retention time of 4 minutes could not be separated. Only eight prominent peaks with significant height and area ( $> 1\%$ ) were seen.

Figure 6.19: HPLC chromatogram of column purified fraction U5 for methanol extract of *Zephyranthes carinata*.

The chromatogram for column purified fraction is shown in Figure 6.19.

Methanol and water [20:80] with 0.1 % TFA was used at a flow rate 1 mL/min. The column purified fraction contained two peaks for retention times 0 to 30 minutes (Table 6.9) indicating two classes of compounds.

Peaks with retention time 10-20 minutes are attributed to the presence of saponin [266, 268, 280]. Apart from the prominent peaks, some peaks having area < 1 % were detected, probably due to presence of other compounds in small quantities.

#### 6.4.5 FTIR Analysis

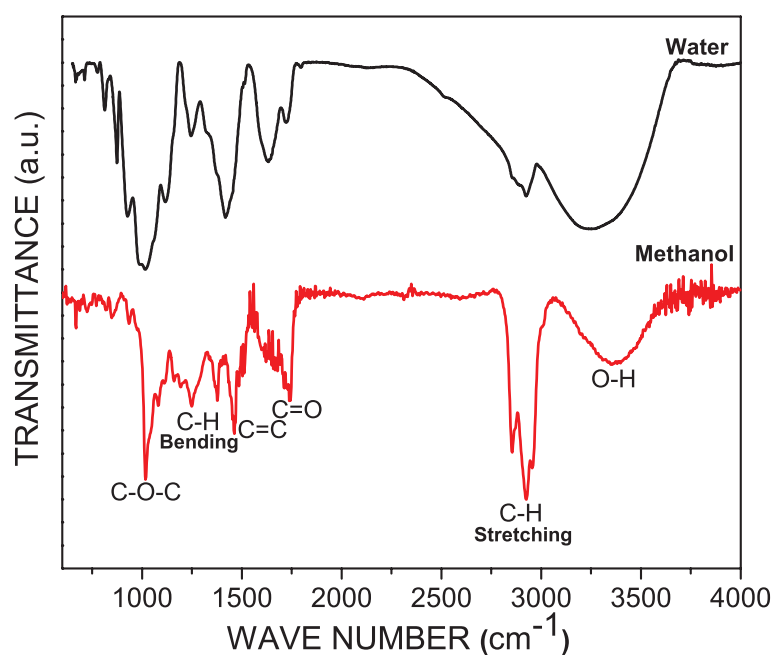


Figure 6.20: FTIR spectra for extracts of *Zephyranthes carinata*.

FTIR spectra are shown in Figure 6.20. Table 6.14 represents the functional groups present. The FTIR spectrum exhibited the presence of broad spectrum of hydroxyl (OH), carbonyl group (C=O), C-H (stretching and

bending), and C=C (skeletal vibration from  $sp^2$  carbon rings) which are characteristic of oleanane triterpenoid saponin absorptions. The water and methanol extracts showed prominent C=O peak indicating the presence of oleanane-type triterpenoid saponins. The prominent C-O-C peak for both the extracts indicated glycoside linkages to sapogenins [269].

Table 6.14: Functional groups present in the extracts of *Zephyranthes carinata*.

Functional Groups	Water Extract $\text{cm}^{-1}$	Methanol Extract $\text{cm}^{-1}$
O-H	3336	3322
C-H Stretching	2920	2919, 2856
C=O	1722	1738
C=C	1631	1632
C-H Bending	1414	1471, 1378
C-O-C	1239,1131,1014	1245,1078,1012

The absorption due to C-H bending indicates a saturation in the compound. The functional group C=C indicates the presence of conjugated unsaturation [270]. Water extract exhibited prominent broad C-O-C peak compared to methanol indicating a bigger molecule. On the other hand, the C-H stretching for methanol extract was more prominent and sharp as compared to water extract. These changes are attributed to different amounts of compounds extracted in the two solvent systems. However, the water and methanol extracts showed presence of similar functional groups. This indicates that saponins are easily detectable in water and methanol extracts [271].



### 6.4.6 GC-MS Analysis

Figure 6.21 shows the graphical representation of GC-MS of methanol extract of *Zephyranthes carinata*. The extract showed the presence of 16 bioactive phytochemical compounds: alcohols, esters, hydrocarbons, fatty acids etc. Among the compounds identified, five compounds were present in high percentage (Table 6.15). The GC-MS spectra showed five major peaks and many small peaks. The presence of fatty acids in the extract highlights the pharmacological properties of the plant [274].

Table 6.15: Chemical constituents for methanol extract of *Zephyranthes carinata* by GC-MS.

Peak No.	Retention Time (minutes)	Peak Area (%)	Molecular Formula	Molecular Mass (g/mol)	IUPAC Name of Compound
1	8.789	8.322	C <sub>5</sub> H <sub>12</sub> N <sub>2</sub> O	116.16	O-Butylisourea
2	8.846	25.856	C <sub>8</sub> H <sub>18</sub> O	130.23	(S)-(+)-5-Methyl-1-heptanol
3	12.244	15.846	C <sub>6</sub> H <sub>12</sub> O <sub>2</sub>	116.15	Formic acid, neopentyl ester
4	13.073	21.563	C <sub>12</sub> H <sub>26</sub> O <sub>2</sub>	202.33	Butane, 1, 1-dibutoxy
5	25.144	8.486	C <sub>21</sub> H <sub>38</sub> O <sub>2</sub>	322	n-Propyl 9,12-octadecadienoate

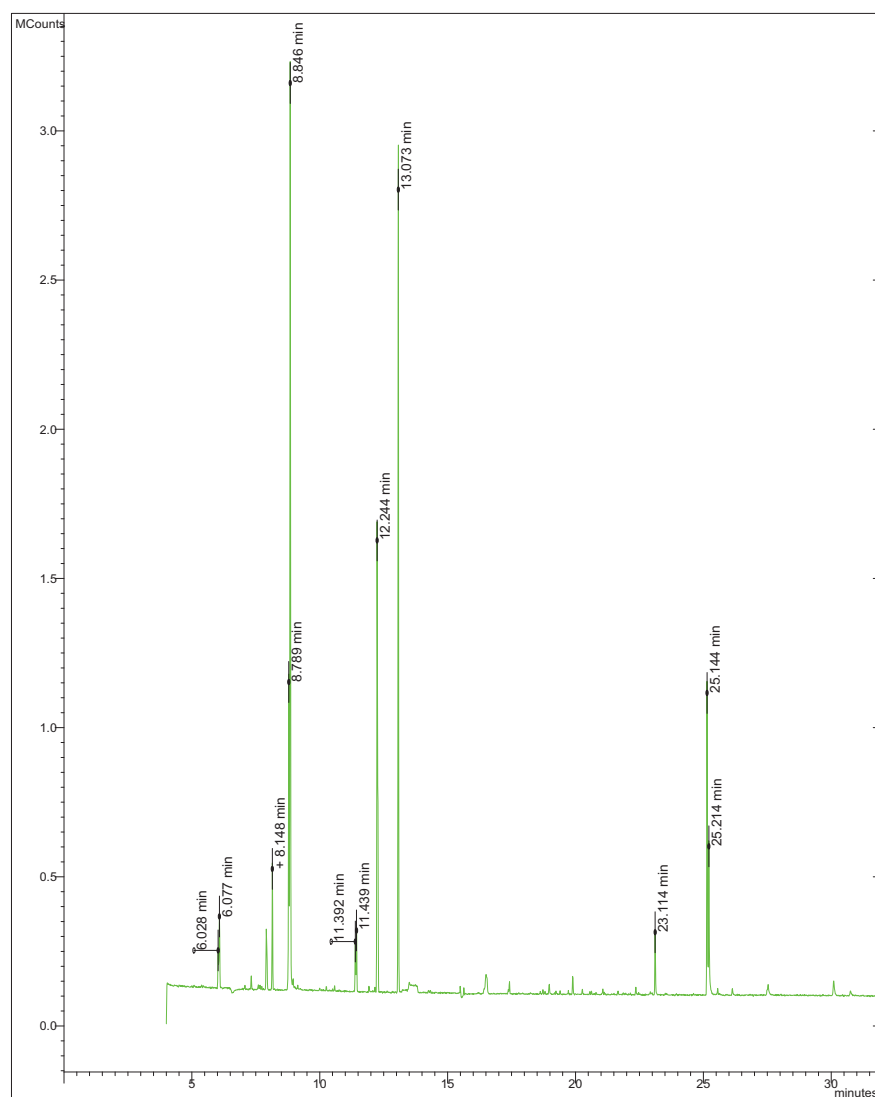


Figure 6.21: GC-MS chromatogram for methanol extract of *Zephyranthes carinata*.

## 6.5 *Sapindus mukorossi*

### 6.5.1 Thin Layer Chromatography Analysis

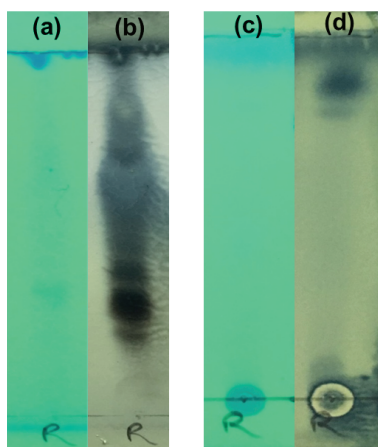


Figure 6.22: TLC plates for methanol extract of *Sapindus mukorossi*: using (Chloroform: Glacial acetic acid: Methanol: Water [8:4:1.5:1]) (a) short wavelength (254nm) (b) derivatized with PMA; using (Petroleum ether: Ethyl acetate [50:50]) (c) short wavelength (d) derivatized with PMA.

Figure 6.22 shows the TLC for methanol extract of *Sapindus mukorossi* using solvent system (Chloroform: Glacial acetic acid: Methanol: Water [8:4:1.5:1]) [192]. The resulting TLC patterns were viewed as given in Table 6.16.

The spots with  $R_f$  values 0.822 (light grey) and 0.711 (grey) were due to non-polar compounds while spots with  $R_f$  values 0.200 (light black), 0.289 (black) and 0.400 (black) were due to polar compounds. The broader spot above  $R_f$  value 0.400 indicated inseparable non-polar components. The  $R_f$  value of 0.400 is attributed to the presence of saponin [258].

A non-polar solvent system (Petroleum ether: Ethyl acetate [50:50]) was used to study the non-polar compounds. Two spots having  $R_f$  value 0.783

Table 6.16:  $R_f$  value on TLC plate for methanol extract of *Sapindus mukorossi*.

Solvent System	No. of Spots	( $R_f$ ) Short wavelength 254 nm	( $R_f$ ) Derivatised with PMA
Chloroform: Glacial acetic acid: Methanol:Water (8:4:1.5:1)	5	-	0.822
		-	0.711
		-	0.400
		0.339	-
		-	0.289
PET.ether:Ethyl acetate (50:50)	2	-	0.870
		-	0.783

and 0.870 were obtained (Figure 6.1).

A large amount of work has already been done on isolation and characterization of *Sapindus mukorossi* [149, 150, 151, 152]. Hence, CC was not performed for this sample.

## 6.5.2 UV-Visible Spectroscopy

Figure 6.23 shows the absorbance peaks for water and methanol extracts of *Sapindus mukorossi*. Absorbance is seen at 214.83 nm for water and 217.05 nm and 248.15 nm for methanol, attributed to  $\pi$ - $\pi^*$  electronic transitions due to presence of C=C multi double bonds in the rings. Absorptions at 214.83 nm for water and 217.05 nm for methanol are attributed to the presence of saponin (Figure 6.23). Absorption peak at longer wavelength (Table 6.17) is observed at 278.13 nm for water, attributed to  $n$ - $\pi^*$  electronic transitions of C=O group. Water and methanol extracts showed similar absorbance.

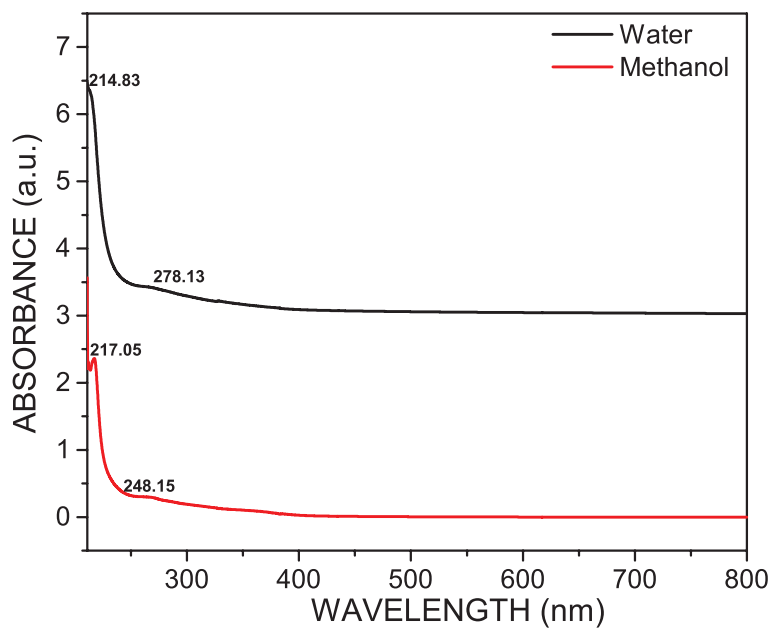


Figure 6.23: UV-Visible absorption spectra for extracts of *Sapindus mukorossi*.

Table 6.17: UV-Vis absorption for extracts of *Sapindus mukorossi*.

Water Extract (nm)	Methanol Extract (nm)
214.83	217.05
-	248.15
278.13	-

### 6.5.3 HPLC Analysis

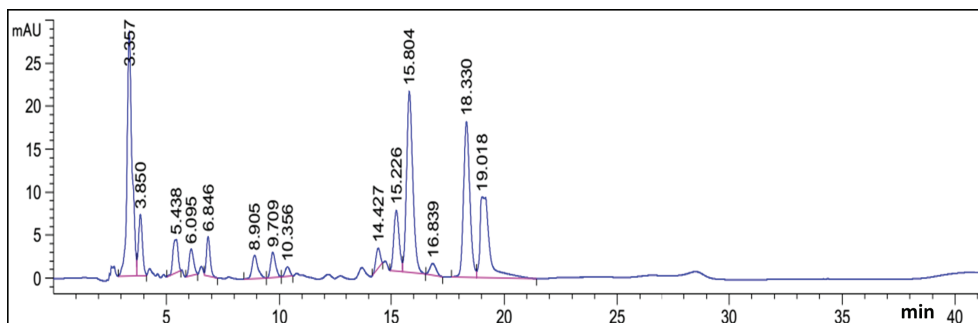


Figure 6.24: HPLC chromatogram for the methanol extract of *Sapindus mukorossi*.

Figure 6.24 shows the HPLC chromatograms of methanol extract at 260 nm. Methanol-water and acetonitrile-water were used as the solvent system. The acetonitrile-water [50:50, 80:20, 70:30, 20:80, 10:90, 15:85] mobile phase could not adequately resolve the peaks. Methanol and water [10:90] with 0.1 % TFA was chosen at a flow rate 1 mL/min.

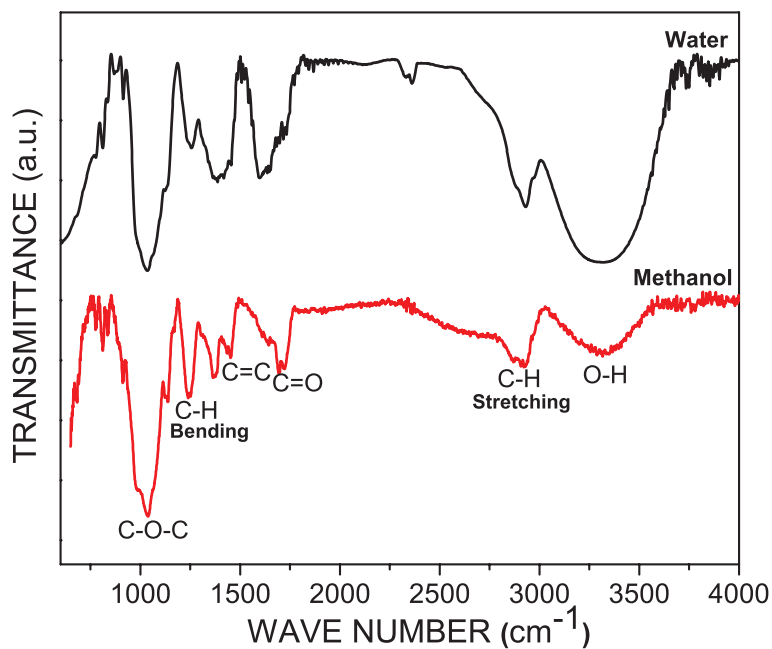
Table 6.18 shows the retention times and areas of the peaks. The chromatogram showed 14 peaks (Figure 6.24) for retention times 0 to 45 minutes. However, only 11 prominent peaks had significant area ( $> 1\%$ ). Peaks with retention time 10-20 minutes are attributed to the presence of saponin [266, 267, 268, 280].

### 6.5.4 FTIR Analysis

FTIR spectra are shown in Figure 6.25. Table 6.19 illustrates the various functional groups present. FTIR spectrum exhibited presence of hydroxyl (OH), carbonyl (C=O), C-H (stretching and bending), and C=C (skeletal

Table 6.18: HPLC chromatogram for the methanol extract of *Sapindus mukorossi*.

Retention Time (minutes)	Area (%)
3.357	21.9293
3.850	4.3849
5.438	2.9985
6.095	2.0979
6.846	2.5823
8.905	2.4176
9.709	2.2128
10.356	0.7729
14.427	1.5980
15.226	5.8063
15.804	20.2603
16.839	1.2955
18.330	17.5963
19.018	14.0475

Figure 6.25: FTIR spectra for extracts of *Sapindus mukorossi*.



vibration from  $sp^2$  carbon rings) characteristic of oleanane-type triterpenoid saponin absorptions. The prominent peak of C-O-C for both the extracts indicated prominent glycoside linkage to sapogenins [269].

Table 6.19: Functional groups present in extracts of *Sapindus mukorossi*.

Functional Groups	Water Extract $\text{cm}^{-1}$	Methanol Extract $\text{cm}^{-1}$
O-H	3298	3258
C-H Stretching	2932	2919, 2864
C=O	1723	1719, 1691
C=C	1594	1643
C-H Bending	1369	1451, 1363
C-O-C	1249, 1034	1240, 1038

The absorption due to the C-H bending for water and methanol indicates a saturation in the compound. The functional group C=C indicates the presence of conjugated unsaturation [270]. Water extract exhibited a broader peak for O-H compared to methanol indicating a bigger molecule. The water and methanol extract showed similar functional groups which indicates that saponins are easily detectable in water and methanol extracts [271].

### 6.5.5 GC-MS Analysis

The GC-MS chromatogram for methanol extract of *Sapindus mukorossi* is presented in Figure 6.26. The extract showed 27 bioactive phytochemical compounds: alcohols, esters, aldehydes, fatty acids etc. Table 6.20 illustrates the six prominent compounds.

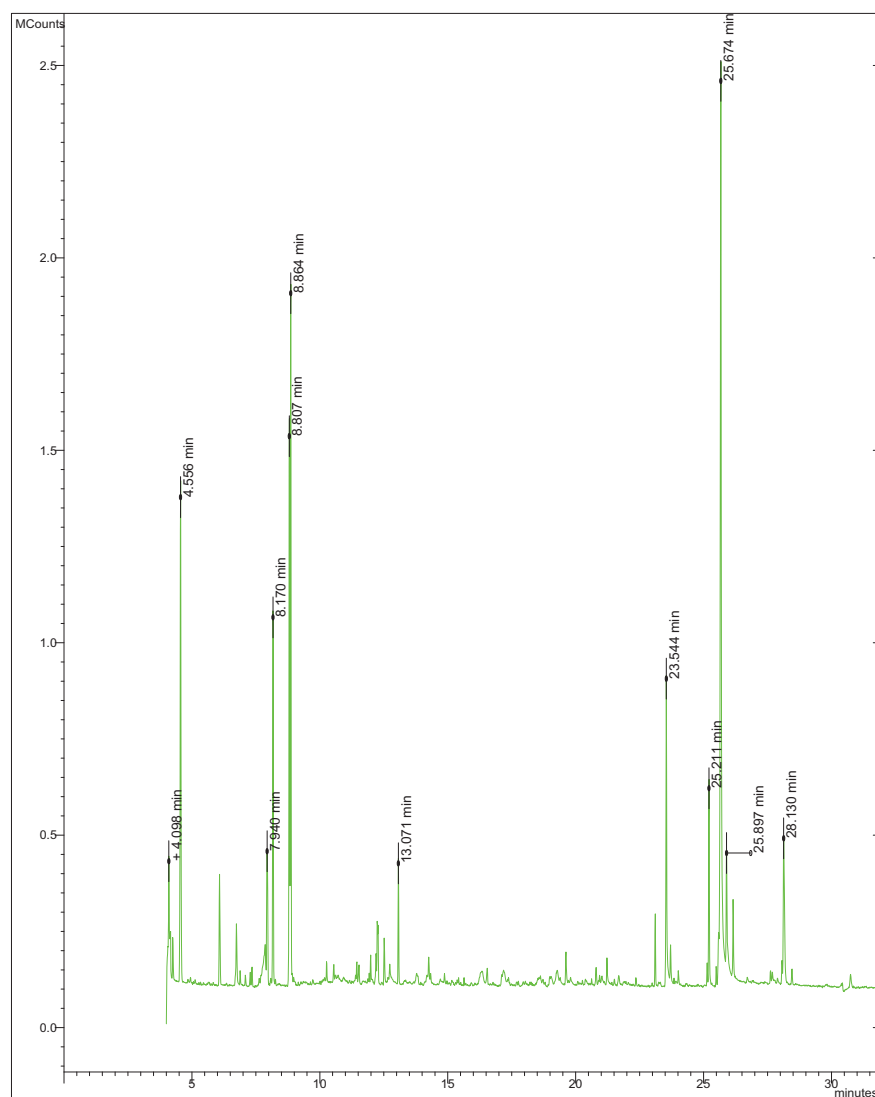


Figure 6.26: GC-MS chromatogram for the methanol extract of *Sapindus mukorossi*.

Table 6.20: Chemical constituents for methanol extract of *Sapindus mukorossi* by GC-MS.

Peak No.	Retention Time (minutes)	Peak Area (%)	Molecular Formula	Molecular Mass (g/mol)	IUPAC Name of Compound
1	4.556	9.524	C <sub>8</sub> H <sub>16</sub> O <sub>2</sub>	144.21	Acetic acid, hexyl ester
2	8.170	5.992	C <sub>8</sub> H <sub>16</sub> O <sub>2</sub>	144.21	Butanoic acid, butyl ester
3	8.807	9.202	C <sub>5</sub> H <sub>12</sub> N <sub>2</sub> O	116.16	O-Butylisourea
4	8.864	10.907	C <sub>8</sub> H <sub>18</sub> O	130.23	1-Hexanol, 2-ethyl
5	23.544	5.899	C <sub>16</sub> H <sub>32</sub> O <sub>2</sub>	256.42	n-Hexadecanoic acid
6	25.674	26.316	C <sub>19</sub> H <sub>36</sub> O	280.49	2-Methyl-Z,Z-3,13-octadecadienol

Some of the compounds present in extracts of *Sapindus mukorossi* is similar to *Albizia procera* extracts. Hexadecanoic acid, methyl ester a palmitic acid compound have biological properties such as anti-oxidant, anti-inflammatory [281], lubricant activities [272]. Palmitic acid is a good source of toiletry and laundry soap [273]. 2-Methyl-Z,Z-3,13-octadecadienol is reported to possess anti-cancer properties [282]. The presence of fatty acids shows the pharmacological characteristics of the plant [274].

## 6.6 *Acacia concinna*

### 6.6.1 Thin Layer Chromatography Analysis



Figure 6.27: TLC plates for methanol extract of *Acacia concinna* derivatized with anisaldehyde-sulphuric acid reagent using (a) (Chloroform: Glacial acetic acid: Methanol: Water [8:4:1.5:1]) (b) (Petroleum ether: Ethyl acetate [80:20]).

TLC of *Acacia concinna* extract was conducted using Chloroform: Glacial acetic acid: Methanol: Water [8:4:1.5:1]. When the TLC plate was derivatized with anisaldehyde-sulphuric acid reagent it showed three spots (Table 6.21) with  $R_f$  values 0.87 (black) due to non-polar compounds and  $R_f$  values 0.48 (dark green) and 0.61 (light brown) due to polar compounds (Figure 6.27(a)). The plate did not show any distinct spots under short or long wavelength. The broad spot above  $R_f$  value 0.48 may be due to inseparable polar compounds. Also, the long tail like structure above the spot with

$R_f$  value 0.87 indicated inseparable non-polar compounds. Anisaldehyde-sulphuric acid reagent showed a dark green coloured spot with a  $R_f$  value of 0.48 indicating saponins [258].

Using a non-polar solvent system (Petroleum ether: Ethyl acetate [60:40]), two spots having  $R_f$  value 0.79 and 0.87 were obtained as shown in Figure 6.27(b).

Table 6.21:  $R_f$  value on TLC plate for methanol extract of *Acacia concinna*.

Solvent System	No. of spots	( $R_f$ ) Derivatised with PMA
Chloroform: Glacial acetic acid: Methanol:Water (8:4:1.5:1)	3	0.87 0.61 0.48
PET.ether:Ethyl acetate (60:40)	2	0.87 0.79

### 6.6.2 Column Chromatography

The methanol extract of *Acacia concinna* was subjected to CC to elute 72 fractions. Four fractions (Figure 6.28) showing distinct spot in TLC were further analysed with UV-Vis and FTIR. One fraction was monitored with HPLC.

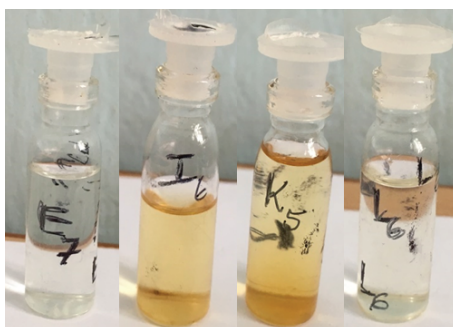


Figure 6.28: Column purified fractions for methanol extract of *Acacia concinna*.

### 6.6.3 UV-Vis Spectroscopy

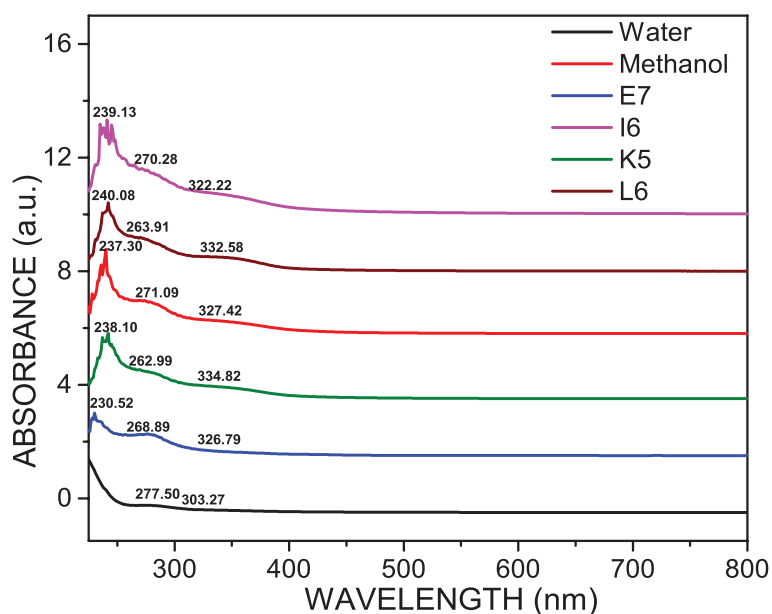


Figure 6.29: UV-Vis absorption spectra for extracts of *Acacia concinna*.

Figure 6.29 shows the absorbance peaks for the extracts of *Acacia concinna*. The results are summarized in Table 6.22. Absorption peaks shown in the first row is in the range 230 nm to 240 nm. This is attributed to  $\pi$ - $\pi^*$  electronic transitions due to presence of C=C multi double bonds in the

rings. Absorption between 200-400 nm indicates the presence of unsaturated groups [256]. The absorption peaks in the range of 230 nm to 240 nm are attributed to the presence of saponin (Figure 6.29).

Table 6.22: UV-Vis absorption for extracts of *Acacia concinna* .

<b>Water Extract nm</b>	<b>Methanol Extract nm</b>	<b>Fract. E7 nm</b>	<b>Fract. I6 nm</b>	<b>Fract. K5 nm</b>	<b>Fract. L6 nm</b>
-	237.30	230.52	239.13	238.10	240.08
277.50	271.09	268.89	270.28	262.99	263.91
303.27	327.42	326.79	322.22	334.82	332.58

Absorption peaks at longer wavelengths are attributed to  $n-\pi^*$  electronic transitions due to the presence of C=O group. The absorption peak suggests that the compounds have chromophores.

Methanol extract and column purified fractions showed similar absorbance. Column purified fractions exhibited prominent peaks which are not observed for water extract. These changes may be attributed to differences in the type of surfactants extracted by the solvents. Absorption peaks in the range of 240-285 nm and 300-500 nm indicates the presence of flavonoids [265].

#### 6.6.4 HPLC Analysis

The methanol extract of *Acacia concinna* and one column purified fraction I6 were subjected to HPLC for further analysis. Figures 6.30 and 6.31 show the chromatograms at a wavelength of 260 nm.

Different solvent systems like methanol-water and acetonitrile-water in

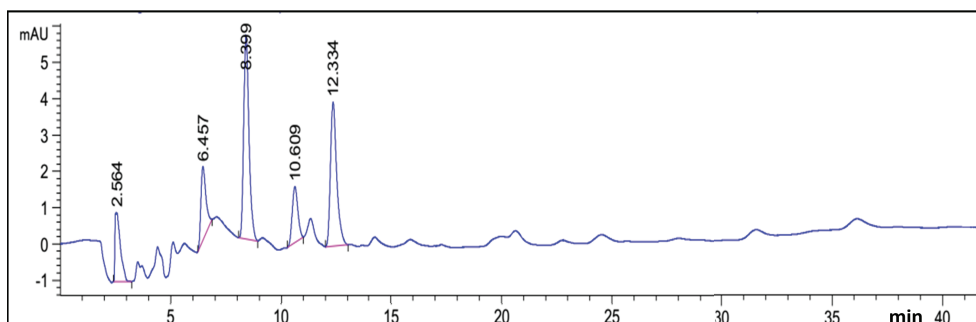


Figure 6.30: HPLC chromatogram for methanol extract of *Acacia concinna*.

varying compositions were used for elution on HPLC. Good peak separations were obtained using methanol and water [15:85] for methanol extract and [20:80] for column purified fraction with 0.1 % TFA at a flow rate 1 mL/min [266].

Table 6.23: HPLC for methanol extracts of *Acacia concinna*.

Methanol Extract		Column Purified Fraction I6	
Retention Time (minutes)	Area (%)	Retention Time (minutes)	Area (%)
2.564	12.1833	2.411	42.7874
6.457	12.0855	3.498	9.9422
8.399	35.6560	4.063	22.4084
10.609	10.4089	5.714	13.0985
12.334	29.6663	7.771	11.7635

The retention time and area of the peaks are illustrated in Table 6.23. The methanol extract showed five distinct peaks (Figure 6.30) for retention times 0 to 45 minutes.

The chromatogram for column purified fraction I6 shown in Figure 6.31 contained five distinct peaks indicating that five classes of compound still exists. The peaks obtained were sharp, distinct and prominent. This could



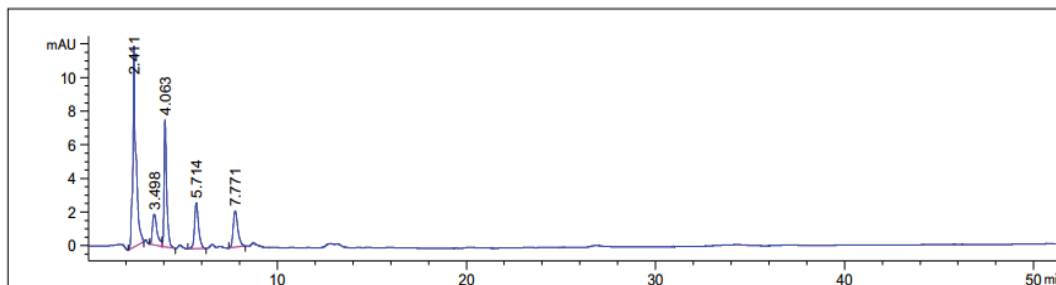


Figure 6.31: HPLC chromatogram of column purified fraction I6 for methanol extract of *Acacia concinna*.

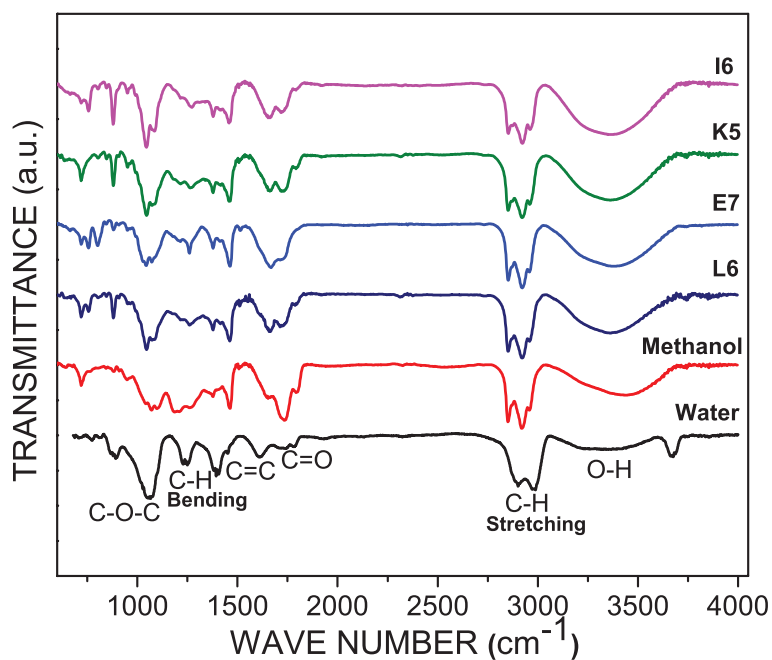
be due to the removal of some compounds during CC.

The elution of the solvent with lower retention time indicates the presence of polar compounds and higher retention time non-polar compounds. Peaks with retention time 10-20 minutes indicated the presence of saponin [266, 268, 280].

### 6.6.5 FTIR Analysis

Figure 6.32 illustrates the FTIR spectra. The different functional groups present are outlined in Table 6.24. Hydroxyl, alkyl, ether and ester groups were seen. Characteristic oleanane triterpenoid saponin absorptions were seen, showing the presence of OH, C=O, C-H, and C=C. Oleanane-type triterpenoid saponins are characterized by the C=O bond due to the presence of oleanolic acid/ester. The absorption peak due to C-O-C indicated glycoside linkages to the sapogenins [269].

Similar functional groups were present in water, methanol and column purified fractions. This showed that saponin can be easily detected in water and methanol extracts [271]. Prominent glycoside linkages to the sapogenins,

Figure 6.32: FTIR spectra for extracts of *Acacia concinna*.Table 6.24: Functional groups present in extracts of *Acacia concinna*.

Functional Groups	Water Extract $\text{cm}^{-1}$	Methanol Extract $\text{cm}^{-1}$	Fract. E7 $\text{cm}^{-1}$	Fract. I6 $\text{cm}^{-1}$	Fract. K5 $\text{cm}^{-1}$	Fract. L6 $\text{cm}^{-1}$
O-H	3228	3409	3381	3360	3359	3353
C-H Stretching	2989	2957	2957	2960	2958	2957
	2971	2920	2922		2921	2922
	2901	2851	2856	2851	2958	2851
C=O	1783	1794	1713	1717	1792	1723
	1742	1734	-	-	1724	1712
	1712	-	-	-	-	-
C=C	1610	1651	1665	1662	1664	1666
	-	-	1513	1653	1654	1657
	-	-	-	1645	-	1651
C-H Bending	1409	1662	1461	1458	1462	1461
	1382	1379	1377	1378	1375	1378
C-O-C	1239	1264	1261	1271	1262	1263
	1075	1186	1072	1086	1075	1072
	1055	1044	1027	1045	1045	1046

C-O-C is seen for water and column purified fractions I6, K5 and L6. The observed changes in FTIR spectrum is attributed to the efficient removal of impurities during purification process making the peak prominent.

### 6.6.6 GC-MS Analysis

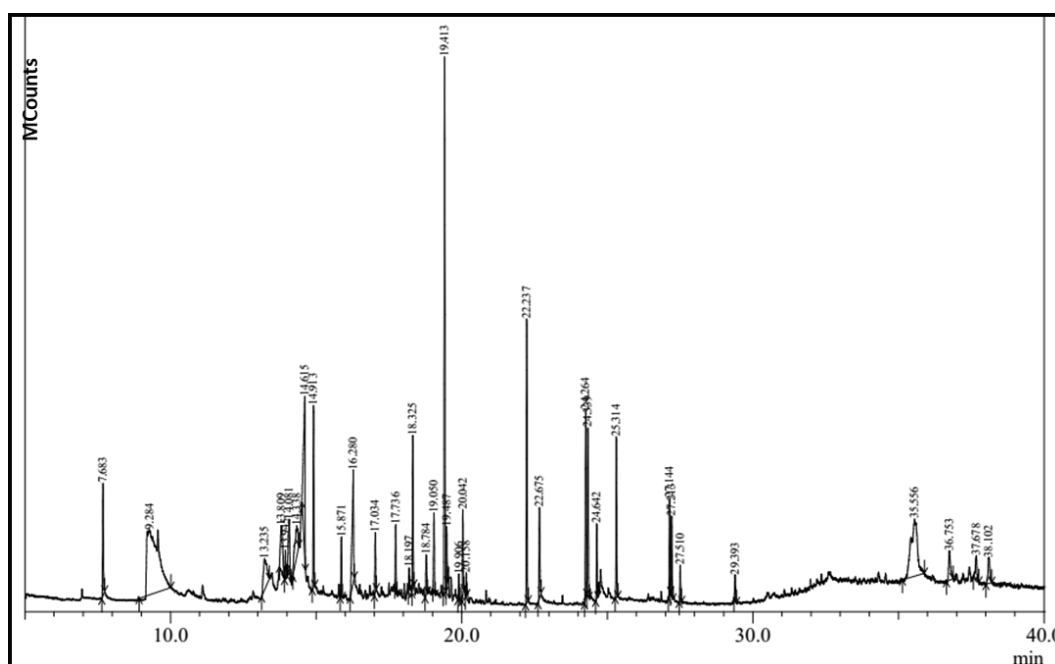


Figure 6.33: GC-MS chromatogram for methanol extract of *Acacia concinna*.

The GC-MS representation for methanol extract of *Acacia concinna* is shown in Figure 6.33 leading to identification of a large number of compounds. The methanol extract showed the presence of 36 bioactive phytochemical compounds: alcohols, esters, aromatic substances, fatty acids etc. The prominent compounds are illustrated in Table 6.25. The presence of fatty acids in the plant extract shows that the plant could have for pharmacological usage [274].

Table 6.25: Chemical constituents for methanol extract of *Acacia concinna* by GC-MS.

Peak No.	Retention Time (minutes)	Peak Area (%)	Molecular Formula	Molecular Mass (g/mol)	IUPAC Name of Compound
1	9.284	18.00	C <sub>7</sub> H <sub>10</sub> O <sub>2</sub>	126.15	1,3-Cyclo-, -hexanedione 2-methyl
2	14.615	5.89	C <sub>10</sub> H <sub>16</sub> O <sub>2</sub>	168.23	Neric acid
3	19.413	9.82	C <sub>15</sub> H <sub>22</sub> O	218.33	(3aR, 4R, 7R) -1,4,9,9- Tetramethyl- 3,4,5,6,7,8- hexahydro-2H-3a, 7-methanoazulen-2-one
4	35.556	8.92	C <sub>34</sub> H <sub>46</sub> N <sub>2</sub> O <sub>6</sub>	578.74	Cholesta-5, 7-dien-3. -ol,3,5- dinitrobenzoate

## 6.7 Conclusion

The results obtained from this study contribute to the knowledge of chemical composition of the extracts of *Albizia procera*, *Juglans regia*, *Zephyranthes carinata*, *Acacia concinna* and *Sapindus mukorossi*. The TLC showed the presence of saponin having large number of polar and non-polar groups. UV-Vis results confirmed the presence of saponin along with smaller amount of flavonoids. FTIR analysis on these extracts suggest the presence of triterpenoid saponins. The results from the HPLC analysis suggest that good separation of compounds is possible using water-methanol solvent system with varying compositions. The GC-MS gave a detailed insight of the chemical profiles of the compounds present. The GC-MS analysis showed the presence

of diverse classes of compounds having biological, industrial and pharmacological importance. The presence of fatty acids in these plant extract provides the pharmacological characteristics of the plants. Thus the natural surfactant contains a wide range of pharmacologically interesting compounds which could be exploited in future.

# Chapter 7

## Two-Dimensional One-Shot Forced Drainage

After studying the surface and foam properties of natural surfactants, it is essential to examine drainage properties of foam, an important factor in analyzing the stability of foam. The drainage profile in natural surfactant systems were investigated by studying the drainage characteristics; the balance between gravity and capillarity over time. This is perhaps the first study of foam drainage on plant based natural surfactant systems.

### 7.1 Introduction

Drainage is the flow of liquid through foam as a result of gravity and capillarity. It is an important aspect to study the physics of foams [82]. The gravitational forces cause most of the liquid to drain, thus destabilizing the foam and changing its rheological properties. It is a complex physico-chemical

hydrodynamic process depending not only on shape and size of the Plateau borders but also on the rate of destruction of foam by bubble coalescence [222]. The liquid flows out of the foam when the hydrostatic pressure at the bottom of foam column becomes larger than the external pressure. When the foam becomes dry, liquid films become thinner, the structure becomes fragile resulting in collapse. Drainage is thus ultimately related to the stability of foam. A study of drainage is important for industries such as brewing, petroleum and separation technology [13].

The drainage process is controlled by surface energy and viscous dissipation of the liquid. Gravity affects the viscous dissipation as greater gravity leads to faster flow of liquid and hence larger viscous dissipation. As the liquid flows along the channels, it pushes the bubbles to adjust their shape by surface tension and also causes rearrangements. This makes the channel wider or narrower, thus affecting liquid flow [82].

The liquid draining from the foam undergoes viscous losses determined by two drainage regimes. The channel dominated/Poiseuille flow (viscous losses dominant in the Plateau borders) and the node dominated/ Plug flow (viscous loss dominant in the nodes) [81, 283]. For Poiseuille flow the scaling law between the velocity of drainage wave  $v$  and input flow rate  $Q$  is given by [79]

$$v \propto Q^{1/2} \quad (7.1)$$

In plug flow the relation is [284].

$$v \propto Q^{1/3} \quad (7.2)$$

Many studies have been carried out on drainage in one-dimension over the years [75, 78, 79, 285, 286]. However, limited amount of work have been performed for two-dimensional drainage [13, 77, 83]. Forced drainage is the downward flow of liquid poured at a constant rate on top of a dry foam [80]. It leads to a propagation of wet wave through the foam. Addition of surfactant solution on top of a foam periodically leads to pulsed drainage, a modification of forced drainage [222].

In this work we have studied one-shot forced drainage in two-dimensions using natural plant based surfactant systems. The foams were produced by passing nitrogen gas in a Hele-Shaw cell containing surfactant solution. The details of the experimental system is described in Chapter 3. This is the first study of drainage profile in plant based natural surfactant systems. Here even though the system is three dimensional, drainage properties of foams are investigated in only one face of a rectangular cell. Thus it is referred to as two-dimensional drainage, the dimensions mentioned are the vertical and the horizontal. The remaining horizontal direction will be similar to the one studied. In addition, I have also tried to investigate the shape of the drainage profile as it flows downstream. This study could provide a valuable insight about the drainage characteristics. Two natural surfactant systems, *Sapindus mukorossi* and *Acacia concinna* have been studied.



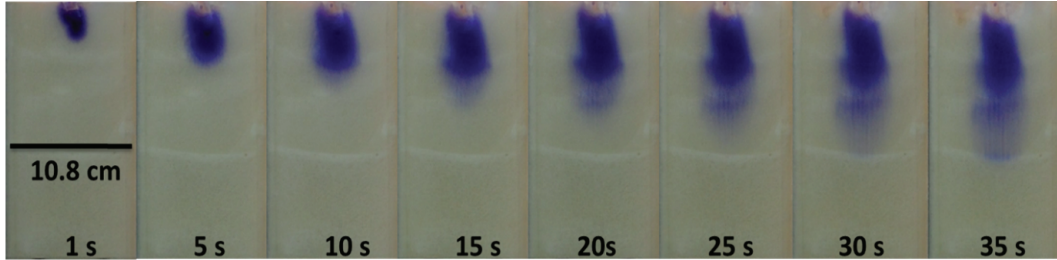


Figure 7.1: Snapshot of 2 D drainage for *Sapindus mukorossi*, 0.5 ml liquid added. Photograph shows precursor movement after 10 seconds.

## 7.2 *Sapindus mukorossi*

### 7.2.1 Drainage Profile

One-shot forced drainage was studied in two-dimension using a Hele-Shaw cell. Foam was prepared on a  $4.69 \times 10^{-2}$  g/cc solution by Bikerman's method. Mono-dispersed foam having small bubbles ( $\sim < 0.5$  mm) was produced. 0.5 ml of the same surfactant solution with a blue dye was added at the top of the foam column. Snapshots of the drainage pattern at different times are shown in Figure 7.1. The intensity of light received by the camera is taken as an indication of liquid fraction, darker foam corresponding to higher liquid fraction. The draining wave travels faster in the vertical direction compared to horizontal direction. The vertical movement is attributed to gravity while the horizontal spreading is due to capillarity.

Figure 7.2(a) shows the propagation of drainage wave in vertical and horizontal directions as a function of time. The vertical front moves linearly while the horizontal front moves initially and then remains fixed. The linear increase in front position indicates that the drainage wave flows downwards with a constant speed. The vertical position of the wave is plotted on a

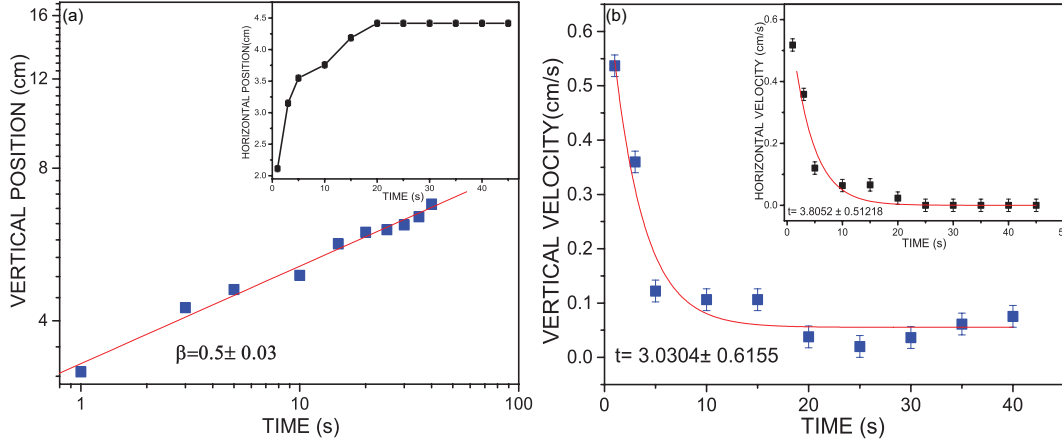


Figure 7.2: (a) Position of wave front along vertical and horizontal directions as a function of time (b) Variation of vertical and horizontal velocity with time.

double logarithmic scale. It is observed that the vertical front position proceeds with time in the form of power law  $v \propto Q^\beta$ . The exponent obtained is  $\beta = 0.5 \pm 0.03$ , similar to the exponent  $\beta = 0.67$  reported by Hutzler et al for synthetic surfactants [13]. The value of the exponent indicates that the flow is Poiseuille type. Horizontal front position moves and then becomes almost constant. Power law behaviour is not seen. This indicates that *Sap-indus mukorossi* system exhibits similar drainage characteristics as synthetic surfactant systems [13].

The variation of velocity of wave front with time is shown in Figure 7.2(b). The velocity of the wave decreases as it descends and spreads out in the horizontal direction. It is observed that the drainage wave front initially spreads in both directions. The wave front stagnates after  $3.81 \pm 0.51$  seconds in the horizontal direction and  $3.03 \pm 0.62$  seconds in the vertical direction. The spreading of drainage wave in horizontal direction may be attributed to diffusion of moving molecules into the foam. The spreading may also

be due to collision of moving molecules with stationary ones. The diffusion of the moving molecules ceases after some time, may be due to molecular collision lowering the energy and momentum of the particles. The decrease in velocity in the vertical direction can be attributed to equilibrium attained between gravitational and drag force on the surfactant solution after  $3.03 \pm 0.62$  seconds. The amount of liquid flowing down the foam column is also reduced due to horizontal spreading as well as some liquid getting stuck to the foam.

## 7.2.2 Drainage Profile Shape

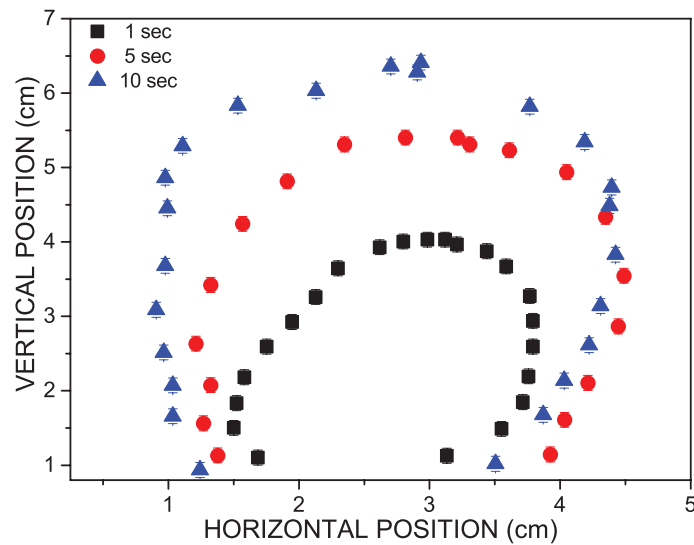


Figure 7.3: Shape of the drainage pattern. The vertical axis is shown upwards, hence the shape should be visualised in reverse.

When solution is added from the top, the liquid drains in the foam, velocities vary widely and the liquid spreads gradually occupying an increasing portion of flow region. Figure 7.3 shows the drainage pattern at 1, 5 and 10 seconds. This microscopic phenomenon is attributed to the combination

of molecular diffusion and hydrodynamic mixing occurring with the laminar flow through the foam. This results in a conic form downstream from a continuous point source producing an expanding ellipsoid [287].

### 7.2.3 Liquid Fraction along Vertical and Horizontal Positions

The gray scale (K) or the intensity of light at any point is taken as an indication of the liquid fraction. Thus the profiles of the liquid fraction represents the beginning of propagation of the drainage wave, it's initial build-up at the top of the foam and finally the flow of the drainage wave downstream. The drainage wave moves downwards from the source and tends to be a normal Gaussian distribution vertically and horizontally, as illustrated in Figure 7.4. The drainage profile obtained for one-shot forced drainage is similar to pulsed drainage profile [75]. The drainage profile exhibits three regions. The first region is the rear which is the injection point. The second region is the middle region, which extends from the injection point to the maximum of liquid fraction. The third region is the front, which is the region below the maximum liquid fraction [75].

The vertical component is larger than the horizontal, which indicates that the major axis of mixing occurs in the direction of flow. The drainage wave along vertical and horizontal direction shows a normal Gaussian shape. The normal Gaussian distribution, along the vertical direction distorts after 10 seconds indicating that there exist two types of flow. This may also indicate that most of the liquid is flowing together through the foam and only a

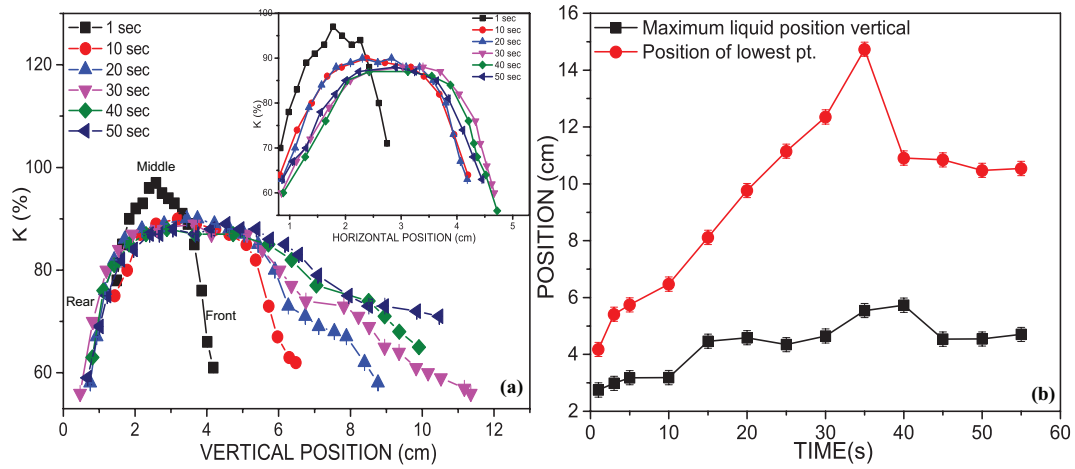


Figure 7.4: (a) Profiles of liquid fraction along the vertical and horizontal (b) Position of the wetting front moving through the foam.

small portion is flowing at a faster rate. The spreading of the wave along the horizontal direction becomes almost constant after 30 seconds. This indicates that most of the liquid is moving together vertically and only a small part is spreading in the horizontal direction or remaining at the point of origin.

Figure 7.4 (b) gives the movement of the position of the maximum liquid fraction (red circles). Also plotted is the position of the lowest point of the wave front (black squares). It is evident that the front position moves faster than the maximum liquid fraction indicating two different movements.

### 7.2.4 Effect of added dye on Surface Tension

The effect of adding indigo dye to *Sapindus mukorossi* solution was studied below CMC, just before CMC and above CMC. The surface tension curves are as illustrated in Figure 7.5. It is observed that below CMC the added dye has little affect on the surface tension. The surface tension reduced as the amount of the dye was increased. The surfactant molecules exist as

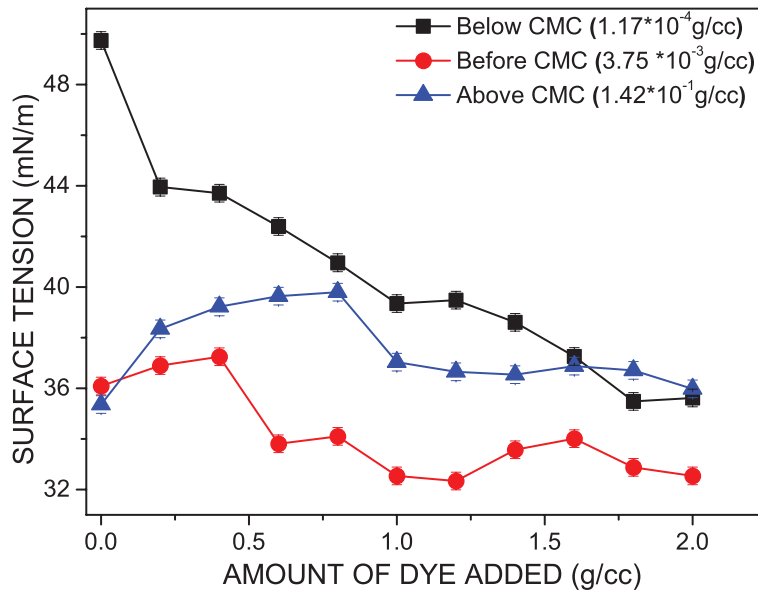


Figure 7.5: Surface tension as a function of amount of dye added.

monomers and the dye particles were able to come up to the surface.

When the dye was added just before CMC, it was observed that the surface tension was not much affected. Just before CMC, more molecules exist at the air-water interface and no dye molecules could be accommodated. This lead to the formation of micelles. The dye particles may have surrounded the micelles due to which no significant change in surface tension was seen. Above CMC, the dye had minimal effect on surface tension. Since we are working on solutions where micelles have already been formed, the dye should not have any significant effect on the drainage process.

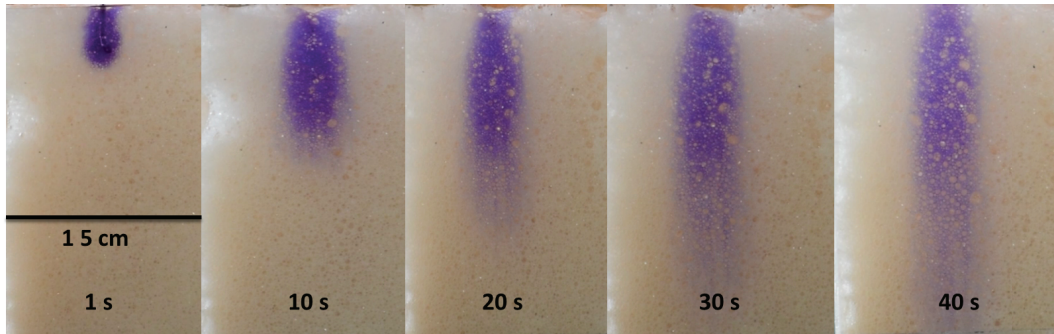


Figure 7.6: Snapshot of 2 D drainage for *Acacia concinna*, 0.5 ml liquid added. Photograph shows precursor movement after 10 seconds.

## 7.3 *Acacia concinna*

### 7.3.1 Drainage Profile

Another surfactant system, *Acacia concinna* was used to investigate one-shot forced drainage. Bikerman's method was used to generate foam with the concentration of the solution  $5.25 \times 10^{-2}$  g/cc. Poly-dispersed foam having large bubble size ( $\sim > 0.5$  mm) was produced by this surfactant system. As in the case of *Sapindus mukorossi* system, a 0.5 ml surfactant solution with a dye was added at the top of the foam column prepared. Figure 7.6 illustrates two-dimensional drainage at different time scale. The draining wave again travelled faster in the vertical direction, as compared to horizontal direction.

The propagation of drainage wave in vertical and horizontal directions with time is shown in Figure 7.7(a). The results were similar to *Sapindus mukorossi* system. The vertical front position increases linearly indicating that the drainage wave flows downwards with a constant speed. The horizontal front position increases and then remains constant with time. Plotting

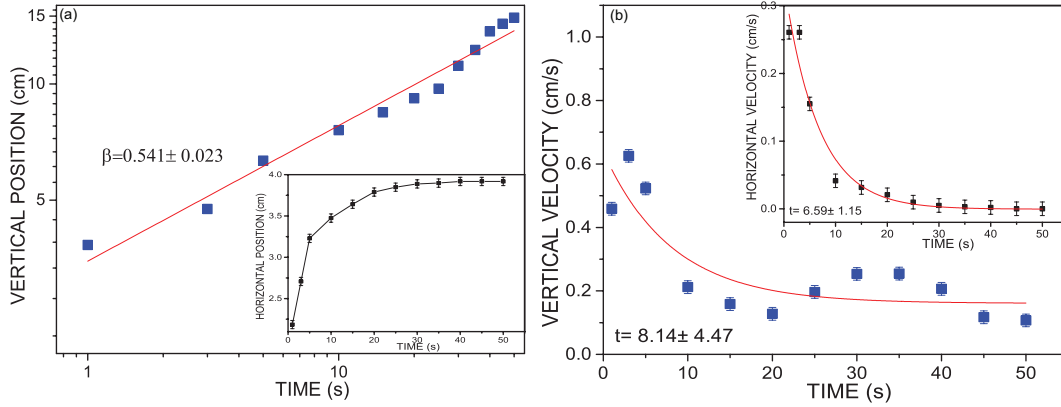


Figure 7.7: (a) Position of wave front along vertical and horizontal directions (b) Variation of vertical and horizontal velocity with time.

the vertical position of the wave on a double logarithmic scale, it is observed that the vertical front position proceeds with time in the form of power law  $v \propto Q^\beta$ . The exponent obtained is  $\beta = 0.541 \pm 0.023$  was similar to *Sapindus mukorossi* and that reported for synthetic surfactants [13]. The flow exhibited is also Poiseuille. The power law is not followed in the horizontal direction as front position moves and then becomes almost constant. This results indicates that *Acacia concinna* system also exhibited similar drainage characteristics as *Sapindus mukorossi* and synthetic surfactant systems.

Figure 7.7(b) illustrates the variation of wave front velocity with time. As in the case of *Sapindus mukorossi* system, the drainage wave front spreads in both directions and stagnates after  $6.59 \pm 1.15$  seconds in the horizontal direction and  $8.14 \pm 4.47$  seconds in the vertical direction.

### 7.3.2 Drainage Profile Shape

Figure 7.8 shows the drainage pattern for 1 second, 5 seconds and 10 seconds. The shape of the drainage pattern is similar to *Sapindus mukorossi* system



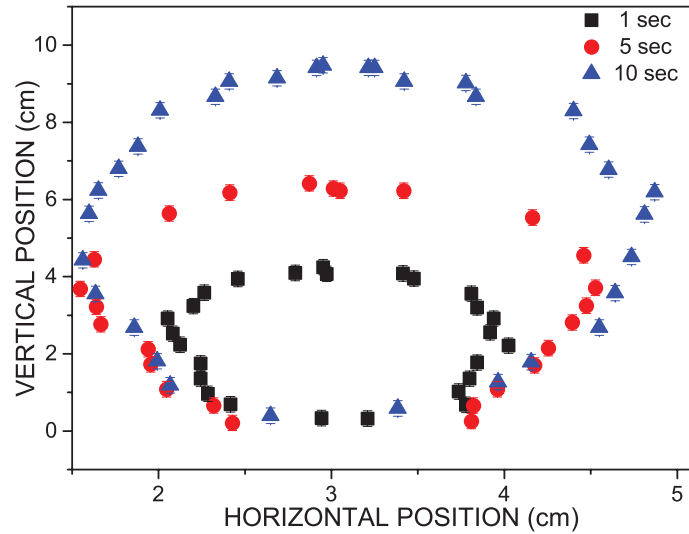


Figure 7.8: Shape of the drainage pattern.

with slight distortion. This distortion may be attributed to the size and nature of the bubbles formed. When liquid is added, it drains in the foam, resulting in variation of velocities. The liquid spreads gradually occupying an increasing portion of flow region. The combination of molecular diffusion and hydrodynamic mixing in the laminar flow through the foam is responsible for this microscopic phenomenon. Thus a conic form is produced resulting in an expanding ellipsoid [287].

### 7.3.3 Liquid Fraction along Vertical and Horizontal Position

The liquid fraction profile is similar to *Sapindus mukorossi* system. Figure 7.9(a) shows that initially the liquid fraction is constant for a short distance and becomes very small immediately after that. This behaviour was not seen for *Sapindus mukorossi*. The constant liquid fraction corresponds to wet

foam and the rapid decrease means that the foam below is dry [81]. After few seconds the drainage wave travels downwards from the source and tends to be a distorted Gaussian distribution vertically and horizontally. This distortion is due to the poly-dispersed foam produced by *Acacia concinna* system.

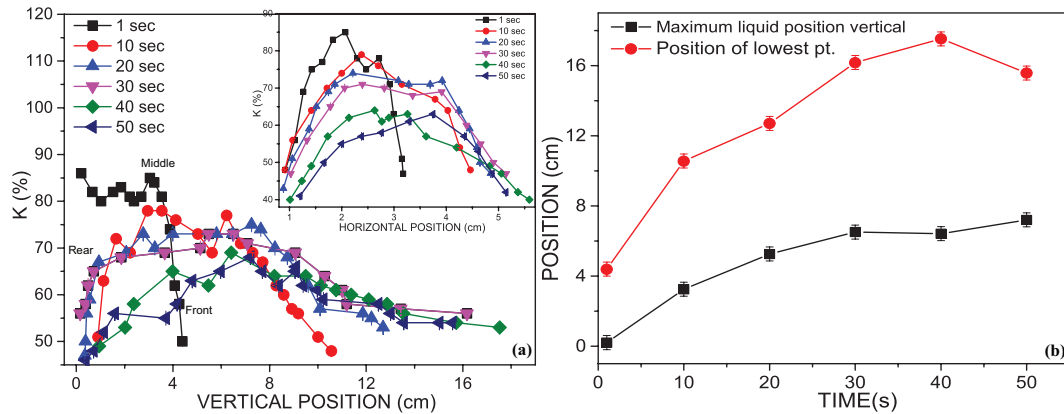


Figure 7.9: (a) Profiles of liquid fraction along the vertical and horizontal (b) Position of the wetting front moving through the foam.

The distorted Gaussian distribution along the vertical direction shows variation in its flow after 10 seconds indicating that there exists two types of flow. The variation in its nature also indicates that most of the liquid is flowing together through the foam and a small portion is flowing at a faster rate. The spreading of the wave along the horizontal direction becomes almost constant after 5.5 seconds. This indicates that most of the liquid is moving together downward and only a small part is spreading in the horizontal direction or remaining stationary.

Figure 7.9 (b) shows the variation of position of maximum liquid fraction along the vertical direction and the lowest point of the wave front along the vertical at a given time. The front position thus moves faster than the maximum liquid fraction.

## 7.4 Conclusion

To quantitatively understand the process of foam drainage, forced drainage experiment in two-dimensions for *Sapindus mukorossi* and *Acacia concinna* system were performed. This is probably the first study of one-shot forced drainage through plant based natural surfactant systems. Similar basic drainage profiles were exhibited by both systems. The drainage wave flows downwards and also spreads horizontally as it descends. The horizontal spreading is attributed to diffusion of added solution into the foam and collision of spreading molecules with the foam. The vertical flow slows down after attaining equilibrium between gravitational force and drag force. The vertical front position for both the systems follows a power law behaviour. The results from the drainage profile indicate a Poiseuille flow, similar to results obtained by Hutzler et al for synthetic surfactants [13].

In addition, we have analysed the shape of the drainage profile for both systems which exhibit a conic form downstream and later produces an expanding ellipsoid. The liquid fraction analysis shows that the drainage profile for *Sapindus mukorossi* is a normal Gaussian distribution along the horizontal and asymmetric Gaussian distribution along the vertical. The *Acacia concinna* system shows distorted Gaussian distribution along the horizontal and vertical directions, attributed to poly-dispersed foam. The vertical movement of the liquid through the foam exhibits two different types of movement. The presence of two different movements of the liquid has not been previously reported in the literature. Whether it is a precursor followed by the main liquid is still a question that has to be further investigated.

CHAPTER 7. TWO-DIMENSIONAL ONE-SHOT FORCED DRAINAGE 199

As a precautionary measure, the effect of added dye on surface tension was studied for *Sapindus mukorossi* system. The results indicate that the added dye did not have any major effect.

## Part IV

# CONCLUSIONS

# Chapter 8

## Concluding Remarks and Future Prospects

This chapter summarizes the research work presented in the thesis. In addition, some suggestions have been made for possible further work in the field.

### 8.1 Conclusion

In the thrust to find an eco-friendly alternative to synthetic surfactants, we investigated the surface and foam properties of five plant based natural surfactants. The plants studied were *Sapindus mukorossi*, *Albizia procera*, *Juglans regia*, *Zephyranthes carinata* and *Acacia concinna*. The surface activity of some synthetic surfactants were studied as a reference. In addition, we studied the chemical profiles of the natural surfactants and carried out a preliminary characterization of the compounds present.

The studies on surface and foam characteristics (Chapter 4) revealed that the plant extracted natural surfactants exhibited similar properties to that of synthetic ones. The surface activities of *Albizia procera*, *Zephyranthes carinata* and *Juglans regia* have been studied for the first time. *Sapindus mukorossi* and *Acacia concinna* exhibited greater surface tension reduction indicating good detergency while *Albizia procera*, *Juglans regia*, *Zephyranthes carinata* showed moderate detergency. *Sapindus mukorossi*, *Acacia concinna*, *Zephyranthes carinata* are acid balanced with respect to human skin while *Albizia procera* and *Juglans regia* are less acidic. Good wetting was shown by *Albizia procera* and *Acacia concinna* and moderate wetting by *Sapindus mukorossi* and *Zephyranthes carinata*. *Juglans regia* did not exhibit any change in wetting from pure water even though the surface tension reduced significantly. All the surfactants exhibited low CMC except *Acacia concinna* indicating that micellar solubilization begin at a lower concentration.

Addition of salt on foaming below and at CMC revealed an optimum limit for maximum foaming. Above CMC, foaming decreases with salt concentration. This could be attributed to enhanced electrostatic repulsion between adsorbed and non-adsorbed particles and also due to reduced adsorption at the air-water interface.

Emulsification studies reveal that emulsion stability decreases in the region of micelle formation. Good emulsification properties were shown by *Sapindus mukorossi* and *Zephyranthes carinata* which could find many industrial applications. The effect of salt on viscosity was minimal for natural surfactants indicating their non-ionic nature. The natural surfactants exhibited surface and foam properties similar to synthetic surfactants making

them potential candidates for good surface activity useful for many cosmetic and food industries.

Exploring the surface and foam properties lead us to study the CMCs of surfactants. Dirt Dispersion (DD) or the amount of dirt present in the foam is an important parameter. We have quantified DD for the first time and have studied its variation with concentration. While quantifying DD we were able to measure the CMCs of surfacants using a digital camera and a computer with appropriate software (Chapter 5). Dirt in foam increases, reaches a maximum and then decreases with increase in concentration. The concentration at which maximum amount of dirt remains in the foam corresponds to CMC. The results illustrate that this approach towards CMC measurement agrees with surface tension measurements. This leads to a new approach of CMC determination which is easy, inexpensive and requires very small amount of sample. In addition, CMC for complex mixtures can also be obtained, leading to easy low cost approach for CMC determination of non-ionic surfactants.

To understand their chemical profile preliminary characterization of the natural surfactants were performed (Chapter 6). TLC analysis revealed the presence of saponin having a large number of polar and non-polar groups. The presence of saponin along with small amount of flavonoids was supported by the UV-Vis results. Investigating FTIR suggest the presence of triterpenoid saponin.

HPLC results indicate the presence of large number of compounds. Good separation of compounds was achieved using water-methanol solvent system. The details of the different chemical profiles of the compounds were investig-



ated by GC-MS which showed the presence of diverse classes of compounds belonging to alcohol, esters, aldehyde and fatty acids classes.

Drainage is an essential factor in analyzing the stability of foam. The stability mechanism of foam was understood by studying one-shot two-dimensional drainage characteristics, a balance between gravity and capillarity over time (Chapter 7). A dye was added to the added surfactant from the top of the foam to make drainage visible. This is the first study of two-dimensional foam drainage on plant based natural surfactants.

The drainage profiles exhibited by *Sapindus mukorossi* and *Acacia concinna* systems were similar. The draining wave flows vertically due to gravity and spreads horizontally as it descends. The drainage profile reveals that the vertical front position proceeds with time in the form of power law. These natural systems exhibit a Poiseuille type flow, similar to the results obtained by Hutzler et al for synthetic surfactants [13].

The drainage wave for both systems reveal a conic form downstream producing an expanding ellipsoid with time. Liquid fraction analysis of *Sapindus mukorossi* system showed normal Gaussian distribution along the horizontal and asymmetric Gaussian distribution along the vertical. *Acacia concinna* system showed distorted Gaussian distribution along the horizontal and vertical directions, attributed to the poly-dispersity of the foam. This asymmetric Gaussian distribution along the vertical is attributed to the existence of two different types of movement as the drainage wave flows downstream. These two movements of the liquid through the foam has not been previously reported in the literature. The reason behind this is still a question that needs to be investigated further.

## 8.2 Future Prospects

From the study of surface and foam properties of natural surfactants (Chapter 4), we have seen that the natural surfactants are appropriate candidates for surface activity. Further studies on surface and foam properties could be performed on mixed surfactant systems which could exhibit better performance than a single surfactant system. This could further give an understanding of the synergistic interaction of the mixed surfactants providing a wider use of the natural surfactants.

Chapter 5 suggests a new approach towards measurement of CMC of non-ionic surfactants. Further studies on other mixed micelle systems should be conducted using this approach which could provide a better understanding micelles and CMC should also be studied using Dynamic Light Scattering technique.

Preliminary characterization for natural surfactants have given interesting results (Chapter 6). Further work on purification of individual compounds would reveal their structures that would be beneficial.

Chapter 7 describes two-dimensional one-shot forced drainage where the drainage profile, shape of drainage and liquid fraction were investigated. The experimental results should further be subjected to theoretical understanding. This would complement the experimental results and allow a better understanding of drainage in foams.

# Part V

## APPENDIX

# Appendix

## Identification of Plants

The letters of identification and authentication of parts of the plant are presented below:



Ph. No. (03592) 231494 (0)  
Fax No. (03592) 231213  
E-mail : arri.gangtok@gmail.com

### आयुर्वेद क्षेत्रीय अनुसंधान संस्थान

तादोंग, गान्तोक - 737102 (सिक्किम)

### AYURVEDA REGIONAL RESEARCH INSTITUTE

TADONG, GANGTOK - 737102 (SIKKIM)

Central Council for Research in Ayurvedic Sciences

Deptt. of AYUSH, Ministry of Health & Family Welfare, Govt. of India

केन्द्रीय आयुर्वेदीय विज्ञान अनुसंधान परिषद

आयुष विभाग, स्वास्थ्य एवं परिवार कल्याण मंत्रालय, भारत सरकार


पत्र सं०.....  
F. No. ३/३९१२/ARRI- GOR/Secy/224

दिनांक.....  
Date: 11.04.2022

### To Whom It May Concern

This is to certify and confirm that the following plant parts collected by Mrs. Ambika Pradhan, IVth Semester (M. Phil- Ph. D.), Department of Physical Science, Sikkim University have been referred, identified and authenticated as detailed below:

S. No	Local Name	Scientific Name	Family	Plant parts
1	Ritha	<i>Sapindus mukorossi</i> Gaertn	<i>Sapindaceae</i>	Fruit Pulp
2	Seto Siris	<i>Albizia procera</i> (Roxb) Benth	<i>Mimosaceae</i>	Leaves
3	Pyagi Phool	<i>Zephyranthes carinata</i> Herbert	<i>Amyrilladaceae</i>	Bulb
4	Shikakai	<i>Acacia concinna</i> DC	<i>Fabaceae</i>	Fruit (Pods)
5	Okhar	<i>Juglans regia</i> Linn.	<i>Juglandaceae</i>	Bark

  
(Dr. T.K. Mandal)  
Research Officer (S-2)  
Incharge



सत्यमेव जयते

**GOVERNMENT OF WEST BENGAL**

☎ 0354 - 2252358(O)

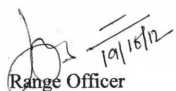
Directorate of Forests  
Office of the Range Officer,  
Lloyd Botanic Garden, Darjeeling  
Silviculture (Hills) Division

**To whom it may concern.**

Certified that Miss. Ambika Pradhan, Department of Physical Science, Sikkim University have visited Lloyd Botanic Garden. She also referred, identified and authenticate the following species with the herbarium of following species.

Local Name	Botanical Name	Family
1. (Rita)	Sapindus mukorossi	-Sapindaceae
2. (Seto siris)	Albizia procera	-Mimosaceae
3. (Pyazi phool)	Zephyranthes Crinate	-Amyrilladaceae
4. (Okher)	Juglams regia	-Juglandaceae

I wish success in her life.

  
Range Officer  
Lloyd Botanic Garden

RANGE OFFICER  
Lloyd Botanic Garden  
DARJEELING

# Bibliography

- [1] M. J. Rosen. *Surfactants and interfacial phenomena*. New Jersey: John Wiley and Sons, Inc., 2004.
- [2] L. L. Schramm. *Surfactants: Fundamentals and applications in the petroleum industry*. United Kingdom: Cambridge University Press, 2000.
- [3] A. Mohr, P. Talbiersky, H-G. Korth, R. Sustmann, R. Boese, D. Blaser, and H. Rehage. A new pyrene-based fluorescent probe for the determination of critical micelle concentrations. *The Journal of Physical Chemistry B*, 111(45):12985–12992, 2007.
- [4] P. Ekwall, L. Mandell, and P. Solyom. The aqueous cetyl trimethylammonium bromide solutions. *Journal of Colloid and Interface Science*, 35(4):519–528, 1971.
- [5] M. Perez-Rodriguez, G. Prieto, C. Rega, L. M. Varela, F. Sarmiento, and V. Mosquera. A comparative study of the determination of the critical micelle concentration by conductivity and dielectric constant measurements. *Langmuir*, 14(16):4422–4426, 1998.

- [6] O. Topel, B. A. Cakir, L. Budama, and N. Hoda. Determination of critical micelle concentration of polybutadiene-block-poly (ethyleneoxide) diblock copolymer by fluorescence spectroscopy and dynamic light scattering. *Journal of Molecular Liquids*, 177:40–43, 2013.
- [7] E. De Vendittis, G. Palumbo, G. Parlato, and V. Bocchini. A fluorimetric method for the estimation of the critical micelle concentration of surfactants. *Analytical Biochemistry*, 115(2):278–286, 1981.
- [8] S. Sunayana. *Wetting of PTFE surface by mixed surfactant solutions in the presence of electrolyte*. PhD thesis, National Institute of Technology, Rourkela, 2010.
- [9] D. L. Weaire and S. Hutzler. *The physics of foams*. New York: Oxford University Press, 2001.
- [10] H. A. Stone, S. A. Koehler, S. Hilgenfeldt, and M. Durand. Perspectives on foam drainage and the influence of interfacial rheology. *Journal of Physics: Condensed Matter*, 15(1):S283–S290, 2003.
- [11] A. Saint-Jalmes, M. U. Vera, and D. J. Durian. Uniform foam production by turbulent mixing: New results on free drainage vs. liquid content. *The European Physical Journal B-Condensed Matter and Complex Systems*, 12(1):67–73, 1999.
- [12] S. A. Koehler, H. A. Stone, M. P. Brenner, and J. Eggers. Dynamics of foam drainage. *Physical Review E*, 58(2):2097–2106, 1998.

- [13] S. Hutzler, S. J. Cox, and G. Wang. Foam drainage in two dimensions. *Colloids and Surfaces A: Physicochemical and Engineering Aspects*, 263(1):178–183, 2005.
- [14] M. Durand and D. Langevin. Physicochemical approach to the theory of foam drainage. *The European Physical Journal E: Soft Matter and Biological Physics*, 7(1):35–44, 2002.
- [15] S. Deshmukh, B. Kaushal, and S. Ghode. Formulations and evaluation of herbal shampoo and comparative studies with herbal marketed shampoo. *International Journal of Pharma and Bio Sciences*, 3(3):638–645, 2012.
- [16] A. Kumar and R. R. Mali. Evaluation of prepared shampoo formulations and to compare formulated shampoo with marketed shampoos. *International Journal of Pharmaceutical Sciences Review and Research*, 3(1):120–126, 2010.
- [17] A. Kabalnov. Thermodynamic and theoretical aspects of emulsions and their stability. *Current Opinion in Colloid and Interface Science*, 3(3):270–275, 1998.
- [18] C. G. Naylor, J. P. Mieure, W. J. Adams, J. A. Weeks, F. J. Castaldi, L. D. Ogle, and R. R. Romano. Alkylphenol ethoxylates in the environment. *Journal of the American Oil Chemists' Society*, 69(7):695–703, 1992.
- [19] C. Edser. Latest market analysis. *Focus on Surfactants*, pages 1–2, 2006.



- [20] T. Ivankovic and J. Hrenovic. Surfactants in the environment. *Archives of Industrial Hygiene and Toxicology*, 61(1):95–110, 2010.
- [21] C. Schmitt, B. Grassl, G. Lespes, J. Desbrieres, V. Pellerin, S. Reynaud, J. Gigault, and V. A. Hackley. Saponins: A renewable and biodegradable surfactant from its microwave-assisted extraction to the synthesis of monodisperse lattices. *Biomacromolecules*, 15(3):856–862, 2014.
- [22] N. R. Biswal. *Studies on adsorption and wetting phenomena associated with solid surfaces in aqueous synthetic and natural surfactant solutions*. PhD thesis, National Institute of Technology, Rourkela, 2012.
- [23] Y. Chevalier. New surfactants: New chemical functions and molecular architectures. *Current Opinion in Colloid and Interface Science*, 7(1):3–11, 2002.
- [24] L. Tmakova, S. Sekretar, and S. Schmidt. Plant-derived surfactants as an alternative to synthetic surfactants: Surface and antioxidant activities. *Chemical Papers*, 70(2):188–196, 2016.
- [25] A. Pradhan and A. Bhattacharyya. Shampoos then and now: Synthetic versus natural. *Journal of Surface Science and Technology*, 30(1-2):59–76, 2014.
- [26] S. A. Ostroumov. Studying effects of some surfactants and detergents on filter-feeding bivalves. *Hydrobiologia*, 500(1):341–344, 2003.

- [27] R. P. Singh, N. Gupta, S. Singh, A. Singh, R. Suman, and K. Annie. Toxicity of ionic and nonionic surfactants to six macrobes found in Agra, India. *Bulletin of Environmental Contamination and Toxicology*, 69(2):265–270, 2002.
- [28] N. R. Biswal and S. Paria. Interfacial and wetting behavior of natural–synthetic mixed surfactant systems. *RSC Advances*, 4(18):9182–9188, 2014.
- [29] P. Piispanen. *Synthesis and characterization of surfactants based on natural products*. PhD thesis, Kungl Tekniska Hogskolan, Stockholm, 2002.
- [30] K. Holmberg. Natural surfactants. *Current Opinion in Colloid and Interface Science*, 6(2):148–159, 2001.
- [31] W. Oleszek and Z. Bialy. Chromatographic determination of plant saponins—an update (2002–2005). *Journal of Chromatography A*, 1112(1):78–91, 2006.
- [32] E. Karimi, H. Z. E. Jaafar, and S. Ahmad. Phytochemical analysis and antimicrobial activities of methanolic extracts of leaf, stem and root from different varieties of *Labisa pumila* Benth. *Molecules*, 16(6):4438–4450, 2011.
- [33] S. Mitra and S. R. Dungan. Micellar properties of Quillaja saponin. 1. Effects of temperature, salt, and pH on solution properties. *Journal of Agricultural and Food Chemistry*, 45(5):1587–1595, 1997.

- [34] P. Molgaard, A. Chihaka, E. Lemmich, P. Furu, C. Windberg, F. Ingerslev, and B. Halling-Sorensen. Biodegradability of the molluscicidal saponins of *Phytolacca dodecandra*. *Regulatory Toxicology and Pharmacology*, 32(3):248–255, 2000.
- [35] P. K. S. M. Rahman and E. Gakpe. Production, characterisation and applications of biosurfactants-Review. *Biotechnology*, 7(2):360–370, 2008.
- [36] C-H. Yang, Y-C. Huang, Y-F. Chen, and M-H. Chang. Foam properties, detergent abilities and long-term preservative efficacy of the saponins from *Sapindus mukorossi*. *Journal of Food and Drug Analysis*, 18(3):155–160, 2010.
- [37] J. Holdaway. *A study of the structure and formation of biocompatible mesostructured polymer-surfactant hydrogel films*. PhD thesis, University of Bath, United Kingdom, 2013.
- [38] S. P. Sulakhe. *Studies in interfacial science: Ecofriendly surfactant*. PhD thesis, Institute of Chemical Technology, Mumbai, 2012.
- [39] D. G. Davies and C. R. Bury. CCLXXXIX.-The partial specific volume of potassium n-octoate in aqueous solution. *Journal of the Chemical Society (Resumed)*, pages 2263–2267, 1930.
- [40] M. Mishra, P. Muthuprasanna, K. S. Prabha, P. S. Rani, I. A. Satish, I. Sarath Ch., G. Arunachalam, and S. Shalini. Basics and potential applications of surfactants-a review. *International Journal of PharmTech Research*, 1(4):1354–1365, 2009.

- [41] A. Nokhodchi, J. Shokri, A. Dashbolaghi, D. Hassan-Zadeh, T. Ghafourian, and M. Barzegar-Jalali. The enhancement effect of surfactants on the penetration of lorazepam through rat skin. *International Journal of Pharmaceutics*, 250(2):359–369, 2003.
- [42] X. M. Li, L. Gu, Y. L. Xu, and Y. L. Wang. Preparation of fenofibrate nanosuspension and study of its pharmacokinetic behavior in rats. *Drug Development and Industrial Pharmacy*, 35(7):827–833, 2009.
- [43] J. W. Logan and F. R. Moya. Animal-derived surfactants for the treatment and prevention of neonatal respiratory distress syndrome: Summary of clinical trials. *Therapeutics and Clinical Risk Management*, 5:251–260, 2009.
- [44] F. H. Pennings, B. L. S. Kwee, and H. Vromans. Influence of enzymes and surfactants on the disintegration behavior of cross-linked hard gelatin capsules during dissolution. *Drug Development and Industrial Pharmacy*, 32(1):33–37, 2006.
- [45] P. Dimmitt. Cerumen removal products. *Journal of Pediatric Health Care*, 19(5):332–336, 2005.
- [46] O. Elmofty. Surfactant enhanced oil recovery by wettability alteration in sandstone reservoirs. Master’s thesis, Missouri University of Science and Technology, USA, 2012.
- [47] N. Venkatesh. *Studies on synthesis of biosurfactants and their applications*. PhD thesis, Anna University, Chennai, 2011.

- [48] J. D. Van Hamme, A. Singh, and O. P. Ward. Physiological aspects: Part 1 in a series of papers devoted to surfactants in microbiology and biotechnology. *Biotechnology Advances*, 24(6):604–620, 2006.
- [49] J. Drelich, C. Fang, and C. L. White. Measurement of interfacial tension in fluid-fluid systems. *Encyclopedia of Surface and Colloid Science*, 3:3158–3163, 2002.
- [50] G. Masutani and M. K. Stenstrom. A review of surface tension measuring techniques, surfactants, and their implications for oxygen transfer in waste water treatment plants. *Water Resources Program, School of Engineering and Applied Science, University of California, Los Angeles*, 1984.
- [51] P. L. du Nouy. An interfacial tensiometer for universal use. *The Journal of General Physiology*, 7(5):625, 1925.
- [52] R. Miller, V. B. Fainerman, K-H. Schano, A. Hofmann, and W. Heyer. Dynamic surface tension determination using an automated bubble pressure tensiometer. *Tenside, Surfactants, Detergents*, 34(5):357–363, 1997.
- [53] J. W. McBain and C. S. Salmon. Colloidal electrolytes-Soap solutions and their constitution. *Journal of the American Chemical Society*, 42(3):426–460, 1920.
- [54] A. S. C. Lawrence. Solubility in soap solutions. Part 10.—Phase equilibrium, structural and diffusion phenomena involving the ternary liquid crystalline phase. *Discussions of the Faraday Society*, 25:51–58, 1958.

- [55] P. H. Elworthy, A. T. Florence, and C. B. Macfarlane. *Solubilization by surface-active agents and its applications in chemistry and the biological sciences*. Chapman and Hall, 1968.
- [56] A. T. Florence and R. T. Parfitt. Micelle formation by some phenothiazine derivatives. II. Nuclear magnetic resonance studies in deuterium oxide. *The Journal of Physical Chemistry*, 75(23):3554–3560, 1971.
- [57] M. Mondal, A. Roy, S. Malik, A. Ghosh, and B. Saha. Review on chemically bonded geminis with cationic heads: Second-generation interfacants. *Research on Chemical Intermediates*, 42(3):1913–1928, 2016.
- [58] R. J. Farn. *Chemistry and technology of surfactants*. United Kingdom: John Wiley and Sons, 2008.
- [59] P. L. Nostro. Cleaning II: Surfactants and micellar solutions. *Nanoscience for the Conservation of Works of Art*, 28:147, 2013.
- [60] K. G. Furton and A. Norelus. Determining the critical micelle concentration of aqueous surfactant solutions: Using a novel colorimetric method. *Journal of Chemical Education*, 70(3):254–257, 1993.
- [61] A. Patist, S. S. Bhagwat, K. W. Penfield, P. Aikens, and D. O. Shah. On the measurement of critical micelle concentrations of pure and technical-grade nonionic surfactants. *Journal of Surfactants and Detergents*, 3(1):53–58, 2000.

- [62] K. P. Ananthapadmanabhan, E. D. Goddard, N. J. Turro, and P. L. Kuo. Fluorescence probes for critical micelle concentration. *Langmuir*, 1(3):352–355, 1985.
- [63] J. J. Bikerman. *Foams*. New York: Springer-Verlag, 1973.
- [64] A. A. Waltermo, P. M. Claesson, S. Simonsson, E. Manev, I. Johansson, and V. Bergeron. Foam and thin-liquid-film studies of alkyl glucoside systems. *Langmuir*, 12(22):5271–5278, 1996.
- [65] L. L. Schramm and F. Wassmuth. *Foams: Basic principles*. ACS Publications, 1994.
- [66] K. S. Lim and M. Barigou. Ultrasound-assisted generation of foam. *Industrial and Engineering Chemistry Research*, 44(9):3312–3320, 2005.
- [67] L. K. Shrestha, D. P. Acharya, S. C. Sharma, K. Aramaki, H. Asaoka, K. Ihara, T. Tsunehiro, and H. Kunieda. Aqueous foam stabilized by dispersed surfactant solid and lamellar liquid crystalline phase. *Journal of Colloid and Interface Science*, 301(1):274–281, 2006.
- [68] A. Patist, P. D. T. Huibers, B. Deneka, and D. O. Shah. Effect of tetraalkylammonium chlorides on foaming properties of sodium dodecyl sulfate solutions. *Langmuir*, 14(16):4471–4474, 1998.
- [69] S. G. Oh and D. O. Shah. Relationship between micellar lifetime and foamability of sodium dodecyl sulfate and sodium dodecyl sulfate/1-hexanol mixtures. *Langmuir*, 7(7):1316–1318, 1991.

- [70] S. Mun and D. J. McClements. Influence of interfacial characteristics on Ostwald ripening in hydrocarbon oil-in-water emulsions. *Langmuir*, 22(4):1551–1554, 2006.
- [71] D. Langevin. Dynamics of surfactant layers. *Current Opinion in Colloid and Interface Science*, 3(6):600–607, 1998.
- [72] R. Aveyard, J. H. Clint, and D. Nees. Small solid particles and liquid lenses at fluid/fluid interfaces. *Colloid and Polymer Science*, 278(2):155–163, 2000.
- [73] G. A. Pankhurst. Foam formation and foam stability: The effect of the adsorbed layer. *Transactions of the Faraday Society*, 37:496–505, 1941.
- [74] G. Narsimhan and Z. Wang. Rupture of equilibrium foam films due to random thermal and mechanical perturbations. *Colloids and Surfaces A: Physicochemical and Engineering Aspects*, 282:24–36, 2006.
- [75] S. A. Koehler, S. Hilgenfeldt, and H. A. Stone. A generalized view of foam drainage: Experiment and theory. *Langmuir*, 16(15):6327–6341, 2000.
- [76] M. Krzan, H. Caps, and N. Vandewalle. High stability of the bovine serum albumine foams evidenced in Hele–Shaw cell. *Colloids and Surfaces A: Physicochemical and Engineering Aspects*, 438:112–118, 2013.
- [77] J. Huang and Q. Sun. Foam drainage with twin inputs in two dimensions. *Colloids and Surfaces A: Physicochemical and Engineering Aspects*, 309(1):132–136, 2007.



- [78] R. A. Leonard and R. Lemlich. A study of interstitial liquid flow in foam. Part I. Theoretical model and application to foam fractionation. *AIChE Journal*, 11(1):18–25, 1965.
- [79] D. Weaire, N. Pittet, S. Hutzler, and D. Paldal. Steady-state drainage of an aqueous foam. *Physical Review Letters*, 71(16):2670–2673, 1993.
- [80] Q. C. Sun, W. Ge, and J. Huang. Influence of gravity on narrow input forced drainage in 2D liquid foams. *Chinese Science Bulletin*, 52(3):423–427, 2007.
- [81] G. Verbist, D. Weaire, and A. M. Kraynik. The foam drainage equation. *Journal of Physics: Condensed Matter*, 8(21):3715–3731, 1996.
- [82] D. Weaire and S. Hutzler. *The Physics of Foams*. New York: Oxford University Press, 1999.
- [83] S. A. Koehler, S. Hilgenfeldt, and H. A. Stone. Flow along two dimensions of liquid pulses in foams: Experiment and theory. *Europhysics Letters*, 54(3):335, 2001.
- [84] R. Mezzenga, P. Schurtenberger, A. Burbidge, and M. Martin. Understanding foods as soft materials. *Nature Materials*, 4(10):729–740, 2005.
- [85] T. J. Martin. *Fire-Fighting Foam Technology*. United Kingdom: John Wiley and Sons, 2012.

- [86] A. Singh, J. D. Van Hamme, and O. P. Ward. Surfactants in microbiology and biotechnology: Part 2. Application aspects. *Biotechnology Advances*, 25(1):99–121, 2007.
- [87] L. L. Schramm and E. E. Isaacs. *Foams in enhancing petroleum recovery*. United Kingdom: John Wiley and Sons, 2012.
- [88] T. M. Madkour and R. Azzam. Self-assembly urethane architecture: Free volume, connolly surface and diffusion coefficients investigation. *International Journal of Mathematical Models and Methods in Applied Sciences*, 2(3):372–381, 2008.
- [89] P. Stevenson and N. W. A. Lambert. *Froth phase phenomena in flotation*. United Kingdom: John Wiley and Sons, 2012.
- [90] K. S. Birdi. *Surface and colloid chemistry: Principles and applications*. Boca Raton: CRC press, 2010.
- [91] M. A. James-Smith, K. Alford, and D. O. Shah. A novel method to quantify the amount of surfactant at the oil/water interface and to determine total interfacial area of emulsions. *Journal of Colloid and Interface Science*, 310(2):590–598, 2007.
- [92] A. Ducret, A. Giroux, M. Trani, and R. Lortie. Characterization of enzymatically prepared biosurfactants. *Journal of the American Oil Chemists' Society*, 73(1):109–113, 1996.

- [93] R. Pichot. *Stability and characterisation of emulsions in the presence of colloidal particles and surfactants*. PhD thesis, University of Birmingham, 2012.
- [94] G. Marrucci. A theory of coalescence. *Chemical Engineering Science*, 24(6):975–985, 1969.
- [95] T. F. Tadros. *Emulsion formation and stability*. United Kingdom: John Wiley and Sons, 2013.
- [96] G. O. Phillips and P. A. Williams. *Handbook of hydrocolloids*. Boca Raton: CRC Press, 2009.
- [97] M. Shields, R. Ellis, and B. R. Saunders. A creaming study of weakly flocculated and depletion flocculated oil-in-water emulsions. *Colloids and Surfaces A: Physicochemical and Engineering Aspects*, 178(1):265–276, 2001.
- [98] P. Taylor. Ostwald ripening in emulsions. *Colloids and Surfaces A: Physicochemical and Engineering Aspects*, 99(2-3):175–185, 1995.
- [99] K. Szymczyk and B. Janczuk. Wettability of a glass surface in the presence of two nonionic surfactant mixtures. *Langmuir*, 24(15):7755–7760, 2008.
- [100] V. Nace. *Nonionic surfactants: Polyoxyalkylene block copolymers*, volume 60. Boca Raton: CRC Press, 1996.

- [101] A. Pradhan and A. Bhattacharyya. Quest for an eco-friendly alternative surfactant: Surface and foam characteristics of natural surfactants. *Journal of Cleaner Production*, 150:127–134, 2017.
- [102] K. Chatterjee. *Wettability of hair using natural and synthetic surfactants in presence of silver nanoparticles as additive*. PhD thesis, National Institute of Technology, Rourkela, 2012.
- [103] P. A. Lara-Martin, A. Gomez-Parra, J. L. Sanz, and E. Gonzalez-Mazo. Anaerobic degradation pathway of linear alkylbenzene sulfonates (LAS) in sulfate-reducing marine sediments. *Environmental Science and Technology*, 44(5):1670–1676, 2010.
- [104] M. Hampel, I. Moreno-Garrido, E. Gonzalez-Mazo, and J. Blasco. Suitability of the marine prosobranch snail *Hydrobia ulvae* for sediment toxicity assessment: A case study with the anionic surfactant linear alkylbenzene sulphonate (LAS). *Ecotoxicology and Environmental Safety*, 72(4):1303–1308, 2009.
- [105] C. F. Mason. *Biology of freshwater pollution*. London: Pearson Education, 2002.
- [106] C. Verge, A. Moreno, J. Bravo, and J. Berna. Influence of water hardness on the bioavailability and toxicity of linear alkylbenzene sulphonate (LAS). *Chemosphere*, 44(8):1749–1757, 2001.
- [107] M. Ghoochani, S. Shekoohiyan, A. H. Mahvi, B. Haibati, and M. Norouzi. Determination of detergent in Tehran ground and surface water.

- American-Eurasian Journal of Agriculture and Environmental Science*, 10(3):464–469, 2011.
- [108] B. Mukherjee, M. Nivedita, and D. Mukherjee. Plankton diversity and dynamics in a polluted eutrophic lake, Ranchi. *Journal of Environmental Biology*, 31(5):827–839, 2010.
- [109] V. Misra, G. Chawla, V. Kumar, H. Lal, and P. N. Viswanathan. Effect of linear alkyl benzene sulfonate in skin of fish fingerlings (*Cirrhina mrigala*): Observations with scanning electron microscope. *Ecotoxicology and Environmental Safety*, 13(2):164–168, 1987.
- [110] C. L. Yuan, Z. Z. Xu, M. X. Fan, H. Y. Liu, Y. H. Xie, and T. Zhu. Study on characteristics and harm of surfactants. *Journal of Chemical and Pharmaceutical Research*, 6(7):2233–2237, 2014.
- [111] T. Cserhati, E. Forgacs, and G. Oros. Biological activity and environmental impact of anionic surfactants. *Environment International*, 28(5):337–348, 2002.
- [112] S. Jobling, M. Nolan, C. R. Tyler, G. Brighty, and J. P. Sumpter. Widespread sexual disruption in wild fish. *Environmental Science and Technology*, 32(17):2498–2506, 1998.
- [113] S. Gupta, A. Pal, P. K. Ghosh, and M. Bandyopadhyay. Performance of waste activated carbon as a low-cost adsorbent for the removal of anionic surfactant from aquatic environment. *Journal of Environmental Science and Health, Part A*, 38(2):381–397, 2003.

- [114] M. A. Lewis. Chronic toxicities of surfactants and detergent builders to algae: A review and risk assessment. *Ecotoxicology and Environmental Safety*, 20(2):123–140, 1990.
- [115] M. Fountoulakis, P. Drillia, C. Pakou, A. Kampioti, K. Stamatelatou, and G. Lyberatos. Analysis of nonylphenol and nonylphenol ethoxylates in sewage sludge by high performance liquid chromatography following microwave-assisted extraction. *Journal of Chromatography A*, 1089(1):45–51, 2005.
- [116] S. Salati, G. Papa, and F. Adani. Perspective on the use of humic acids from biomass as natural surfactants for industrial applications. *Biotechnology Advances*, 29(6):913–922, 2011.
- [117] S-T. Muntaha and M. N. Khan. Natural surfactant extracted from *Sapindus mukurossi* as an eco-friendly alternate to synthetic surfactant—a dye surfactant interaction study. *Journal of Cleaner Production*, 93:145–150, 2015.
- [118] S. D. Barma. Wettability of hair using natural surfactants in presence of silver nanoparticles as additive. Master’s thesis, National Institute of Technology, Rourkela, 2014.
- [119] K. Hostettmann and A. Marston. *Saponins*. United Kingdom: Cambridge University Press, 2005.
- [120] C. R. Kensil. Saponins as vaccine adjuvants. *Critical Reviews in Therapeutic Drug Carrier Systems*, 13(1-2):1–55, 1996.

- [121] D. Oakenfull. Saponins in food—a review. *Food Chemistry*, 7(1):19–40, 1981.
- [122] G. Francis, Z. Kerem, H. P. S. Makkar, and K. Becker. The biological action of saponins in animal systems: A review. *British Journal of Nutrition*, 88(6):587–605, 2002.
- [123] A. V. Rao and D. M. Gurfinkel. *Dietary saponins and human health*, pages 255–270. Netherlands:Springer, 2000.
- [124] E. Madland. Extraction, isolation and structure elucidation of saponins from *Herniaria incana*. Master’s thesis, Institutt for Kjemi, 2013.
- [125] K-J. Hong, S. Tokunaga, and T. Kajiuchi. Evaluation of remediation process with plant-derived biosurfactant for recovery of heavy metals from contaminated soils. *Chemosphere*, 49(4):379–387, 2002.
- [126] Z-W. Wang, M-Y. Gu, and G-Z. Li. Surface properties of Gleditsia saponin and synergisms of its binary system. *Journal of Dispersion Science and Technology*, 26(3):341–347, 2005.
- [127] W. Oleszek and A. Hamed. *Saponin-based surfactants*. United Kingdom: John Wiley and Sons, 2010.
- [128] D. G. Oakenfull. Aggregation of saponins and bile acids in aqueous solution. *Australian Journal of Chemistry*, 39(10):1671–1683, 1986.
- [129] O. Guclu-Ustundaug and G. Mazza. Saponins: Properties, applications and processing. *Critical Reviews in Food Science and Nutrition*, 47(3):231–258, 2007.

- [130] J. S. Negi, P. S. Negi, G. J. Pant, M. S. M. Rawat, and S. K. Negi. Naturally occurring saponins: Chemistry and Biology. *Journal of Poisonous and Medicinal Plant Research*, 1(1):006–011, 2013.
- [131] M. F. Balandrin. *Commercial utilization of plant-derived saponins: An overview of medicinal, pharmaceutical, and industrial applications*, pages 1–14. United States: Springer, 1996.
- [132] M. J. Olmstead. Organic toothpaste containing saponin, November 26 2002. US Patent 6,485,711.
- [133] B. Yoo, B. Kang, M. Yeom, D. Sung, S. Han, H. Kim, and H. Ju. Nanoemulsion comprising metabolites of Ginseng saponin as an active component and a method for preparing the same, and a skin-care composition for anti-aging containing the same, 3 2003. US Patent App. 10/336,024.
- [134] E. Bombardelli, P. Morazzoni, A. Cristoni, and R. Seghizzi. Pharmaceutical and cosmetic formulations with antimicrobial activity, 5 2002. US Patent 6,475,536.
- [135] Y. Zhan. Animal feed compositions and uses of triterpenoid saponin obtained from *Camellia* L. plants, December 28 1999. US Patent 6,007,822.
- [136] G. M. Henderson. Bio-enhancer, May 8 2001. US Patent 6,228,265.



- [137] D. Roy, R. R. Kommalapati, S. S. Mandava, K. T. Valsaraj, and W. D. Constant. Soil washing potential of a natural surfactant. *Environmental Science and Technology*, 31(3):670–675, 1997.
- [138] C. R. Kensil, A. X. Mo, and A. Truneh. Current vaccine adjuvants: An overview of a diverse class. *Frontiers in Bioscience*, 9:2972–2988, 2004.
- [139] D. J. Meyer. Fire fighting foams utilizing saponins, April 18 2000. US Patent 6,051,154.
- [140] J. D. Dhar, V. K. Bajpai, B. S. Setty, and V. P. Kamboj. Morphological changes in human spermatozoa as examined under scanning electron microscope after in vitro exposure to saponins isolated from *Sapindus mukorossi*. *Contraception*, 39(5):563–568, 1989.
- [141] M. Banerjee, A. Hazra, Y. P. Bharitkar, and N. B. Mondal. Insights of spermicidal research: An update. *Journal of Fertilization: In Vitro, IVF-Worldwide, Reproductive Medicine, Genetics and Stem Cell Biology*, 3(1):138, 2014.
- [142] P. K. Soni, G. Luhadia, D. K. Sharma, and P. C. Mali. Antifertility activities of traditional medicinal plants in males with emphasis on their mode of action: A review. *Journal of Global Biosciences*, 4(1):1165–1179, 2015.
- [143] A. B. Chhetri, K. C. Watts, M. S. Rahman, and M. R. Islam. Soapnut extract as a natural surfactant for enhanced oil recovery. *Energy*

- Sources, Part A: Recovery, Utilization, and Environmental Effects*, 31(20):1893–1903, 2009.
- [144] W. Zhou, X. Wang, C. Chen, and L. Zhu. Enhanced soil washing of phenanthrene by a plant-derived natural biosurfactant, Sapindus saponin. *Colloids and Surfaces A: Physicochemical and Engineering Aspects*, 425:122–128, 2013.
- [145] M. B. Sarma, S. B. Gogoi, D. Devi, and B. Goswami. Degumming of muga silk fabric by biosurfactant. *Journal of Scientific and Industrial Research*, 71:270–272, 2012.
- [146] K. Shikha and Y. R. Chauhan. Biodiesel production from non edible-oils: A review. *Journal of Chemical and Pharmaceutical Research*, 4(9):4219–4230, 2012.
- [147] K. R. Aneja, R. Joshi, and C. Sharma. In vitro antimicrobial activity of Sapindus mukorossi and Emblica officinalis against dental caries pathogens. *Ethnobotanical Leaflets*, 14:402–412, 2010.
- [148] M. Du, S. Huang, J. Zhang, J. Wang, L. Hu, and J. Jiang. Toxicological test of saponins from Sapindus mukorossi Gaerth. *Open Journal of Forestry*, 5(7):749–753, 2015.
- [149] Y-H. Kuo, H-C. Huang, L-M. Yang Kuo, Y-W. Hsu, K-H. Lee, F-R. Chang, and Y-C. Wu. New dammarane-type saponins from the galls of Sapindus mukorossi. *Journal of Agricultural and Food Chemistry*, 53(12):4722–4727, 2005.

- [150] H-C. Huang, W-J. Tsai, S. L. Morris-Natschke, H. Tokuda, K-H. Lee, Y-C. Wu, and Y-H. Kuo. Sapinmusaponins F- J, bioactive tirucallane-type saponins from the galls of *Sapindus mukorossi*. *Journal of Natural Products*, 69(5):763–767, 2006.
- [151] R. Li, Z. L. Wu, Y. J. Wang, and L. L. Li. Separation of total saponins from the pericarp of *Sapindus mukorossi* Gaerten. by foam fractionation. *Industrial Crops and Products*, 51:163–170, 2013.
- [152] W. Heng, Z. Ling, W. Na, G. Youzhi, W. Zhen, S. Zhiyong, X. Deping, X. Yunfei, and Y. Weirong. Analysis of the bioactive components of *Sapindus* saponins. *Industrial Crops and Products*, 61:422–429, 2014.
- [153] R. Ghagi, S. K. Satpute, B. A. Chopade, and A. G. Banpurkar. Study of functional properties of *Sapindus mukorossi* as a potential bio-surfactant. *Indian Journal of Science and Technology*, 4(5):530–533, 2011.
- [154] J. A. Parotta and J. M. Roshetko. *Albizia procera*–white siris for reforestation and agroforestry. *Winrock International*, FACT Net 97-01, 1997.
- [155] S. S. Krishnan, A. K. Muthu, and J. Kavitha. GC-MS analysis of ethanolic extract of aerial parts of *Albizia procera* (roxb.) Benth. *International Journal of Pharmacy and Pharmaceutical Sciences*, 5(3):702–704, 2013.

- [156] K. Kokila, S. D. Priyadharshini, and V. Sujatha. Phytopharmacological properties of Albizia species: A review. *International Journal of Pharmacy and Pharmaceutical Sciences*, 5(5):70–73, 2013.
- [157] S. Sivakrishnan and A. K. Muthu. Evaluation of hepatoprotective activity of squalene isolated from *Albizia procera* against paracetamol induced hepatotoxicity on Wistar rats. *World Journal of Pharmacy and Pharmaceutical Sciences*, 3(3):1351–1362, 2014.
- [158] L. Pachuau and B. Mazumder. *Albizia procera* gum as an excipient for oral controlled release matrix tablet. *Carbohydrate Polymers*, 90(1):289–295, 2012.
- [159] P. Panthong, K. Bunluepuech, N. Boonnak, P. Chaniad, S. Pianwanit, C. Wattanapiromsakul, and S. Tewtrakul. Anti-HIV-1 integrase activity and molecular docking of compounds from *Albizia procera* bark. *Pharmaceutical Biology*, 53(12):1861–1866, 2015.
- [160] T. S. C. Li. *Chinese and related North American herbs: Phytopharmacology and therapeutic values*. Boca Raton: CRC Press, 2002.
- [161] H. H. Hume. Duplications in *Zephyranthes*. *Bulletin of the Torrey Botanical Club*, 62(7):403–411, 1935.
- [162] S. Kobayashi, H. Ishikawa, M. Kihara, T. Shingu, and T. Hashimoto. Isolation of carinatine and pretazettine from the bulbs of *Zephyranthes carinate* herb.(Amaryllidaceae). *Chemical and Pharmaceutical Bulletin*, 25(9):2244–2248, 1977.

- [163] A. Kaur, S. S. Kamboj, J. Singh, R. Singh, M. Abrahams, G. J. Kotwal, and A. K. Saxena. Purification of 3 monomeric monocot mannose-binding lectins and their evaluation for antipoxviral activity: Potential applications in multiple viral diseases caused by enveloped viruses. *Biochemistry and Cell Biology*, 85(1):88–95, 2007.
- [164] K. Kojima, M. Mutsuga, M. Inoue, and Y. Ogihara. Two alkaloids from *Zephyranthes carinata*. *Phytochemistry*, 48(7):1199–1202, 1998.
- [165] M. Mutsuga, K. Kojima, M. Nose, M. Inoue, and Y. Ogihara. Cytotoxic activities of alkaloids from *Zephyranthes carinata*. *Natural Medicines*, 55(4):201–204, 2001.
- [166] N. Cortes, R. A. Posada-Duque, R. Alvarez, F. Alzate, S. Berkov, G. P. Cardona-Gomez, and E. Osorio. Neuroprotective activity and acetylcholinesterase inhibition of five Amaryllidaceae species: A comparative study. *Life Sciences*, 122:42–50, 2015.
- [167] K. Mote, S. Pore, G. Rashinkar, S. Kambale, A. Kumbhar, and R. Sallunkhe. *Acacia concinna* pods: As a green catalyst for highly efficient synthesis of acylation of amines. *Archives of Applied Science Research*, 2(3):74–80, 2010.
- [168] H. V. Chavan and B. P. Bandgar. Aqueous extract of *Acacia concinna* pods: An efficient surfactant type catalyst for synthesis of 3-carboxycoumarins and cinnamic acids via Knoevenagel condensation. *ACS Sustainable Chemistry and Engineering*, 1(8):929–936, 2013.

- [169] R. Kukhetpitakwong, C. Hahnvajjanawong, P. Homchampa, V. Leelavatcharamas, J. Satra, and W. Khunkitti. Immunological adjuvant activities of saponin extracts from the pods of *Acacia concinna*. *International Immunopharmacology*, 6(11):1729–1735, 2006.
- [170] T. Sekine, N. Fukasawa, F. Ikegami, K. Saito, Y. Fujii, and I. Murakoshi. Structure and synthesis of a new monoterpenoidal carboxamide from the seeds of the Thai medicinal plant *Acacia concinna*. *Chemical and Pharmaceutical Bulletin*, 45(1):148–151, 1997.
- [171] I. P. Varshney and K. M. Shamsuddin. Saponins and sapogenins XXV—the sapogenin of *Acacia concinna* DC pods and the constitution of acacic acid. *Tetrahedron Letters*, 5(30):2055–2058, 1964.
- [172] A. S. R. Anjaneyulu, L. R. Row, and A. Sree. Acacidiol, a new nor-triterpene from the sapogenins of *Acacia concinna*. *Phytochemistry*, 18(7):1199–1201, 1979.
- [173] M. A. Gafur, T. Obata, F. Kiuchi, and Y. Tsuda. *Acacia concinna* saponins. I. Structures of prosapogenols, concinnosides AF, isolated from the alkaline hydrolysate of the highly polar saponin fraction. *Chemical and Pharmaceutical Bulletin*, 45(4):620–625, 1997.
- [174] F. Kiuchi, M. A. Gafur, T. Obata, A. Tachibana, and Y. Tsuda. *Acacia concinna* saponins. II. Structures of monoterpenoid glycosides in the alkaline hydrolysate of the saponin fraction. *Chemical and Pharmaceutical Bulletin*, 45(5):807–812, 1997.

- [175] Y. Tezuka, K. Honda, A. H Banskota, M. M. Thet, and S. Kadota. Kinmoonosides A- C, three new cytotoxic saponins from the fruits of *Acacia concinna*, a medicinal plant collected in Myanmar. *Journal of Natural Products*, 63(12):1658–1664, 2000.
- [176] G. Pratap and V. S. Bhaskar Rao. Evaluation of surface active properties of saponins isolated from *Acacia concinna* dc pods. *European Journal of Lipid Science and Technology*, 89(5):205–208, 1987.
- [177] A. M. Alkhawajah. Studies on the antimicrobial activity of *Juglans regia*. *The American Journal of Chinese Medicine*, 25(2):175–180, 1997.
- [178] R. M. Kunwar and N. Adhikari. Ethnomedicine of Dolpa district, Nepal: The plants, their vernacular names and uses. *Lyonia*, 8(1):43–49, 2005.
- [179] K. Bhatia, S. Rahman, M. Ali, and S. Raisuddin. In vitro antioxidant activity of *Juglans regia* L. bark extract and its protective effect on cyclophosphamide-induced urotoxicity in mice. *Redox Report*, 11(6):273–279, 2006.
- [180] D. Brown. *Encyclopedia of Herbs and their Uses*. London: Dorling Kindersley, 1995.
- [181] T. Fujita, E. Sezik, M. Tabata, E. Yesilada, G. Honda, Y. Takeda, T. Tanaka, and Y. Takaishi. Traditional medicine in Turkey VII. Folk medicine in middle and west Black Sea regions. *Economic Botany*, 49(4):406–422, 1995.

- [182] M. Kaileh, W. V. Berghe, E. Boone, T. Essawi, and G. Haegeman. Screening of indigenous Palestinian medicinal plants for potential anti-inflammatory and cytotoxic activity. *Journal of Ethnopharmacology*, 113(3):510–516, 2007.
- [183] K. J. Spaccarotella, P. M. Kris-Etherton, W. L. Stone, D. M. Bagshaw, V. K. Fishell, S. G. West, F. R. Lawrence, and T. J. Hartman. The effect of walnut intake on factors related to prostate and vascular health in older men. *Nutrition Journal*, 7(1):13, 2008.
- [184] J. E. Robbers and V. E. Tyler. *Tyler's herbs of choice. The therapeutic use of phytomedicinals*. New York:Haworth Press Inc., 1999.
- [185] R. Haque, B. Bin-Hafeez, S. Parvez, S. Pandey, I. Sayeed, M. Ali, and S. Raisuddin. Aqueous extract of walnut (*Juglans regia* l.) protects mice against cyclophosphamideinduced biochemical toxicity. *Human and Experimental Toxicology*, 22(9):473–480, 2003.
- [186] E. Noumi, M. Snoussi, N. Trabelsi, H. Hajlaoui, R. Ksouri, E. Valentin, and A. Bakhrouf. Antibacterial, anticandidal and antioxidant activities of *Salvadora persica* and *Juglans regia* L. extracts. *Journal of Medicinal Plants Research*, 5(17):4138–4146, 2011.
- [187] V. Upadhyay. Antifungal activity and preliminary phytochemical analysis of stem bark extracts of *Juglans regia* Linn. *International Journal of Pharmaceutical and Biological Archive*, 1(5):442–447, 2010.
- [188] E. Noumi, M. Snoussi, H. Hajlaoui, E. Valentin, and A. Bakhrouf. Antifungal properties of *Salvadora persica* and *Juglans regia* L. extracts



- against oral *Candida* strains. *European Journal of Clinical Microbiology and Infectious Diseases*, 29(1):81–88, 2010.
- [189] R. R. Deshpande, A. A. Kale, A. D. Ruikar, P. S. Panvalkar, A. A. Kulkarni, N. R. Deshpande, and J. P. Salvekar. Antimicrobial activity of different extracts of *Juglans regia* L. against oral microflora. *International Journal of Pharmacy and Pharmaceutical Sciences*, 3(2):200–201, 2011.
- [190] G. Tagarelli, A. Tagarelli, and A. Piro. Folk medicine used to heal malaria in Calabria (southern Italy). *Journal of Ethnobiology and Ethnomedicine*, 6(1):1–16, 2010.
- [191] R. R. Kommalapati, K. T. Valsaraj, W. D. Constant, and D. Roy. Aqueous solubility enhancement and desorption of hexachlorobenzene from soil using a plant-based surfactant. *Water Research*, 31(9):2161–2170, 1997.
- [192] H. Wagner and S. Bladt. *Plant drug analysis: A thin layer chromatography atlas*. New York: Springer Science & Business Media, 1996.
- [193] C. R. Adao, B. P. da Silva, and J. P. Parente. A new steroidal saponin with antiinflammatory and antiulcerogenic properties from the bulbs of *Allium ampeloprasum* var. *porrum*. *Fitoterapia*, 82(8):1175–1180, 2011.
- [194] H. Ritacco, P-A. Albouy, A. Bhattacharyya, and D. Langevin. Influence of the polymer backbone rigidity on polyelectrolyte–surfactant

- complexes at the air/water interface. *Physical Chemistry Chemical Physics*, 2(22):5243–5251, 2000.
- [195] S. I. Karakashev, P. Georgiev, and K. Balashev. Foam production–ratio between foaminess and rate of foam decay. *Journal of Colloid and Interface science*, 379(1):144–147, 2012.
- [196] E. Tyrode, A. Pizzino, and O. J. Rojas. Foamability and foam stability at high pressures and temperatures. I. Instrument validation. *Review of Scientific Instruments*, 74(5):2925–2932, 2003.
- [197] E. Iglesias, J. Anderez, A. Forgiarini, and J-L. Salager. A new method to estimate the stability of short-life foams. *Colloids and Surfaces A: Physicochemical and Engineering Aspects*, 98(1-2):167–174, 1995.
- [198] A. Bhattacharyya, F. Monroy, D. Langevin, and J-F. Argillier. Surface rheology and foam stability of mixed surfactant–polyelectrolyte solutions. *Langmuir*, 16(23):8727–8732, 2000.
- [199] K. Lunkenheimer and K. Malysa. Simple and generally applicable method of determination and evaluation of foam properties. *Journal of Surfactants and Detergents*, 6(1):69–74, 2003.
- [200] M. E. Purchase. *Dynamic surface tension measurements and their use in prediction of wetting ability*. PhD thesis, Digital Repository@ Iowa State University, 1957.

- [201] A. H. Saad and R. B. Kadhim. Formulation and evaluation of herbal shampoo from *Ziziphus spina* leaves extract. *International Journal of Research in Ayurveda and Pharmacy*, 2(6):1802–1806, 2011.
- [202] S. C. Kothekar, A. M. Ware, J. T. Waghmare, and S. A. Momin. Comparative analysis of the properties of tween-20, tween-60, tween-80, arlancel-60, and arlancel-80. *Journal of Dispersion Science and Technology*, 28(3):477–484, 2007.
- [203] S. Balakrishnan, S. Varughese, and A. P. Deshpande. Micellar characterisation of saponin from *Sapindus mukorossi*. *Tenside Surfactants Detergents*, 43(5):262–268, 2006.
- [204] H. H. Kohler and J. Strnad. Evaluation of viscosity measurements of dilute solutions of ionic surfactants forming rod-shaped micelles. *Journal of Physical Chemistry*, 94(19):7628–7634, 1990.
- [205] J. Mata, D. Varade, and P. Bahadur. Aggregation behavior of quaternary salt based cationic surfactants. *Thermochimica Acta*, 428(1):147–155, 2005.
- [206] R. M. Sharma, K. Shah, and J. Patel. Evaluation of prepared herbal shampoo formulations and to compare formulated shampoo with marketed shampoos. *International Journal of Pharmacy and Pharmaceutical Sciences*, 3(4):402–405, 2011.
- [207] V. G. Berezkin. Contributions from NA Izmailov and MS Schraiber to the development of thin-layer chromatography (on the 70th anniversary

- of the publication of the first paper on thin-layer chromatography). *Journal of Analytical Chemistry*, 63(4):400–404, 2008.
- [208] R. M. Scott. The stationary phase in thin layer chromatography. *Journal of Liquid Chromatography*, 4(12):2147–2174, 1981.
- [209] T. Lalitha, R. Seshadri, and L. V. Venkataraman. Isolation and properties of saponins from *Madhuca butyracea* seeds. *Journal of Agricultural and Food Chemistry*, 35(5):744–748, 1987.
- [210] W. Oleszek, I. Kapusta, and A. Stochmal. *20 TLC of triterpenes (including saponins)*. Boca Raton: CRC Press, 2008.
- [211] L. R. Snyder. *Principles of adsorption chromatography; the separation of nonionic organic compounds*. New York: Marcel Dekker, 1968.
- [212] H-C. Huang, S-C. Liao, F-R. Chang, Y-H. Kuo, and Y-C. Wu. Molluscicidal saponins from *Sapindus mukorossi*, inhibitory agents of golden apple snails, *Pomacea canaliculata*. *Journal of Agricultural and Food Chemistry*, 51(17):4916–4919, 2003.
- [213] J. S. Negi, P. Singh, G. J. N. Pant, and M. S. M. Rawat. High-performance liquid chromatography analysis of plant saponins: An update 2005-2010. *Pharmacognosy Reviews*, 5(10):155–158, 2011.
- [214] V. Sharma and R. Paliwal. Isolation and characterization of saponins from *Moringa oleifera* (Moringaceae) pods. *International Journal of Pharmacy and Pharmaceutical Sciences*, 5(1):179–183, 2013.

- [215] L. R. Snyder, J. J. Kirkland, and J. L. Glajch. *Practical HPLC method development*. United Kingdom: John Wiley and Sons, 2012.
- [216] B. J. Clark, T. Frost, and M. A. Russell. *UV Spectroscopy: Techniques, instrumentation and data handling*, volume 4. London: Chapman and Hall, 1993.
- [217] A. Primer. *Fundamentals of UV-visible spectroscopy*. Number 12-5965. Hewlett-Packard publication, 1996.
- [218] H-H. Perkampus and H-C. Grinter. *UV-VIS Spectroscopy and its Applications*. Springer, 1992.
- [219] B. H. Stuart. *Organic molecules*. United Kingdom: John Wiley and Sons, Ltd., 2004.
- [220] H. Hausdorff. Analysis of polymers by infrared spectroscopy. In *Analytical Chemistry*, volume 23, pages 683–683. American Chemical Society 1155 16th ST, NW, Washington, DC 20036, 1951.
- [221] I. G. Medina-Meza, N. A. Aluwi, S. R. Saunders, and G. M. Ganjyal. GC–MS profiling of triterpenoid saponins from 28 Quinoa varieties (*Chenopodium quinoa* Willd.) grown in Washington State. *Journal of Agricultural and Food Chemistry*, 64(45):8583–8591, 2016.
- [222] P. M. Kruglyakov, S. I. Karakashev, A. V. Nguyen, and N. G. Vilkova. Foam drainage. *Current Opinion in Colloid and Interface Science*, 13(3):163–170, 2008.

- [223] X. Wei, Z. Chang, and H. Liu. Influence of sodium dodecyl sulfate on the characteristics of bovine serum albumin solutions and foams. *Journal of Surfactants and Detergents*, 6(2):107–112, 2003.
- [224] A. R. Mainkar and C. I. Jolly. Evaluation of commercial herbal shampoos. *International Journal of Cosmetic Science*, 22(5):385–392, 2000.
- [225] D. A. Vaz, E. J. Gudina, E. J. Alameda, J. A. Teixeira, and L. R. Rodrigues. Performance of a biosurfactant produced by a *Bacillus subtilis* strain isolated from crude oil samples as compared to commercial chemical surfactants. *Colloids and Surfaces B: Biointerfaces*, 89:167–174, 2012.
- [226] N. A. Negm and A. S. Mohamed. Surface and thermodynamic properties of diquaternary bola-form amphiphiles containing an aromatic spacer. *Journal of Surfactants and Detergents*, 7(1):23–30, 2004.
- [227] S. Paria, N. R. Biswal, and R. G. Chaudhuri. Surface tension, adsorption, and wetting behaviors of natural surfactants on a PTFE surface. *AIChE Journal*, 61(2):655–663, 2015.
- [228] E. A. M. Gad, M. M. A. El-Sukkary, and D. A. Ismail. Surface and thermodynamic parameters of sodium N-acyl sarcosinate surfactant solutions. *Journal of the American Oil Chemists' Society*, 74(1):43–47, 1997.
- [229] P. S. Piispanen, M. Persson, P. Claesson, and T. Norin. Surface properties of surfactants derived from natural products. Part 2: Struc-

- ture/property relationships—foaming, dispersion, and wetting. *Journal of Surfactants and Detergents*, 7(2):161–167, 2004.
- [230] K. Kumpabooth, J. F. Scamehorn, S. Osuwan, and J. H. Harwell. Surfactant recovery from water using foam fractionation: Effect of temperature and added salt. *Separation Science and Technology*, 34(2):157–172, 1999.
- [231] E. T. Akintayo, A. A. Oshodi, and K. O. Esuoso. Effects of NaCl, ionic strength and pH on the foaming and gelation of pigeon pea (*Cajanus cajan*) protein concentrates. *Food Chemistry*, 66(1):51–56, 1999.
- [232] Q. Zhang, X. Wei, J. Liu, D. Sun, X. Zhang, C. Zhang, and J. Liu. Effects of inorganic salts and polymers on the foam performance of 1-tetradecyl-3-methylimidazolium bromide aqueous solution. *Journal of Surfactants and Detergents*, 15(5):613–621, 2012.
- [233] G. S. Canto, J. Treter, S. Yang, G. L. Borre, M. P. G. Peixoto, and G. G. Ortega. Evaluation of foam properties of saponin from *Ilex paraguariensis* A. St. Hil. (Aquifoliaceae) fruits. *Brazilian Journal of Pharmaceutical Sciences*, 46(2):237–243, 2010.
- [234] R. S. Powale and S. S. Bhagwat. Influence of electrolytes on foaming of sodium lauryl sulfate. *Journal of Dispersion Science and Technology*, 27(8):1181–1186, 2006.
- [235] L. Zhou, G. Xu, Z. Zhang, H. Li, and P. Yao. Surface activity and safety of deamidated zein peptides. *Colloids and Surfaces A: Physicochemical and Engineering Aspects*, 540:150–157, 2018.

- [236] M. O. Agu and J. T. Barminas. Evaluation of violet plant (*Securidaca longepedunculata*) roots as an emulsifying agent. *Journal of Applied Chemistry*, 4(4):05–09, 2013.
- [237] M. Nadeem, C. Rangkuti, K. Anuar, M. R. U. Haq, I. B. Tan, and S. S. Shah. Diesel engine performance and emission evaluation using emulsified fuels stabilized by conventional and gemini surfactants. *Fuel*, 85(14-15):2111–2119, 2006.
- [238] E. Carey, S. R. Patil, and C. Stubenrauch. Conductivity measurements as a method for studying ionic technical grade surfactants. *Tenside Surfactants Detergents*, 45(3):120–125, 2008.
- [239] B. Dong, N. Li, L. Zheng, L. Yu, and T. Inoue. Surface adsorption and micelle formation of surface active ionic liquids in aqueous solution. *Langmuir*, 23(8):4178–4182, 2007.
- [240] P. Mukerjee. The nature of the association equilibria and hydrophobic bonding in aqueous solutions of association colloids. *Advances in Colloid and Interface Science*, 1(3):242–275, 1967.
- [241] A. K. Chattopadhyay, L. Ghaicha, S. G. Oh, and D. O. Shah. Salt effects on monolayers and their contribution to surface viscosity. *The Journal of Physical Chemistry*, 96(15):6509–6513, 1992.
- [242] S. D. Williams and W. H. Schmitt. *Chemistry and technology of the cosmetics and toiletries industry*. London:Chapman and Hall, 2012.



- [243] D. Yu, F. Huang, and H. Xu. Determination of critical concentrations by synchronous fluorescence spectrometry. *Analytical Methods*, 4(1):47–49, 2012.
- [244] A. Prieu, S. Zalipsky, R. Cohen, and Y. Barenholz. Determination of critical micelle concentration of lipopolymers and other amphiphiles: Comparison of sound velocity and fluorescent measurements. *Langmuir*, 18(3):612–617, 2002.
- [245] S. Mondal and S. Ghosh. Role of curcumin on the determination of the critical micellar concentration by absorbance, fluorescence and fluorescence anisotropy techniques. *Journal of Photochemistry and Photobiology B: Biology*, 115:9–15, 2012.
- [246] C. H. Tan, Z. J. Huang, and X. G. Huang. Rapid determination of surfactant critical micelle concentration in aqueous solutions using fiber-optic refractive index sensing. *Analytical Biochemistry*, 401(1):144–147, 2010.
- [247] C-E. Lin and K-S. Lin. Determination of critical micelle concentration and interactions between cephalosporins and charged surfactants. *Journal of Chromatography A*, 868(2):313–316, 2000.
- [248] J. F. Yan and M. B. Palmer. A nuclear magnetic resonance method for determination of critical micelle concentration. *Journal of Colloid and Interface Science*, 30(2):177–182, 1969.

- [249] K. Bijma and J. B. F. N. Engberts. Effect of counterions on properties of micelles formed by alkylpyridinium surfactants. 1. conductometry and  $^1\text{H-NMR}$  chemical shifts. *Langmuir*, 13(18):4843–4849, 1997.
- [250] R. Zana. *Dynamics of surfactant self-assemblies: Micelles, microemulsions, vesicles and lyotropic phases*, volume 125. Boca Raton: CRC press, 2005.
- [251] N. Jain, S. Trabelsi, S. Guillot, D. McLoughlin, D. Langevin, P. Letellier, and M. Turmine. Critical aggregation concentration in mixed solutions of anionic polyelectrolytes and cationic surfactants. *Langmuir*, 20(20):8496–8503, 2004.
- [252] A. Popadyuk, H. Kalita, B. J. Chisholm, and A. Voronov. Evaluation of soy-based surface active copolymers as surfactant ingredients in model shampoo formulations. *International Journal of Cosmetic Science*, 36(6):537–545, 2014.
- [253] S. Reis, C. G. Moutinho, C. Matos, B. de Castro, P. Gameiro, and J. L. F. C. Lima. Noninvasive methods to determine the critical micelle concentration of some bile acid salts. *Analytical Biochemistry*, 334(1):117–126, 2004.
- [254] D. T. Piorkowski and D. J. Mc Clements. Beverage emulsions: Recent developments in formulation, production, and applications. *Food Hydrocolloids*, 42:5–41, 2014.
- [255] Y. Yang, M. E. Leser, A. A. Sher, and D. J. Mc Clements. Formation and stability of emulsions using a natural small molecule surfactant:

- Quillaja saponin (Q-Naturale®). *Food Hydrocolloids*, 30(2):589–596, 2013.
- [256] P. K. Jain, A. Soni, P. Jain, and J. Bhawsar. Phytochemical analysis of *Mentha spicata* plant extract using UV–VIS, FTIR and GC/MS technique. *Journal of Chemical and Pharmaceutical Research*, 8(2):1–6, 2016.
- [257] D. C. Liebler, J. A. Burr, L. Philips, and A. J. L. Ham. Gas chromatography–mass spectrometry analysis of vitamin E and its oxidation products. *Analytical Biochemistry*, 236(1):27–34, 1996.
- [258] X-F. Zhang, S-L. Yang, Y-Y. Han, L. Zhao, G-L. Lu, T. Xia, and L-P. Gao. Qualitative and quantitative analysis of triterpene saponins from tea seed pomace (*Camellia oleifera* abel) and their activities against bacteria and fungi. *Molecules*, 19(6):7568–7580, 2014.
- [259] M. Yamunadevi, E. G. Wesely, and M. Johnson. Chromatographic finger print studies on saponins of *Aerva lanata* L. Juss. ex schultes by using HPTLC. *International Journal of Current Pharmaceutical Research*, 4(2):52–57, 2012.
- [260] K. Karthika, S. Jamuna, and S. Paulsamy. TLC and HPTLC fingerprint profiles of different bioactive components from the tuber of *Solena amplexicaulis*. *Journal of Pharmacognosy and Phytochemistry*, 3(1):198–206, 2014.
- [261] S. Sowmya, P. C. Perumal, and V. K. Gopalakrishnan. Chromatographic and spectrophotometric analysis of bioactive compounds from

- Cayratia trifolia (L.) stem. *International Journal of Pharmacy and Pharmaceutical Sciences*, 8(6):57–64, 2016.
- [262] M. Yoshikawa, T. Murakami, H. Matsuda, T. Ueno, M. Kadoya, J. Yamahara, and N. Murakami. Bioactive saponins and glycosides. II. Senegae radix.(2): Chemical structures, hypoglycemic activity, and ethanol absorption-inhibitory effect of E-senegasaponin c, Z-senegasaponin c, and Z-senegin II, III, and IV. *Chemical and Pharmaceutical Bulletin*, 44(7):1305–1313, 1996.
- [263] L. S. Gonzalez-Valdez, N. Almaraz-Abarca, J. B. Proal-Najera, F. Robles-Martinez, G. Valencia-Del-Toro, and M. Quintos-Escalante. Surfactant properties of the saponins of Agave durangensis, application on arsenic removal. *International Journal of Engineering*, 4(2):8269, 2013.
- [264] S. Kudou, M. Tonomura, C. Tsukamoto, T. Uchida, T. Sakabe, N. Tamura, and K. Okubo. Isolation and structural elucidation of DDMP-conjugated soyasaponins as genuine saponins from soybean seeds. *Bioscience, Biotechnology, and Biochemistry*, 57(4):546–550, 1993.
- [265] P. F. Pinheiro and G. C. Justino. *Structural analysis of flavonoids and related compounds-a review of spectroscopic applications*. InTech, www.intechopen.com, 2012.

- [266] M. Burnouf-Radosevich and N. E. Delfel. High-performance liquid chromatography of triterpene saponins. *Journal of Chromatography. A*, 368:433–438, 1986.
- [267] D-J. Yang, T-J. Lu, and L. S. Hwang. Simultaneous determination of furostanol and spirostanol glycosides in Taiwanese yam (*Dioscorea* spp.) cultivars by high performance liquid chromatography. *Journal of Food and Drug Analysis*, 11(4):271–276, 2003.
- [268] I-S. Park, E. M. Kang, and N. Kim. High-performance liquid chromatographic analysis of saponin compounds in *Bupleurum falcatum*. *Journal of Chromatographic Science*, 38(6):229–233, 2000.
- [269] P. G. Kareru, J. M. Keriko, A. N. Gachanja, and G. M. Kenji. Direct detection of triterpenoid saponins in medicinal plants. *African Journal of Traditional, Complementary and Alternative medicines*, 5(1):56–60, 2008.
- [270] N. B. Omodara, J. S. Amoko, O. A. Obijole, and B. M. Ojo. Infrared and ultraviolet spectroscopic analysis of methanol extract of *Phyllanthus muellerianus* root. *Greener Journal of Physical Science*, 3(4):159–164, 2013.
- [271] M. S. Almutairi and M. Ali. Direct detection of saponins in crude extracts of soapnuts by FTIR. *Natural Product Research*, 29(13):1271–1275, 2015.

- [272] M. Sermakkani and V. Thangapandian. GC-MS analysis of *Cassia italica* leaf methanol extract. *Asian Journal of Pharmaceutical and Clinical Research*, 5(2):90–94, 2012.
- [273] M. Krishnaveni, R. Dhanalakshmi, and N. Nandhini. GC-MS analysis of phytochemicals, fatty acid profile, antimicrobial activity of *Gossypium* seeds. *International Journal of Pharmaceutical Sciences Review and Research*, 27(1):273–276, 2014.
- [274] S. Chanda, Y. Baravalia, and K. Nagani. Spectral analysis of methanol extract of *Cissus quadrangularis* L. stem and its fractions. *Journal of Pharmacognosy and Phytochemistry*, 2(4):149–157, 2013.
- [275] S. Honda and T. Masuda. Identification of pyrogallol in the ethyl acetate-soluble part of coffee as the main contributor to its xanthine oxidase inhibitory activity. *Journal of Agricultural and Food Chemistry*, 64(41):7743–7749, 2016.
- [276] Y. H. Han, S. Z. Kim, S. H. Kim, and W. H. Park. Pyrogallol inhibits the growth of lung cancer Calu-6 cells via caspase-dependent apoptosis. *Chemico-Biological Interactions*, 177(2):107–114, 2009.
- [277] W. Janssens. Photographic material suited for use in diffusion transfer photography and method of diffusion transfer photography using such material, November 4 1980. US Patent 4,232,107.
- [278] P. Velayutham and C. Karthi. GC-MS profile of in vivo, in vitro and fungal elicited in vitro leaves of *Hybanthus enneaspermus* (L.)

- F. Muell. *International Journal of Pharmacy and Pharmaceutical Sciences*, 7(1):260–267, 2015.
- [279] P. Vivekraj, S. Vinotha, A. Vijayan, and G. V. Anand. Preliminary phytochemical screening and GC–MS analysis of methanolic extract of *Turnera subulata* Smith (Passifloraceae). *The Journal of Phytopharmacology*, 6(3):174–177, 2017.
- [280] H. O. A. Ahmed and C. Wang. Determination of tea saponin in *Camellia* seed oil with UV and HPLC analysis. *World Journal of Engineering and Technology*, 3(04):30–37, 2015.
- [281] E. Thomas, T. P. Aneesh, D. G. Thomas, and R. Anandan. GC–MS analysis of phytochemical compounds present in the rhizomes of *Nervilia aragoana* gaud. *Asian Journal of Pharmaceutical and Clinical Research*, 6(3):68–74, 2013.
- [282] G. J. Hase, K. K. Deshmukh, R. D. Pokharkar, T. R. Gaje, and N. D. Phatanagre. Phytochemical studies on *Nerium oleander* l. using GC–MS. *International Journal of Pharmacognosy and Phytochemical Research*, 9(6):885–891, 2017.
- [283] S. J. Cox, G. Bradley, S. Hutzler, and D. Weaire. Vertex corrections in the theory of foam drainage. *Journal of Physics: Condensed Matter*, 13(21):4863, 2001.
- [284] S. Koehler, S. Hilgenfeldt, and H. A. Stone. Liquid flow through aqueous foams: The node-dominated foam drainage equation. *Physical Review Letters*, 82(21):4232–4235, 1999.

- [285] D. Weaire, S. Hutzler, G. Verbist, and E. A. J. F. Peters. A review of foam drainage. *Advances in Chemical Physics*, 102:315–374, 1997.
- [286] S. Hutzler, G. Verbist, D. Weaire, and J. A. Van der Steen. Measurement of foam density profiles using AC capacitance. *Europhysics Letters*, 31(8):497–502, 1995.
- [287] D. K. Todd. *Groundwater Hydrology*. New York: John Wiley and Sons Inc, 1980.